Interaction of Polymers with Polluted Atmosphere

Authors:
Gennady Zaikov
Evgenii Davydov
Georgii Pariiskii
Irina Gapanova
Tat'yana Pokholok

SMITHERS
iSmithers

Interaction of Polymers with Polluted Atmosphere Nitrogen Oxides

Authors:

Gennady Zaikov, Evgenii Davydov

Georgii Pariiskii, Irina Gapanova

Tat'yana Pokholok

***i*Smithers – A Smithers Group Company**

Shawbury, Shrewsbury, Shropshire, SY4 4NR, United Kingdom
Telephone: +44 (0)1939 250383 Fax: +44 (0)1939 251118
http://www.rapra.net

First Published in 2009 by

***i*Smithers**

Shawbury, Shrewsbury, Shropshire, SY4 4NR, UK

A catalogue record for this book is available from the British Library.

ISBN: 9781847353795 (hardback)
9781847353771 (softback)

Typeset by Argil Services
Printed and bound by Lightning Source Inc.

Preface

'A man who dares to waste one hour of time has not discovered the value of life'

Charles Robert Darwin (12 February 1809 to 19 April 1882) English biologist, naturalist, evolutionist

'Simplicity is the ultimate Sophistication' Leonardo da Vinci (15 April 1452 to 2 May 1519) Italian polymath: scientist, mathematician, engineer, inventor, anatomist, sculptor, painter, architect, musician and writer

If one was to estimate the world production of polymers and metals not in units of weight (tons), but in units of volume (cubic meters), then humans produce as much polymers, polymeric blends and composites as pig iron, steel, rolled metal and nonferrous metals taken together. The dynamics of the manufacturing process are also important: the growth of polymer production has surpassed that of metals by 15–20% each year in the past 20–25 years.

Humans lived in the Stone age, then in the Bronze age, Iron age, and have already entered into the 'Polymeric age'. Progress appears to involve replacement of one problem by another. When there were no polymers, there were no problems with their application. However, history and progress do not stop, and we should solve new problems connected with using polymers in engineering, life, agriculture, and medicine.

The important problems are the stability of polymeric materials, prolongation of their reliable operating time, predicting the service life of polymeric materials, and the recycling and utilization of polymers. To solve these problems, it is necessary to study the processes of polymer degradation, namely, thermal degradation, oxidation, ozonolysis, photo-ageing, radiolysis, hydrolysis, biodegradation, and mechanical degradation.

Mention should be made of the outstanding scientists working in this area: Alexandr S. Kuz'minskii (Rubber Research Institute, Moscow, Russia), Norman Grassie (Glasgow University, Scotland, UK), Ian McNeill (Glasgow University, Scotland, UK), Georges

Geuskens (Universite de Libre de brusel, Belgium), Rainer Wolf (Sandoz Company, Hunige, Elsas, France), Paul Edwin Stott (Uniroyal Chemical Company, Middlebury, CT, USA), Gerald Scott (Aston University, Birmingham, UK), Moisei B. Neiman (Institute of Chemical Physics, Moscow, Russia), Nikolai M. Emanuel (Institute of Chemical Physics, Moscow, Russia), Frank Mayo (Stanford Research Institute, Palo Alto, CA, USA), Glenn Russel (Iowa State University, Amis, IO, USA), Keith Ingold (National Research Council of Canada, Ottawa, Ontario, Canada), Eli M. Pearce (Brooklyn Polytechnic University, Brooklyn, NY, USA), Herman Mark (Brooklyn Polytechnic University, Brooklyn, NY, USA), Herbert Morawets (Brooklyn Polytechnic University, Brooklyn, NY, USA), Tsutomo Kagya (Kyoto University, Kyoto, Japan) and Ferenz Tüdos (Institute of Chemistry, Budapest, Hungary).

One of the major problems is ascertainment of the mechanism of interaction of polymers with air pollutants, for example, with nitrogen oxides. This monograph is devoted to this matter. The results obtained in studies of the interaction of polymers of different classes with nitrogen oxides are presented. Special attention is given to investigations carried out by electron spin resonance (ESR) spectroscopy, permitting us to draw conclusions from the structure of nitrogen-containing macroradicals on the mechanism of the free-radical stages of the polymer degradation process involving nitrogen oxides. The use of reactions of nitrogen oxides with polymers for obtaining spin-labelled macromolecules is also noteworthy. The stable nitrogen-containing radicals generated in this way can be used for investigations of the molecular dynamics of macromolecules. The capability of nitrogen trioxide for cross-linking of polyvinylpyrrolidone in photo processes provoked our intention to write this book. It is quite possible that hydrogels obtained in this way can serve as specific sorbents for medical use. The interaction of polymers with nitrogen oxides is therefore not only degradation, but sometimes a purposeful modification of polymers.

This monograph has seven chapters. The first chapter is devoted to consideration of the properties of stable aminoxyl radicals, their application in the polymer chemistry, and for investigations of molecular dynamics and the physical structure of polymers. In the second chapter, the classification of polymers differing in stability toward aggressive gases including nitrogen dioxide based on performed chemical and physical-chemical researches. In Chapters 3–6, the effect of nitric oxide, nitrogen dioxide and nitrogen trioxide on various polymers and model low-molecular compounds are discussed. These gases are most important for reactions with polymers because they form eight known nitrogen oxides thought to be air pollutants. The final chapter is concerned with features of the oxidative ion-radical mechanism of interaction of polymers with diamagnetic nitrogen dioxide dimers in the form of nitrosyl nitrate.

The monograph will be useful to scientists, engineers, students and postgraduate students working in the field of chemistry and physics of polymers.

E. Ya. Davydov

I. S. Gaponova

G. B. Pariiskii

T. V. Pokholok

G. E. Zaikov

Contents

Introduction

The mechanism of the influence of atmospheric pollutants on structural materials (specifically polymers) has attracted interest since the 1950s. It was recognised that increasing amounts of discharge from industrial and transport of aggressive compounds such as sulphur oxides, chlorine, hydrocarbons, nitrogen oxides, and ozone give rise to acid rain and smog, which can cause deterioration of polymeric materials. Studies of the kinetics and mechanism of reactions initiated by nitrogen oxides are important for predicting the behaviour of polymeric materials in various service conditions. The concentrations of nitrogen oxides in the atmosphere are from 10^{-9} mol/l to 10^{-8} mol/l. At such low concentrations, the rates of reactions of nitrogen oxides in natural conditions are extremely low. Therefore, these reactions are usually studied at the concentrations of the gases which are several orders of magnitude higher than their atmospheric concentrations, and the results obtained under these conditions, as a rule, extrapolated to the atmospheric concentrations. However, such extrapolation should be done with precaution because the contributions of separate stages to the overall degradation process under accelerated tests can differ from those in natural conditions. In addition, the ageing process due to other factors (thermal, photo-oxidation, ozone) can compete with the reactions involving nitrogen oxides.

Nitrogen oxides are widely used in synthetic organic chemistry and can be successfully applied for chemical modification of high-molecular compounds, for instance, grafting stable nitrogen-containing radicals to macromolecules. For preparation of spin-labelled macromolecules, various synthetic methods are applied. These complicated methods are based, as a rule, on the interaction of stable aminoxyl radicals or their precursors with functional groups of polymers, or the acceptance of spins by nitroso compounds and nitrones. However, as shown in recent years, spin-labelled macromolecules can be obtained in the reactions of polymers of various classes with nitrogen oxides. The generation of spin labels takes place in this case as consecutive process, including formation and conversion of specific intermediate molecular products and active free radicals. If the polymers are capable of reacting with nitrogen oxides, the formation of stable radicals takes place spontaneously or by thermolysis of the molecular products of nitration. Thus, the detection of stable radicals provides also a possibility of ascertainment of the mechanism of the free-radical stages of polymer ageing under the action of nitrogen oxides.

The studies of the initiating reaction mechanism and of the dependence of nitrogen oxides reactivity on specific interactions with functional groups of macromolecules are of particular importance. For an understanding of the reaction mechanism, the detection of primary radical species of substrate molecules is of special interest. The results of the latest investigations relating to this problem are considered in this monograph.

1 Classification of Polymers with respect to Reactivity toward Nitrogen Oxides

A general review of the influence of pollutants on polymers has been presented by Jellinek and co-workers [1]. Therein the characterisation of the reactivity of polymeric materials toward aggressive gases is given. Various polymers were used as films of 20-μm thickness. In most cases, the thickness is sufficiently small to exclude diffusion as the determining factor of pollutant action. Films were investigated under different conditions:

- pollutant action;
- oxygen (O_2) action;
- UV-light action;
- UV-light and oxygen;
- UV-light, oxygen and pollutants.

For nitrogen dioxide (NO_2), the exposure of samples was usually realised under a pressure of 15 mm Hg during 30 hours at 308 K. However, in the case of Nylon 66 and butyl rubber, NO_2 pressure was lowered to 1 mm Hg during 30 minutes. Polyisoprene and polybutadiene were exposed to NO_2 during 5 minutes under a pressure of 1 mm Hg. As a light source ($\lambda > 290$ nm), a mercury lamp was used. The intrinsic viscosity of polymer solutions was measured before and after exposure of samples in the chosen conditions. The high concentration of NO_2 in these situations was used to confirm that certain effects could be observed for a reasonable time.

Polymers can be divided into two main classes on the basis of their reactivity to NO_2 [1]. Saturated polymers such as polyethylene (PE) and polypropylene (PP) belong to the first group, but Nylon 66 does not. The second group covers elastomers. Butyl rubber (BR) undergoes scissions of the main chain, and polybutadiene is extensively cross-linked under the action of NO_2. These elastomers have approximately the same reactivity to NO_2 as to ozone. All films exposed to NO_2 become yellow, and their infrared (IR) spectra show that nitro groups enter into macromolecules. In polyvinylchloride in the presence of NO_2, a decrease in the amount of chlorine, along with the appearance of nitro and nitrite groups, are observed from IR spectra.

It is the author's opinion [1] that some estimations concerning the effects of low concentrations of nitrogen dioxides in the atmosphere ($2 \cdot 10^{-9}$–$2 \cdot 10^{-8}$ mol/l) on polymeric materials can be obtained from using gas concentrations of several orders of magnitude higher. The formulated assumption says that there is linear dependence of the concentration effect of aggressive pollutants. This means that the effect of aggressive gases at low concentrations can be determined by the linear extrapolation of results obtained under the influence of high concentrations. The author pointed out that this procedure contains an element of risk because scissions of macromolecules in some cases are not always linearly decreased with the pressure reduction of the aggressive gas, but the rate of breaks can change drastically at very low concentrations.

Extrapolation was used for estimation of the scission average number $\overline{S}$ under the action of aggressive gases at concentrations of 1–5 ppm within 1 hour [1]. This value is given by the equation:

$$\overline{S} = \frac{DP_{n,0}}{DP_{n,t}} - 1 \tag{1.1}$$

where $DP_{n,0}$ and $DP_{n,t}$ are lengths of macrochains at $t = 0$ and t, correspondingly. On the basis of these estimations, it was concluded that aggressive gases, for instance NO_2 and sulphur dioxide (SO_2), have a slight effect on vinyl polymers in concentrations readily available in polluted air. Even in combination with UV light, deterioration of these polymers is hardly noticeable. However, Nylon 66 is subjected to the action of small concentrations of NO_2 with essential degradation.

1.1 Interaction of Carbon-chain Polymers with NO_2

Pioneering studies of the reaction of NO_2 with PE and PP have been carried out by Ogihara and co-workers [2, 3]. Using IR spectroscopy, they found that NO_2 cannot abstract secondary and tertiary hydrogen atoms from PE and PP at 298 K. It can only add to the vinylene and vinylidene units that are formed in the synthesis of the polymers. These reactions resulted in dinitro compounds and nitro nitrites:

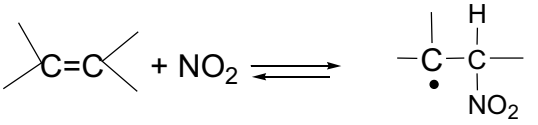

(1.2)

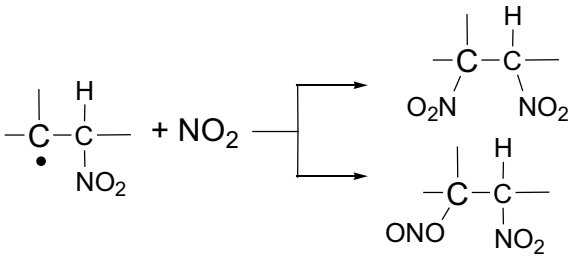

(1.3)

(1.4)

At $T > 373$ K, nitro, nitrite, nitrate, carbonyl and hydroxy groups are formed in these polymers. The following reaction mechanism at high temperatures was proposed:

$$RH + NO_2 \rightarrow R^{\bullet} + HNO_2 \quad (1.5)$$

$$R^{\bullet} + NO_2 \rightarrow RNO_2 \quad (1.6)$$

$$R^{\bullet} + ONO \rightarrow RONO \quad (1.7)$$

$$RONO \rightarrow RO^{\bullet} + NO \quad (1.8)$$

$$RO^{\bullet} + NO_2 \rightarrow RONO_2 \quad (1.9)$$

$$RH + RO^{\bullet} \rightarrow R^{\bullet} + ROH \quad (1.10)$$

$$\sim CH_2\text{-}CH_2\text{-}CH_2\text{-}O^{\bullet} \rightarrow \sim CH_2\text{-}CH_2\text{-}CHO + H \quad (1.11)$$

This scheme allows rationalisation of the accumulation of nitro groups (which proceeds at a constant rate) and auto-accelerated formation of nitrates, alcohols and carbonyl compounds.

However, it provides no explanation for the *S*-shaped dependence of the accumulation of nitrites. The activation energies for the NO_2 addition to the double bonds of PE are 8–16 kJ/mol. The activation energy for hydrogen abstraction is within 56 and 68 kJ/mol for PE, and 60 kJ/mol for PP.

At room temperature and at NO_2 concentrations of 5.4×10^{-4} to 5.4×10^{-3} mol·l^{-1}, the characteristics of PE, PP, polyacrylonitrile and polymethylmethacrylate are changed only slightly even if they simultaneously undergo the combined action of NO_2, O_2 and UV radiation [4]. Reactions of NO_2 with polyvinylchloride and polyvinyl fluoride resulted in a slight decrease in the content of chlorine and fluorine atoms, respectively [1, 4].

In the temperature range 298–328 K, NO_2 (7.8×10^{-3} to 3.4×10^{-2} mol/l) can abstract tertiary hydrogen atoms from polystyrene (PS) molecules to introduce nitro and nitrite groups into macromolecules in subsequent reactions [1]. This process proceeds at low rates and is accompanied by chain scissions [1, 5, 6]. The effect of the number of chain scissions on time $\alpha(t)$ was determined from intrinsic viscosity using Equation (**1.1**). Experiments have been carried out at 298–328 K. According to Jellinek, dependence of the decrease in the degree of polymerisation of PS on exposure time in NO_2 has three linear regions: initial, middle and final. A decrease in the apparent degradation rate was observed in the middle region of the dependence. Presumably this was related to the association of the macromolecules in solution, which is due to the effect of polar groups and can affect the results of viscosimetric measurements. Subsequent increase in the apparent degradation rate was attributed to the consumption of these nitrogen-containing groups and to a decrease in the degree of association of the macromolecules. PS films were also simultaneously exposed to NO_2 (1.1×10^{-4} mol/l) and light ($\lambda > 280$ nm) [6]. No polymer degradation was observed in the initial stage during 10 hours; chain scission then occurred at a constant rate.

An attempt to determine the quantitative characteristics of the ageing of PS and poly-*t*-butylmethacrylate (PTBMA) under the action of NO_2 has been undertaken by Huber [7]. Samples were exposed to a stream of air containing NO_2 (2.5×10^{-6} to 3.7×10^{-5} mol/l) at 300 K and simultaneously irradiated with light (λ>290 nm). The number of chain scission per 10,000 monomer units $\alpha(t)$ can be described by the empirical equation:

$$\alpha = \frac{P}{Q}(\exp Qt - 1) \tag{1.12}$$

where P and Q are constants. This equation describes an autocatalytic process. At $Q \rightarrow 0$, degradation occurs at a constant rate. The autocatalytic process is more pronounced for thin films. Degradation of thin PS films under the same conditions occurs slower than that of PTBMA films, and its autocatalytic nature is more pronounced.

The autocatalytic path of degradation of PTBMA was associated [7] with the photo-induced formation of isobutylene, which reacts with NO_2, thus initiating free-radical degradation processes of macromolecules. The IR spectrum of PS exposed to NO_2 and light exhibits two bands at 1686 cm^{-1} and 3400 cm^{-1} corresponding to carbonyl and hydroxyl groups, respectively. The formation of nitrogen-containing products has not been observed in PTBMA and PS. The following reactions have been proposed [7] in PS:

$$\sim CH_2{-}C(Ph)H \sim + NO_2 \rightarrow HNO_2 + \sim CH_2{-}C^{\bullet}(Ph) \sim \ (R_1^{\bullet}) \tag{1.13}$$

$$R_1^{\bullet} + O_2 \rightarrow R_1O_2^{\bullet} \tag{1.14}$$

$$R_1O_2^{\bullet} + RH \rightarrow ROOH + R_1^{\bullet} \quad (1.15)$$

$$R_1^{\bullet} + NO_2 \rightarrow R_1NO_2 \quad (1.16)$$

$$R_1^{\bullet} + NO_2 \rightarrow R_1ONO \quad (1.17)$$

$$R_1ONO \xrightarrow{h\nu} R_1O^{\bullet} + NO \quad (1.18)$$

$$R_1OOH + NO \rightarrow R_1O^{\bullet} + {}^{\bullet}OH + NO \quad (1.19)$$

$$R_1OOH \xrightarrow{h\nu} R_2^{\bullet} + {}^{\bullet}OH \quad (1.20)$$

$$R_1O^{\bullet} \rightarrow R_2^{\bullet} + \text{degradation products} \quad (1.21)$$

It is believed that the decomposition of hydroperoxides exposed to NO_2 and light leads to autocatalytic degradation of PS.

1.2 Interaction of Rubbers with NO_2

Rubbers are much more susceptible to NO_2 than polymers containing no double bonds. First, this is due to the ability of NO_2 to add reversibly to carbon-carbon double bonds to give nitroalkyl radicals (reaction (1.2)), thus initiating free-radical conversions of elastomers. Second, NO_2 can abstract hydrogen atoms in the β-position to the double bond to give allyl radicals, which then recombine with NO_2 [8]. Depending on the structure of the alkene, the reaction resulting in the formation of the allyl radical can be weakly exothermic or weakly endothermic. For instance, the strength of the weakest C–H bond in the structure $CH_2=C(CH_3)CH_2–H$ is only 314 kJ/mol [9].

The exposure of polyisoprene and polubutadiene to NO_2 leads to degradation and cross-linking of macromolecules, whereas BR (a copolymer of 36% isobutylene and 54% isoprene units) only undergoes degradation [10]. Detailed study of ageing BR exposed to NO_2 (5.2×10^{-7} to 5.2×10^{-5} mol/l) alone, and a NO_2–O_2 mixture and a NO_2–O_2 mixture plus UV light ($\lambda > 280$ nm) at 298–358 K has been done by Jellinek and co-workers [11, 12]. IR spectra before and after exposure of samples showed that the band at 1540 cm^{-1} of ~ C=C ~ bonds disappears, and a new band at 1550 cm^{-1} arises. The latter belongs to nitro groups appearing as a result of addition to double bonds by the reaction (1.2).

The chain scission process in BR is caused by the following scheme:

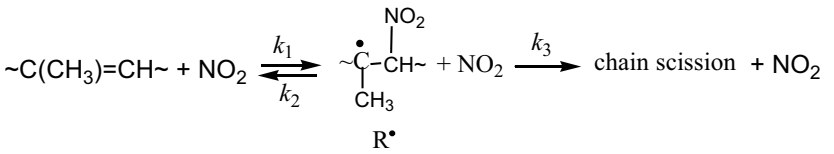

(1.22)

Then the rate of scission is:

$$-\frac{d[n']}{dt} = k_3[R^{\cdot}][NO_2] \tag{1.23}$$

where n' is a number of isoprene units in BR. After integration of (1.23) taking into account a stationary concentration of R•, the following equation for the degradation degree is derived:

$$\alpha = \frac{k_1 k_3 [n']_0 [NO_2] t}{[n]_0 (k_2 + k_3 [NO_2])} \tag{1.24}$$

where $[n']_0$ and $[n]_0$ are the initial concentrations of isoprene units and all units. The amount of double bonds remains practically constant because only a few double bonds are destroyed. Only 1/50 of macromolecules of BR are subjected to scissions. Taking into account low concentrations of NO_2, the linear dependence on time is obtained:

$$\alpha = k_{exp} t \tag{1.25}$$

where k_{exp} is the experimentally determined constant. This constant is represented by the following Arrhenius equation: $k_{exp} = 3.8 \cdot 10^{-2} e^{-7450/RT}$, h^{-1}.

BR degradation in a polluted atmosphere runs in three directions:

- action of NO_2 alone;
- action of O_2;
- combined (synergetic) action of these gases.

The general scheme of the process can be represented as follows:

$$RH + O_2 \xrightarrow{k_4} R^{\bullet} + HO_2 \tag{1.26}$$

$$R^{\bullet} + O_2 \xrightarrow{k_5} RO_2^{\bullet} \tag{1.27}$$

$$RO_2^{\bullet} + RH \xrightarrow{k_6} ROOH + R^{\bullet} \tag{1.28}$$

$$ROOH \xrightarrow{k_7} \text{stable products} \tag{1.29}$$

$$ROOH \underset{k_9}{\overset{k_8}{\rightleftharpoons}} [\text{cage}_1] + O_2 \xrightarrow{k_{10}} \text{chain scission products} + O_2 \tag{1.30}$$

The effect of $NO_2 + O_2$:

$$ROOH + NO_2 \xrightarrow{k_{11}} NO_2\text{–}ROOH \tag{1.31}$$

$$NO_2\text{-}ROOH \underset{k_{13}}{\overset{k_{12}}{\rightleftharpoons}} [\text{cage}_2] \xrightarrow{k_{14}} \text{chain scission products} \tag{1.32}$$

$$2\,R^{\bullet} \xrightarrow{k_{15}} [\text{cage}_3] \tag{1.33}$$

$$[\text{cage}_3] + O_2 \xrightarrow{k_{16}} 2\,R^{\bullet} \tag{1.34}$$

$$[\text{cage}_3] \xrightarrow{k_{17}} R\text{–}R \tag{1.35}$$

The synergetic action of NO_2 and O_2 can be seen from the scheme:

$$\sim CH_2C(CH_3)=CHCH_2CH_2\sim + O_2$$
$$\rightarrow \sim CH_2C(CH_3)=CHCH(OO^{\bullet})CH_2\sim + HO_2^{\bullet} \tag{1.36}$$

$$\sim CH_2C(CH_3)=CHCH(OO^{\bullet})CH_2\sim + RH$$
$$\rightarrow \sim CH_2C(CH_3)=CHCH(OOH)CH_2\sim + R^{\bullet} \tag{1.37}$$

$$\sim CH_2C(CH_3)=CHCH(OOH)CH_2\sim + NO_2$$

$$\rightarrow \sim CH_2C(CH_3)=C(NO_2)CH(OOH)CH_2\sim \qquad (1.38)$$

BR is not sensitive to UV light ($\lambda > 290$ nm) alone. UV light in the presence of NO_2 probably affects the nitro groups of macromolecules.

1.3 Interaction of NO_2 with Aliphatic Polyamides and Polyurethanes

Polymers containing amide groups and urethane groups form a particular class of materials sensitive to NO_2. Jellinek and co-workers [13, 14] showed that exposure of Nylon 66 films of different morphology to NO_2 (10^{-5} to 2.6×10^{-1} mol/l) causes main-chain scission in the polymers. The degradation of Nylon is a diffusion-controlled reaction. Its rate and depth depend essentially on the degree of crystallinity of samples and on the size of crystallites. Degradation is accelerated in the presence of air and UV light in addition to NO_2. The following mechanism for polymer degradation under the action of NO_2 was proposed:

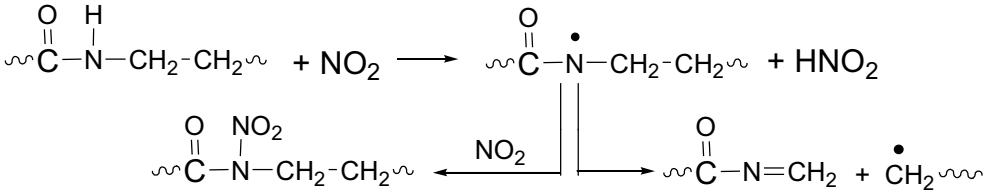

(1.39)

The degradation process is inhibited by small amounts of benzaldehyde or benzoic acid. It is believed that these compounds block the amide groups and that only a few of them (the ones not involved in hydrogen bonding) enter into the reaction:

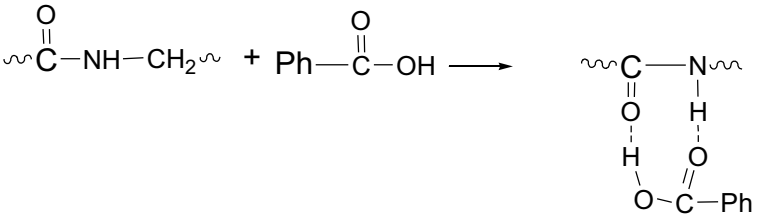

(1.40)

Jellinek and co-workers [14, 15] studied the effect of NO_2 on films of linear polyurethane synthesised from tetramethylene glycol and hexamethylene diisocyanate. It was found that the degradation of polyurethanes is accompanied by cross-linking of macromolecules, and that the degree of degradation and yield (weight percentage)

of the gel fraction are complex functions of the exposure time. For instance, the yield of gel fraction initially increases up to 20%, and then decreases down to nearly zero at 330 K and NO_2 concentration of 0.001 mol/l. The number of chain scissions in the sol fraction (degree of degradation) increases initially, then decreases and eventually increases again; however, the final degradation rate is lower than the initial one. Exposure of the polyurethane films to NO_2 is accompanied by release of carbon dioxide (CO_2). The IR spectra of the films allow assessment of the consumption of NH bonds (ν = 3300 cm^{-1}).

The reaction mechanism proposed [15, 16] involves the abstraction of hydrogen atoms from two types of structures: a carbamate structure (A) and a tertiary amide structure (B):

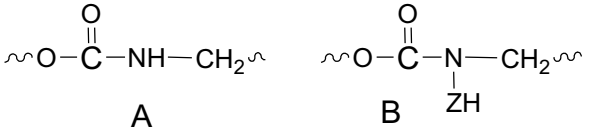

where Z is a side alkyl group. The next stages are represented as follows:

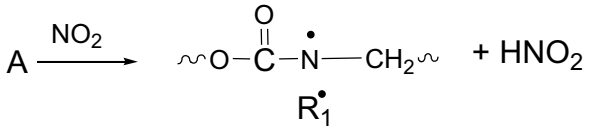

(1.41)

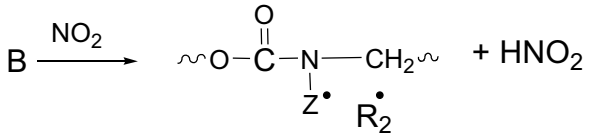

(1.42)

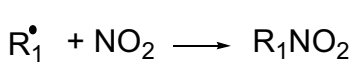

(1.43)

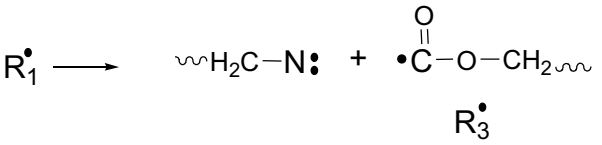

(1.44)

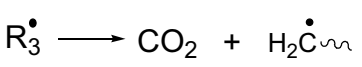

(1.45)

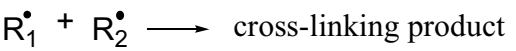

(1.46)

According to the Jellinek, recombination of $R_1^{\bullet}$ and $R_2^{\bullet}$ radicals leads to cross-linking

of the polymer chains, while decomposition of $R_1^{\bullet}$ radicals results in the degradation of macromolecules and the CO_2 release. Energetically, decomposition of the $R_1^{\bullet}$ radicals seems to be improbable because this reaction results in the formation of terminal macroradical $R_3^{\bullet}$ and a nitrene, which is a very reactive species. On the other hand, the $R_1^{\bullet}$ decomposition reaction involving cleavage of C-C or C-O bonds does not produce alkoxycarbonyl macroradicals $R_3^{\bullet}$, which can undergo decarboxylation subsequently [16]. Therefore, the ageing of polyurethanes in an NO_2 atmosphere can be represented as follows [17]:

Reaction (1.41)

Reaction (1.42)

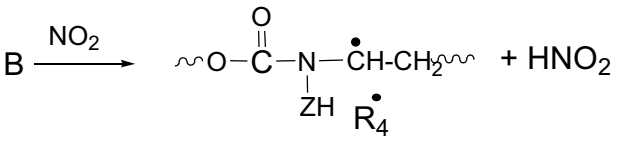

(1.47)

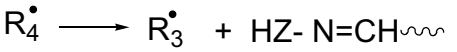

(1.48)

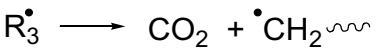

(1.49)

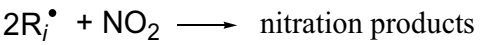

(1.50)

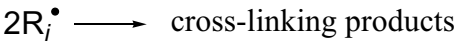

(1.51)

where i = 1–4.

This scheme expresses the degradation accompanied by cross-linking of macromolecules, the consumption of NH groups of the polymer, as well as the release of CO_2 upon degradation.

The investigations carried out earlier characterise the reactivity of different classes of polymers with NO_2. However, the mechanisms of free-radical processes proposed on the basis of the results considered are rather formal. As a rule, they take account of changing molecular weights and the composition of final molecular products of the nitration. In connection with this, the study of structures of free radicals forming in primary and intermediate stages of polymer conversions attracts special interest. Such research allows drawing conclusions on the mechanism of initiation of free-radical conversions dependent on the nature of functional groups of macromolecules. As

shown by electron spin resonance (ESR) measurements, different stable nitrogen-containing macroradicals are formed on exposure of polymers to NO_2 [17]. The analysis of the radical composition from ESR spectra allows estimation of polymer stability by a simple method.

References

1. H.H.D. Jellinek, *Degradation and Stabilisation of Polymers*, Elsevier, New York, NY, USA, 1978.

2. T. Ogihara, *Bulletin of the Chemical Society of Japan*, 1963, **31**, 58.

3. T. Ogihara, S. Tsuchiya and K. Kuratani, *Bulletin of the Chemical Society of Japan*, 1965, **38**, 978.

4. H.H.D. Jellinek in *Proceedings of The 2nd International Symposium on Degradation and Stabilisation of Polymers (Abstracts of Reports)*, Dubrovnik, Croatia, 1978.

5. H.H.D. Jellinek and Y. Toyoshima, *Journal of Polymer Science: Polymer Chemistry Edition*, 1967, **5**, 12, 3214.

6. H.H.D. Jellinek and F. Flajsman, *Journal of Polymer Science: Polymer Chemistry Edition*, 1969, **7**, 4, 1153.

7. A. Huber, *Diss Doktor Naturwiss,* Fakultät Chemie der Universität Stuttgart, Germany, 1988.

8. D.H. Giamalva, G.B. Kenion, D.F. Church and W.A. Pryor, *Journal of the American Chemical Society*, 1987, **109**, 23, 7059.

9. B. Rånby and J.F. Rabek, *Photodegradation, Photo-oxidation and Photostabilisation of Polymers*, Wiley, London, UK, 1975.

10. H.H.D. Jellinek, F. Flajsman and F.J. Kryman, *Journal of Applied Polymer Science*, 1969, **13**, 1, 107.

11. H.H.D. Jellinek and F. Flajsman, *Journal of Polymer Science: Polymer Chemistry Edition*, 1970, **8**, 3, 711.

12. H.H.D. Jellinek and P. Hrdlovi , *Journal of Polymer Science: Polymer Chemistry Edition*, 1971, **9**, 5, 1219.

13. H.H.D. Jellinek and A.K. Chandhuri, *Journal of Polymer Science: Polymer Chemistry Edition*, 1972, **10**, 6, 1773.

14. H.H.D. Jellinek, A.R. Yokata and Y. Itoh, *Polymer Journal*, 1973, **4**, 601.

15. H.H.D. Jellinek and T.J.Y. Wang, *Journal of Polymer Science: Polymer Chemistry Edition*, 1973, **11**, 12, 3227.

16. H.H.D. Jellinek, F.H. Martin and H. Wegener, *Journal of Applied Polymer Science*, 1974, **18**, 6, 1773.

17. G.B. Pariiskii, I.S. Gaponova, E.Ya. Davydov, *Russian Chemical Reviews*, 2000, **69**, 11, 985.

2 Properties and Applications of Aminoxyl Radicals in Polymer Chemistry

Free-radical reactions initiated by nitrogen dioxide (NO_2) and other nitrogen oxides in polymers are accompanied by the generation of stable nitrogen-containing radicals. Analysis of their structures and kinetics of formation provides information on the free-radical stages of complex processes of polymer nitration under various conditions [1]. These studies can be used in synthetic chemistry in particular for the development of methods of polymer modification, for example, for the preparation of spin-labelled macromolecules. The generation of spin labels thus occurs in consecutive reactions, including formation and conversions of specific intermediate molecular products and active free radicals.

Most of the traditional developing methods of preparing spin-labelled macromolecules are based on organic compounds capable of interacting with polymers to form stable aminoxyl radicals (ARs). Grafting these radicals can be carried out by means of nitroso compounds and nitrones which capture active radicals. ARs represent a vast class of stable radicals widely used in chemistry. Numerous articles and monographs are devoted to the synthesis and properties of these radicals [2, 3]. The insertion of ARs to macromolecules allows changing the physical, chemical and operational characteristics of polymers. In general, this effect is conditioned by the presence of >N–O• fragments in polymer chains, and the interaction of these radical centres with components of polymeric materials. In the present chapter, the structures and properties of ARs and the pathways of stable radical generation using organic synthesis are considered.

2.1 Structure and Physical Properties of Stable Radicals

Within the framework of resonance theory, AR structure can be represented by the following resonant structures [4]:

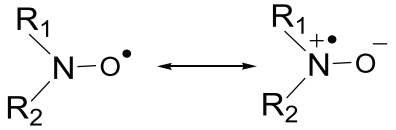

(2.1)

The schemes of electronic shell formation of the paramagnetic centre from AR and levels of the molecular orbitals of AR are respectively shown in **Figure 2.1** and **Figure 2.2**.

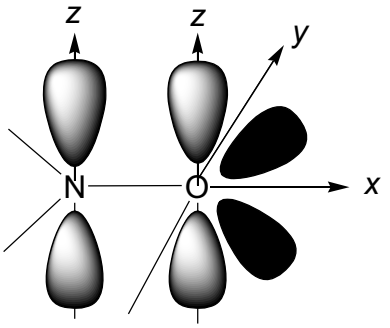

Figure 2.1 The electron shells of AR: π orbital of unpaired electron is along the *z* axis; the electron pair orbital is black

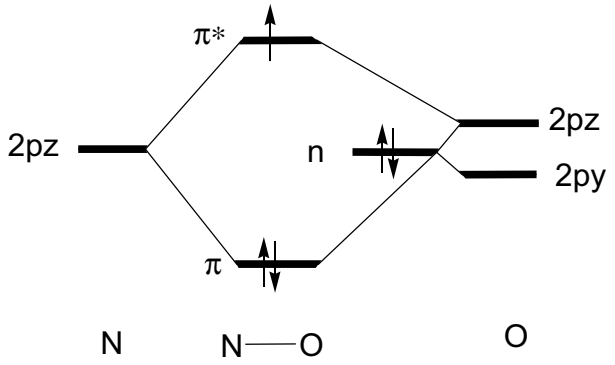

Figure 2.2 Molecular orbitals of the paramagnetic fragment of AR

The length of the N–O bond in all types of ARs is 1.27–1.30 Å. This value corresponds to the length of a three-electronic bond, i.e., for an electronic structure in which binding σ and π orbitals are occupied by electron pairs, whereas the unpaired electron occupies the nonbinding π* orbital formed by the p_z orbitals of nitrogen and oxygen atoms and is located approximately equally between them. Delocalisation of the unpaired electron between N and O atoms with lowering of its energetic level (134 kJ/mol) is the main reason for the high stability of ARs [3].

The geometrical structure of the radical centre depends appreciably on the character of the R_1 and R_2 groups. The angle between the CNC plane and the N–O bond in different radicals varies from 0° to 30° [3]. Deviation of the nitrogen atom from coplanarity does not result in energy change, but hybridisation of the nitrogen atom determines the characteristics of electron spin resonance (ESR) spectra of ARs. Most ARs do not form dimers > N–O–O–N < in a wide range of temperatures and various solvents [5]. AR dimerisation is a thermodynamically inefficient process connected with loss of the stabilisation energy of two radical fragments.

ARs have two absorption bands in their electronic spectrum. Di-*t*-alkylaminoxyls have bands at 240 nm (ε = 3000 l/mol/cm) and at 410–460 nm (ε = 5 l/mol/cm). The first is caused by a $\pi \rightarrow \pi^*$ transition, the second belongs to a $n \rightarrow \pi^*$ transition (**Figure 2.2**). Because of conjugation of an aromatic ring with aminoxyl groups, the bathochrome shift occurs for absorption bands. Shifts up to 335–340 nm and 490–510 nm are observed for diarylaminoxyls [3]. The vibration frequencies of ARs should appear in IR spectra at 1340–1370 cm^{-1} [3]. Unfortunately, bands in this region are frequently connected with vibrations of alkyl groups. According to studies of solid IR, solution IR, and the Raman spectra of 1,1,3,3-tetramethylisoindolin-2-yloxyl radicals [6], the N–O• stretching frequency is 1431 cm^{-1}. This apparently anomalous peak position was confirmed by isotopic substitution studies and *ab initio* density functional theory calculations. Therefore, IR spectroscopy can be carefully applied for IR identification. The dissociation energy of the C–N bond determined by the electronic impact method is 121.5 kJ mol^{-1} [7]. The low energy makes the decay of ARs feasible due to breakage of the C–N bond under certain conditions. The ionisation potential of ARs is sufficiently high (7 eV) [8]. This enables the increased stability of ARs in reactions in which cations and radical cations are the primary active centers, i.e., in reactions induced by irradiation and oxidation.

2.2 ESR Spectroscopy of ARs

The ESR spectra of ARs are quantitatively described by spin Hamiltonian [2]:

$$H = -\beta\overline{H_0}\,\overline{g}\overline{S} + \overline{STI} \tag{2.2}$$

where β is the Bohr magneton, $\overline{H_0}$ is the external magnetic field intensity, $\overline{g}$ is g-tensor, $\overline{S}$ is the electron spin operator, $\overline{T}$ is the tensor of hyperfine interaction (HFI), $\overline{I}$ is the nuclear spin operator. Spin Hamiltonian consists of isotropic and anisotropic parts:

$$H = H_i + H_a \tag{2.3}$$

$$H_i = -\beta g \overline{H_0}\,\overline{S} + a\overline{IS} \tag{2.4}$$

$$H_a = -\beta \overline{H_0}\,\overline{g'S} + \overline{ST'I} \tag{2.5}$$

where g and a are isotropic values of g-factor and HFI constant. They are determined by the following equations:

$$g = 1/3(g_x + g_y + g_z) = 1/3r\overline{g'} \tag{2.6}$$

$$a = 1/3(T_x + T_y + T_z) = 1/3r\overline{T'} \tag{2.7}$$

where $\overline{g'}$ and $\overline{T'}$ are diagonal tensors. The constituents of these tensors are connected with common $\overline{g'}$- and $\overline{T'}$- tensors by the equations:

$$g_i = g_i' + g \tag{2.8}$$

$$T_i = T_i^{'} + a \tag{2.9}$$

($i = x + y + z$)

In solutions with low viscosity, ARs are rapidly rotated with total averaging $\overline{g}$ -and $\overline{T}$ -tensors. Therefore, ESR spectra of ARs in solutions are characterised by a triplet signal with the component intensity ratio of 1:1:1 owing to interaction of unpaired electrons with the ^{14}N nucleus having $I = 1$. This triplet splits because of interactions with magnetic nuclei in α and β positions. Isotropic HFI constants a_N dependent on AR structure are given below [9]:

	a_N, mT
Dialkylaminoxyl	1.4–1.7
Alkylarylaminoxyl	1.1–1.4
Diarylaminoxyl	09–1.1
Acylaminoxyl	0.67–1.1
Alkoxyalkylaminoxyl	2.4–2.8

Alkoxyarylaminoxyl	1.3v1.5

The analysis of HFI using quantum-chemical calculations has allowed determination of the spin density ρ on N and O atoms. For example, the ρ-value in di-*t*-alkylaminoxyls is distributed practically 50-50 between N and O atoms, and an unpaired electron is almost completely located on a radical fragment [10]. In alkylaryl- and diarylaminoxyl radicals, an unpaired electron can be delocalised onto an aryl fragment with considerable decreasing ρ on N atom. Therefore, the constant of splitting a_N in these radicals is less than in dialkylaminoxyl radicals. In viscous liquids, the rotation of radicals becomes slower, and *g*- and HFI tensors are not completely averaged. As a result, HFS components are broadened out, and the high-field component shows this broadening to a greater extent. For various components ($M = 0, \pm 1$) of the AR spectrum, one can obtain the following equations for the correlation time τ of radical rotation [2]:

$$\tau' = \left(\frac{\Delta H_1}{\Delta H_0} - \frac{\Delta H_{-1}}{\Delta H_0} \right) \frac{15\pi\sqrt{3}\Delta H_0}{8Hb\Delta\gamma} \tag{2.10}$$

$$\tau'' = \left(\frac{\Delta H_1}{\Delta H_0} - \frac{\Delta H_{-1}}{\Delta H_0} - 2 \right) \frac{4\pi\sqrt{3}h}{8\beta b^2} \tag{2.11}$$

where ΔH_i is the width of components M_i, $b = 2/3[T_2 - 1/2(T_x + T_y)]$ and $\Delta\gamma = \frac{\beta}{h}[g_z - 1/2(g_x + g_y)]$

The equations (**Equation 2.10**) and (**Equation 2.11**) are valid for = 5 ×10^{-11} to 5 ×10^{-9} s. The correlation time is connected with the radius of rotating molecules and viscosity of the solvent η by the Stokes equation:

$$\tau = \frac{4\pi\eta r^3}{3kT} \tag{2.12}$$

For determining τ in the range of slow movements (τ > 5 × 10^{-9} s), the dependence of τ on shift of the high-field line Δ relative to its position in the ESR spectrum can be used [11]:

$$\Delta = \text{const} \cdot \tau^{3/2} \tag{2.13}$$

Using the equation (**Equation 2.13**) one can calculate τ in the range of 5 × 10^{-9} to 5 × 10^{-7} s, and use these values in studies of the rotational diffusion of macromolecules.

The correlation time can be expressed as a function of the parameter $S = A_z' / A_z$ where A_z' is half of distance between extremes of the outside lines of the triplet ESR spectrum and A_z is the same value in conditions of extremely slow movements of ARs [12]:

$$\tau = a(1 - S)^b \tag{2.14}$$

where *a* and *b* depend on the diffusion model. The equation (**Equation 2.14**) is convenient for using in the range of $10^{-8} < \tau < 10^{-6}$

2.3 Chemical Properties of ARs

The stability of ARs is conditioned by tautomeric conversions and depends on the chemical structure of substituents at the N atom, temperature and solvent [5, 9]. The general mechanism of AR decay is a disproportionation reaction with formation of nitrones and hydroxylamines. ARs having primary or secondary alkyl groups are short-lived species because they easily undergo disproportionation by the scheme:

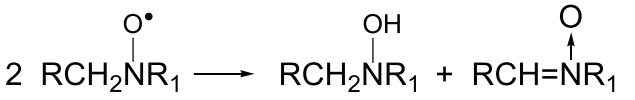

(2.15)

In several cases, the arising products, for example, hydroxylamines, can be effective acceptors of short-lived radicals. They are readily oxidised by nitroso compounds, ARs, oxygen or other oxidisers which accumulate as a result of side reactions. In this case, one can observe the post-accumulation of radical adducts [13, 14].

Nitrones formed by reaction (2.15) represent spin traps and can accept ARs. In some cases, such adducts can be more stable than radical adducts of the initial generation, so only adducts of the second and third generations will be observed in ESR experiments. ARs of high stability are formed when the nitrogen is connected with the tertiary carbon atom and the disproportionation is excluded [3]. Such radicals are, for example, di-*t*-butylaminoxyl (1), derivatives of 4,4-dimethyloxazolidineoxyl (2), 2,2,5,5,-tetramethylpyrrolinoxyl (3) and derivatives of piperidine-1-oxyl (4).

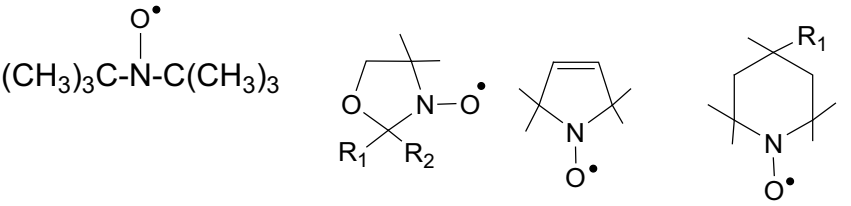

(I) (II) (III) (IV)

Changes in the structure of nitrogen substituents make ARs susceptible to dimerisation. In such a case the electron delocalisation degree increases and, hence, an opportunity appears for reactions via other centers. *Tert*-butylphenylaminoxyl (V) is much less stable than radical (I) due to unpaired electron delocalisation to an aromatic ring. Delocalisation enables an attack of the *p*-position of the phenyl ring by a second AR:

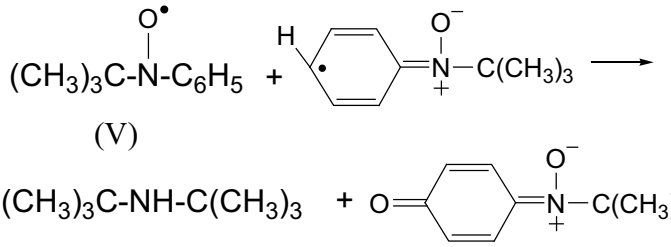

(V)

(2.16)

Although the mechanisms of decay of ARs of this type in different, they always include attack of aminoxyl groups to the *o*- or *p*- positions of aromatic rings. The *o*-substituents stabilise ARs owing to violation of the coplanarity and the decrease of spin density in an aromatic ring [15]. The bulky substituents in *p*- and *m*- positions also stabilise ARs (as in this case) because steric hindrances arise for radical attack [16]. The triphenyl-*t*-butylaminoxyl (VI) decays in an unusual way. The spatial strain of the radical centre results in N–C dissociation in ARs [17]:

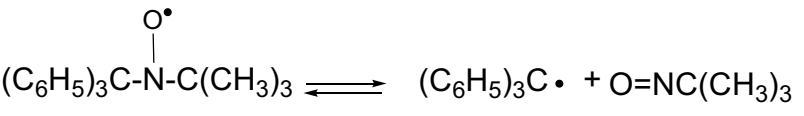

(VI)

(2.17)

Solvents essentially influence the decay rate. Rate constants in polar solvents are less because of AR blocking due to formation of hydrogen bonds with solvents. In conditions where hydrogen-atom abstraction from surrounding molecules is difficult, aminoxyls are stable up to 200–220 °C [18]. ARs can accept one radical with the formation of diamagnetic compounds:

$$N{-}O^{\bullet} + R^{\bullet} \rightarrow >N{-}O{-}R \qquad (2.18)$$

The rate constants of reactions of ARs with solvated electrons, H atoms, $OH^{\bullet}$, and $CH_3^{\bullet}$ amount to 10^9–10^{10} l/mol/s, and 10^8·l/mol/s with the radical $C^{\bullet}HOH$ [19]. This property of ARs serves as the basis for their use as 'counters' of radicals. The unique property of ARs is their ability to react without participation of unpaired electrons with retention of paramagnetism. Such reactions are widely used for synthesis of new ARs with various substituents [3], for synthesis of metalorganic radicals containing Tl, Hg, and Fe. [20]. In this way, polyradicals were obtained in which paramagnetic fragments were interconnected in a uniform molecular system [21]. These reactions represent a method of spin labels used in chemistry, biochemistry and molecular biology [22].

The properties of ARs as oxidisers can be shown by their interaction with hydrocarbons [23]:

$$>N{-}O^{\bullet} + RH \rightarrow >N{-}OH + R^{\bullet}$$

$$>N{-}O^{\bullet} + R^{\bullet} \rightarrow >N{-}OR \qquad (2.19)$$

By the voltammeter method, ionisation potentials of oxidation of several ARs were measured in acetonitrile [24]. It was concluded that strong oxidisers are required for AR oxidation. Bromine and chlorine easily and quantitatively oxidise ARs into reactive oxoammonium salts [25, 26]. Stable diarylaminoxyls under the action of halogens also form oxoammonium salts, and the ease of oxidation of the radicals is determined by the nature of the substituents:

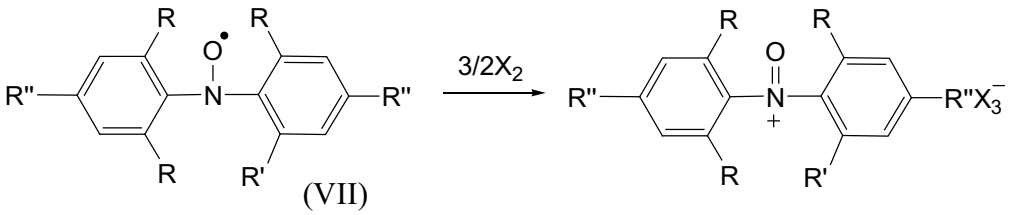

(VII)

(2.20)

If R = R′ = H, R″ = OCH_3, then radical VII is oxidised by bromine. In the case of R = R′ = R″ = OCH_3, radical VII is readily oxidised (even by iodine). The basic products of the vigorous reaction of radical I with ozone are nitro-*t*-butane and oxygen [27]. The oxidation of alcohols into carbonyl compounds can be carried out via the interaction of piperidinoxyl with copper (II) [28]:

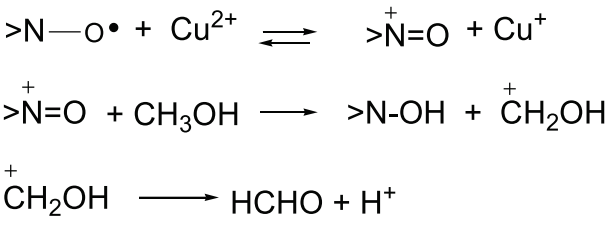

(2.21)

Under the action of strong acids, the protonation of ARs takes place [3]:

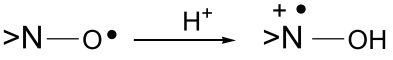

(2.22)

The protonation of ARs is the first stage of their interaction with mineral acids, which results in the products of disproportionation [29]:

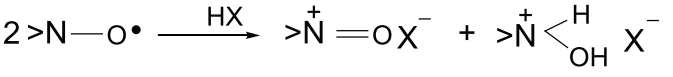

(2.23)

The ARs of piperidine, hydrogenated pyrrole and nitronylaminoxyls disproportionate. Aminoxyls also disproportionate under the action of allyl and benzyl bromide by the following scheme [30]:

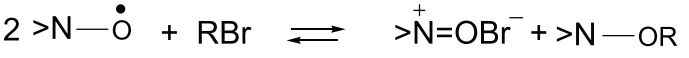

(2.24)

Along with reactions without the participation of the radical centre, ARs react as typical radicals. At elevated temperatures, they abstract hydrogen atoms, chlorine, bromine and other elements. There are examples of sufficiently reactive ARs in H-atom abstraction at standard temperatures. The benzotriazole-*N*-oxyl (BTNO) generated by the oxidation of 1-hydroxybenzotriazole (HBT) with a Ce^{IV} salt in acetonitrile spontaneously decays with a first-order rate constant of 6.3×10^{-3} s^{-1} at room temperature [31]. The decay of this aminoxyl is strongly accelerated in the presence of H-donor substrates such as alkylarenes, benzyl and allyl alcohols:

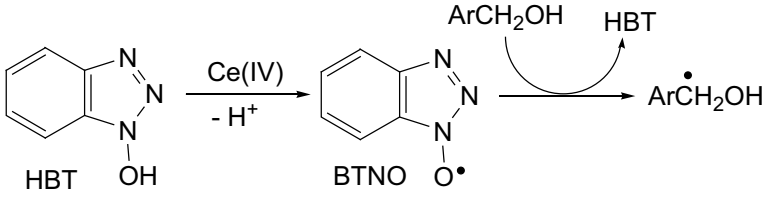

(2.25)

The kinetic isotope effect confirms the H-abstraction step to be rate-determining.

ARs recombine with many radicals participating in chain chemical reactions and add to multiple bonds. Dialkylaminoxyl radicals actively react with alkyl radicals [5, 32], sulphur-containing radicals [33], solvated electrons and with radicals generated by the γ-radiolysis of organic compounds [34]. ARs recombine with hydroxyl radicals, but do not react with $HO_2^{\bullet}$ radicals [35].

As distinct from dialkylaminoxyl radicals, aromatic ARs react with peroxide radicals [36]. If alkyl radicals or hydrogen atoms participate in reactions, the basic products of such reactions are the corresponding ethers and hydroxylamines [34]. Hydroxyalkyl radicals are captured by ARs [34] with the formation of unstable ethers, which decompose to yield the aldehyde and hydroxylamine:

$$>N-\dot{O} + \dot{C}H_2OH \longrightarrow >N-O-CH_2OH \longrightarrow >N-OH + CH_2O \qquad (2.26)$$

ARs are useful 'counters' of active alkyl radicals [37] and inhibitors of radical polymerisation [38]. Aliphatic and aromatic ARs have approximately identical inhibition. These radicals are similar to quinines, and are considerably stronger radical inhibitors than nitroso compounds. The comparison of reactivity of spin traps and ARs shows that ARs are 2–5 orders of magnitude more effective radical acceptors than nitrones and nitroso compounds. Therefore, new effective acceptors of radicals are generated already at the early stages of short-living radical trapping.

Calculations in the framework of density functional theory [39] for the model AR $H_2NO^{\bullet}$ indicate that addition to the carbonyl carbon is exothermic by 18.7 kcal/mol [40]. This prediction was tested experimentally in reactions of AR IV with ketenes [41]. In this case, a facile reaction occurred. On the basis of theoretical as well as kinetic and product studies, the reactions were interpreted as proceeding through attack of one IV at the carbonyl carbon, forming an α-acyl radical intermediate. Then the intermediate radical reacts with another IV at C_β:

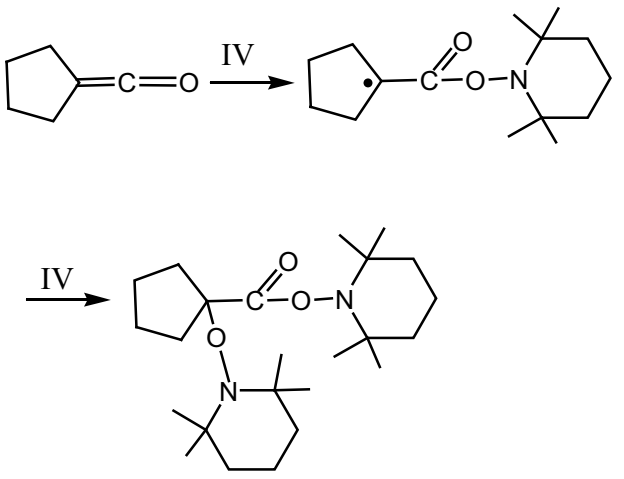

(2.26)

The adducts of ARs with organic free radicals have attracted considerable attention because of their potential utility as free radical initiators, and because of the important role of reversible dissociation of adducts of IV in living radical polymerisation.

This wide development is observed in the study of the participation of ARs in various photochemical reactions, and the phototransfer of electrons and electronic energy. For some radicals the basic process is dissociation with the detachment of nitric oxide, whereas other types of ARs mainly abstract hydrogen atoms from solvents. The quantum yield of such process is very high (~0.5) [42]. Di-*t*-alkylaminoxyls are poorly stable under exposure to UV light. The photolysis of radical IV (R_1 = OH) by light with λ = 350 nm in toluene completely converts them into equal quantities of hydroxylamine and benzyl ether of hydroxylamine [43]. Thus, the capability of some excited ARs to abstract a hydrogen atom with the subsequent recombination of formed radicals and ARs provides a method of the functionalisation of macromolecules.

The radical III (R=$CONH_2$) decays during photolysis with breakage of N–C bonds [44]:

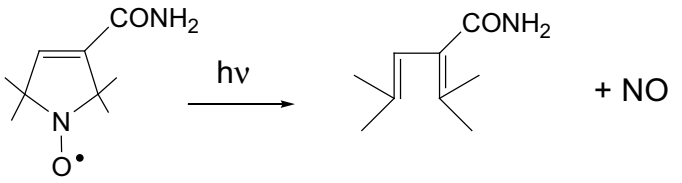

(2.27)

The photochemical transformations of ARs depend not only on the type of radical, but also on the chemical properties of the solvent [42, 45]. Radical I in pentane

dissociates with the detachment of *t*-butyl groups during photolysis by light with $\lambda < 300$ nm in the band of $\pi \rightarrow \pi^*$ transitions:

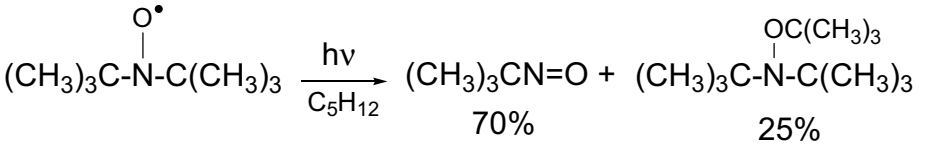

(2.28)

In the solution of radical I in carbon tetrachloride, there is an absorption in the range of 300–400 nm corresponding to the charge-transfer band. The irradiation of the solution by light with $313 < \lambda < 360$ nm results in the decomposition of radical I with the quantum yield of 1.7:

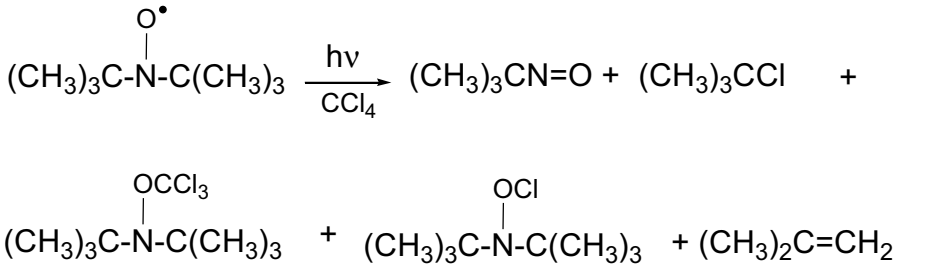

(2.29)

That is, the decay of radical I takes place under the action of light and in secondary reactions with products of the solvent photolysis, in particular with $CCl_3^{\bullet}$ radicals.

2.4 Applications of ARs

Stable radicals (also known as 'spin labels') find wide applications in various areas of scientific research and manufacture. AR applications include organic chemistry and photochemistry, chemical kinetics and catalysis, analytical chemistry, chemistry of polymeric materials, molecular biology and medicine. In experimental chemistry, ARs are used to recognise the mechanism of chemical reactions, and the structures of active radicals in a wide temperature range [46]. The important feature of ARs is the regular change of their ESR spectra depending on mobility, nature of surrounding molecules and mutual distances. They are widely applied in research of the physics and chemistry of polymers [18]. For these purposes, a small quantity of spin labels is introduced into the studied polymer so that 200–600 monomer units account for

one stable radical. In these conditions, the widening of ESR spectra caused by a spin exchange is excluded.

With the help of spin labels one can determine the parameters of molecular movements and their change under various external effects, study the dynamics of the conformations of macromolecules in solutions, investigate the molecular dynamics in solid polymers, carry out the analysis of the compatibility of components of complex polymer blends, and investigate cross-linked and filled polymers. An important area of applications of spin labels is study of the mechanism and kinetics of reactions in heterogeneous systems, interfaces, and defects of packing [18]. The capability of recombining with other active particles provides a way for AR application as inhibitors and regulators of polymerisation, effective stabilisers of polymer oxidation, and the thermal, mechanical and photodegradation of polymers. The kinetic features of the inhibited oxidation of polypropylene and polyethylene by 2,2,6,6-tetramethyl-4-benzoyloxypiperidine-1-oxyl have been studied [47, 48].

ARs in the grafted form can be also used as inhibitors. In rubbers containing one aminoxyl group per 1000-3000 monomer units, the induction periods of the oxidation at 140o are several times more than in polymers without such groups [49]. High-molecular-weight inhibitors are favourable for high-temperature stabilisation and for polymers with high molecular mobility. These conditions provide more homogeneous distribution of such stabilisers, and show the basic advantage of their nonvolatility [50].

Increase of the nitrocellulose working life in the presence of 2,2,6,6-tetramethyl-4-ethyl-4-oxypiperidine-1-oxyl was observed during mechanical actions. Additives of this stabiliser at 0.3 wt% increase the durability of the polymer by a factor of one hundred. The breaking strength is also increased several times, and the creep rate of the material decreases by 100-fold [51]. These results were confirmed by investigations of mechanical degradation of polypropylene in the presence of radical IV (R=$OOCNHC_6H_5$) [52]. ARs grafted on polypropylene considerably increase their stability during treatment in the stirrer [53, 54].

ARs can be used as effective quenchers of exited states and controlling agents in photochemical and radiating processes. ARs have been used as photostabilisers of films and fibres [54, 55]. These radicals have been used in the synthesis of polymers with strong magnetic properties (e.g., polyradicals). On the basis of polyacetylene containing ARs, a polymer ferromagnetic having a residual magnetisation of 1 G has been prepared [56].

ARs are used in molecular biology for obtaining spin-labelled macromolecules. These labels register slight changes in the macromolecule state [22]. With the help of spin labels, the conformational transformations of biopolymer macromolecules as well as changes in the structure of biomembranes and nucleic acids, have been studied.

2.5 Generation of ARs in Reactions of Spin Trapping

The possibility of stabilising short-living radicals was shown for the first time using their reactions with nitroso compounds and nitrones [57, 58]:

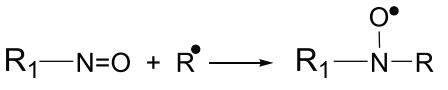

(2.30)

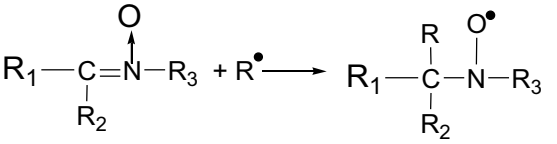

(2.31)

All aliphatic nitroso compounds are dimers in the solid phase, but they dissociate in solutions and the gas phase. The monomer form of nitroso compounds accepts radicals. Aliphatic nitroso compounds form sufficiently stable adducts with short-living radicals of a very different structure. The characteristics of ESR spectra of radical adducts with tertiary nitroso compounds is practically identical for all spin traps of a given type, and is determined by a number of β-hydrogen atoms or other atoms for >N–O• fragments. The most frequently used spin trap is *t*-nitroso butane (TNB). The irradiation of a reacting mixture during photochemical generation of radicals is accompanied by the formation of some symmetric ARs in the following way [59]:

(2.32)

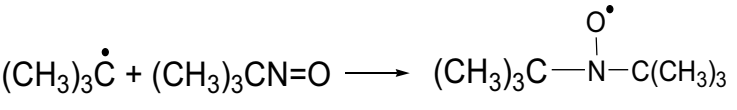

(2.33)

Concentrations of symmetric ARs are usually less than those for basic radicals, but the superposition of the spectra of two radicals frequently complicates the interpretation.

Alkyl hydroperoxides react with nitroso compounds giving ARs [60]:

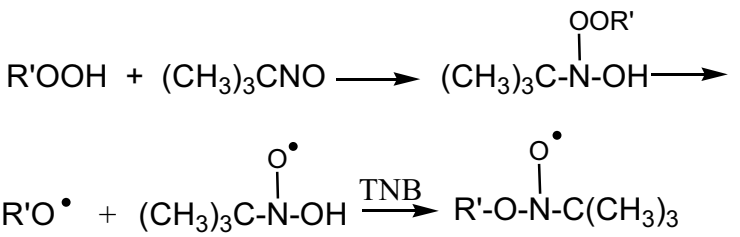

(2.34)

Nitroso compounds also readily react with certain anions [61] with the formation of oxyanions, which are oxidised into ARs by the nitroso compound or traces of O_2:

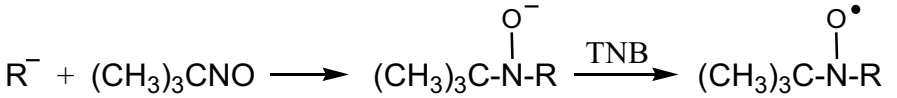

(2.35)

Therefore the interpretation of data of radical acceptance by TNB in the presence of oxidisers and in electron-donor media is complicated. 2-methyl-2-nitosobutanone-3 is close to TNB in chemical properties and ESR spectra of radical adducts [59], and sometimes it is a more effective acceptor of radicals.

The defect of TNB connected with its sensitivity to light, oxidisers, strong acids and some anions limits the application of this trap. Aromatic nitroso compounds have some advantages in comparison with aliphatic ones. Most aromatic nitroso compounds except 2,4,6-tri-*t*-butylnitroso benzene (BNB) are dimers which dissociate in solutions The monomer form of aromatic nitroso compounds accepts radicals. The characteristics of ESR spectra of aromatic nitroso compounds are determined by the number of substituents in the aromatic rings and β-hydrogen atoms in a radical fragment. They form sufficiently stable adducts with many short-living radicals, but do not form stable adducts with $RO^{\bullet}$, $RO_2^{\bullet}$, $^{\bullet}OH$ radicals and halogen atoms. Sufficiently detailed consideration of the capability of aromatic nitroso compounds for the detection and identification of metalorganic radicals containing Co, Mo, Fe, V, Mn, Re, Cr, Os has been completed [62, 63].

Among aromatic nitoso compounds, nitroso benzene (NB) has found the greatest application. It is more accessible and not sensitive to visible and near-UV light. Only light at $\lambda < 310$ nm gives rise to the formation of diphenylaminoxyl. Spin adducts with NB are usually stable at room temperature. The basic imperfection of NB is the complexity of the analysis of ESR spectra because of additional lines from the protons of phenyl groups. The other essential restriction for NB applications is the impossibility of its use in solutions containing alkalis, alcoholates and other electron donors. In similar conditions, the stable radical anions of NB $C_6H_5NO^{\bullet -}$ are formed [64].

Nitroso durene (ND) is also used as a spin trap. The main advantage of ND is the simplicity of ESR spectra of radical adducts, insensitivity to UV light, and high stability of the adducts at room temperature. The drawback of ND is poor solubility in many solvents, broadening of lines because of interaction with protons of methyl groups, and instability of adducts with $RO^{\bullet}$ radicals [65]. Certain advantages for studying reactions of spin trapping are inherent to BNB [66]. It is well dissolved in many solvents, and

exists in the active monomer form in solid state and solutions. BNB is a bifunctional trap, and radicals join to nitrogen and oxygen atoms. The properties of substituted NB such as 2,4,6-trimethylcarbonylnitrosobenzene, 2,4,6-trimethoxynitrosobenzene and pentafluoronitrosobenzene have been investigated [65].

Nitrones are also widely used as spin traps. Nitrones have the much greater thermal and photochemical stability than nitroso compounds. They are monomers and have activity to free radicals even in the solid state. As a result of accepting of radicals by reaction (2.31), ARs are formed. As a rule, fragment R_3 of these AR represents the tertiary alkyl group, and fragment R_1 is the substituted aromatic group. The inconvenience of using of nitrones as spin traps is the absence (in most cases) of hyperfine splitting (HFS) from atoms of the attached radical in the ESR spectra of formed ARs.

Information on the structure of the captured radical, as well as in the case of nitroso compounds, can be obtained from a_N and a_H^β constants. In general, the three most accessible nitrones are applied as spin traps:

diphenylnitrone (DPN) [67, 68]

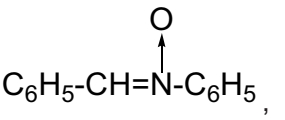

methylene-*t*-butylnitrone (MN) [69-71]

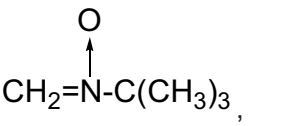

C-phenyl-N-*t*-butylnitrone (PBN) [72, 73]

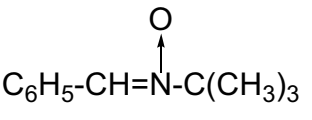

Obtained from DPN, ARs are reactive and transform into diamagnetic molecules by recombining with radicals. This disadvantage has caused poor applicability of DPN as a spin trap. MN [69–71] is more active trap than other nitrones. The carbon atom, which is attacked by short-living radicals, is less shielded. MN forms considerably more stable adducts with $^{\bullet}OH$, $HO_2^{\bullet}$ and $(CH_3)_3COO^{\bullet}$ radicals [74]. The essential advantage of MN in comparison with TNB is that this nitrone catches aminoradicals, whereas nitroso compounds do not add them [69]. Alongside TNB, PBN is the basic trap widely used in studies of short-living free radicals [75]:

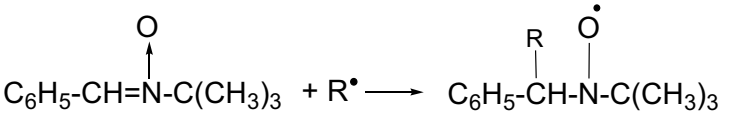

(2.36)

PBN is stable to the action of light, O_2, and water, and is well dissolved in many solvents. Radical adducts with PBN are stable at room temperature and in several cases can be isolated in the pure state. PBN catches a more extensive variety of radicals than TNB, for example, F•, Cl•.

The insertion of two functional groups OH and >C=N→O into structure of one molecule has been carried out in the work [76]. As a spin trap, -(3,5-di-*t*-butyl-4-hydroxyphenyl)N-*t*-butylnitrone was used. This bifunctional trap forms phenoxyl radicals in reaction with radicals having pronounced oxidising properties (RO•, R•C=O, PhCOO•) and ketones in triplet-exited states. The radicals with an unpaired electron on carbon atoms add to the β-carbon of the nitrone-forming AR:

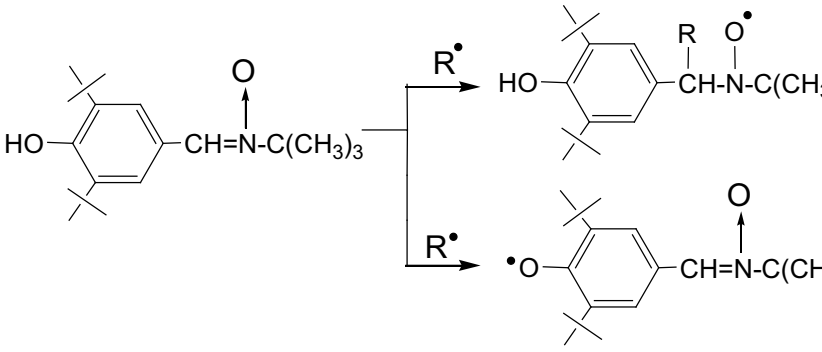

(2.37)

(2.38)

The study of oxidation by the spin trap method is associated with identification of adducts of nitrones with $RO_2^{\bullet}$ radicals [77, 78]. Adducts of $RO_2^{\bullet}$ radicals with PBN are unstable and even at 263 K rapidly decay. During decomposition of these adducts, the products of interaction with RO• radicals are formed:

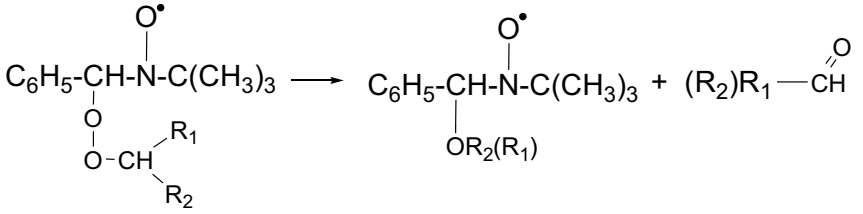

(2.39)

Thus, though the $RO_2^{\bullet}$ radicals cannot be detected in concrete conditions of oxidation of hydrocarbons, the formation of PBN adducts with $RO^{\bullet}$ radicals is the qualitative indication on occurrence of peroxide radicals in the reacting system.

The composition of products of interaction of aliphatic nitrones with $OH^{\bullet}$ radicals can be very varied. For nitrones containing aromatic groups, for example PBN, three paths of reactions are possible: hydrogen-atom abstraction from alkyl groups, addition of $OH^{\bullet}$ to aromatic rings, and nitrone groups with formation of ARs [79, 80]:

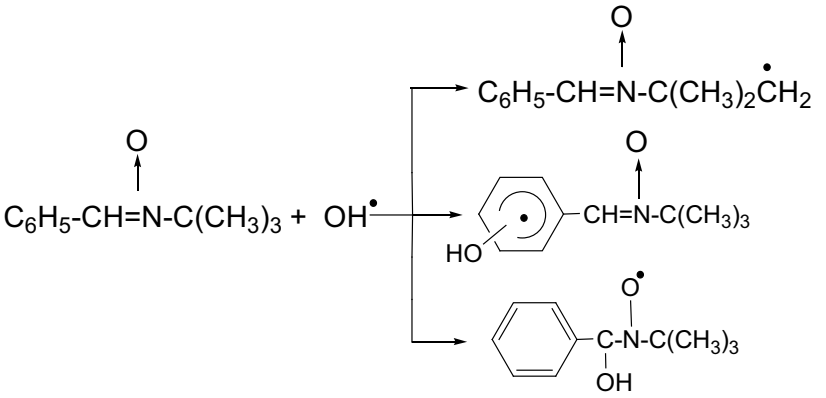

Nitrones can accept various atoms and radicals. The convincing evidence of hydrogen-atom addition to nitrones has been obtained by the example of PBN [19]. The attachment of H atoms to aromatic rings gives cyclohexadienyl radicals [81]. Adducts of PBN with H atoms are unstable and are not observed in non-polar solvents. The spin trapping of fluorinated radicals and Cl atoms by PBN takes place [82, 83].

A series of 3-aryl-2*H*-benzo[1,4]oxazin-4-oxides

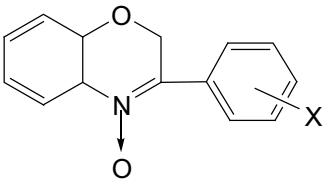

was prepared, and their ability to trap free radicals investigated by ESR spectroscopy [84]. In organic solvents, these compounds could efficiently scavenge all carbon- and oxygen-centred radicals tested, giving very persistent aminoxyls (except with the superoxide anion whose spin adducts were unstable). The main feature of these nitrones as spin traps lies in the potential to recognise the initial radical trapped.

Besides a *g*-factor and aminoxyl nitrogen coupling constant dependent on the species trapped, the ESR spectra also showed different patterns due to hyperfine splitting characteristic of the radical scavenged. This last important feature was investigated by means of density functional theory calculations. The overall summary of the ESR characteristics of various ARs produced in nitrones has been completed [19, 72]. In these studies, the various aspects and features of application of the spin trap method in invetigations of the mechanism of chemical reactions are considered.

2.6 Synthesis of Polymers Containing Stable ARs

The chemical properties of polymeric ARs are determined by the >N O• fragment and are basically similar to those of low-molecular ARs. They are characterised by high chemical stability in a wide range of pH in water solutions, thermal stability up to 180 °C, and oxidative stability. The life time of such radicals can be many years and is not limited to inert media. The interaction of ARs having functional groups with those of macromolecules is the most widespread procedure for obtaining aminoxyl-containing polymers [18]. The preparation methods of ARs have been summarised in monographs [2, 3]. As an example of such reactions, one can consider the graft of AR III (R=COOH or $COOCH_3$) to polyethylene glycol having end hydroxyl groups [85]. The first stage of the reaction includes the treatment of radical III by sulphochloride to obtain ARs containing chloranhydride groups. The attachment of synthesised aminoxyl to the polymer is then carried out by the following scheme:

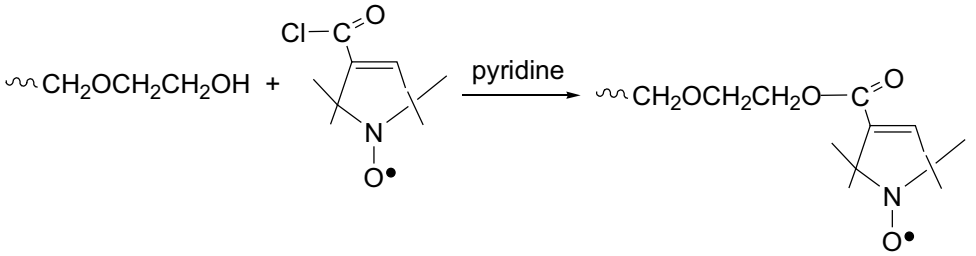

(2.43)

Polyvinylacetate with ARs was obtained by the reaction with radical III (R=COOH) [86]. Macromolecules of modified polyvinylacetate contain from 1 to 10 ARs.

Polyacrylates, polymethylacrylates and polymethylmethacrylate with ARs are synthesised by reaction of the copolymer containing chloranhydride groups with a radical IV (R=OH) [87]:

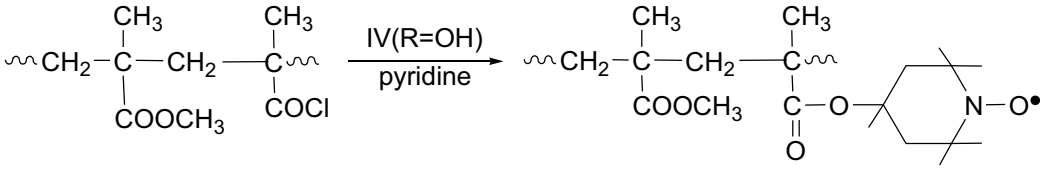

(2.44)

Synthesis of spin-labelled polystyrene has been carried out by the reaction of the polymer containing chlormethyl groups with radical IV (R=OH) [88, 89]:

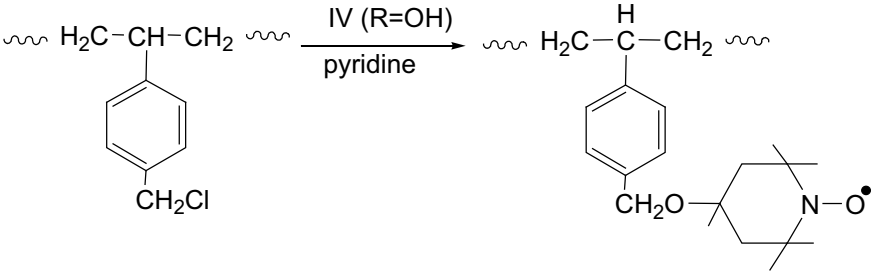

(2.45)

AR (VIII) was introduced to macromolecules of polyvinylacetate by partial saponification [90]:

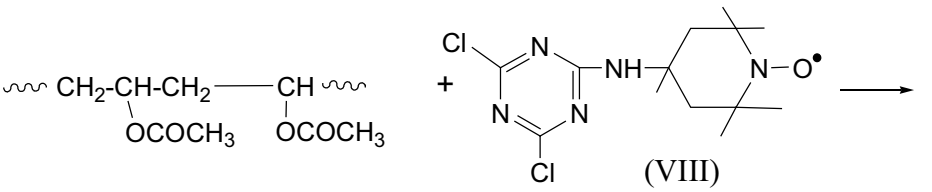

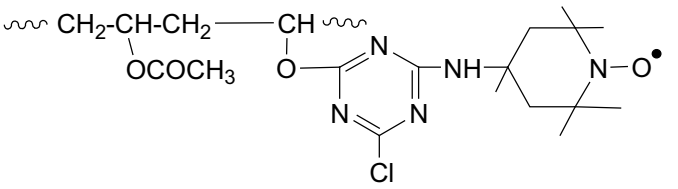

(2.46)

Polyethylene films containing carbonylhydrazide groups were treated by radical IV (R = –N=C=S) [91]. The spin-labelled polyethylene was obtained by the following reaction:

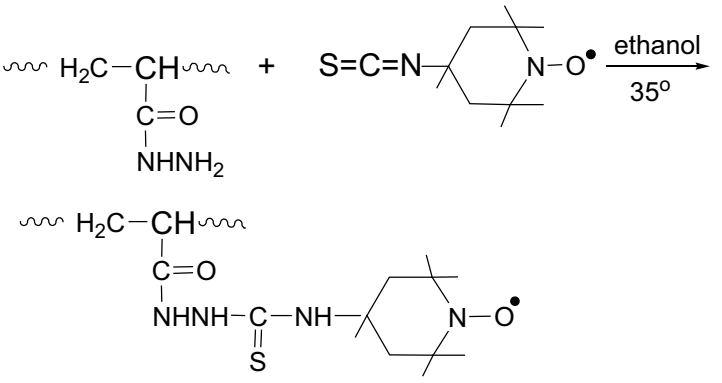

(2.47)

Synthesis of the spin-labelled copolymer of styrene with maleic anhydride has been carried out on heating a solution of the copolymer and radical IV (R=NH_2) in anhydrous tetrahydrofuran (THF) [92]:

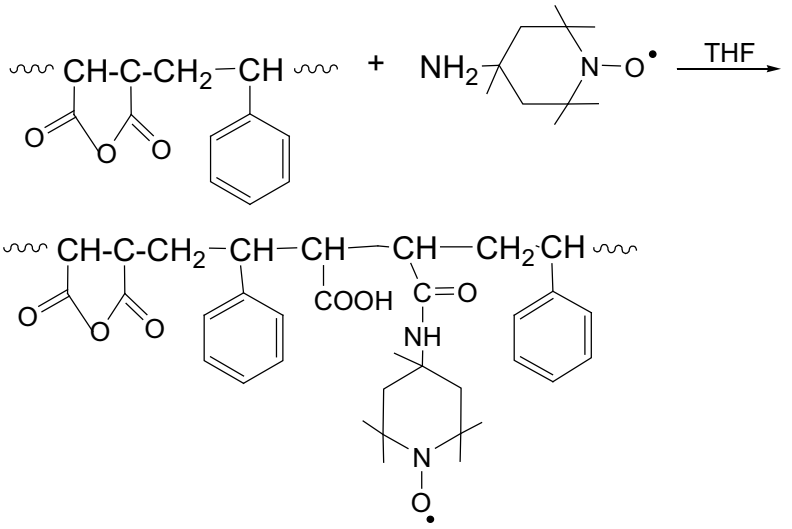

(2.48)

However, most of synthetic polymers have no suitable reactive groups. ARs can be inserted into such polymers only via copolymerisation or chemical modification of macromolecules. Using reactions of ARs without participation of unpaired electrons, polymers were synthesised from monomers containing one or two free-radical fragments [93]. The paramagnetism of such polymers amounts to 1.5–2.1 10^{21} spin. AR (IX) on the basis of radical-containing diacetylenes

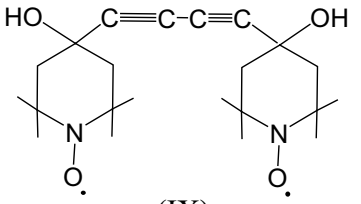

(IX)

undergoes polymerisation, being converted to polymeric polycrystals under the action of light or on heating (80–100 °C) [56, 94]. A polyacetylene chain with stable radical substituents (R•) is similar to the hypothetical polyene polyradical

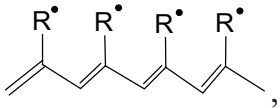

, which serves a theoretical model for a 'ferromagnetic' macroradicals. The solid-state polymerisation of such diacetylenes was thought to be a prospective or at least a feasible route to conjugated polyradicals. Several features of the polymerisation approach seem to be advantageous. Owing to monomer lattice control, exact stereospecificity of the polyradical may be guaranteed. The crystalline nature of the polymerisation products should facilitate characterisation of the latter. Catalysts are not used for the polymerisation, so the probability of contamination of the reaction products is reduced. Based on gel permeation chromatography (GPC) analysis, the polymerisation products are oligomers with polymerisation degree n = 4–10 [94]. A broad structureless absorption band in their optical spectra, peaking at λ_{max} = 380 nm, is indicative of a short conjugation length. After thermal treatment, X-ray analysis revealed almost total amorphisation of polymerisation products of some monomers similar to IX. ESR showed also that the magnetic behaviour of the products was typical for a spin-labelled oligomer chain (triplet signal and a typical τ-correlation times *vs* molecular mass dependence in solution) without signs of ferromagnetic ordering of spins. Thus, the ferromagnetic properties of polyconjugated polyradicals produced from aminoxyl-substituted diacetylenes seem to be ellusive.

AR (X)

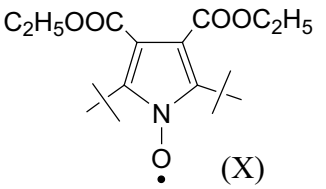

(X)

has been incorporated into the main chain of 'living' polystyrene obtained by anionic polymerisation in the presence of butyl lithium [95]:

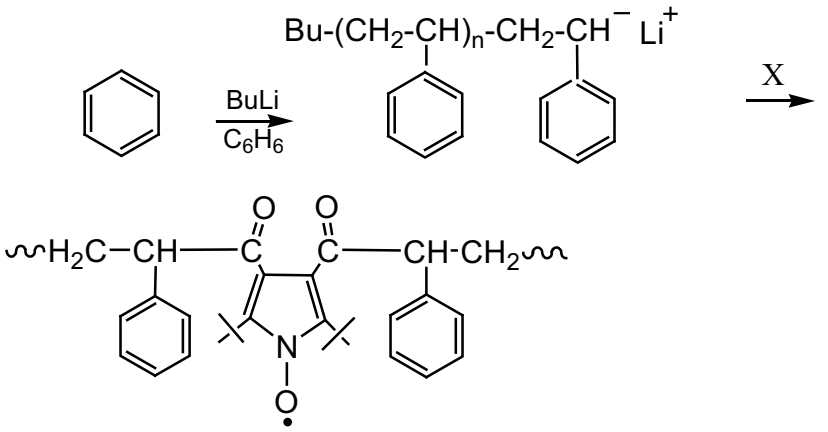

(2.49)

By the same method of 'living' radical polymerisation, a series of block copolymers of poly(ethylene oxide-styrene) with narrow polydispersity were synthesised by the following two-step approach [96]. Initially, 'living' anionic polymerisation of ethylene oxide with sodium-4-oxy-2,2,6,6-tetramethyl-1-piperidinoxyl as initiator yields polyethylene oxide with ARs at the chain end:

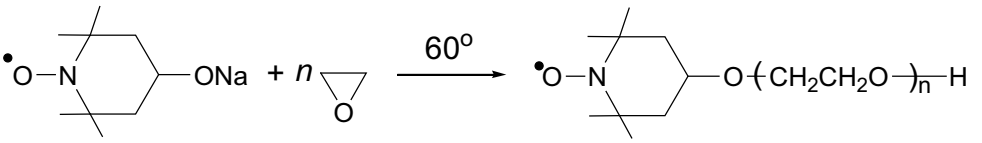

(2.50)

A stable free radical polymerisation of styrene gives a block copolymer:

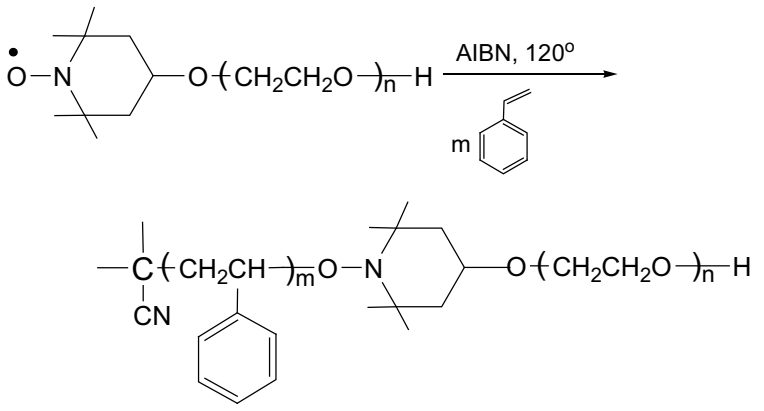

(2.51)

By the polycondensation of 1,10-decandiol with chloranhydride of terephthalic acid in the presence of AR (XI),

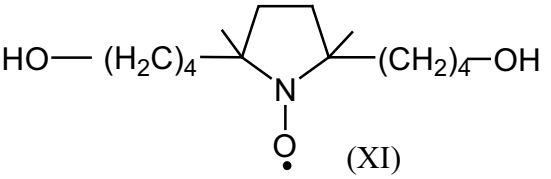

(XI)

a polymer of the following structure has been obtained [97]:

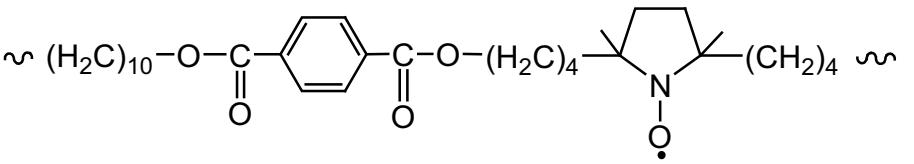

However, polymerisation or copolymerisation of monomers with ARs does not always occur without participation of unpaired electrons. For example, attempts to synthesise polymers from monomers containing radical IV [R = –O (C=O) C (CH_3) =CH_2] have not been successful because radicals of growing chains actively react with aminoxyl groups [98, 99]. Therefore, for preparation of spin-labelled polymers, one can use monomers containing appropriate amines with subsequent oxidation of the polymer. In such a manner, the spin-labelled polymer has been synthesised [100] from the monomers:

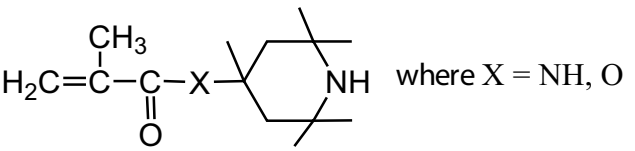

where X = NH, O

The oxidation of polyacrylamides having diphenylamine groups using lead dioxide gives polymers with ARs [101]:

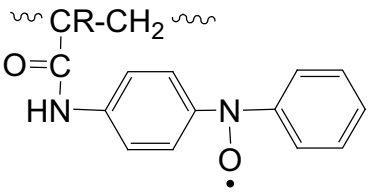

where R = H, CH_3.

Aminoxyl-containing polyvinylpyrrolidone and polyvinylcaprolactam have been obtained by the copolymerisation of corresponding monomers and amines

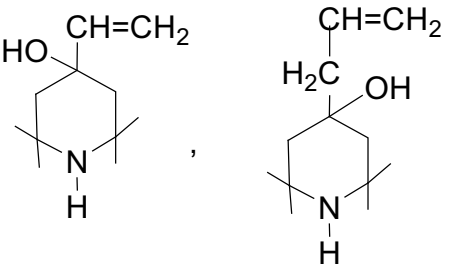

with further oxidation of amine groups in the copolymers [102]:

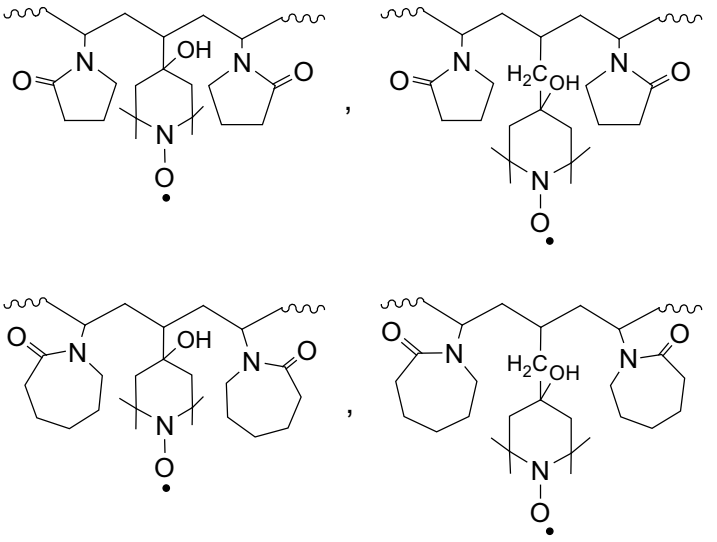

The grafting of ARs to polyethylene has been done in the reaction of copolymers containing carbonyl groups (0.5%) with 2-amine-2-methyl propanol [103]:

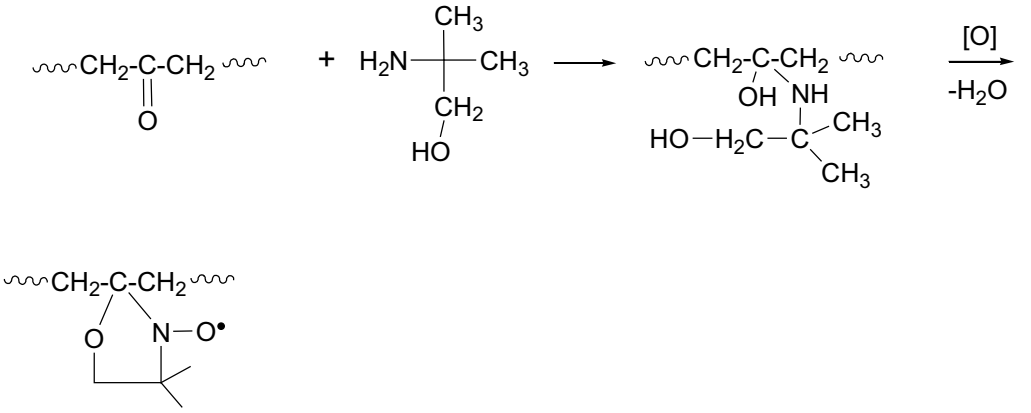

(2.52)

Polymers containing nitrone and aminoxyl groups have been obtained by the reaction of polystyrene containing formaldehyde groups in the *p*-position of phenyl rings with 2,3-bis(hydroxylamino)-2,3-dimethylbutane [104]:

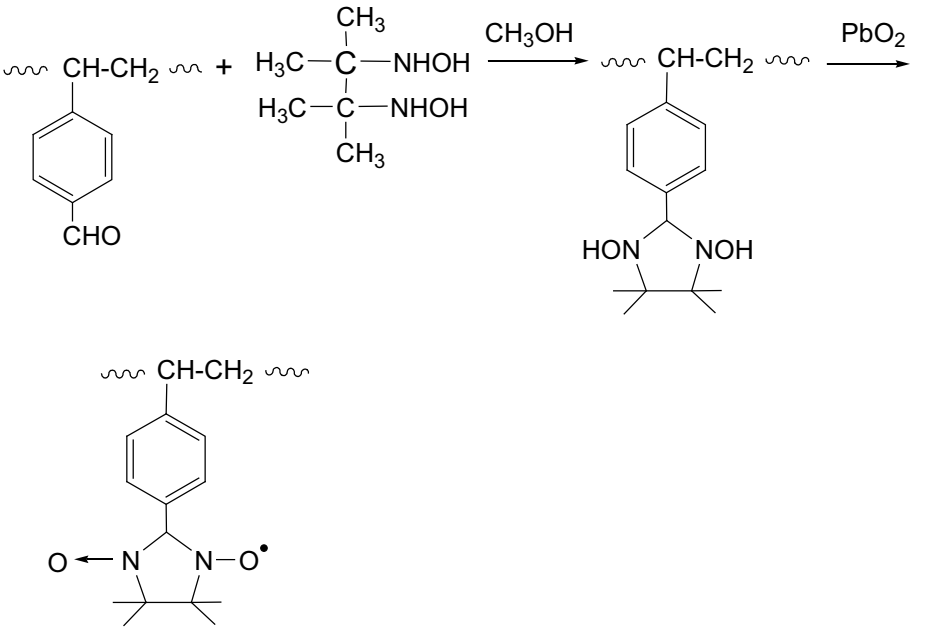

(2.51)

Polymers with grafted ARs can be also produced in reactions of macroradicals formed by mechanodegradation, photolysis or radiolysis in the presence of aminoxyl biradicals. By this method, for example, AR (XII)

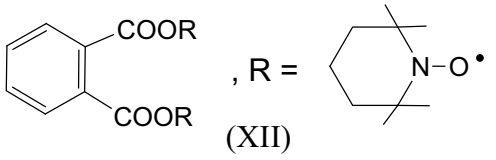

(XII)

has been introduced into macromolecules of polyolefins in the course of their mechanodestruction [105]. Biradicals are grafted upon macromolecules by one of two radical fragments. By ESR [106], the nature of polymeric ARs formed during the photooxidation of films of isotactic polypropylene containing bis-(2,2,6,6-tetramethyl-4-piperidyne)-sebacinate has been studied:

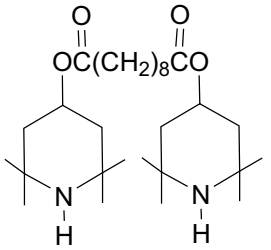

Only one of the amine groups of this stabiliser is oxidised to ARs during photolysis. The part of monoradicals formed recombines with alkyl macroradicals of polypropylene, and then the second amine group is converted into ARs.

To obtain spin-labelled polymers, various nitroso compounds are widely used. The wide set of reactions represents a variety of methods of polymer modification by these compounds. In most cases, ARs can be generated by reactions of nitroso compounds with metalorganic reactants:

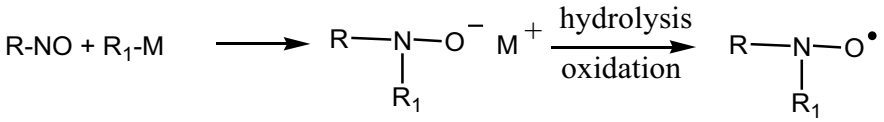

(2.52)

When ARs are introduced into the phenyl rings of polystyrene, the first stage is mercuration of the polymer. Under the action of nitrosyl chloride, the mercurated polystyrene is converted into one containing nitroso groups. The synthesis of modified

polystyrene includes stages of polymer treatment by phenylmagnesium bromide and silver oxide [107]:

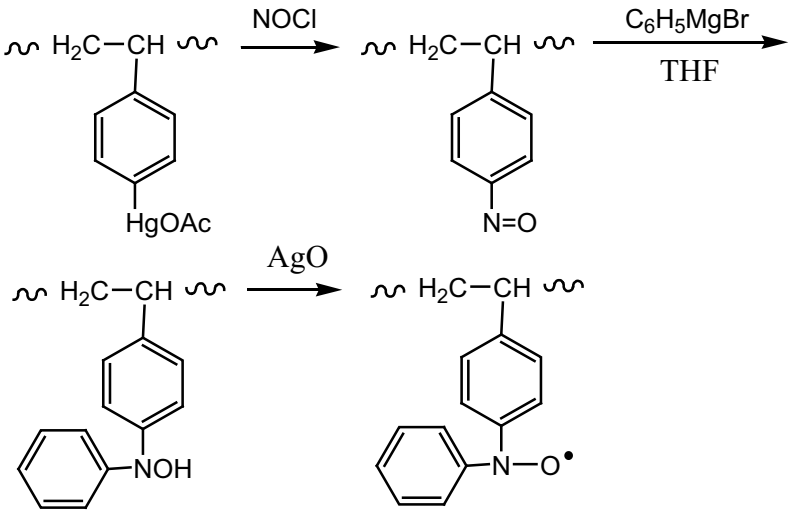

(2.53)

The spin-labelled polystyrene contains one AR per 1000 monomer units. If *t*-butylmagnesium chloride is used instead of phenylmagnesium bromide, a polymer with *t*-butylaminoxyl groups can be obtained [108]:

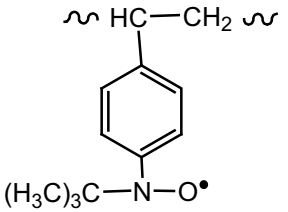

Synthesis via scheme (2.53) has several drawbacks. The mercurated polystyrene is inclined to cross-link, and the polymer containing nitroso groups is unstable. A more suitable method of synthesis of spin-labelled polystyrene is given below [109]:

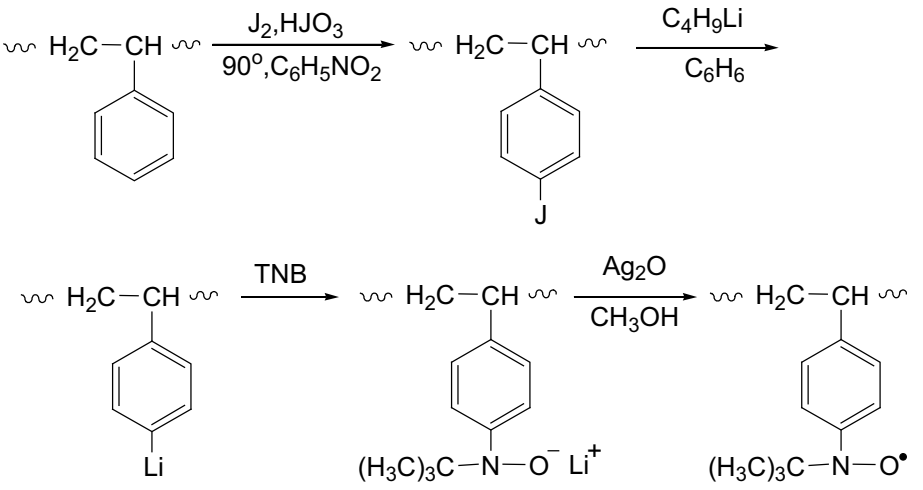

(2.54)

This synthesis is not accompanied by the destruction or cross-linking of macromolecules.

TNB can be used use as a trap for carbanions which are converted into ARs by the following reaction:

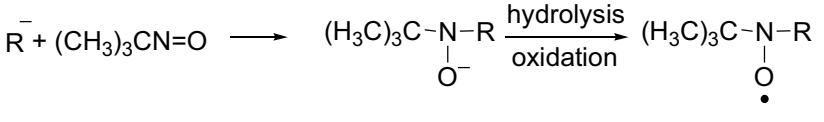

(2.55)

The choice of suitable initiating system allows preparation of polystyrene containing ARs on one (*n*-butyl lithium) or two (naphthalate sodium) ends of macromolecules. By this method, aminoxyl-containing polymethylstyrene, poly-2-vinylpiridine and a copolymer of styrene with methylstyrene have been obtained [61].

Polymethylmethacrylate with end *t*-butylaminoxyl groups was synthesised by a similar method [110]. However, anionic polymerisation of methylmethacrylate is accompanied by side reactions influencing the efficiency of the process (especially on the site of label attachment). The optimal conditions of synthesis are using THF as the solvent, 70 °C, and initiators: *n*-butyl lithium, sodium naphthalate or 9-lithium fluorine. In these conditions, one can obtain polymethylmethacrylate with the end AR:

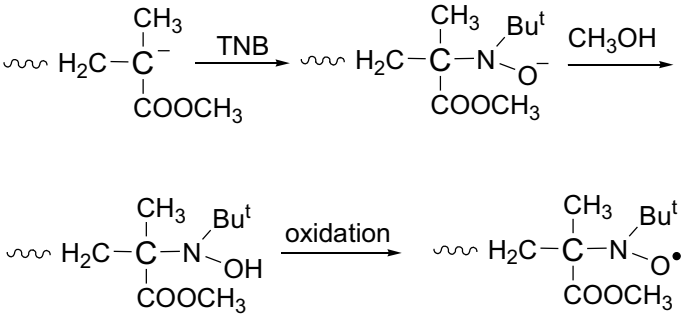

(2.56)

The important reaction of nitroso compounds resulting in spin-labelled polymers is radical capture. Polystyrene containing *t*-butyl aminoxyl was obtained by radical polymerisation in the presence of TNB and t-butylperoxyoxalate [111]:

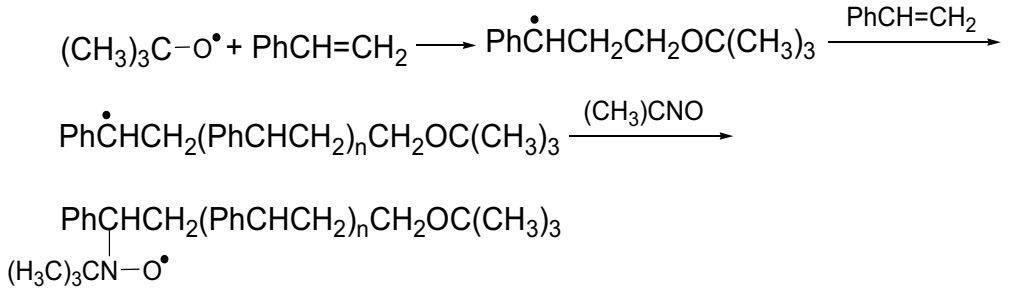

(2.57)

ARs can also be introduced into macromolecules by the reaction of nitroso compounds with macroradicals generated by mechanodestruction, thermal degradation, or the photolysis of polymers. The experimental data and schemes of TNB conversions in reactions with alkyl macroradicals of polypropylene under shearing forces or photolysis have been attained [53]. During polyethylene grinding in a mixture with NB at 77 K, ARs appeared on a surface of particles of the polymer as a result of interactions of the spin trap with macroradicals [112]. The multiple treatment of cross-linked rubbers containing TNB by repeated swelling–cooling leads to occurrence of ARs as a result of bond scissions with the formation of macroradicals [113]. The synthesis of polyethylene containing ARs has also been done by thermal destruction of the polymer films with BNB additives [114]. The films with BNB were prepared by combined dissolutions of the polymer and BNB in benzene with subsequent removal of the solvent.

Spin-labelled rubbers (polybutadiene, polyisoprene, copolymer of isobutylene with isoprene) were prepared by reactions with 2,6-dichloronitrosobenzene in toluene

solutions [115]. The ESR signal of ARs occurs immediately after mixing solutions of rubbers and the nitroso compound. ARs formed are stable for months. The method proposed allows obtaining various spin-labelled polymers having > C=C < bonds.

Spin labels were grafted on polyethylene under γ-radiolysis in the presence of PBN [116]:

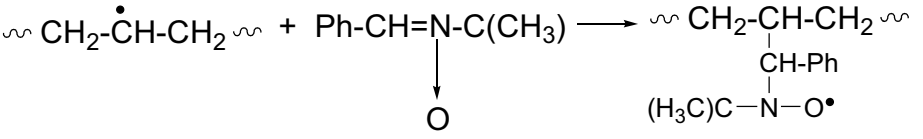

(2.58)

The γ-radiolysis at –196 °C generates alkyl macroadicals ~ CH_2-C•H-CH_2~ detected by the ESR spectrum. The formation of ARs was observed at –70 °C via reaction 2.58.

A peculiar example of spin-labelling is 1,3-dipolar addition of paramagnetic nitrones (XIV) to the double bonds of rubbers [117]:

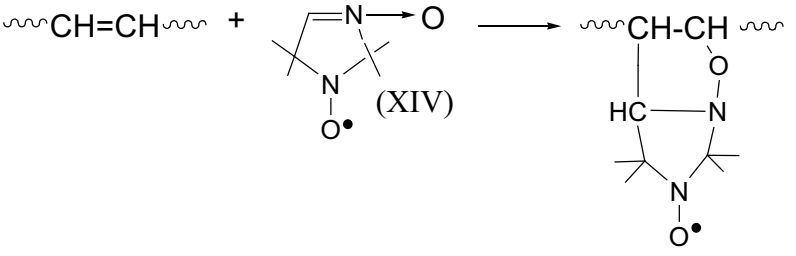

(2.59)

As with spin-labelled methylvinylpyridine, chloroprene and divinyl rubbers have been obtained.

The method of incorporation of ARs into the polymer matrix has been demonstrated by the polymerisation of pyrrole [118]. In the presence of protons, radical IV causes polymerisation of pyrrole to polypyrrole with the incorporated reduced (hydroxylamine) form and oxidised (nitrosonium ion) form of ARs in the polymer matrix. In electrochemical oxidation of pyrrole in the presence of ARs, a coupled electrochemical–chemical synthesis produces polypyrrole films with incorporated nitrosonium ions. They can by reduced to ARs by partial film reduction.

The successful use of spin labels in the analysis of functionalisation of macromolecules has been demonstrated by the copolymer of styrene–divinylbenzene with different

content of carboxy groups. The radical IV (R_1 = OH) and 6-(3-aminophenyl)-2,4-diphenylverdazil:

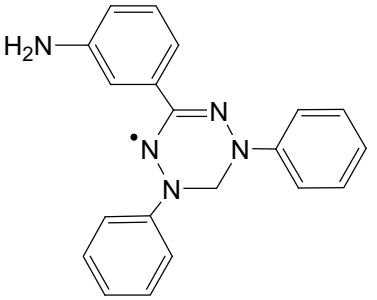

were selected as spin labels with consideration of their distinct ESR spectra and the presence of reactive hydroxyl and amino groups. A carboxy-containing copolymer was converted into the corresponding acid chloride. The resin was then treated with dimethylacetamide (DMAA) solutions of IV and verdazyl spin labels in various concentrations. The concentrations of radicals in the spin-labelled polymer measured by ESR and initial concentrations of radicals had a discrepancy of about 1–1.5%. Hence, some polymer containing the functional groups –COOH, –NCO, or epoxy capable of binding the functional groups of the spin labels can be analyzed rapidly and accurately using the considered procedure.

Thus, different ways are suitable for AR formation in polymers, including purely chemical synthetic methods as well as radiation-initiated, photo- and mechano-chemically initiated processes. The choice of one or other depends on the chemical structure of the polymer, and the availability or lack of reactive functional groups in macromolecules [119].

References

1. G.B. Pariiskii, I.S. Gaponova, and E.Ya Davydov, *Russian Chemical Reviews*, 2000, **69**, 985.

2. P. Tormala and J.J. Lindberg, *Structural Studies of Macromolecules by Spectroscopic methods*, Ed., K.J. Ivin, Khimiya, Moscow, 1980, p.236.

3. E.G. Rozantsev and V.D. Sholle, *Organic Chemistry of Free Radicals*, Khimiya, Moscow, Russia, 1979.

4. D.C. Nonhebel, J.M. Tedder and J.C. Walton, *Radicals*, Cambridge University Press, Cambridge, UK, 1979.

5. E.G. Rozantsev, *Free Nitroxyl Radicals*, Plenum Press, New York, NY, USA, 1970.

6. L. Rintoul, A.S. Micallef, D.A. Reid and S.E. Bottle, *Spectrochimica Acta Part A*, 2006, **63**, 2, 398.

7. P.J. Carmichael, B.G. Gowwnlock and C.A.F. Johnson, *Journal of the Chemical Society-Perkin Transactions II*, 1973, **14**, 1853.

8. M.M. Lipey, V.K. Potapov and R.G. Kostyanovsky, *Khimiia Vysokikh Energii*, 1974, **8**, 496.

9. A.L. Buchachenko and A.M. Wasserman, *Stable Radicals*, Khimiya, Moscow, Russia, 1973.

10. H.G. Aurich, K. Hahn, K. Stork and W. Weiss, *Tetrahedron*, 1977, **33**, 969.

11. R.C. McCalley, E.J. Shimshick and H.M. McConnell, *Chemical Physics Letters*, 1972, **13**, 2, 115.

12. S.A. Goldman, G.V. Bruno and J.H. Freed, *Journal of Physical Chemistry*, 1972, **76**, 13, 1858.

13. A. Bluhm and J. Weinstein, *Journal of the American Chemical Society*, 1970, **92**, 5, 1444.

14. T. Doba, S. Noda and H. Yoshuda, *Bulletin of the Chemical Society of Japan*, 1979, **52**, 21.

15. A.R. Forrester and S.P. Hepburn, *Journal of the Chemical Society C: Organic Articles*, 1970, **9**, 1277.

16. A. Calder and A.R. Forrester, *Journal of the Chemical Society C: Organic Articles*, 1969, 10, 1459.

17. O.W. Mender and E.J. Janzen, *Journal of Organic Chemistry*, 1969, **34**, 12, 4072.

18. A.M. Wasserman and A.L. Kowarsky, *Spin Labels and Probes in Physical Chemistry of Polymers*, Nauka, Moscow, Russia, 1986.

19. V.E. Zubarev, V.N. Belewsky and L.T. Bugaenko, *Russian Chemical Reviews*, 1979, **48**, 1361.

20. A.B. Shapiro and E.G. Rozantsev, *Izvestiya Akademii Nauk SSSR Seriya Khimicheskaya*, 1966, 1650.

21. M.B. Neiman, E.G. Rozantsev and V.A. Golubev, *Akademii Nauk SSSR Seriya Khimicheskaya*, 1965, 548.

22. L.J. Berliner, *Spin Labeling Theory and Applications*, Academic Press, New York, NY, USA, 1974.

23. A.L. Buchachenko and O.P. Tkacheva, *Kinetika i Kataliz*. 1966, **7**, 777.

24. W. Summermann and U. Deffner, *Tetrahedron Letters*, 1975, **31**, 593.

25. V.A. Golubev, R.I. Zjdanov and E.G. Rozantsev, *Akademii Nauk SSSR Seriya Khimicheskaya*, 1970, 184.

26. R.I. Zjdanov, V.A. Golubev and E.G. Rozantsev, *Akademii Nauk SSSR Seriya Khimicheskaya*, 1970,186.

27. P.S. Bailey and J.E. Keller, *Journal of Organic Chemistry*, 1970, **35**, 8, 2782.

28. J.W.F. Keana, *Chemical Reviews*, 1978, **78**, 1, 37.

29. V.A. Golubev, R.I. Zjdanov, V.M. Gida and E.G. Rozantsev, *Akademii Nauk SSSR Seriya Khimicheskaya,* 1971, 853.

30. H. Low, I. Paterson and J.M. Tedder, *Journal of the Chemical Society, Chemical Communications*, 1977, **6**, 171.

31. P. Brandi, C. Galli and P. Gentili, *Journal of Organic Chemistry*, 2005, **70**, 23, 9521.

32. A.L.J. Beckwith and J.S. Polle, *Journal of the American Chemical Society*, 2002, **124**, 32, 9489.

33. K. Murayama and T. Yoshioka, *Bulletin of the Chemical Society Japan*, 1969, **42**, 1942.

34. S. Nigan, K.D. Asmus and R.L. Willson, *Journal of Chemical Society, Faraday Transactions 1*, 1976, **72**, 2324.

35. S.I. Skuratova, Yu.N. Kozlov, N.V. Zakatova and V.A. Sharpaty, *Zhurnal Fizicheskoi Khimii*, 1971, **45**, 1821.

36. O.N. Karpukhin, T.V. Pokholok and V.Ya. Shlyapintokh, *Vysokomolekulyarnye Soedineniya Seria A*, 1971, **13**, 22.

37. M.S. Khloplyankina, A.L. Buchachenko, M.B. Neiman and A.G. Vasil'eva, *Kinetika i Kataliz*, 1965, **6**, 394.

38. L.V. Ruban, A.L. Buchachenko, M.B. Neiman, Yu.V. Kohanov, *Vysokomolekulyarnye Soedineniya Seria A*, 1971, **8**, 1642.

39. A.D. Becke, *Physical Review*, 1988, **38**, 3098.

40. H. Huang, H. Henry-Riyad and T.T. Tidwell, *Journal of the American Chemical Society*, 1999, **121**, 16, 3939.

41. A.D. Allen, B. Cheng, M.H. Fenwick, B. Givehchi, H. Henry-Riyad, V.A. Nikolaev, E.A. Shikhova, D. Tahmassebi, T.T. Tidwell and S. Wang, *Journal of Organic Chemistry*, 2001, **66**, 8, 2611.

42. M.Ya. Melnikov and V.A. Smirnov, *Photochemistry of Organic Radicals*, Moscow State University, Moscow, Russia, 1994.

43. J.F.W. Keana, R.J. Dinerstein and F. Baitis, *Journal of Organic Chemistry*, 1971, **36**, 1, 209.

44. J.F.W. Keana and F. Baitis, *Tetrahedron Letters*, 1968, **9**, 3, 365.

45. A.I. Bogatyreva and A.L. Buchachenko, *Russian Chemical Reviews*, 1975, **44**, 2171.

46. S.A. Maslov and G.E. Zaikov, *Russian Chemical Reviews*, 1977, **46**, 1253.

47. Yu.B. Shilov, R.M. Batalova and E.T. Denisov, *Doklady Akademii Nauk SSSR*, 1972, **207**, 388.

48. Yu.B. Shilov and R.E.T. Denisov, *Vysokomolekulyarnye Soedineniya Seria A*, 1974, **16**, 2313.

49. T.G. Ilieva, E.E. Potapov and E.A. Polenov, *Kautchuk i Rezina*, 1989, 39.

50. N.M. Emanuel and A.L. Buchachenko, *Chemical Physics of Polymer Degradation and Stabilisation*, Science Press, Utrecht, The Netherlands, 1987.

51. V.A. Malchevsky and V.A. Zakrevsky, *Mekhanika Polimerov*, 1978, **2**, 342.

52. Yu.N. Rogov, F.V. Deyun, V.A. Anisin, L.P. Smirnov and G.B. Manelis, *Doklady Akademii Nauk SSSR*, 1983, **230**, 637.

53. K.B. Chakraborty and G. Scott, *Journal of Polymer Science, Part C: Polymer Letters Edition*, 1984, **22**, 10, 553.

54. K.B. Chakraborty and G. Scott, *Journal of Applied Polymer Science*, 1985, **30**, 8, 3267.

55. S. Al-Malaika and G. Scott in *Degradation and Stabilisation of Polyolefins*, Ed., N.S. Allen, Applied Science Publications, New York, NY, USA, 1983, p.219.

56. Yu.V. Korshak, A.A. Ovchinnikov, A.B. Shapiro, T.V. Medvedeva and V.N. Spector, *Journal of Experimental and Theoretical Physics Letters*, 1986, **43**, 309.

57. M. Iwamura and N. Inamoto, *Bulletin of the Chemical Society Japan*, 1967, **40**, 703.

58. A. Mackor, T.A. Wajer, T.J. De Boer and J.D. Van Voorat, *Tetrahedron Letters*, 1967, 2757.

59. S. Forshult, Z.C. Laggercrant and K. Torselle, *Acta Chemica Scandinavica*, 1969, **23**, 522.

60. S. Terabe and R. Kanoka, *Journal of the Chemical Society, Perkin Transactions 2*, 1972, **2**, 14, 2163.

61. A.R. Forrester and S.P. Hepburn, *Journal of the Chemical Society C: Organic Articles*, 1971, 701.

62. D. Rehorec and H. Hennig, *Canadian Journal of Chemistry*, 1982, **60**, 12, 1565.

63. A. Hudson, M.F. Lappert, P.W. Lednor, J.J. MacQuitty and B.K. Nicholson, *Journal of the Chemical Society Dalton Transactions*, 1981, **11**, 2159.

64. G. Russell, J. Geels and F.J. Smentowsti, *Journal of the American Chemical Society*, 1967, **89**, 15, 3821.

65. S. Terabe, K. Kuruma and R. Konaka, *Journal of the Chemical Society, Perkin Transactions 2*, 1973, **9**, 1252.

66. S. Terabe and R. Konaka, *Journal of the American Chemical Society*, 1971, **93**, 17, 4306.

67. M. Iwamura and N. Inamoto, *Bulletin of the Chemical Society Japan*, 1970, **43**, 756.

68. A. Bluhm and J. Weinstein, *Journal of Organic Chemistry*, 1972, **37**, 11, 1748.

69. N. Anderson and R. Norman, *Journal of the Chemical Society B: Physical Organic Articles*, 1971, 993.

70. E.G. Janzen and I. Lopp, *Journal of Magnetic Resonance*, 1972, **7**, 107.

71. Success in Chemistry and Biochemistry: Mind's Flight in Time and Space, Volume 4, Ed., G.E. Zaikov, Nova Science Publishers, NY, USA, 2009, p.626.

72. E.G. Janzen, *Accounts of Chemical Research*, 1971, **4**, 31.

73. E.G. Janzen and B.J. Blackburn, *Journal of the American Chemical Society*, 1969, **91**, 16, 4481.

74. R. Konaka, S. Terabe, T. Mizuta and S. Sakata, *Canadian Journal of Chemistry*, 1982, **60**, 12, 1532.

75. D.F. Church, *Journal of the American Chemical Society*, 1984, **106**, 18, 5073.

76. J.G. Paifici and H.L. Browning, *Journal of the American Chemical Society*, 1970, **92**, 17, 5231.

77. J.A. Howard and J.C. Tait, *Canadian Journal of Chemistry*, 1978, **56**, 2, 176.

78. V.E. Zubarev, V.N. Belevsky and S.P. Yarkov, *Doklady Akademii Nauk SSSR*, 1979, **244**, 1392.

79. C.L. Greenstock and R.H. Wiebe, *Canadian Journal of Chemistry*, 1982, **60**, 12, 1560.

80. P. Neta, S. Steenken and E.G. Janzen, *Journal of Physical Chemistry*, 1980, **84**, 5, 532.

81. W.A. Pryor, T.H. Lin and J.P. Stanley, *Journal of the American Chemical Society*, 1973, **95**, 6993.

82. E.G. Janzen, B. Knauer and J. Gerlock, *Journal of Physical Chemistry*, 1970, **74**, 9, 2037.

83. E.G. Janzen, B. Knauer and S.L. William, *Journal of Physical Chemistry*, 1970, **74**, 15, 3025.

84. P. Astolfi, M. Marini and P. Stipa, *Journal of Organic Chemistry*, 2007, **72**, 23, 8677.

85. P. Tormala, H. Lattila and J.J. Lindberg, *Polymer*, 1973, **14**, 10, 481.

86. F.D. Bluhm, J.E. Dikson and W.G. Miller, *Journal of Polymer Science Part B: Polymer Physics Edition*, 1984, **22**, 2, 211.

87. A.T. Bullock, G.G. Cameron and V. Krajewski, *Journal of Physical Chemistry*, 1976, **80**, 16, 1792.

88. S.L. Regan, *Journal of the American Chemical Society*, 1974, **96**, 16, 5275.

89. S.L. Regan, *Journal of the American Chemical Society*, 1975, **97**, 11, 3108.

90. T.A. Aleksandrova, A.M. Wasserman and A.A. Tager, *Vysokomolekulyarnye Soedineniya Seria A*, 1977, **99**, 1, 137.

91. J.R. Rasmussen, D.E. Bergbreiter and G.M. Whitesides, *Journal of the American Chemistry Society*, 1977, **99**, 14, 4746.

92. N.V. Kulikov, G.I. Likhtenshtein, E.G. Rozantsev, V.I. Suskina and A.B. Shapiro, *Biofizika*, 1972, **17**, 42.

93. E.G. Rozantsev and G.Ph. Novelko, *Vysokomolekulyarnye Soedineniya Seria B*, 1967, **9**, 866.

94. O.L. Lazareva, M.V. Motyakin, A.B. Shapiro and A.N. Shchegolikhin, *Synthetic Metals*, 1997, **85**, 1-3, 1685.

95. C. Freidrich, C. Noel, R. Ramassuel and A. Rassat, *Polymer*, 1980, **21**, 2, 232.

96. F.J. Hua and Y.L. Yang, *Polymer*, 2001, **42**, 4, 1361.

97. F. Sundholm, A.M. Wasserman, I.I. Barashkova, V.P. Timofeev and A.L. Buchachenko, *European Polymer Journal*, 1984, **20**, 7, 733.

98. O.H. Griffith, W.P.J. Keana, S. Rottshalffer and T.A. Warlick, *Journal of the American Chemical Society*, 1967, **89**, 19, 5072.

99. A.R. Forrester and P. Hepburn, *Journal of the Chemical Society C: Organic Articles*, 1971, **20**, 3322.

100. A.K. Kurusaki, K.W. Lee and M. Okawara, *Journal of Polymer Science Part A: Polymer Chemistry Edition*, 1972, **10**, 11, 3295.

101. D. Braun and S. Hauge, *Makromolekulare Chemie*, 1971, **150**, 57.

102. A.M. Wasserman, V.P. Timofeev, T.A. Aleksandrova and A.B. Shapiro, *European Polymer Journal*, 1983, **19**, 4, 333.

103. A.T. Bullok, G.G. Cameron and P.N. Smith, *European Polymer Journal*, 1975, **11**, 9, 617.

104. Y. Miura, K. Nakai and M. Kinoshita, *Makromolekulare Chemie*, 1973, **172**, 233.

105. V.A. Radzig, A.B. Shapiro and E.G. Rozantsev, *Vysokomolekulyarnye Soedineniya Seria B*, 1972, **14**, 685.

106. D.K.C. Hodgeman, *Journal of Polymer Science Part A: Polymer Chemistry Edition*, 1980, **18**, 2, 533.

107. G. Drefahl, H.H. Horhold and K.D. Hofmann, *Journal fur Praktische Chemie*, 1968, **37**, 137.

108. A.T. Bullok, G.G. Cameron and P.M. Smith, *Journal of Physical Chemistry*, 1973, **77**, 13, 1635.

109. A.T. Bullok, G.G. Cameron and P.M. Smith, *Polymer*, 1972, **13**, 2, 89.

110. A.T. Bullok, G.G. Cameron and J.M. Elson, *Polymer*, 1974, **15**, 2, 74.

111. G.R. Chalfont and M.J. Perkins, *Journal of the American Chemical Society*, 1968, **90**, 25, 7141.

112. S. Vivatpanachart, H. Nomura and Y. Miyahara, *Polymer*, 1981, **22**, 7, 896.

113. P. Zander and A. Karl-Friedrich, *Plaste und Kautsch*, 1986, **33**, 288.

114. T. Kitahara, S. Shimada and H. Kashiwabara, *Polymer*, 1980, **21**, 11, 1299.

115. G. Miclos, A. Rockenbauer and P. Tüdos, *Macromolecules*, 1987, **20**, 12, 3083.

116. N. Kusumoto and T. Sakai, *Polymer*, 1979, **20**, 10, 1175.

117. I.I. Barashkova, V.V. Martin, B.N. Anfimov and L.B. Volodarsky, *Vysokomolekulyarnye Soedineniya Seria B*, 1987, **29**, 354.

118. P. Rapta, A. Bartl and L. Dunsch, *Synthetic Metals*, 1997, **84**, 1-3, 187.

119. A.R. Katritzky, S.A. Belyakov, S. Strab, B. Cage and N.S. Dalal, *Tetrahedron Letters*, 1999, 407.

3 Interaction of Polymers with Nitric Oxide

Nitric oxide (NO) has a key role in many bioregulatory systems, including immune stimulation, platelet inhibition, neurotransmission, and relaxation of smooth muscle [1]. Its biosynthesis derives from nitric oxide synthases which catalyse the conversion of L-arginine to L-citrulline, resulting in NO release. Among the proposed NO storage components are protein-bound thionitrosyls and protein-bound dinitrosyl iron complexes (DNIC) $[Fe(NO)_2]_{protein}$ [2, 3]. The latter are derived from iron-sulphur cluster degradation in the presence of excess NO. Mobilisation of protein-bound NO could involve NO or $Fe(NO)_2$ unit transfer to small serum molecules such as glutathione, free cysteine, or other S-containing biomolecules. The hypothetical scheme can be expressed as follows [3]:

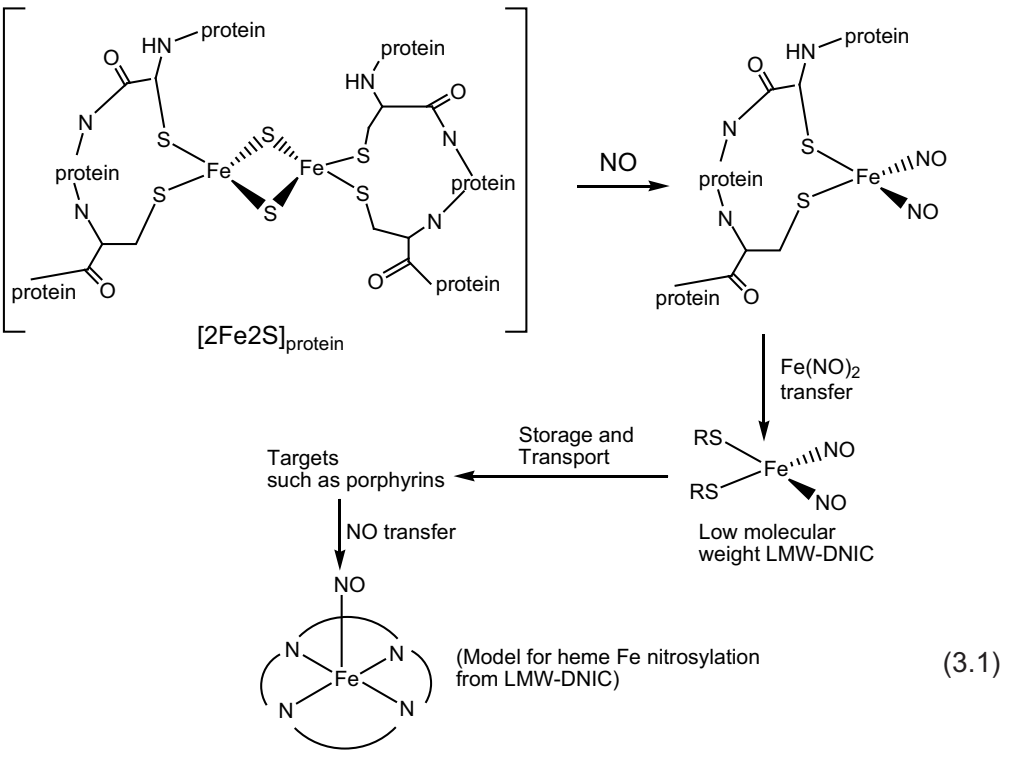

(3.1)

From the 1950s, NO has been known as air pollutant along with nitrogen dioxide (NO_2), but not so many data are available concerning its reactivity. Although NO contains an unpaired electron, on the scale of free radical reactivity it lies at the low rates for reactions with radical transfer and cannot abstract at room temperature even tertiary or allylic hydrogen atoms because the H–NO bond with a strength of 205 kJ/mol [4] is weaker than any C–H bonds in organic compounds. However, NO actively recombines with free radicals, and it is a well known inhibitor of chain radical reactions, and is the indicator for short-lived radicals generated by thermal and photochemical decompositions of organic molecules [5].

3.1 Interaction of NO with Organic Compounds

The fast reaction between NO and methyl radical has been studied repeatedly over the years [6–10]. The initial product of the interaction of methyl radical and NO is nitroso methane isomerising next into formaldoxime:

$$CH_3^{\bullet} + NO \rightarrow CH_3NO \rightarrow CH_2{=}N\text{-}OH \qquad (3.2)$$

The features of the mechanism of the reaction between methyl radical and NO were explained adequately on the basis of the formation and subsequent decomposition of formaldoxime [4]. This compound was first identified among the products of the thermal decomposition of di-*t*-butyl peroxide in an atmosphere of NO at 225 °C [7]. The rate constant for the reaction (**Equation 3.21**) has been determined through mass spectrometric studies of the thermal decomposition of dimethylmercury in NO [8]. In short reaction times at 480–900 °C, the major product of the interaction is CH_3NO (CH_2=N-OH). With long reaction times, NH_3, H_2O, HCN, CO_2, N_2, CO_2 and CH_3CN were also detected. Nitroso methane or its reaction products have not been found in the flash photolysis of azomethane-NO-neopentane mixtures [11]. However, the analysis procedure in this case required repeated condensation and evaporation of the products and excess reactants. Dimerisation and isomerisation to the non-volatile products $(CH_3NO)_2$ and $(CH_2{=}N\text{-}OH)_2$ probably resulted under these conditions, and nitroso methane (formaldoxime) and possible other products would not be detected by infrared (IR) measurements on the volatilised fraction of the condensate.

Acetone and a stable dimer of nitroso methane are major products of the photodecomposition of *t*-butyl nitrite at 25 °C [12]. It was suggested that dimer formation from nitroso methane monomer follows the primary process:

$$(CH_3)_3CONO \xrightarrow{h\nu} CH_3COCH_3 + CH_3NO \qquad (3.3)$$

The product composition indicates the formation of intermediate methyl radicals and NO which recombine. Nitroso methane dimers have *cis* and *trans*-isomer forms [13]

The IR technique has been used to determine directly the concentration of nitroso methane formed in the photolysis of azomethane in NO [9]. The following simple mechanism adequately describes the results obtained:

$$(CH_3)_2N_2 \xrightarrow{h\nu} 2CH_3^{\bullet} + N_2 \quad (3.4)$$

$$CH_3^{\bullet} + NO \longrightarrow CH_3NO \quad (3.5)$$

$$2\,CH_3NO \longrightarrow (CH_3NO)_2\ (gas) \quad (3.6)$$

$$(CH_3NO)_2\ (gas) \longrightarrow (CH_3NO)_2\ (solid\ at\ wall) \quad (3.7)$$

Dimers formed during the gas-phase reaction deposit as white powder on the walls of the reactor.

All other products observed in reactions $R^{\bullet}$ + NO can be considered to be a result of adding radicals and NO to the initial monomer product. For instance, photolysis of trifluoronitroso methane produces N,N-bis-trifluoremethylhydroxylamine nitrite [14]:

$$CF_3NO \xrightarrow{h\nu} CF_3^{\bullet} + NO \quad (3.8)$$

$$CF_3NO \xrightarrow{CF_3^{*}} [(CF_3)_2NO^{\bullet}] \xrightarrow{NO} (CF_3)_2NONO \quad (3.9)$$

In this process, the interaction of nitroso methane with NO formed can take place, so the thermal reactions of polyfluorinated nitroso compounds with NO have been studied in detail. It has been shown that NO interacts extremely easily at room temperature with examined nitroso compounds, and these mixtures in the gas phase give the characteristic brown colour of NO_2. A noticeable decay of nitroso compounds is not observed over several hours, i.e., nitroso compounds catalyse the redox disproportionation of NO. Within a few weeks, trifluoronitro methane and some quantities of *N*,*N*-bis-trifluoremethylhydroxylamine nitrite appear in reacting mixtures. The interaction of CF_3NO with NO is represented by the scheme:

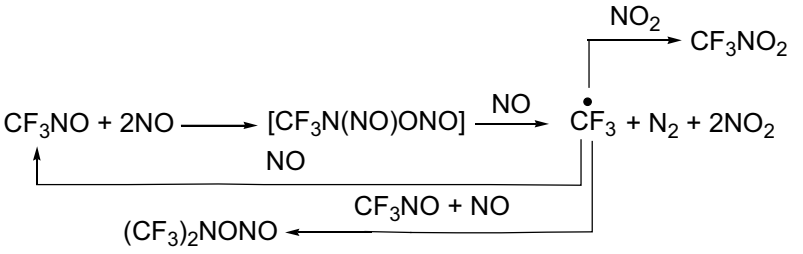

(3.10)

The study of reactions of polyfluorinated nitroso alkanes shows that nitroso groups actively accept NO with the formation of a nitroso-derivative of hydroxylamines.

The spin trapping of NO as aminoxyl radicals (ARs) R_1–NO•–R_2 was observed by electron spin resonance (ESR) spectroscopy in various radical reactions. For example, such ARs are formed in the course of the photodecomposition of 2,2'-azobisisobutyronitrile (AIBN) in aliphatic alcohols (methanol, ethanol, 2-propanol) [15]. In this case, R_1 is the radical N≡C–$C(CH_3)_2$ from AIBN, and R_2 is derived from alcohol molecules as a result of a hydrogen atom abstraction by R_1.

The distinctive feature of NO is the capability of forming weak reversible complexes with some stable free radicals. The formation of such complexes is characteristic of tyrosyl radicals identified in a number of enzyme systems [16]. The interaction of tyrosyl radicals with NO has been shown to inhibit enzyme activity. The reaction between photogenerated tyrosyl radicals and NO is near diffusion-limited with the rate constant of 1–2 × 10^9/M/s and gives 3-nitrosocyclohexadienone intermediate species. These species can reversibly regenerate the tyrosyl radical and NO or undergo rearrangement to form 3-nitrosotyrosine:

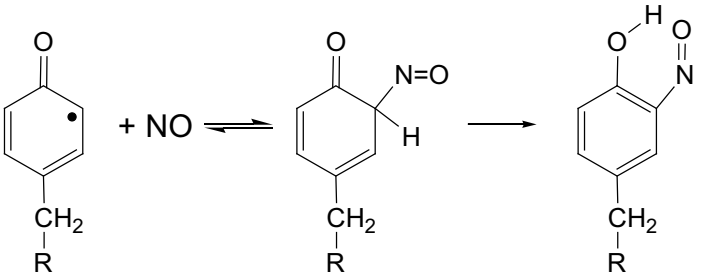

(3.11)

The 3-nitrosotyrosine is in equilibrium with its oxime tautomer which, as a result of one-electron oxidation, is converted into the tyrosine iminoxyl radical:

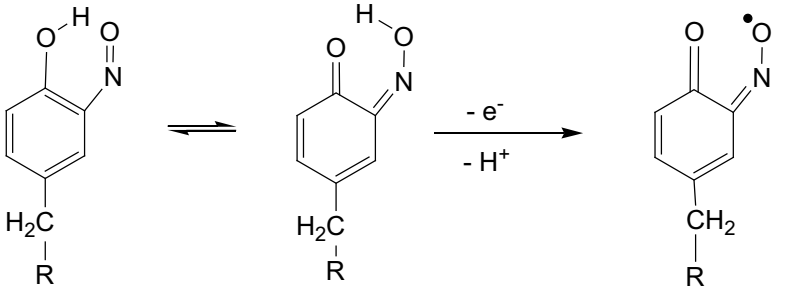

(3.12)

Iminoxyl radicals were detected in this system by ESR spectra on the basis of large isotropic HFI constants (a_N = 2.93 mT). As a source of the oxidation, light-driven reactions have been proposed.

Analogous reversible coupling NO was observed for stable phenoxyl radicals of phenolic antioxidants [17]: 2,4,6-tri-*tert*-butylphenol, 2,6-di-*tert*-butyl-4-methylphenol, α–tocopherol, 4,4′-methylene-bis-(2,6-di-*tert*-butylphenol), and phenyl-4,4′-methine-bis-(2,6-di-*tert*-butylphenol). The structures of the coupled products could be the nitrite or either the 2- or 4-nitrosocyclohexadienone, and for 2,4,6-tri-*tert*-butylphenol their formation can be represented by the scheme:

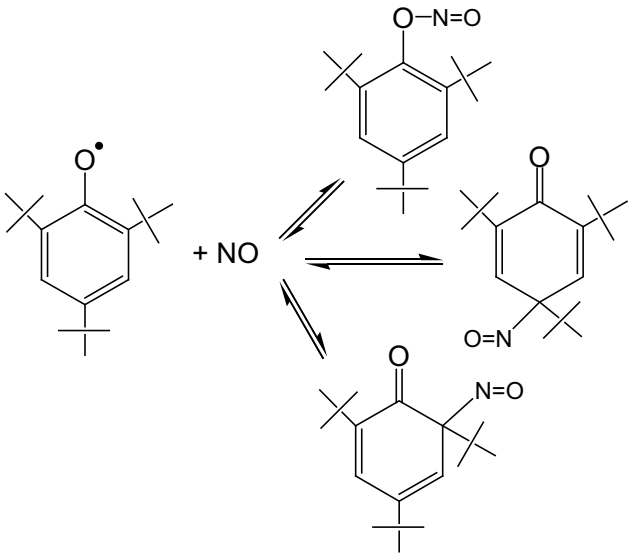

(3.13)

Analysis by chromatographic and nuclear magnetic resonance (NMR) methods shows that C-nitroso compounds are the major products of the reactions. The ratio of *para* isomer:*ortho* isomer is approximately 4:1. The reacting mixture in cyclohexane shows an ESR signal consisting of one broad line of low intensity. However, this signal

resolves into a triplet spectrum characteristic of 2,4,6-tri-*tert*-butylphenoxyl radical (a_H = 0.2 mT), when nitrogen is bubbled into the cyclohexane solution previously saturated with NO. The intensity of this signal is much greater than found in the presence of NO (approximately 20×). Thus, when excess NO is removed, the nitric oxide adduct slowly dissociates back to phenoxyl radical and NO.

Many studies are directed toward examining the mechanism of the NO interaction with unsaturated organic compounds. It has been reported that 5,6-di(propan-2-ylidene)cyclohexa-1,3-diene (I) reacts with NO to form a persistent AR [18]. Thus, (I) is the real nitric oxide trap:

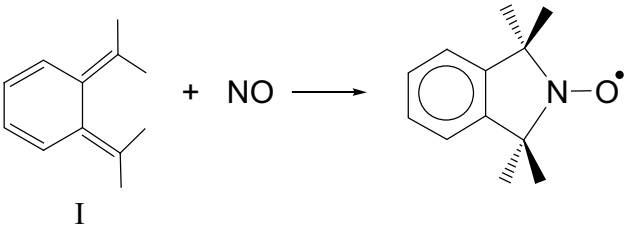

I (3.14)

The invention of (I) was driven by the need to monitor NO production. Formation of a persistent AR permits such monitoring by ESR. However, it is necessary to produce the diene trap (I) by the photolysis just prior to trapping NO because this compound is unstable:

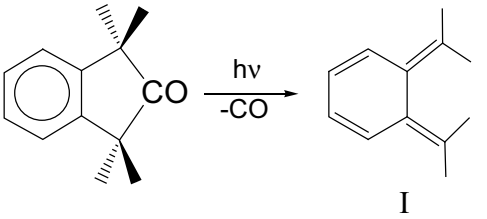

I (3.15)

A similar concept of NO trapping was proposed by the following reactions [19]:

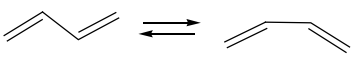

(3.16)

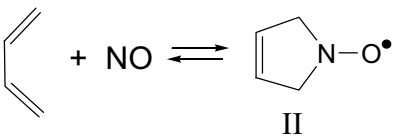

II (3.17)

This mechanism has been disputed. There was no reaction with butadiene itself, although ARs were formed when NO_2 was added. However, a variety of substituted butadienes did react with pure NO. Dilute solutions of 2,3-dimethylbuta-1,3-diene in inert solvents reacted very rapidly to give ARs having a quintet of triplets in the ESR spectrum indicative of four equivalent protons: a_N = 1.42 mT; a_H = 0.95 mT. In 2,5-dimethylhexa-2,4-diene, ARs have the typical value of isotropic HFI constant a_N = 1.45 mT. Solutions of phorone 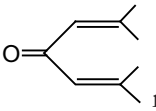 reacted completely in <60 s to give ESR triplets characteristic of ARs with a_N = 1.49 mT and a_H = 0.07 mT (2 H). The radical formed from 2,3-dimethylbuta-1,3-diene with four strongly coupled protons had the cyclic structure II. For phorone, all the results seem to favour simple addition, in which the only reasonable structure is III:

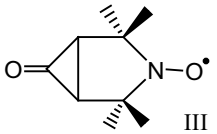

III

As the mass spectral analysis shows, electronically exited NO produced by ultraviolet (UV) light irradiation (λ = 226.5 nm and 214.4 nm) induces the decomposition of ethylene to acetylene and hydrogen [20]. Besides, a yellow solid deposit identical to that found from the photolysis of NO–acetylene mixtures is obtained in these conditions. The IR spectrum of the solid is consistent with an oxime or an amide group. Although its structure is uncertain, the solid appears to result from the addition of NO to C_2H_2. The radical formed may then add to another C_2H_2 and ultimately be terminated by collision with NO followed rearrangement to the oxime structure. As is known [21], NO inhibits the photosensitised polymerisation of acetylene. It is not clear what primary reactions lead to the formation of acetylene and molecular hydrogen. It is suggested that these products result from a molecular detachment process during the photolysis of NO-ethylene mixtures.

In the reactions using NO as a reagent, there is always a problem that the true active species is unidentified. This is due to the possibility that a trace amount of oxygen or a metal ion can function as a catalyst for the reaction of NO. Pure NO does not react with alkenes, for example, isobutene or similar alkyl-substituted olefins [22]. The main isolated products were found to be nitroalkenes, and it was postulated that the small amounts of NO_2 formed from the oxidation of NO:

$$2NO + O_2 \longrightarrow 2NO_2 \qquad (3.18)$$

added to the least sterically hindered end of the alkene double bond to produce β–nitroalkyl radicals:

$$NO_2 + CH_2{=}CR_2 \rightleftharpoons O_2NCH_2{-}C^{\bullet}R_2 \tag{3.19}$$

which were converted in several steps to nitroalkenes.

The product of the reaction of NO with cyclohexene under 7-atm pressure was shown to be bis (1-nitroso-2-nitrocyclohexane) [23]. That is, the dimer of the nitroso compound formed by initial addition of NO_2 to cyclohexene and subsequent coupling of the β–nitrocyclohexyl radical with NO:

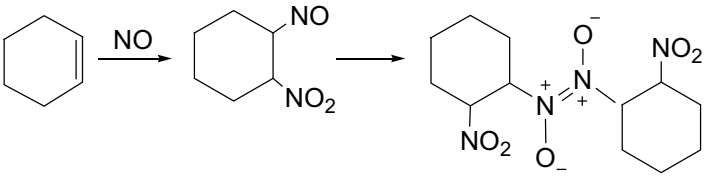

(3.20)

NO_2 arose from the disproportionation of NO:

$$3NO \longrightarrow N_2O + NO_2 \tag{3.21}$$

The disproportionation is important at high pressures and it was still significant at 7-atm pressure.

It was considered that direct addition of NO to alkenes or polyenes may be favoured by the presence of stabilising substituents or by additional double bonds in the substrate because both of these situations lead to increased resonance stabilisation of the adduct radical by delocalisation of the unpaired electron:

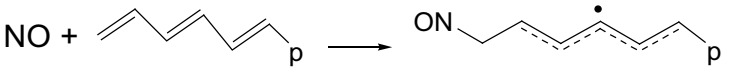

(3.22)

This affirmation has been tested by ESR spectroscopy and product analysis of the reactions of pure NO and of NO-air mixtures with alkenes containing electron-withdrawing and electron-releasing substituents as well as dienes [22], fatty acids [24] and β-carotene [25]. It has been shown that ARs can be detected in the reaction of NO with all these compounds. In the complete absence of air, no ESR spectra in alkenes were obtained. However, when some quantity of air was introduced into the NO gas stream, ESR spectra appeared. Pure NO therefore does not add directly to alkenes containing acceptor or donor substituents or to dienes. The thermodynamic stabilisation due to electron delocalisation (**Equation 3.18**) was not sufficient to alter

the balance in favour of formation of β-nitroso alkyl radicals. The reaction could be initiated by addition of NO_2 to the double bond of each unsaturated molecule [26–28]. Brown [26] conducted an exhaustive study of the NO-isobutylene reaction and concluded that the major products of the reaction were formed via a free-radical mechanism initiated by addition of the NO_2 impurity to the double bond. He reported that rigorously purified NO did not react with liquid olefins, even on prolonged contact. The main question here is the source of NO_2, i.e., the oxidative reaction (**Equation 3.18**) of NO with traces of oxygen or the disproportionation reaction (**Equation 3.21**). By the example of 2,5-dimethylhexa-2,4-diene (IV), a mechanism of AR formation in dienes under the action of NO can be represented as follows [22]:

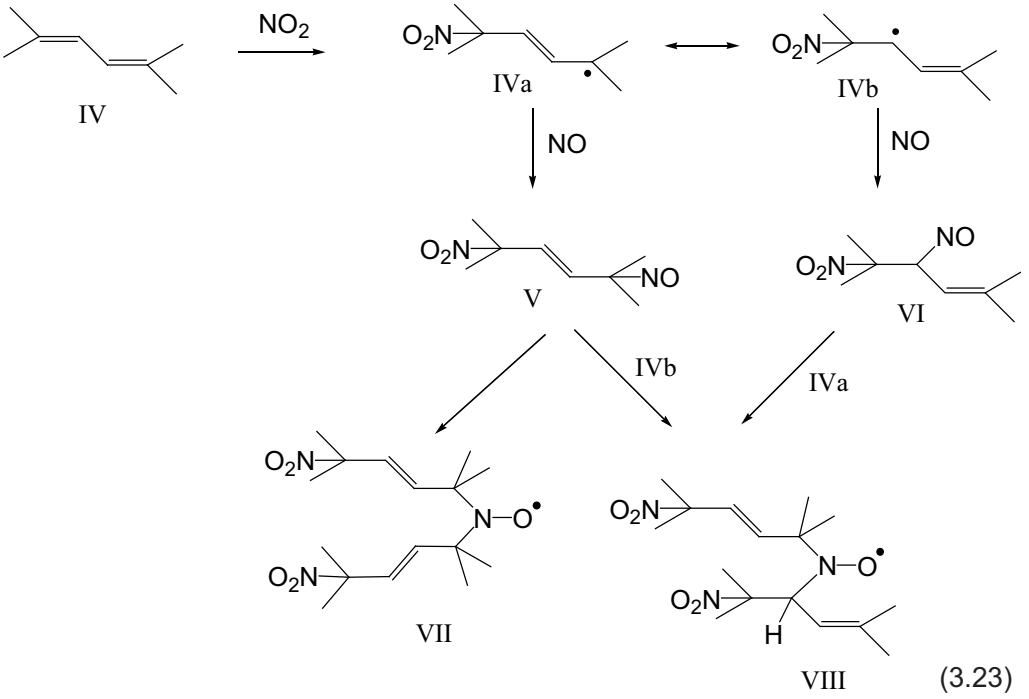

(3.23)

The important feature of radicals IVa and IVb is that they contain a delocalised allyl unit. It follows that NO can couple at each end of the allyl system to give two different nitroso compounds V and VI, both of which may couple with other allyl radicals IVa and IVb at either end to give a mixture of the dialkylaminoxyl radicals VII and VIII. The AR VII will be the most stable and hence dominates. The one β-hydrogen of the radical VIII enables disproportionation to occur, and its lifetime will be much shorter and its stationary state concentration much lower.

Pure NO does not react directly with many organic compounds, but it becomes a strong nitrosating agent in the presence of molecular oxygen via reaction (**Equation 3.18**) and subsequent conversion into N_2O_3. For instance, the interaction of NO-O_2 mixture with cycloalkyl alcohols in acetonitrile produces the corresponding nitrites [29]:

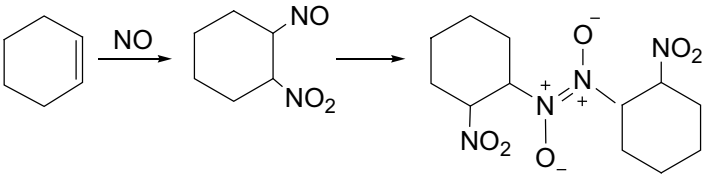

(3.24)

This process can be considered to be a direct method for preparing alkyl nitrites in very good yields in organic solvents, thus avoiding many restrictions caused by the low solubility of organic compounds in aqueous medium:

$$ROH + N_2O_3 \longrightarrow RONO + HNO_2 \qquad (3.25)$$

This reaction apparently may be used for converting polyalcohols (e.g., ribose or glucose) or other substrates of biological interest into the corresponding nitrites.

The action of NO containing traces of O_2 at room temperature causes a cleavage of epoxide rings [30, 31]. The reactions proceed in a highly stereoselective manner with the formation of hydroxy nitrates in 91% yield:

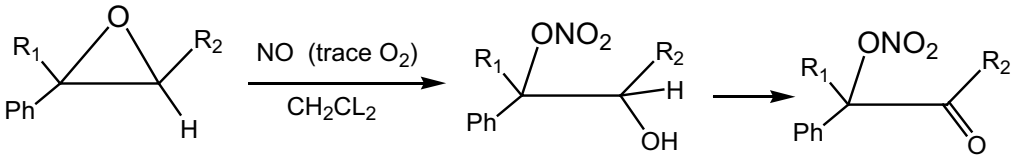

(3.26)

The reaction is assumed to be initiated by NO_2 impurities.

In the presence of O_2, NO shows sufficiently high reactivity in reactions with nitrogen-containing organic compounds. It has been found that primary aromatic amine reacted with NO + O_2 in benzene to give triazene derivatives in 60–64% yield [32]. The proposed reaction mechanism includes the formation of intermediate N-nitroso compounds in reaction with dimers of NO_2:

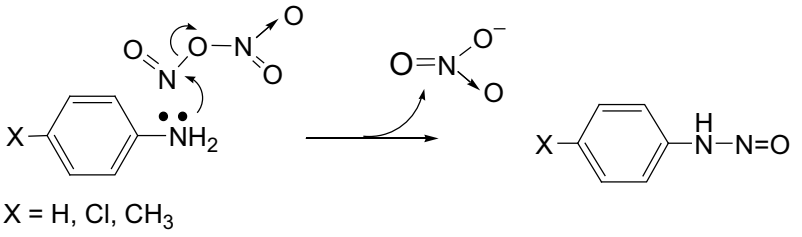

(3.27)

The nitroso compound containing the α-hydrogen atom turns into corresponding oxime and then the diazonium ion:

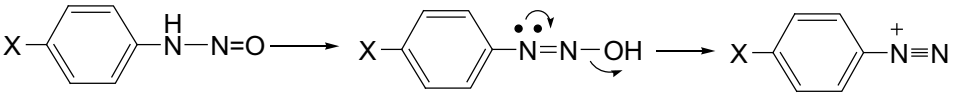

(3.28)

Triazenes are formed in the subsequent reactions:

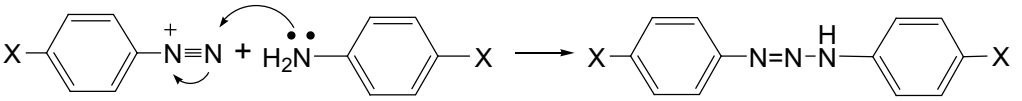

(3.29)

In the course of study of the reaction of NO with aromatic amines, the effect of solvents on the reaction mechanism has been established. NO reacts in ethereal solvents (tetrahydrofuran (THF), dioxane, ethoxy ethane (EtOEt), dimethylether (DME)) or chloroform to give deamination products [33]. This solvent effect was explained by the competitive decomposition of diazonium ions via accepting an electron from NO to give the phenyl radical, and hydrogen (H)-atom abstraction from the solvent leads to the deamination product:

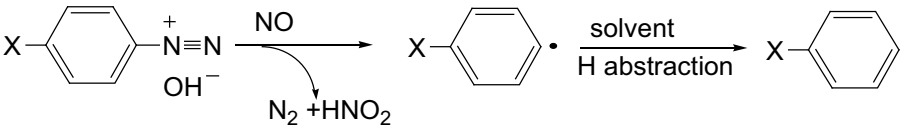

(3.30)

In benzene, the reaction pathway connected with the H-atom abstraction from solvent molecules is not realised, and triazene derivatives are mainly formed in similar conditions. The reaction of NO with secondary and tertiary amines in the presence of oxygen gives *N*-nitrosamines as the main products [34]. These compounds cannot apparently isomerise into oximes similar to reaction (**Equation 3.28**) and are stabilised.

The action of NO has been used as a simple and easy method of the oxidation of 1,4-dihydropyridines [35]:

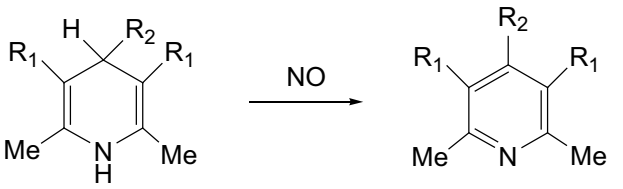

(3.31)

This process of aromatisation occurs in quantitative yields (98%) in benzene or CH_3CN solutions in absence and presence of oxygen. However, a plausible reaction mechanism remains unclear.

Thus, compounds which contain an N-H bond may react with NO in various ways under the influence of O_2. When arylhydrazines reacted with NO in THF in the presence of oxygen, benzene derivatives were obtained (60–80%) accompanied by small amounts of arylazides (3–9%) [36]:

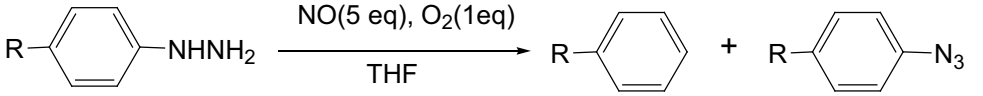

R = NO_2, Cl, H, Me, OMe

(3.32)

There is a slight tendency for electron-withdrawing substituents to afford lower selectivity in the reaction (**Equation 3.32**); the ratio of yields of benzene derivatives to arylazides changes from 9 for R = OMe to 2.44 for R = NO_2.

There has been much interest in the synthesis and investigation of *N*-nitrosoamides, which are known to be potent carcinogens. Nitrosation by the use of NO has been reported [37]:

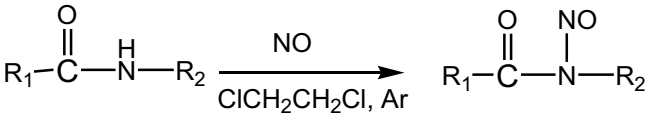

(3.33)

This reaction system can exclude oxygen at least to the order of 1 µl of O_2 in 22.4 ml of NO. The solvent effect was investigated using Ph-C(=O)-NH-CH_2Ph as a substrate. The yields of *N*-nitrosoamides suggest that oxygen-containing solvents (acetone,

THF, CH_3OH, dimethylformamide (DMF)) are totally ineffective. On the contrary, the use of non-oxygen solvents such as CCl_4 or 1,2-dichloroethane resulted in the formation of *N*-nitrosoamides in good yields (77–94%). The influence of oxygen was investigated for elucidation of the active species of the reaction (**Equation 3.32**). The addition of O_2 linearly increased the yield of *N*-nitrosoamides. Thus, it is undeniable that the reaction proceeded by participation of a trace amount of N_2O_3.

Because of the deep interest of the chemistry of α–aminoacide–*N*–carboxyanhydrid es in peptide synthesis, many attempts have been undertaken to develop an efficient method of obtaining these compounds. Nitrosation of *N*–carbamoyl–valine with the system NO/O_2 yields the N–nitroso–*N*–carbamoyl–valine which decomposes into α–isocyanatoacid which is converted into the anhydride [38]:

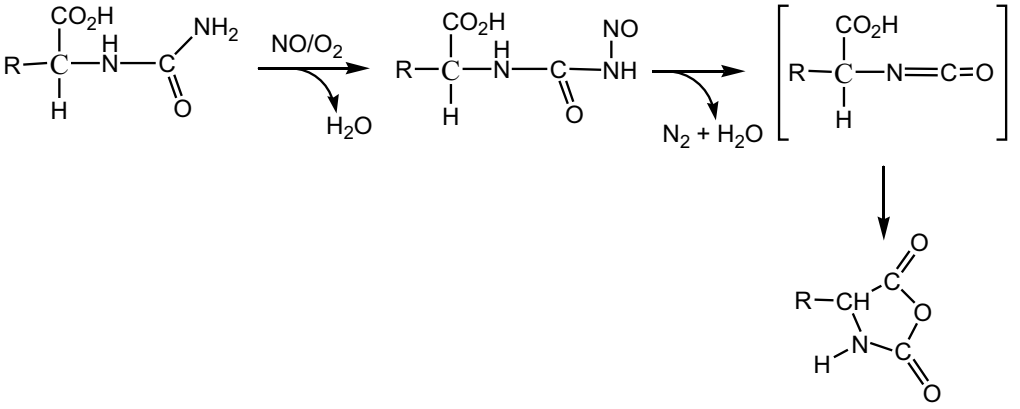

(3.34)

This method uses mild conditions, works quantitatively, and liberates only H_2O and N_2 as accompanying products. This reaction has been done with other amino acids (alanine, phenylalanine, leucine) with the same quantitative yield.

Although in many reactions NO behaves as a monomeric species or in the form N_2O_3, it undergoes a pressure- and temperature-dependent dimerisation in anaerobic conditions. The NO electrophilic dimer has been spectrally characterised at low temperatures [39]. The structure of the dimers in the gas phase was determined from measurements of rotational transition frequencies for $^{14}NO–^{14}NO$, $^{15}NO–^{15}NO$. The NO dimer is weakly bound with a binding energy of ~16 kJ/mol. Solid-phase data were interpreted to be due to a planar *cis*-structure with the NNO angle of 99.6°, and with NN and NO distances of 2.23 Å and 1.16 Å, respectively. As has been shown by kinetic means [40], these dimers are important in reactions with bromine, chlorine, oxygen, and hydrogen. The kinetics of the reaction $2NO + Cl_2 \rightarrow 2NOCl$ may be

treated in the same manner as the reaction of NO with O_2; the activation energy of the reaction is 4.78 kcal/mol.

On the basis of the structure of the products established, it has been proposed that NO dimers can behave as an electron pair-acceptor in reactions with a series of Lewis bases [41]. In particular, diethylamine reacts by the following scheme:

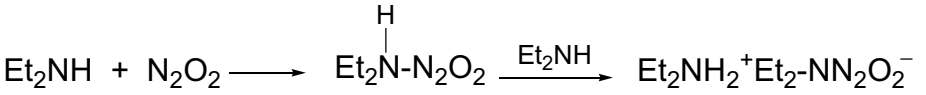

(3.35)

Many nucleophiles can add to two NO molecules with the resulting adducts being a diazeniumdiolate ($B\text{-}N^+(O^-)=N\text{-}O^-$) [42]:

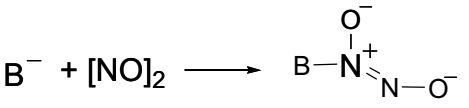

(3.36)

These *N*-bound diazeniumdiolates decompose in aqueous media, releasing NO. They are useful as NO donors in biomedical research. On the basis of their thermal decomposition behaviour, C-diazeniumdiolate compounds can be considered as high energy density materials. Similar to traditional explosives, diazeniumdiolate-substituted compounds also derive energy from the oxidation of the carbon backbone during their decomposition. To understand the NO reaction chemistry with carbanions and to synthesise potentially high-energy compounds, the reactions of NO with enolates derived from aliphatic methyl ketones containing α-methylene or α-methyne groups and with enolates derived from α,α′-dimethylene or α,α′-dimethine groups have been studied [42]. It has been shown that the reactions of the ketones with NO progress more rapidly at lower temperatures (–20 °C) than at room temperature. The solvent for these reactions is ideally methanol because it reacts comparatively slowly (or not at all) with NO under these conditions. In a typical reaction, 1 equiv of the substrate is added to freshly prepared solution of 1–5 equiv of sodium metal or potassium metal dissolved in absolute methanol. The reaction of NO with a *cis*- and *trans*-isomeric mixture (1:4) of 2,6-dimethylcyclohexanone in the presence of potassium methoxide proceeds smoothly, yielding the *cis*- and *trans*-α,α′-bisdiazeniumdiolated products:

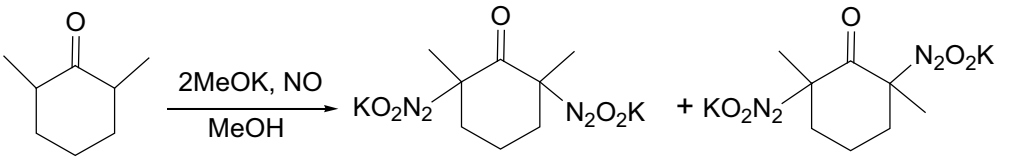

(3.36)

There are specific substrate preferences for the observed diazeniumdiolations which follow the trend α-CH > α-CH_2 > α-CH_3 for the ketones.

The reaction of NO with the double bonds of enamines also produces compounds containing the diazeniumdiolate functional group bound to carbon, and some of the compounds prepared in this way have the potential to serve as spontaneous NO donors [43]. The compounds chosen for study were enamines 1–4 derived from condensation of cyclopentanone or cyclohexanone with morpholine or pyrrolidine. When these enamines were dissolved in acetonitrile and treated with NO gas (5-atm pressure) at room temperature, a vigorous exothermic reaction resulted, accompanied by high uptake of NO and formation of a brown precipitate. Attempts to isolate the solid precipitates often resulted in rapid decomposition, with the release of large volumes of gaseous NO. At –78 °C in diethyl ether, the reaction of 4-(1-cyclohexen-1-yl) morpholine (IX) afforded a good yield of crystalline NO addition product (X):

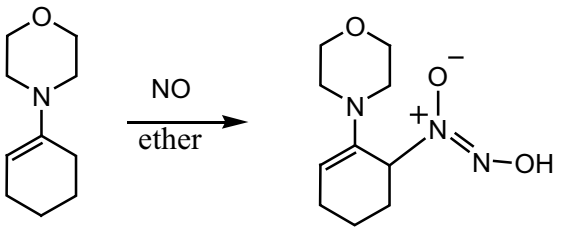

IX X

(3.37)

When a sample of X was dissolved in CD_3CN, the proton NMR spectrum obtained was fully consistent with structure X. However, when sample X was dissolved in D_2O, the proton spectrum revealed that the preferred tautomer was a zwitterion (XI):

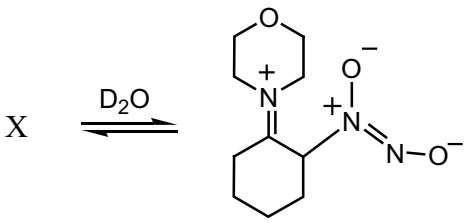

XI

(3.38)

The reaction of NO with more hindered enamines was confirmed by direct formation of a zwitterion (XIII) from 4-(cyclohexylidenemethyl)morpholine (XII) in good yield:

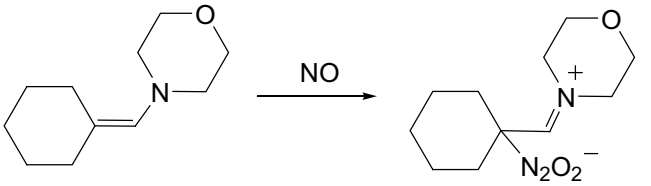

XII XIII (3.39)

Thus, the results stated above demonstrate that pure NO does not react with mono olefins, and that NO_2 impurities are responsible for the observed reactions of alkenes with NO. Traces of NO_2 are present in reactions with enamines and ketones, and the electrophilic reaction prevails. This may have implications for interpreting the behaviour of NO produced in physiological processes. Oxygen is present in most of the environments (atmospheric or biological) where NO chemistry occurs. It is essential to consider radical and ionic chemistry in developing an understanding of these systems.

3.2 Reactions of NO with Macroradicals Generated by the Photolysis and Radiolysis of Polymers

Because of the low reactivity of pure NO in reactions of atom abstraction as well as addition to double bonds, direct interaction of this reactant with most synthetic polymers does not occur. However, the chemical modification of macromolecules in an atmosphere of NO in conditions of the simultaneous generation of macroradicals takes place due to spin trapping via the formation of nitroso compounds. The structure of stable nitrogen-containing radicals formed from nitroso compounds in the subsequent reactions gives information on the mechanism of proceeding processes in polymers under the action of various radical-initiating factors.

3.2.1 Synthesis of Spin-Labelled Fluorinated Polymers by Free-Radical Reaction in the Presence of NO

It is a difficult problem to introduce spin traps in fluorinated polymers, for instance, polytetrafluoroethylene (PTFE), which is chemically inert, rigid, and insoluble. Rexroad and Gordy [44] observed the ESR spectrum of stable nitrogen-containing radicals when PTFE samples were γ-irradiated in NO. The three components of the

spectrum are approximately equal in intensity and have equal spacing of 2.8 mT. The radical produced by X- or γ-irradiation of PTFE in a vacuum has the structure ~ $CF_2CF^{\bullet}CF_2$ ~ (XIV). When NO is admitted to a sample previously irradiated in a vacuum, the signal from the fluorocarbon macroradical quickly disappears by direct addition of NO. When a PTFE sample is irradiated in the presence of NO, probably all free radicals produced from the PTFE itself decay immediately in recombination with NO. The authors [44] do not give an interpretation of the triplet ESR spectra, assuming that the radicals must be formed by addition of NO to molecular fragments or ions which have an even number of electrons.

The mechanism of reactions of NO with γ-irradiated PTFE and a copolymer of tetrafluoroethylene with hexafluoropropylene (TFE-HFP) has been considered in detail [45–51]. Stable ARs were not detected in PTFE samples irradiated in an atmosphere of NO at room temperature, only a signal of stable iminoxyl radicals ~ $F_2C-\overset{\overset{N-O^{\bullet}}{\|}}{C}-CF_2$ ~ (XV) was recorded in this polymer [46]. The splitting between components of its ESR spectrum of 2.8 mT and g = 2.0040 coincide with those observed in [44]. After pumping of irradiated samples, the intensity of ESR signals increases by 3–4 times. The intensity increase with moving of NO denotes the formation of weak non-paramagnetic complexes of radicals XV with NO. The formation of iminoxyl radicals XV in the course of radiolysis of PTFE in the presence of NO is the result of the following reactions [46]:

$$\text{PTFE} \xrightarrow{\gamma} \sim CF_2{-}CF^{\bullet}{-}CF_2 \sim + NO \rightarrow \sim CF_2{-}CF(NO){-}CF_2 \sim \xrightarrow{\gamma}$$

$$\sim CF_2{-}C^{\bullet}(NO){-}CF_2 \sim \longrightarrow \text{XV} \qquad (3.40)$$

It has also been demonstrated [52] that interaction of NO with radiation-produced macroradicals XIV at 150–200 °C leads to their decay without the production of ARs. The absence of ARs in irradiated PTFE was explained by the hindrance of spatial migration of the free valence within the rigid matrix of the fluorinated polymer in which the nitroso compounds formed by recombination of XIV with NO cannot serve as spin traps. It has been noted [52] that PTFE samples irradiated in air and exposed to NO at room temperature exhibit an ESR spectrum tentatively assigned to aminoxyl macroradicals, but the conditions under which these radicals are formed have not been clearly defined. Furthermore, to reliably identify the radicals by their solid-phase spectra, one should assess isotropic values with the appropriate parameters of low-molecular perfluoroalkylaminoxyl radicals studied thoroughly in the liquid phase [53, 54].

The spectra of powdered PTFE samples furnish insufficient information to permit similar estimations. Oriented PTFE films were used to: (i) ascertain the nature of the radicals; (ii) gain additional information about the mechanism of their formation; and (iii) show the feasibility of their application as spin labels [47]. It has established that:

1. Exposure of fluoroalkyl macroradicals at 25–250 °C to NO does not produce nitrogen-containing radicals,
2. If peroxy radicals were synthesised by post-radiation oxidation of alkyl radicals, nitrogen-containing radicals were not detected after exposure of the samples to NO for 120 hours,
3. Exposure to NO of PTFE powder containing a mixture of middle and terminal peroxy radicals and γ-irradiation at room temperature in air leads to the formation of nitrogen-containing radicals whose ESR spectrum is displayed in **Figure 3.1**:

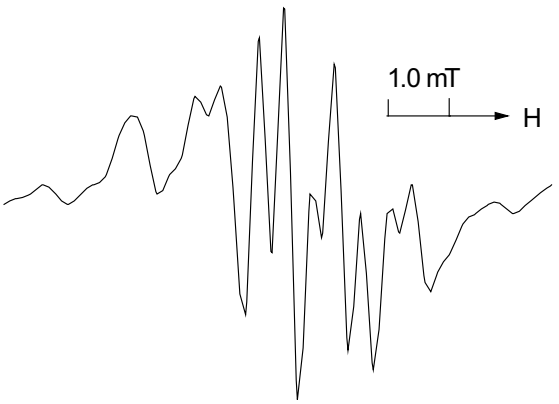

Figure 3.1 ESR spectrum of oriented PTFE films γ-irradiated in air and exposed to NO for 96 h at 298 K

Formation of these radicals required a long time of sample exposure to NO (≥48 hours). The amount of radicals accumulated after 70-hour exposure to NO was 1.5×10^{-4} mol/kg.

4. Formation of nitrogen-containing radicals is not associated with the reactions of NO_2 produced by NO interaction with peroxy radicals. This was evidenced by

experiments in which NO was removed immediately after decay of the peroxy radicals, and the samples were exposed for 96 hours to NO_2. Nitrogen-containing radicals were not detected in this case.

Thus, to produce nitrogen-containing radicals distinguishable in their structure from radical XV one should initially conduct γ-radiolysis of PTFE samples in air to accumulate peroxy radicals. The presence of $RO_2^{\bullet}$ radicals alone is insufficient. Some other products arising in PTFE in the course of radiolysis in air must be present. Nitrogen-containing radicals form as a result of the secondary reactions in which valence-saturated compounds participate, transforming in an atmosphere of NO.

After γ-irradiation of non-oriented PTFE films in air, evacuation, and subsequent long-term exposure to NO, the same spectrum as in powder samples was recorded. Oriented PTFE films were investigated by two procedures. In the first case, the axis of sample rotation was perpendicular to the film-stretching direction and to the constant magnetic field. In this case, rotation of samples leads to changes in angle α between the magnetic field and stretching direction, and an unambiguous dependence of ESR parameters on angle α is obtained. At room temperature and α = 0°, the spectrum is a triplet consisting of quintets with splittings of 0.46 mT in the triplet, 1.11 mT in the quintet, and with a *g*-factor of 2.0060. At α = 90°, splitting increases to 1.12 mT in the triplet and to 1.61 mT in the quintet; *g* = 20071. Triplet splitting is associated with coupling between unpaired electrons and the nitrogen nucleus, and quintet splitting with four magnetically equivalent fluorine atoms.

The observed interval of the *g*-factor values at various α is characteristic of ARs. Therefore, in analyzing ESR spectra, the anisotropic magnetic parameters determined for low-molecular ARs were used [47]. It is commonly recognised for low-molecular ARs that the *z* axis is aligned with the 2*p*-orbital of the unpaired electron of the N atom, and that this direction determines the maximum value of the A^N-tensor and *g*-tensor value close to that for free electrons. The *x* axis is aligned with the N–O bond characterised by the maximum value of the *g*-tensor (2.0088–2.0104) and small (0.5–0.7 mT) A^N value. The *y* axis determines a *g*-tensor value of 2.006–2.007, and the hyperfine coupling (HFC)-tensor value approximately corresponds to A_{xx}^{N} [55].

If we assume that PTFE macromolecules are mostly aligned with the direction of film stretching, then the *y* axis of ARs is parallel to the macromolecule axis: $g_{II} = g_{xx}$ and $A_{II}^{N} = A_{yy}^{N}$. In the case of alkyl and peroxy PTFE macroradicals, rotational or torsional vibrations around the axes of macromolecules average g_{xx} and g_{zz} values, as well as A_{xx} and A_{zz}. Then within the model of the magnetic field perpendicular to the stretching direction, $g_{\perp} = (g_{xx} + g_{zz})/2$ and $A_{\perp} = (A_{xx} + A_{zz})/2$. The isotropic values of the *g*-factor and HFC constants are $g = (2\,g_{\perp} + g_{II})/3 = 2.0067$ and $a^N = (2\,A_{\perp} +$

A_{II})/3 = 0.90 mT. These isotropic values can be compared with the appropriate values for perfluoroaminoxyl radicals in the liquid phase. For example, for $(n - C_3F_7)_2NO^{\bullet}$ and $(n - C_7F_{15})_2NO^{\bullet}$ radicals at room temperature, the *g*-factor values are 2.0070 and a_N = 0.877 and 0.875 mT, respectively [56]. Thus, the dataset obtained shows that the radicals observed (**Figure 3.1**) are ARs with the structure $\sim F_2C-\overset{\overset{O^{\bullet}}{|}}{N}-CF_2\sim$. Hyperfine coupling of the unpaired electron with fluorine β-atoms is also anisotropic with the minimum and maximum values observed at α = 0° and α = 90°, respectively. The isotropic HFC constants for fluorine atoms can be assessed by the formula $\alpha_{\beta}^{F} = (A_{II}^{F} + 2A_{\perp}^{F})/3 = (1.1 + 3.23)/3 = 1.4$ mT. This value is greater than α_{β}^{F} for $(n - C_3F_7)_2NO^{\bullet}$ and $(n - C_7F_{15})_2NO^{\bullet}$ radicals in the liquid phase equal to 0.966 and 0.974, respectively [56]. However, a close value ($\alpha_{\beta}^{F} = 1.38$ mT) was observed in the liquid phase for $(CH_3COOCF_2)_2NO^{\bullet}$ radicals [53].

As indicated above, to form ARs one should carry out PTFE radiolysis in air. That is, both peroxy radicals directly reacting with NO and some product formed in radiolysis under these conditions participate in their synthesis. The mechanism must be such that ARs formed as a result of a sequence of a few reactions in stretched films should be oriented in space identically. Oriented radicals may form whenever the process producing them does not require significant displacements of the reagents in space. That is, they are obtained from adjacent intermediate products and retaining the initial orientation of macromolecules. Based on the aforesaid, the following mechanism of aminoxyl macroradical synthesis has been proposed. In an oxygen-containing atmosphere, part of the middle alkyl radical XIV formed in the course of irradiation under the effect of high-energy factors can decompose with rupture of the main chain:

$$\sim CF_2-CF_2-CF^{\bullet}-CF_2\sim \xrightarrow{\gamma} \sim CF_2^{\bullet} + CF_2=CF-CF_2\sim \qquad (3.41)$$

In the absence of oxygen in the rigid PTFE matrix, the reverse reaction of these radical proceeds efficiently. In the presence of oxygen, the terminal alkyl macroradicals can be oxidised to form terminal peroxy radicals which interact with double bonds much slower. Under the action of NO on samples containing neighbouring terminal double bonds and peroxy radicals, the latter are converted into macromolecular nitrates and nitrites [47]:

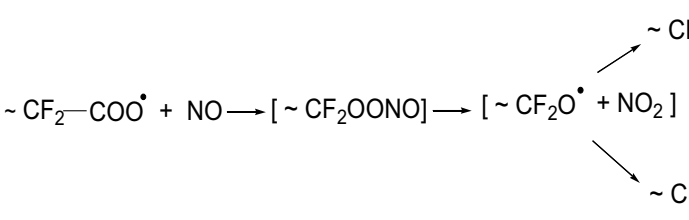

(3.42)

(3.43)

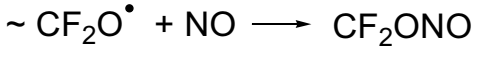

(3.44)

As has been established [45], one or both of the nitrogen-containing products and alkoxy radicals decompose at 90 °C at a significant rate to produce terminal alkyl macroradicals:

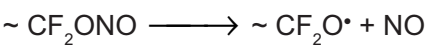

(3.45)

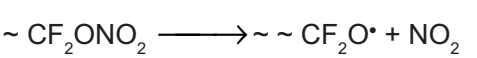

(3.46)

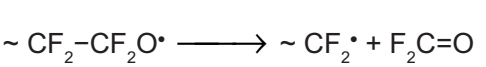

(3.47)

Terminal alkyl macroradicals recombine with NO to produce terminal nitroso groups neighbouring to the terminal double bonds. Similar decomposition and formation of terminal nitroso groups also takes place at room temperature. This supposition is supported by the fact that ARs are synthesised only after long-term exposure of irradiated PTFE to NO. The adjacent terminal double bonds and formed terminal nitroso compounds can enter in a reaction to synthesise ARs:

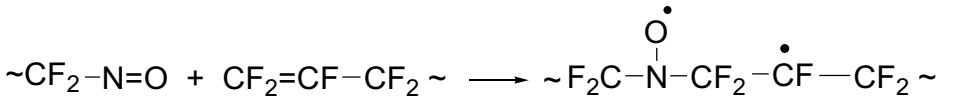

(3.48)

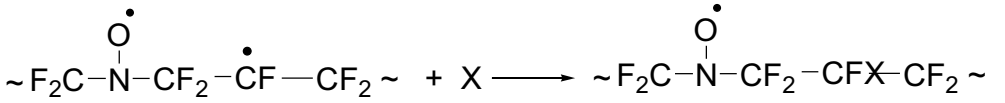

(3.49)

where X = NO or NO_2.

Thus, free-radical PTFE conversions in an NO atmosphere synthesise in the polymer bulk thermally stable spin-labelled macromolecules whose concentration is sufficient to investigate the molecular dynamics of this polymer by ESR spectroscopy. The advantage of the suggested method is that the AR fragment is incorporated in the main macromolecule chain without disturbing its orientation and motion.

A similar procedure was used to obtain spin-labelled TFE-HFP [49]. The presence of hexafluoropropylene (HFP) groups in this polymer leads to disturbance of the structural ordering typical of PTFE to more complex dynamics of their motion. After γ-irradiation of powders and films of TFE-HFP copolymer in air, there are three types of stable peroxy macroradicals in the samples: end radicals ~ CF_2–$CF_2O_2^{\bullet}$, secondary middle-chain radicals ~ CF_2–$CF(OO^{\bullet})$–CF_2 ~, and tertiary middle-chain radicals ~ CF_2–$C(CF_3)(OO^{\bullet})$–CF_2 ~. In contrast to PTFE, prolonged exposure (>100 hours) of these samples in a NO atmosphere at room temperature does not lead to the formation of aminoxyl macroradicals. However, two types of macroradicals are formed if TFE-HFP is heated with evacuation after the decay of radicals in a NO atmosphere. At 90 °C, the ESR spectrum demonstrates the presence of tertiary alkyl macroradicals ~ CF_2–$C^{\bullet}(CF_3)$–CF_2 ~ formed upon decay of the tertiary nitroso compounds [57]. On further increasing of the temperature up to 180 °C, the tertiary alkyl macroradicals radicals disappear, and the signal of ARs ~ $F_2C-\overset{\overset{O^{\bullet}}{|}}{N}-CF_2$ ~ is retained in the ESR spectrum. ARs in TFE-HFP form non-paramagnetic complexes with NO, which readily decompose at 25 °C in a vacuum.

The analysis of ESR spectra of ARs was done on oriented films of TFE-HFP [49]. Two series of oriented samples were studied. In the first series, the direction of the film drawing, coinciding with the long axis of macromolecules, was perpendicular to the axis of the rotation in the external magnetic field. The dependence of the values of *g*-factor and hyperfine splitting on nitrogen nuclei and fluorine nuclei on the angle α between the directions of drawing and magnetic field was obtained for these samples: α = 0°, g = 2.0060, A_N = 0.54 mT, A_F = 1.09 mT, and α = 90°, g = 2.0071, A_N = 1.09 mT, A_F = 1.51 mT. In the second series, the direction of the macromolecular orientation coincided with the axis of sample rotation, whereas the magnetic field was perpendicular to the axis of molecules for all values of α. In this case, the ESR spectra remained unchanged during sample rotation, and the values of *g*-factor and hyperfine splitting coincided with the corresponding values obtained in the previous series of experiments for the macromolecular axis oriented perpendicular to the magnetic field.

It has been concluded from the above results that the *g*-tensor and HFC tensor have axial symmetry with one of the tensor axes coinciding with the macromolecular axis. The data obtained allow us to calculate the isotropic values of the *g*-factor and the constants of splitting on nitrogen nuclei and fluorine nuclei: $g_{iso} = (g_{I} + 2g_{\perp})/3 = 2.0068, a_{N} = (A_{I}^{N} + 2A_{\perp}^{N})/3 =$ 91 mT and $a_{F} = (A_{I}^{F} + 2A_{\perp}^{F})/3 =$ 37mT. A comparison of the isotropic parameters of the ESR spectra of ARs in PTFE and TFE-HFP copolymers demonstrates that both polymers have the same values of *g*-factor, constants of splitting on the nitrogen nucleus, and similar a_{F} values. These data indicate that the radicals in both polymers not only have identical chemical structure, but also identical conformations.

ARs 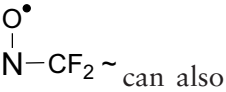 can also be generated in samples initially containing alkyl macroradicals. If the gaseous products of radiolysis are removed from the samples preliminarily γ-irradiated in a vacuum, and then NO is admitted into the tube, alkyl radicals exhibit fast decay. The ESR spectrum recorded upon heating of these samples in a vacuum at >90 °C contains the signals of alkyl and aminoxyl macroradicals. At 180 °C, the samples show an almost pure spectrum of aminoxyl macroradicals. A disadvantage of this method of preparation of aminoxyls is a lower yield compared with that for samples irradiated in air. This is evidently connected to the fact that nitroso compounds formed by the action of NO on alkyl macroradicals are less stable than the products of NO interaction with peroxy radicals. These nitroso compounds begin to decompose with NO emission at >130 °C, and prolonged heating of samples at ≥180 °C is necessary for decay of the macroradicals formed. ARs also partially decay at this temperature, so the yield of stabilised ARs is lower for the sample irradiated in a vacuum than that for samples irradiated in air.

One more type of aminoxyl macroradicals is observed in a powdered TFE-HFP γ-irradiated in air after exposure in a NO atmosphere and subsequent evacuation, followed by photolysis in a He atmosphere by light at λ > 260 nm at 25 °C [49]. In this case, a new type of aminoxyl macroradical is formed. The ESR spectrum of these radicals consists of eight HFC lines with 6.7-mT splitting between the edge lines and *g* = 2.0067. The radicals are stable up to 180–190 °C, do not interact with oxygen, and readily form decomposing nonparamagnetic complexes with NO. An ESR spectrum of this type is expected for ~ CF_2–NO•–CF_3 radicals if their five β-fluorine atoms are magnetically equivalent and $A_N = A_F(CF_3) = A_F(CF_2)$. Photolysis of TFE-HFP samples γ-irradiated in a vacuum and then exposed to NO does not lead to the formation of ARs. This indicates that one step of AR synthesis is photolysis of the products formed upon the interaction of NO with peroxy macroradicals of the copolymer.

The mechanism of the conversion of free radicals in fluorinated polymers reflects the introduction of NO into the middle of the main chain without changing its orientation and the possible formation of $CF_3^{\bullet}$ radicals in the system under the action of light. The ARs appear in the temperature range where the tertiary nitroso compounds decay in the vacuum with the regeneration of tertiary alkyl macroradicals ~ CF_2–$C^{\bullet}(CF_3)$–CF_2 ~. As has been established [58], these tertiary macroradicals decay in an inert atmosphere. Decay of these radicals requires spatial transfer of free valence. The first step of radical decay is β-decomposition by the reaction [59]:

$$\sim CF_2{-}C^{\bullet}(CF_3){-}CF_2{-}CF_2 \sim \longrightarrow \sim CF_2{-}C(CF_3){=}CF_2 + {}^{\bullet}CF_2{-}CF_2 \sim \tag{3.50}$$

In the presence of NO formed upon decomposition of the tertiary nitroso compounds, the terminal radicals can be converted into terminal nitroso compounds reacting with the adjacent double bond and forming aminoxyl macroradicals:

$$NO + {}^{\bullet}CF_2{-}CF_2 \sim \longrightarrow ON{-}CF_2{-}CF_2 \sim \tag{3.51}$$

$$\sim CF_2{-}C(CF_3){=}CF_2 + ON{-}CF_2{-}CF_2 \sim \longrightarrow \sim$$
$$CF_2{-}C^{\bullet}(CF_3){-}CF_2{-}NO^{\bullet}{-}CF_2 \sim \xrightarrow{+X}$$
$$\sim CF_2{-}C(CF_3)(X){-}CF_2{-}NO^{\bullet}{-}CF_2 \sim \tag{3.52}$$

where X is a low-molecular radical, for example, NO or NO_2.

This mechanism explains why ARs are formed in TFE-HFP samples irradiated in a vacuum and in air. The ~ CF_2–$NO^{\bullet}$–CF_3 radicals can be formed by interaction between the $CF_3^{\bullet}$ radical and the terminal nitroso compound ~ CF_2–N=O or between the CF_3NO and terminal fluoroalkyl macroradicals ${}^{\bullet}CF_2$–CF_2 ~. The scheme of the process presented below along with reactions explains radical formation in the system under the action of light [49]:

$$\sim CF_2{-}CF(OO^{\bullet}){-}CF_2 \sim + NO \longrightarrow \sim CF_2{-}CF(ONO_2){-}CF_2 \sim \tag{3.53}$$

$$\sim CF_2{-}CF_2{-}OO^{\bullet} + NO \longrightarrow \sim CF_2{-}CF_2{-}ONO_2 \tag{3.54}$$

$$\sim CF_2{-}C^{\bullet}(CF_3){-}CF_2 \sim + NO \longrightarrow \sim CF_2{-}C(CF_3)(NO){-}CF_2 \sim \tag{3.55}$$

$$\sim CF_2{-}CF(ONO_2){-}CF_2 \sim \xrightarrow{h\nu} \sim CF_2{-}CF(O^{\bullet}){-}CF_2 \sim + NO_2 \quad (3.56)$$

$$\sim CF_2{-}CF_2{-}OONO_2 \sim \xrightarrow{h\nu} \sim CF_2{-}CF_2O^{\bullet} + NO_2 \quad (3.57)$$

$$\sim CF_2{-}C(CF_3)(NO){-}CF_2 \sim \xrightarrow{h\nu} \sim CF_2{-}C^{\bullet}(CF_3){-}CF_2 \sim + NO \quad (3.58)$$

$$\sim CF_2{-}CF(O^{\bullet}){-}CF_2 \sim \longrightarrow \sim CF_2{-}CF{=}O + {}^{\bullet}CF_2{-}CF_2 \sim \quad (3.59)$$

$$\sim CF_2{-}CF_2O^{\bullet} \longrightarrow \sim CF_2{-}CF_2^{\bullet} + F_2C{=}O \quad (3.60)$$

$$\sim CF_2{-}CF_2^{\bullet} + NO \longrightarrow \sim CF_2{-}CF_2{-}NO \quad (3.61)$$

$$\sim CF_2{-}C^{\bullet}(CF_3){-}CF_2 \sim + NO_2 \longrightarrow \sim CF_2{-}C(CF_3)(ONO){-}CF_2 \sim$$

$$\xrightarrow{h\nu} \sim CF_2{-}C(CF_3)(O^{\bullet}){-}CF_2 \sim + NO \longrightarrow CF_3^{\bullet} + \sim CF_2{-}CO{-}CF_2 \sim \quad (3.62)$$

$$CF_3^{\bullet} + NO \longrightarrow CF_3NO \quad (3.63)$$

$$CF_3^{\bullet} + ON{-}CF_2{-}CF_2 \sim \longrightarrow CF_3{-}NO^{\bullet}{-}\ CF_2{-}CF_2 \sim \quad (3.64)$$

$$CF_3NO + {}^{\bullet}CF_2{-}CF_2 \sim \longrightarrow CF_3{-}NO^{\bullet}{-}\ CF_2{-}CF_2 \sim \quad (3.65)$$

This sequence of reactions explains why $CF_3{-}NO^{\bullet}{-}\ CF_2{-}CF_2 \sim$ radicals are not formed during the photolysis of polymer samples irradiated in a vacuum and then exposed to NO. Under these conditions, there is no formation of the nitrates whose photolysis produces the NO_2 necessary for the conversion of tertiary alkyl radicals to the corresponding alkoxide macroradicals and then to $CF_3^{\bullet}$. Thus, aminoxyl macroradicals obtained in the TFE-HFP copolymer are optimal spin labels. Behaviour of $\sim CF_2{-}C(CF_3)(X){-}CF_2{-}NO^{\bullet}{-}CF_2 \sim$ radicals can reflect the motion of the segments located in the middle of polymer chain, whereas the ESR spectra of $CF_3{-}NO^{\bullet}{-}CF_2{-}CF_2 \sim$ radicals contain information about the movements of terminal groups of macromolecules.

3.2.2 Photolysis of Polymethylmethacrylate and Acetyl Cellulose in NO

During the photolysis of polymethylmethacrylate (PMMA) in an atmosphere of NO by unfiltered light of a mercury lamp at room temperature, the formation of acylalkylaminoxyl radicals such as R_1–NO•–C(=O)–OR_2 was observed with typical parameters of the anisotropic triplet ESR spectrum in a solid phase: $A_{II}^{N} = 2.1 \pm 0.1$ mT and $g_{II} = 2.0027 \pm 0005$ [48, 50, 51, 60]. If photolysis of the same samples is carried out at 383 K, dialkylaminoxyl radicals R_1–NO•–R_2 in addition to acylalkylaminoxyl radicals are produced with parameters of the ESR spectrum: $A_{II}^{N} = 3.2 \pm 0.1$ mT and $g_{II} = 2.0026 \pm 0005$. Under the action of filtered UV light (260–400 nm) at room temperature, there is a third type of stable radical, namely iminoxyls R_1–C(=NO•)–R_2, which in the benzene solution of PMMA is characterised by a triplet ESR spectrum with the isotropic parameters: $a_N = 2.8$ mT and $g = 2.005$. The occurrence of acylalkylaminoxyl radicals is evidence of eliminating methoxycarbonyl radicals in the course of polymer photolysis:

$$\sim(CH_3)C(COOCH_3)–CH_2–(CH_3)C(COOCH_3)\sim \xrightarrow{h\nu}$$

$$\sim(CH_3)C(COOCH_3)–CH_2–(CH_3)C^{\bullet}\sim (R^{\bullet}) + {}^{\bullet}COOCH_3 \qquad (3.66)$$

The subsequent reaction with participation of NO gives acylalkylaminoxyl radicals:

$${}^{\bullet}COOCH_3 + NO \rightarrow O{=}N–COOCH_3 \xrightarrow{+R^{\bullet}} R–NO^{\bullet}–COOCH_3 \qquad (3.67)$$

Macroradicals $R^{\bullet}$ can decompose [61], and dialkylaminoxyl radicals are formed as follows:

$$R^{\bullet} \xrightarrow{kT} \sim(CH_3)C(COOCH_3)–CH_2–(CH_3)C{=}CH_2$$

$$+ {}^{\bullet}C(CH_3)(COOCH_3)\sim \xrightarrow{+NO,R^{\bullet}}$$

$$R–NO^{\bullet}–C(CH_3)(COOCH_3)\sim \qquad (3.68)$$

Iminoxyl radicals appear as a result of the generation of macroradicals ~(CH_3) $C(COOCH_3)$–$C^{\bullet}H$–$(CH_3)C(COOCH_3)\sim$ ($R_1^{\bullet}$), for example, in the reaction of PMMA

macromolecules with methoxycarbonyl radicals:

$$\sim(CH_3)C(COOCH_3)–CH_2–(CH_3)C(COOCH_3)\sim + {}^{\bullet}COOCH_3 \rightarrow R_1^{\bullet} + HCOOCH_3 \quad (3.69)$$

The radical $R_1^{\bullet}$ in an atmosphere of NO is converted into nitroso compounds and further into oximes:

$$R_1^{\bullet} + NO \longrightarrow R_1–NO \longrightarrow$$

$$\sim(CH_3)C(COOCH_3)–C(=NOH)–(CH_3)C(COOCH_3) \sim (R_1–NOH) \quad (3.70)$$

As a result of the mobile hydrogen-atom abstraction from oximes by reactive methoxycarbonyl radicals, iminoxyls are formed:

$$R_1–NOH + {}^{\bullet}COOCH_3 \rightarrow HCOOCH_3 + R_1N{=}O^{\bullet} \quad (3.71)$$

A limiting stage of reaction (**Equation 3.67**) is NO diffusion into a polymeric matrix. The rate of reaction (**Equation 3.68**) should depend much more on the mobility of macromolecular reagents. Therefore, the distinction in the composition of radicals in PMMA photolysed at room temperature and 383 K is observed. At room temperature, acylalkylaminoxyl radicals are formed due to acceptance of low-molecular methoxycarbonyl radicals ${}^{\bullet}COOCH_3$ by nitroso compounds. At 383 K, when molecular mobility essentially grows, dialkylaminoxyl radicals $R_1–NO^{\bullet}–R_2$ are formed because the meeting of two macromolecular particles occurs. The results obtained demonstrate an opportunity of using NO for elucidation of the polymer photolysis mechanism. With the help of this reactant, it was possible to establish the nature and mechanism of formation of intermediate short-lived radicals in photochemical process using ESR spectra of stable ARs.

In acetyl cellulose (AC) photolysed at room temperature in the presence of NO, the ESR spectra of dialkylaminoxyl ($A_{II}^{N} = 3.1$ mT, $g = 2.0026$) and acylalkylaminoxyl ($A_{II}^{N} = 2.0$mT, $g = 2.0032$) radicals are recorded [60]. The removal of NO from AC samples leads to increasing the signal of acylalkylaminoxyl radicals. This effect is connected to the formation of non-paramagnetic complexes of the radicals with NO. Dialkylaminoxyl radicals do not form such complexes in AC. The accumulation of acylalkylaminoxyl radicals in AC is determined by acetoxyl radicals ${}^{\bullet}C(=O)CH_3$, which split-off from macromolecules owing to light absorbance. Dialkylaminoxyls are formed with participation of methyl radicals also generated by photolysis.

3.2.3 Radiolysis of Acetyl Cellulose and Polymethylmethacrylate in NO

After irradiation of AC in an atmosphere of NO, a very weak ESR signal is observed. After evacuation, the intensity of the ESR spectrum increases sharply, at that the quantity of radicals increases with elevation in temperature and duration of pumping [60]. As in the case of PMMA, the effect observed is conditional on the decomposition of non-paramagnetic complexes of NO with radicals. The ESR spectrum is interpreted as an anisotropic triplet with the axial symmetry of *g*-tensor and HFI-tensor: $A_{II}^{N} = 4.5 \pm 0.1$ mT, $A_{\perp}^{N} = 2.4 \pm 0.1$ mT, $g_{II} = 2.0025 \pm 0005$, $g_{\perp} = 2.0054 \pm 0005$. Such values of ESR parameters enable identification of the radicals as iminoxyls [62]. Iminoxyl radicals decay gradually in the solution of AC in benzene, and the signal of acylalkylaminoxyl radicals R_1–NO•–C(=O)–R_2 remains in the ESR spectrum. In contrast with photolysed AC, dialkylaminoxyl radicals in γ-irradiated samples were not observed. In the solid phase and an inert atmosphere, iminoxyl radicals are sufficiently stable and decay at T > 120 °C with complete disappearance at 165 °C.

The γ-radiolysis of PMMA at room temperature in an atmosphere of NO as well as photolysis leads to the formation of acylalkylaminoxyl radicals. The evacuation of samples at elevated temperatures gives rise to the appearance of the signal of iminoxyl radicals in the ESR spectrum. As distinct from photolysis, γ-radiolysis can stimulate hydrogen-atom detachment from the C–H bonds of macromolecules and, consequently, the formation of primary and secondary macromolecular nitroso compounds takes place in an atmosphere of NO. Such nitroso compounds are rapidly isomerised into oximes [63]. The abstraction of hydrogen atoms from the OH groups of oximes by active free radicals results in the formation of iminoxyl radicals [64]. This viewpoint is confirmed by the observation of ESR spectra of iminoxyl radicals in γ-irradiated PMMA and AC in the presence of NO.

3.3 Interaction of Polymeric Hydroperoxides with NO

The phenomenon of hydroperoxide decomposition under the action of NO was studied using macromolecular peroxides and their low-molecular analogues [65, 66]. It has been shown [66] that NO-induced decomposition of polypropylene (PP) hydroperoxides leads to the formation of low-molecular hydrocarbons, which is indicative of the degradation of macromolecules. The primary stage of the decomposition is represented by the reaction [65, 66]:

$$\text{ROOH} + \text{NO} \longrightarrow \text{RO}^{\bullet} + \text{HONO} \qquad (3.72)$$

The reaction of hydroperoxides with NO can also proceed with the formation of peroxy radicals:

$$ROOH + NO \longrightarrow ROO^{\bullet} + HNO \quad (3.73)$$

At high hydroperoxide concentrations in solution, the process was described as decomposition of hydroperoxide dimers by NO [65]:

$$(ROOH)_2 + NO \longrightarrow ROH + HONO + ROO^{\bullet} \quad (3.74)$$

Pryor and co-workers [67] gave evidence that NO_2, which is a more active radical as compared with NO, cannot directly decompose hydroperoxides. The reaction is induced by non-paramagnetic dimers of N_2O_4. In this context, the scheme including the reactions (**Equations 3.72–74**) is not evident.

Important information on the nature of reactions involved in the decomposition of hydroperoxides in an atmosphere of NO can be extracted from kinetic data of ROOH consumption, and dependence of the overall process rate on NO pressure Kinetics were studied at room temperature using PP hydroperoxides [68]. The consumption rate of hydroperoxide is initially low and then increases sharply (**Figure 3.2**).

The character of the kinetic curves cannot be explained from the mechanism presented by the reactions (**Equation 3.72–74**). According to these reactions, based on the direct interaction of hydroperoxides with NO, the rate of decomposition is maximal at the beginning of the process and decreases with a decrease in the concentration of ROOH. The shape of the kinetic curves is characteristic of autoaccelerated reactions with an induction period.

According to ESR data [68], the decomposition of PP hydroperoxides in NO is accompanied by the formation of dialkylaminoxyl radicals (anisotropic triplet with $g_{II} = 2.0024 \pm 0.0003$ and $A_{II}^{N} = 3.1 \pm 0.1$mT). Upon pumping out NO, the ESR spectrum displays an additional signal due to acylalkylaminoxyl radicals with $g_{II} = 2.0026 \pm 0.0003$ and $A_{II}^{N} = 2.1 \pm 0.1$ mT. This signal is not observed in the ESR spectrum of non-evacuated samples because acylalkylaminoxyl radicals form non-paramagnetic complexes with NO molecules [59]. ARs were not found in the control PP samples free of hydroperoxides. Similar to the kinetics of hydroperoxide decomposition, the accumulation of ARs exhibits an induction period which depends on the concentration of NO. However, the limiting concentrations of radicals differ only slightly and amount to ~2.2×10^4 mol/kg.

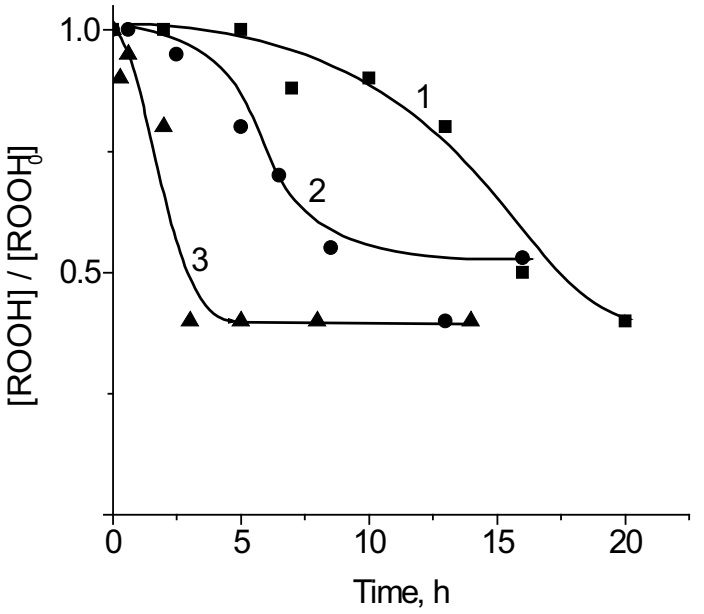

Figure 3.2 Kinetics of consumption of PP hydroperoxides at [NO] = 1.6×10^{-3} (1), 3.2×10^{-3} (2), and 4.1×10^{-3} mol/l (3)

An analysis of the kinetic data shows that the induction period of AR accumulation is well reproduced for a given NO concentration in the same series of measurements. However, the duration of this period varies from one series to another, and may significantly change depending on experimental conditions. For example, prolonged (for several days) evacuation of the vacuum line, employed to fill the tubes with NO, resulted in a marked increase in the induction period. The period increased even more when thorough evacuation of the system was followed by slow admission of NO into tubes with oxidised PP via a U-shaped trap cooled to –95 °C. These results lead to the conclusion that the induction periods for hydroperoxide decomposition and AR accumulation are very sensitive to trace amounts of impurities of higher nitrogen oxides (or substances capable of producing these oxides upon interaction with NO). Indeed, adding 3×10^{-6} mol/l NO_2 to 3×10^{-3} mol/l NO results in the complete disappearance of the initial slow period of hydroperoxide decomposition by the reaction of ROOH with NO_2 alone. The impurities introduced into the system with NO and affecting the induction period serve as a 'seed' in the autoaccelerated process. The maximum rates of hydroperoxide decomposition and AR accumulation depend primarily on the gas-phase concentration of NO that determines the formation of a product responsible for the accelerated decomposition of hydroperoxide. Note that the catalytic effect of trace concentrations of NO_2 was observed in the reactions of NO with alkenes [26].

In general, autoacceleration kinetics is characteristic of autocatalytic processes and degenerate-branched chain reactions. The process involves the stages of initiation, accumulation of the product responsible for the accelerated hydroperoxide decomposition, and free-radical reactions leading to the formation of ARs.

The reactions (**Equation 3.72–73**) cannot be the initiating factors of hydroperoxide decomposition. The reaction (**Equation 3.72**) is exothermic, but its stable products are nitrites and alcohols. However, the products of PP hydroperoxide conversion in an atmosphere of NO consist predominantly of macromolecular nitrates. The reaction (**Equation 3.73**) is strongly endothermic and, hence, unlikely to proceed at room temperature. Dependence of the induction period on the degree of purity of NO indicates that reactions involving trace amounts of higher nitrogen oxides control the initiation process. Consequently, the interaction of hydroperoxide with NO proceeds according to the reaction:

$$ROOH + N_2O_3 \longrightarrow [ROONO] + HNO_2 \qquad (3.75)$$

with the formation of thermally unstable peroxynitrite. The latter exhibits a high rate of conversion according to the scheme:

$$[ROONO] \longrightarrow [RO^{\bullet} + NO_2] \longrightarrow RONO_2 \qquad (3.76)$$

$$[RO^{\bullet} + NO_2] \longrightarrow RO^{\bullet} + NO_2 \qquad (3.77)$$

In the solid phase, the recombination of radicals in the 'cage' is highly efficient, whereas the escape of NO_2 and $RO^{\bullet}$ radicals from the 'cage' is quite low. Alkoxy radicals $RO^{\bullet}$ generated in reactions (**Equation 3.77**) decompose or enter into substitution reactions with neighbouring macromolecules to form chain $R_c^{\bullet}$ and end $R_e^{\bullet}$ alkyl macroradicals as well as low-molecular alkyl radicals $r^{\bullet}$. The appearance of the latter radicals in the reaction of PP hydroperoxide with NO was verified in [66]:

$$RO^{\bullet} \longrightarrow R_c^{\bullet}(R_e^{\bullet}, r^{\bullet}) \qquad (3.78)$$

The reaction of alkyl radicals with NO leads to the formation of macromolecular and low-molecular nitroso compounds:

$$R_c^{\bullet}(R_e^{\bullet}, r^{\bullet}) + NO \longrightarrow R_cNO(R_eNO, rNO) \qquad (3.79)$$

The increase in the rate of hydroperoxide decomposition with time relates to reactions proceeding with participation of such nitroso compounds. There are two variants of these processes. As is known, the interaction of nitroso compounds with hydroperoxides in the liquid phase results in intensive decomposition of the latter into free radicals [69]:

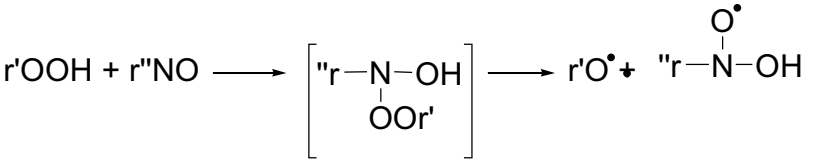

(3.80)

The alkoxyalkylaminoxyl radicals have low stability and decompose according to the reaction:

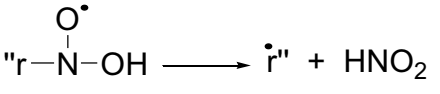

(3.81)

The alkyl radicals formed in the system stimulate the hydroperoxide decomposition:

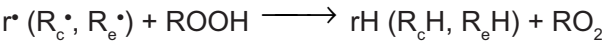

(3.82)

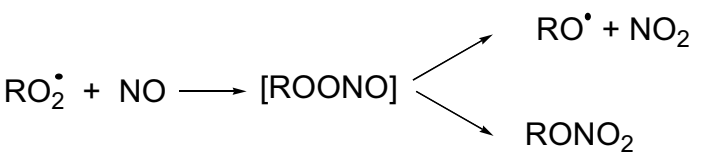

(3.83)

(3.84)

Thus, the set of reactions (**Equations 3.78–3.84**) leads to degenerate chain branching. Moreover, the nitrous acid formed in reactions (**Equations 3.75 and 3.81**) increase the initiation rate via the reaction:

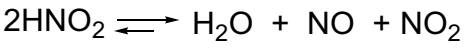

(3.85)

with the equilibrium shifted to the right at room temperature.

Another process that increases the rate of hydroperoxide decomposition is disproportionation of NO to N_2 and $NO_3^{\bullet}$, which proceeds with the participation of nitroso compounds and favours accumulation of NO_2 in the reacting system [26]:

$$RNO + 2NO \longrightarrow [R{-}N{=}N{-}ONO_2] \longrightarrow$$

$$[R^{\bullet} + N_2 + {}^{\bullet}ONO_2] \rightarrow RONO_2 + N_2 \quad (3.86)$$

$$[R^{\bullet} + N_2 + {}^{\bullet}ONO_2] \rightarrow R^{\bullet} + N_2 + NO_3^{\bullet} \quad (3.87)$$

$$NO + NO_3^{\bullet} \longrightarrow 2NO_2 \quad (3.88)$$

Reactions (**Equations 3.87 and 3.88**) stimulate an increase of NO_2 concentration, resulting in the acceleration of reaction (**Equation 3.75**) and the formation of nitrates. Alkyl radicals R• formed in the NO disproportionation in the cage reaction (**Equation 3.86**) also give nitrates.

The formation of nitroso compounds in PP is confirmed by the synthesis of ARs via the reaction

$$R_1^{\bullet} + R_2NO \longrightarrow R_1{-}NO^{\bullet}{-}R_2 \quad (3.88)$$

in which one of the reagents can be a low-molecular species. ARs were not found to form when hydroperoxide decomposition was induced by pure NO. The reactions presented above suggest that trace amounts of NO_2 introduced together with NO into the system may act as a 'catalytic seed' for hydroperoxide decomposition.

Thus, irrespective of the particular mechanism involved in the PP hydroperoxide decomposition by NO at room temperature, this process has an autoaccelerated character and proceeds with the participation of free radicals.

References

1. P.G. Wand, M. Xian, X. Tang, X. Wu, Z. Wen, T. Cai and J. Janczuk, *Chemical Reviews*, 2002, **102**, 4, 1091.

2. A.F. Vanin, V.P. Mokh, A.F. Serezhenkov and E.I. Chazov, *Nitric Oxide*, 2007, **16**, 322.

3. C.Yi. Chiang and N.Y. Darensbourg, *Journal of Biological Inorganic Chemistry*, 2006, **11**, 3, 359.

4. B. Ranby and J.F. Rabek, *Photodegradation, Photo-Oxidation and Photostabilisation of Polymers*, Wiley, London, UK, 1975.

5. J.G. Calvert and J. Pitts, *Photochemistry*, Wiley, New York, NY, USA, 1966.

6. H.A. Taylor and H. Bender, *Journal of Chemical Physics*, 1941, **9**, 1968.

7. J. H. Raley, F.F. Rust and W.E. Vaughan, *Journal of the American Chemical Society*, 1948, **70**, 2, 761.

8. W.A. Bryce and K.U. Ingold, *Journal of Chemical Physics*, 1955, **23**, 1968.

9. J.G. Calvert, S.S. Thomas and P.L. Hanst, *Journal of the American Chemical Society*, 1960, **82**, 1, 1.

10. D.E. Hoare, *Canadian Journal of Chemistry*, 1962, **40**, 10, 2012.

11. W.C. Steppy and J.G. Calvert, *Journal of the American Chemical Society*, 1959, **81**, 4, 769.

12. C.S. Coe and T.F. Doumani, *Journal of the American Chemical Society*, 1948, **70**, 4, 1516.

13. B.G. Gowenlock. and J. Trotman, *Journal of the Chemistry Society*, 1955, 4190.

14. A.Ya. Yacubovitch, S.P. Makarov, V.A. Ginzburg, N.F. Privezentceva and L.L. Martynova, *Doklady Akademii Nauk SSSR*, 1961, **141**, 125.

15. C. Lagercrantz, *Free Radical Research Communications*, 1993, **19**, 387.

16. B.E. Sturgeon, R.E. Glover, Y.R. Chen, L.T. Burks and R.P. Mason, *Journal of Biological Chemistry*, 2001, **276**, 49, 45516.

17. E.G. Janzen, A.L. Wilcox and V. Manoharan, *Journal of Organic Chemistry* 1993, **58**, 14, 3597.

18. H.G. Korth, R. Sustman, P. Lommes, T. Paul, A. Ernst, H. de Groot, L. Hughes, K.U. Ingold, *Journal of the American Chemical Society*, 1994, **116**, 7, 2767.

19. I. Gabr and M.C.R. Symons, *Journal of the Chemical Society Faraday Transactions*, 1996, **92**,10, 1767.

20. J.J. McGee and J. Heicklen, *Journal of Chemical Physics*, 1964, **41**, 2977.

21. D.J. Le Roy and E.W. Stracie, *Journal of Chemical Physics*, 1944, **12**, 117.

22. J.S.B. Park and J.C. Walton, *Journal of the Chemical Society - Perkin Transactions II*, 1997, **12**, 12, 2579.

23. K.W. Chiu, P.D. Savage, G. Wilkinson and D.J. Williams, *Polyhedron*, 1985, **4**, 11, 1941.

24. M. d'Ischia, N. Rega and V. Barone, *Tetrahedron Letters*, 1999, **55**, 9297.

25. I. Gabr, R.P. Patel, M.C.R. Symons and M.T. Wilson, *Journal of the Chemical Society - Chemical Communications*, 1995, **9**, 915.

26. J.F. Brown, *Journal of the American Chemical Society*, 1957, **79**, 10, 2480.

27. A. Rockenbauer and L. Korecz, *Journal of the Chemical Society Chemical Communications*, 1994, 2, 145.

28. A. Rockenbauer, M. Gyor and F. Tüdos, *Tetrahedron Letters*, 1986, 3425.

29. L. Grossi and S. Strazzari, *Journal of Organic Chemistry*, 1999, **64**, 8076.

30. W. Wu, Q. Liu, Yi. Shen, R. Li and L. Wu, *Tetrahedron Letters*, 2007, **48**, 1653.

31. Z. Liu, R. Li, D. Yang and L. Wu, *Tetrahedron Letters*, 2004, **45**, 1565.

32. T. Nagano, H. Takizawa and M. Hirobe, *Tetrahedron Letters*, 1995, **36**, 8239.

33. T. Itoh, Y. Matsuya, K. Nagata and A. Ohsawa, *Tetrahedron Letters*, 1996, **37**, 4165.

34. T. Itoh, Y. Matsuya, H. Maeta, M. Miyazaki, K. Nagata and A. Ohsawa, *Chemical and Pharmaceutical Bulletin*, 1999, **47**, 6, 819.

35. T. Itoh, K. Nagata, M. Okada and A. Oshawa, *Tetrahedron Letters*, 1995, **36**, 2269.

36. T. Itoh, Y. Matsuya, K. Nagata and A. Ohsawa, *Tetrahedron Letters*, 1997, **38**, 4117.

37. T. Itoh, K. Nagata, Y. Matsuta, M. Miyazaki and A. Ohsawa, *Tetrahedron Letters*, 1997, **38**, 5017.

38. H. Collet, C. Bied, L. Mion, J. Taillades and A. Commeyras, *Tetrahedron Letters*, 1996, **37**, 9043.

39. S.G. Kukolich, *Journal of the American Chemical Society*, 1982, **104**, 17, 4715.

40. H. Gershinowitz and H. Eyring, *Journal of the American Chemical Society*, 1935, **57**, 6, 985.

41. R.S. Drago and F.E. Paulik, *Journal of the American Chemical Society*, 1960, **82**, 1, 96.

42. N. Arulsamy and D.S. Bohle, *Journal of Organic Chemistry*, 2006, **71**, 2, 572.

43. J.A. Hrabie, E.V. Arnold, M.L. Citro, C. George and L.K. Keefer, *Journal of Organic Chemistry*, 2000, **65**, 18, 5745.

44. H.N. Rexroad and W. Gordy, *Journal of Chemical Physics*, 1959, **30**, 399.

45. I.S. Gaponova, G.B. Pariiskii and D.Ya. Toptygin, *Vysokomolekulyarnye Soedineniya Seria A*, 1983, **25**, 862.

46. I.S. Gaponova, G.B. Pariiskii and D.Ya. Toptygin, *Vysokomolekulyarnye Soedineniya Seria A*, 1989, **31**, 1238

47. I.S. Gaponova and G.B. Pariiskii, *Chemical Physics Report*, 1997, **16**, 1795.

48. G.B. Pariiskii, I.S. Gaponova and E.Ya. Davydov, *Russian Chemical Reviews*, 2000, **69**, 985.

49. I.S. Gaponova and G.B. Pariiskii, *Journal of Polymer Science Part B: Polymer Physics Edition*, 1998, **40**, 394.

50. E.Ya. Davydov, I.S. Gaponova, T.V. Pokholok, A.P. Vorotnikov, G.B. Pariiskii and G.E. Zaikov, *Polymers for Advanced Technologies*, 2008, **19**, 6, 475.

51. E.Ya. Davydov, G.B. Pariiskii, I.S. Gaponova, T.V. Pokholok and G.E. Zaikov, *Chemistry and Chemical Technology*, 2008, **2**, 33.

52. Ya.S. Lebedev, Yu.D. Tsvetkov and V.V. Voevodsky, *Vysokomolekulyarnye Soedineniya Seria A*, 1963, **5**, 1500.

53. E.G. Janzen, *Russian Chemical Reviews*, 1974, **43**, 2247.

54. C. Chatgillaloglu, V. Malatesta and K.U. Ingold, *Journal of Physical Chemistry*, 1980, **84**, 26, 3597.

55. A.L. Buchachenko and A.M. Vasserman, *Stable Radicals*, Khimiya, Moscow, Russia, 1974.

56. C.X. Zhao, X.K. Jing, G.F. Chen, Y.L. Qu, X.S. Wang and J.Y. Lu, *Journal of the American Chemical Society*, 1986, **108**, 11, 3132.

57. I.S. Gaponova, G.B. Pariiskii and D.Ya. Toptygin, *Vysokomolekulyarnye Soedineniya Seria B*, 1985, **27**, 129.

58. M. Iwasaki, K. Torriyama, T. Sawaki and M. Inoe, *Journal of Chemical Physics*, 1967, **47**, 554.

59. K.V. Scherer, T. Ono, K. Yamanouchi, R. Fernandez, P. Henderson and H. Goldwhite, *Journal of the American Chemical Society*, 1985, **107**, 3, 718.

60. I.S. Gaponova, G.B. Pariiskii and D.Ya. Toptygin, *Vysokomolekulyarnye Soedineniya Seria A*, 1988, **30**, 262.

61. E.Ya. Davydov, G.B. Pariiskii and D.Ya. Toptygin, *Vysokomolekulyarnye Soedineniya Seria A*, 1977, **19**, 977.

62. W.M. Fox and M.C.R Symons, *Journal of the Chemical Society A: Inroganic, Physical, Theoretical,* 1966, 1503.

63. J.D. Roberts and M. Caserio, *Basic Principles of Organic Chemistry*, W. A. Benjamin, Inc, New York, NY, USA, 1964.

64. J.L. Brokenshire, J.D. Roberts and K.U. Ingold, *Journal of the American Chemical Society*, 1972, **94**, *20,* 7040.

65. J.R. Shelton and R.F. Kopczewski, *Journal of Organic Chemistry*, 1967, **32**, 9, 2908.

66. L.A. Tatarenko and V.S. Pudov, *Vysokomolekulyarnye Soedineniya Seria B*, 1980, **22**, 671.

67. W.A. Pryor, L. Castle and D.F. Church, *Journal of the American Chemical Society*, 1985, **107**, 1, 211.

68. I.S. Gaponova and G.B. Pariiskii, *Journal of Polymer Science Part A: Polymer Chemistry Edition*, 1995, **37**, 1133.

69. S. Terabe and R. Konaka, *Journal of the Chemical Society, Perkin Transactions II*, 1972, **14**, 2163.

4 Free-Radical Conversions of Polymers Initiated by Nitrogen Trioxide

Radicals of nitrogen trioxide (NO_3) have a significant role in the chemical processes occurring in the top layers of the atmosphere [1]. They are produced in the gas phase by the reaction of nitrogen dioxide (NO_2) with ozone:

$$NO_2 + O_3 \longrightarrow NO_3 + O_2 \tag{4.1}$$

During daylight, the primary loss mechanism of NO_3 is by photolysis:

$$NO_3 \xrightarrow{h\nu} NO_2 + O \tag{4.2}$$

while at night it is the reaction with NO_2:

$$NO_3 + NO_2 \longrightarrow N_2O_5 \tag{4.3}$$

and the reaction with gas-phase organic compounds is thought to be the principal depletion mechanism. The lifetime of NO_3 in the atmosphere decreases dramatically at a relative humidity of >40–50%. This suggests that one major source of nitric acid (NO) in the atmosphere is the insertion of gas phase NO_3 into atmospheric droplets. This is possibly most important at night, since daytime photolysis of NO_3 is very rapid. In addition, NO_3 can react with other constituents of the droplets and initiate the autoxidation of sulfur dioxide. This, in turn, leads to the formation of sulfuric acid. Therefore, nitrogen trioxide enhances the acidification of atmospheric droplets both directly and indirectly.

4.1 Methods of Generation of NO_3

The NO_3 radical has been produced via photolysis of solutions of ceric (IV) nitrates in mixtures of water with nitric acid (HNO_3) [2–7] and acetic acid [8] as well as pure HNO_3 [8]. Using flash photolysis of ceric ammonium nitrate (CAN) $(NH_4)_2Ce(NO_3)_6$ solutions, Martin and co-workers [2–5, 8] first postulated the primary photochemical process:

$$Ce^{IV}NO_3^- \xrightarrow{h\nu} Ce^{III} + NO_3 \quad (4.4)$$

The ceric nitrate extinction coefficient is much lower in pure water then in HNO_3 solution. In the presence of HNO_3, the ceric nitrate spectrum is red-shifted from that observed in water. This phenomenon is thought to result from the fact that the inner coordination sphere of Ce (IV) is occupied by OH groups in water or dilute HNO_3 by NO_3^- in more concentrated HNO_3 solution. The quantum yield for NO_3 formation is constant for 5 M < $[HNO_3]$ <14 M ($\varphi \approx 1$), but tends to zero as $[HNO_3] \rightarrow 0$.

They major pathway for NO_3 disappearance is the following process:

$$Ce^{III} + NO_3 \xrightarrow{k_1} Ce^{IV}NO_3^- \quad (4.5)$$

In 6.0 M HNO_3 solutions, Martin and co-workers reported $k_1 = (1.70 \pm 0.04) \times 10^6$ M^{-1} s^{-1} at room temperature with an activation energy 10 ± 0.2 kcal/mol.

However, Hayon and co-workers [6, 9] suggested that the NO_3 radical was not formed by the direct photolysis of Ce^{IV} ion, but rather by the direct photolysis of the non-dissociated HNO_3 molecules, whence they presumed the OH radical was a precursor to NO_3 in this system:

$$HONO_2 \longrightarrow OH + NO_2 \quad (4.6)$$

$$OH + HONO_2 \longrightarrow H_2O + NO_3 \quad (4.7)$$

This assumption was formulated on the basis of the electron spin resonance (ESR) study of NO_3 produced upon ultraviolet (UV) photolysis of aqueous HNO_3 and $K_2Ce(NO_3)_6$ ices at 77 K. The kinetics of decay of NO_3 generated by flash photolysis of aqueous $HONO_2$ solutions of $K_2Ce(NO_3)_6$ at room temperature was studied [6]. The authors agreed with Martin and co-workers that the Ce^{IV} cations were involved in explaining the generation of NO_2. However, they maintained that the primary process

$$Ce^{IV}{\cdot}H_2O \xrightarrow{h\nu} Ce^{III} + OH + H^+ \quad (4.8)$$

was necessary to produce NO_3. The decay follows first-order kinetics with a rate constant of 0.95×10^3 s^{-1}. The conclusions of the work [6] differ substantially with those made in the works [2–5] on the same system not only with regard to the primary process and the kinetic order of NO_3 decay, but also in the contention that these radicals do not react with the species Ce^{III} generated from the primary process (**Equation 4.8**); the NO_3 radicals react with excess Ce^{III} added before the flash.

According to the whole data array [3], the overall mechanism of NO_3 conversions in 1–15 M aqueous HNO_3 solutions of CAN includes reactions (**Equation 4.4**), (**Equation 4.5**) as well as the following reactions:

$$NO_3 + NO_3 \xrightarrow{k_2} N_2O_6 \tag{4.9}$$

$$N_2O_6 + 2\,Ce^{IV} \longrightarrow 2\,NO_2^+ + O_2 + 2\,Ce^{III} \tag{4.10}$$

$$NO_2^+ + NO_3^- + H_2O \rightleftharpoons 2\,HONO_2 \tag{4.11}$$

This mechanism explains the generation of NO_3 and provides concurrent processes (**Equation 4.5**) and (**Equation 4.9**). The observed Ce^{IV} bleaching results from the sequence of reactions (**Equation 4.9**) and (**Equation 4.10**). On the basis of this mechanism, a rate equation for the decay of NO_3 is represented as:

$$-d[NO_3] / dt = k_1[Ce^{III}]\cdot[NO_3] + 2k_2[NO_3]^2 \tag{4.12}$$

This equation cannot be simply integrated, but it allows some simplifications to estimate rate constants. With excess of Ce^{III} in the solution, the second term becomes negligible and equation (**Equation 4.12**) reduces to the following equation:

$$-d[NO_3] / dt = k_1[Ce^{III}]\cdot[NO_3] \tag{4.13}$$

used in the pseudo-first-order kinetic study [6]. The first term in (**Equation 4.12**) leads to the disappearance of Ce^{III} from the system, whereas the second term leads to an increase in Ce^{III} due to the sequence of (**Equation 4.9**) and (**Equation 4.10**). The estimation of k_2 is possible in conditions when $[Ce^{III}]_t \approx [NO_3]_t$. Then (**Equation 4.12**) transforms to the expression:

$$-d[NO_3] / dt = (k_1 + 2k_2)\cdot[NO_3]^2 \tag{4.14}$$

NO_3 radicals have been also produced via the pulse radiolysis of concentrated HNO_3 [10] or sodium nitrate solutions [11–13]. On evidence derived from the data of these works, the occurrence of NO_3 radicals is caused by the reaction of hydroxyl radicals (**Equation 4.7**) formed as a result of the indirect action of ionising radiation or the reaction:

$$NO_3^- + OH + H^+ \longrightarrow H_2O + NO_3 \tag{4.15}$$

In accordance with [11], a source of NO_3 is also a direct action of radiation on nitrate anions:

$$NO_3^- \rightsquigarrow NO_2 + O + e^- \quad (4.16)$$

$$O + H^+ \rightleftharpoons OH^+ \quad (4.17)$$

$$NO_3^- + OH^+ \longrightarrow NO_3 + OH \quad (4.18)$$

The kinetic data for NO_3 decay in the radiolysis conditions are questionable. As noted in [11], the order of the reaction depends on the concentration of solutions. At low concentrations of HNO_3, the disappearance of NO_3 is described by first-order kinetics, but this process obeys second-order kinetics at high concentrations. At intermediate concentrations, the process has a mixed order.

A detailed study of the kinetics of decay of NO_3 over a wide range of HNO_3 concentrations up to 20 M has been carried out [10]. It was found that with an increase in acid concentration from 0 M to 5 M, the initial concentration of NO_3 sharply increases, reaching a maximum value, and then there is an appreciable decrease in radical concentration. Such dependence is explained by growth of the fraction of OH radicals arising under the radiolysis of water and participating in reactions (**Equation 4.7**) with a rate constant of $(1.4 \pm 0.1) \times 10^8$ s^{-1} [10] or (**Equation 4.15**) when HNO_3 concentration increases. The increase of the acid concentration is accompanied by the growth of the radiation yield of NO_2 due to the direct action of radiation on NO_3^- or HNO_3. For interpretation of decreasing the radiation yield of NO_3 at $[HNO_3] > 5$–8 M, it is necessary to accept that in these conditions the essential part of HNO_3 is non-dissociated. In this case, the direct action of radiation on HNO_3 is represented by the following process:

$$HNO_3 \rightsquigarrow NO_2 + OH \quad (4.19)$$

As is seen, the direct action of radiation on HNO_3 leads to the formation of only one radical NO_3 (reaction (**Equation 4.7**) per one acid molecule destroyed in the reaction (**Equation 4.19**), whereas the pulse radiolysis of less concentrated solutions produces two radicals NO_3 according to reactions (**Equation 4.15**)–(**Equation 4.18**). The evidence for the reaction (**Equation 4.19**) is the absorption band of NO_2 at 400 nm [14] in an optical spectrum appearing in 15 M HNO_3 immediately after advancing the electronic pulse. Such absorption was not observed for diluted 3M solutions. The approximate calculation of the NO_3 radiation yield for 5–8 M solutions of HNO_3 gives a minimum value of ~10 radicals per 100 eV [10]. The yield of direct radiation decomposition of nitrate anions was estimated to be 8–17 ions per 100 eV [11].

The rate of the NO_3 disappearance depends on concentration of acid solutions and on the doze of radiation. From the kinetic analysis of NO_3 disappearance, the rate

constants of first-order decay k_1 and bimolecular decay k_2 were determined: $k_1 = 8 \times 10^3\ s^{-1}$; $k_2 = 1.8 \times 10^8$/M/s [10]. The most probable process of first-order decay is thermal decomposition:

$$NO_3 \longrightarrow NO_2 + O \tag{4.20}$$

NO_3 radicals have been detected, along with NO_3^{-2} and ONOO•, by the ESR method in the course of the action of X-radiation on monocrystals of potassium permanganate at 77 K [15]. At such temperature, NO_3 radicals are unstable and progressively disappear.

For the NO_3 source, the reaction of the fluorine atom with HNO_3 can be used [16–19]:

$$F + HNO_3 \longrightarrow HF + NO_3 \tag{4.21}$$

This reaction is carried out by passing a 1% mixture of F_2 in helium through a microwave discharge to produce F atoms. HNO_3 was introduced into the flow tube upstream of the microwave discharge inlet port by passing He through a bubbler containing the pure acid. HNO_3 concentration was at least ten-times higher than that of F atoms. Excess HNO_3 prevents the secondary reaction

$$F + NO_3 \longrightarrow FO + NO_2 \tag{4.22}$$

taking away NO_3. Microwave power to the discharge tube is kept at <5 W to minimise the production of oxygen atoms. The presence of O atoms in the flow system results in a background source of NO_2 due to the reaction of O atoms with NO_3:

$$O + NO_3 \longrightarrow NO_2 + O_2 \tag{4.23}$$

The use of CF_4 as a precursor of F atoms instead of F_2 is preferable [16] because possible complications due to F_2 reactions cannot occur.

Generation of NO_3 via the reaction (**Equation 4.21**) also takes place during photolysis of a mixture of molecular fluorine (5.0×10^{15} molecule/cm^3) and HNO_3 (2.0×10^{16} molecule/cm^3) at $\lambda \geq 180$ nm [20]. Two other methods used in the work [20] for this purpose are based on photolysis of a mixture of chlorine (2.0×10^{16} molecule/cm^3) and chlorine nitrate or the photolysis of chlorine nitrate:

$$Cl_2 \xrightarrow{h\nu\ (\lambda > 280nm)} 2\ Cl \tag{4.24}$$

$$Cl + ClONO_2 \longrightarrow Cl_2 + NO_3 \tag{4.25}$$

$$ClONO_2 \xrightarrow{h\nu\ (\lambda > 280nm)} Cl + NO_3 \tag{4.26}$$

To investigate the kinetics of the gas-phase reactions of NO_3 radicals with organic compounds, the method based on thermal decomposition of N_2O_5 into NO_2 and NO_3 was applied [21–26]. It has been noticed that some organics react rapidly with a mixture of O_3 and NO_2, but rather slowly with O_3 and NO_2 alone. N_2O_5 and NO_3 can be produced in the O_3–NO_2 system by the reactions [21]:

$$O_3 + NO_2 \xrightarrow{k_1} NO_3 + O_2 \tag{4.27}$$

$$NO_3 + NO_2 \underset{k_{-2}}{\overset{k_2}{\rightleftharpoons}} N_2O_5 \tag{4.28}$$

where $k_1 = 4.4 \times 10^{-17}$ cm^3/molecule/sec and $K = k_2 / k_{-2} = 8 \times 10^{-10}$ molecule/cm^3 [27]. The determination of rate constants for NO_3 reactions are based on measuring the rate of disappearance of N_2O_5 in the presence and absence of added organic reactant. The acceleration of N_2O_5 decay observed with the organic reactant is attributed to the NO_3–organic molecule reaction.

4.2 Photochemistry of NO_3

The photochemistry of NO_3 is potentially important in the balance of ozone in the troposphere and lower stratosphere [1, 28–30]. The absorption spectrum of NO_3 shows three absorption maxima in the wavelength range 350–770 nm at 600, 640 and 680 nm. The strongest absorption is at 640 nm [1, 6, 12, 28, 29, 31]. The value of the molar extinction coefficient of NO_3 at 635 nm and room temperature reported in [3] is 250 ± 90/M/cm. However, from data obtained by Wine and co-workers, $\varepsilon_{NO_3}^{635} = 832 \pm 112$/M/cm [7].

The two modes of photolysis of NO_3 have different effects on ozone. If the photolysis products are NO_2 + O by reaction (**Equation 4.2**), ozone is produced in an oxygen system via the reaction:

$$O + O_2 + M \longrightarrow O_3 + M \tag{4.29}$$

The photolysis of NO_3 gives one NO molecule that in subsequent reactions destroys

ozone [29]:

$$NO_3 \xrightarrow{h\nu} NO + O_2 \tag{4.30}$$

$$NO + O_3 \longrightarrow NO_2 + O_2 \tag{4.31}$$

In the 470–610-nm region, the quantum yields are 0.23 for (**Equation 4.30**) and 0.77 for (**Equation 4.2**). The quantum yield for (**Equation 4.30**) in the 610–700-nm region is only 0.07 [29].

The NO_3 radical has D_{3h} symmetry and a $^2A_2'$ ground electronic state as predicted in the work [32]. The extended Hückel and intermediate neglect of differential overlap (INDO) molecular orbital methods have been applied to NO_3 with a view to understanding its ground-state geometry and electronic structure [33]. The computational model predicts a Y-shaped geometry (C_{2v} symmetry) for the radical. Its ground state is found to be of $^2B_2$ symmetry. Whether NO_3 has a symmetrical D_{3h} structure or a Y-shaped structure, the reaction coordinate to form NO + O_2 does not have the symmetry of a symmetric stretch, but more nearly that of an antisymmetric stretch. The absorption of light with $\lambda > 580$ nm leads to the dissociation of NO_3 as in (**Equation 4.30**). Below 580 nm, NO_3 dissociates to NO_2 + O with a quantum yield close to unity [28, 29].

4.3 Interaction of NO_3 with Organic Compounds

Several organic compounds are emitted into the atmosphere from natural sources. The largest amounts of hydrocarbons are released from various types of plants and trees. For example, isoprene is a natural hydrocarbon emitted by trees in tropical forests [34]. Peak concentrations of about 3 parts per billion by volume of isoprene were observed around noon.

Tropospheric mixing ratios of methane, C_2–C_{10} hydrocarbons, and carbon monoxide were measured over the Amazon tropical forest [35]. The emission strength of these substances on a global scale is much larger than that of anthropogenic organics. These compounds have a significant role in the chemistry of atmospheric oxidant formation. At present, attention is being focussed on the degradation process of these natural hydrocarbons and in particular on those processes leading to the formation of oxidants that may develop toxic properties.

NO_3 can react actively with several organic compounds and may dominate the nighttime chemistry of volatile biogenic compounds. Kinetic and product data are required for a wide variety of classes and structures of organics to investigate

the reactivity of the NO_3 radical, and to assess the importance of its reactions in atmospheric chemistry (in particular the formation of HNO_3 as a key component of acid deposition). Two experimental techniques for the determination of rate constants for the gas-phase reactions of NO_3 have been described [23, 24]. The first of these techniques was based upon observing the increased decay rate of N_2O_5, prepared by the method of Schott and Davidson [36], in the presence of a reactive organics [21, 22]. In these N_2O_5 – NO_2 organic mixtures, along with the equilibrium (**Equation 4.28**), the following reactions are:

$$N_2O_5 \xrightarrow{k_3} \text{loss of } N_2O_5 \tag{4.32}$$

$$NO_3 + \text{organic} \xrightarrow{k_4} \text{products} \tag{4.33}$$

where reaction (**Equation 4.32**) may be a background wall reaction. Then:

$$\frac{d[N_2O_5]}{dt} = -k_{-2}[N_2O_5] + k_2[NO_2][NO_3] - k_3[N_2O_5] \tag{4.34}$$

$$\frac{d[NO_3]}{dt} = k_{-2}[N_2O_5] - k_2[NO_2][NO_3] - k_4[NO_3][\text{organic}] \tag{4.35}$$

Combining (**Equation 4.34**) and (**Equation 4.35**) leads to the expression:

$$\frac{d[N_2O_5]}{dt} + \frac{d[NO_3]}{dt} = -k_3[N_2O_5] - k_4[NO_3][\text{organic}] \tag{4.36}$$

and under conditions where the equilibrium (**Equation 4.28**) is attained, then [23]:

$$-\frac{d\ln[N_2O_5]}{dt} = \left(k_3 + \frac{k_4[\text{organic}]}{K[NO_2]}\right)\left(\frac{K[NO_2]}{1+K}\right) \tag{4.37}$$

where $K = \dfrac{k_2}{k_{-2}} = \dfrac{[N_2O_5]}{[NO_2][NO_3]}$

Becasuse under the experimental conditions $K[NO_2] >> 1$, equation (**Equation 4.37**) can be simplified to

$$-\frac{d\ln[N_2O_5]}{dt} = k_3 + \frac{k_4[\text{organic}]}{K[NO_2]} \tag{4.38}$$

Thus, under conditions such that the [organic]/[NO_2] ratio remains constant during an experiment, then from a series of such experiments the plot (**Equation 4.38**) should

yield k_4. Typical initial reactant concentrations are as follows: $[N_2O_5] = (2–5) \times 10^{13}$ molecule/cm^3; $[NO_2] = (2 – 280) \times 10^{13}$ ·molecule/cm^3; [organic] = $(6 – 340) \times 10^{13}$ ·molecule/cm^3.

The second experimental method is based upon monitoring the relative decay rates of a series of organics, including at least one organic whose NO_3 radical reaction rate constant was also determined from the enhanced N_2O_5 decay rates in $N_2O_5 – NO_2$ organic mixtures. If the organics react essentially negligibly with N_2O_5 and NO_2, then the chemical loss process of these organics is due to the reaction with NO_3 radicals includes (**Equation 4.30**) and the reaction:

$$NO_3 + \text{reference organic} \longrightarrow \text{products} \tag{4.39}$$

Small amounts of dilution occur from the incremental additions of N_2O_5 to the reaction mixture. The dilution factor at time t is measured by pressure change within the chamber. This factor D_t is given by

$$D_t = \ln \frac{(\text{pressure chamber})_t}{(\text{pressure chamber})_{t_0}} \tag{4.40}$$

The dilution factor D_t is typically 0.006 (i.e., ~ 0.6%) per N_2O_5 addition. Thus:

$$\ln \frac{[\text{organic}]_{t_0}}{[\text{organic}]_t} = k_4 \int_{t_0}^{t} [NO_3]dt + D_t \tag{4.41}$$

$$\ln \frac{[\text{reference organic}]_{t_0}}{[\text{reference organic}]_t} = k_4 \int_{t_0}^{t} [NO_3]dt + D_t \tag{4.42}$$

Eliminating the integrated NO_3 radical concentration from equations (**Equation 4.41**) and (**Equation 4.42**) leads to

$$\ln \frac{[\text{organic}]_{t_0}}{[\text{organic}]_t} - D_t = \frac{k_4}{k_5} \ln \left(\frac{[\text{reference organic}]_{t_0}}{[\text{reference organic}]_t} - D_t \right) \tag{4.43}$$

where $[\text{organic}]_{t_0}$ and $[\text{reference organic}]_{t_0}$ are the concentrations of the organic and reference organic, respectively, at time t_0, $[\text{organic}]_t$ and $[\text{reference organic}]_t$ are the corresponding concentrations at time t. Hence, the plot (**Equation 4.40**) gives a possibility to determine k_4/k_5. For this technique, the initial concentrations of the organic reactants were $(2–3) \times 10^{13}$ molecule/cm^3, and $(0.5–5) \times 10^{13}$ molecule/cm^3 of N_2O_5 per addition were added to the chamber throughout the experiments. For

the studies involving the more reactive alkenes, (2–20) × 10^{14} molecule/cm^3 of NO_2 were also included in the reaction mixtures to extend the reaction time [24].

For the experiments in which N_2O_5 decay rates are used to determine individual NO_3 radical reaction rate constants, N_2O_5, NO_2 and the organics are quantitatively monitored by Fourier transform infrared technology (FT-IR) spectroscopy. For the relative rate constant studies, the reacting organics are analysed prior to and during these reactions by gas chromatography.

As a free radical, NO_3 participates in reactions of abstraction of the hydrogen (H) atom. Relative rate constants have been reported for the gas-phase reactions of NO_3 with a series of alkanes [23]. The data obtained show that the rate constants increase monotonically along the *n*-alkane series. These reactions must proceed via H-atom abstraction:

$$NO_3 + RH \longrightarrow HNO_3 + R \qquad (4.44)$$

with this pathway being exothermic by 3.2, 6.7, and 9.2 kcal/mol for primary, secondary, and tertiary C–H bonds, respectively. If to assume that H atom abstraction from $–CH_3$ groups is slow compared with abstraction from $–CH_2–$ groups, the kinetic data for *n*-alkanes (butane–nonane) and cyclohexane give rate constants of·10^{-17}–10^{-16} cm^3 ·$molecule^{-1}$·s^{-1} for the reaction·of NO_3 radicals with $–CH_2–$ groups. The available data are not sufficiently precise to allow further differentiations into $–CH_2–$ groups bonded to $–CH_2–$ or $–CH_3$ groups.

The rate constants for reactions of NO_3 radicals with isobutane and 2,3-dimethylbutane refer to the rate constants for H-atom abstraction from tertiary C–H group bonded respectively to three $–CH_3$ groups and one tertiary C–H group and two $–CH_3$: k(isobutene) = 2.9 × 10^{17} cm^3/molecule/s and k (2,3-dimethylbutane) = 6.0 × 10^{-17} cm^3/molecule/s. The rate constants obtained in the work [23] show that for nighttime NO_3 radical concentrations of 2 × 10^9 molecule/cm^3, 37 of these nighttime reactions are one order of magnitude or more less effective as total loss processes for the alkanes compared with the daytime reaction with the OH radical ([OH] = 10^6 molecule/cm^3). These nighttime reactions of alkanes with NO_3 lead to the formation of the HNO_3 constituent of acid deposition.

Rate constants for reactions of H-atom abstraction by NO_3 radicals from alcohols in neutral and acidic aqueous solutions were determined using pulse radiolysis [1]. The following values were obtained: k_{HOCH_2-H} = 7 × 10^4, $k_{(HO)(CH_3)HC-H}$= 7 × 10^5, and $k_{(HO)(CH_3)_2C-H}$ = 2.4 × 10^6 M^{-1}·s^{-1}. The H-atom abstraction from other C–H bonds in the molecules was not considered. Nevertheless, a plot of the logarithm of the rate constant against C–H bond strength shows a quite reasonable

linear relationship, suggesting that abstraction of the indicated alkyl hydrogen is the dominant reaction path. Other studies on the reactions of NO_3 with alcohols in the aqueous phase carried out by flash photolysis [6] and pulse radiolysis [10] give rate constant values twofold higher for ethyl alcohol and fivefold higher for methyl alcohol.

Gaseous mixtures of N_2O_5, O_2 and aldehydes give as a major reaction product peroxyacyl nitrates $RCOO_3NO_2$ [21, 37]. In view of the potential role of these reactions in the formation of photochemical smogs, the kinetics and mechanism of the N_2O_5 + aldehyde system have been studied. The $RCOO_2NO_2$ formation involves the reactions of NO_3 and NO_2 radicals in equilibrium with N_2O_5:

$$NO_3 + RCHO \longrightarrow HNO_3 + RC^{\bullet}=O \quad (4.45)$$

$$RC^{\bullet}=O + O_2 \longrightarrow RCOOO^{\bullet} \quad (4.46)$$

$$RCOOO^{\bullet} + NO_2 \longrightarrow RCOO_2NO_2 \quad (4.47)$$

The first-order decay of N_2O_5 was found to be proportional to CH_3CHO concentration [21]. The addition of NO_2 reduces the rate of the reaction. The addition of ozone increases the decay rate of N_2O_5. This is consistent with the occurrence of reaction (**Equation 4.45**) because the addition of O_3 increases the NO_3 concentration. Several experiments carried out at a low partial pressure of oxygen (<1 133,322 Pa) resulted in non-first-order decay of N_2O_5. A change in mechanism is expected under these conditions because the other reactions can compete with reaction (**Equation 4.46**). The yield of peroxyacetyl nitrate per N_2O_5 consumed is >0.8. The yield of HNO_3 was at least 50% of the amount of N_2O_5 reacted. The experimental data were used to derive a rate constant for the H-abstraction reaction (**Equation 4.45**) by a numerical integration of reactions (**Equation 4.28**), (**Equation 4.45**) – (**Equation 4.47**). The value of (**Equation 4.45**) rate constant for acetaldehyde used in this calculation was adjusted until the calculated N_2O_5 decay matched that observed experimentally. This procedure gives a value of $k_{(IV.45)}(CH_3CHO)$ of 1.2×10^{-15} cm^3/molecule/s, which is much higher than the rate constants for H-atom abstraction from the C–H bonds of alkanes [23].

The kinetics of reaction (**Equation 4.45**) for formaldehyde have been studied using long-path infrared (IR) and visible spectroscopy to follow the reactants and products in dilute mixtures of O_3, NO_2 and CH_2O (700 Torr) at room temperature [37]. It was accepted that only reactions (**Equation 4.27**), (**Equation 4.28**), (**Equation 4.45**) and (**Equation 4.46**) are important in the simplified reaction mechanism of the loss of CH_2O and N_2O_5/NO_3. A more detailed consideration of the chemistry of the system

points to several other potentially important reactions. First, there are several sources of NO (a potential reactant for NO_3) which must occur in this system [27, 29, 38]:

$$NO_3 + NO_2 \longrightarrow NO + NO_2 + O_2 \quad (4.48)$$

$$O_3 + NO_2 \longrightarrow NO + 2O_2 \quad (4.49)$$

$$NO_3 + M \longrightarrow O_2 + NO + M \quad (4.50)$$

The generation of NO in the $NO_2 - NO_3 - CH_2O$ system makes available various other reaction pathways for NO_3 and other species present. Thus, NO_3 and O_3 react as follows:

$$NO_3 + NO \longrightarrow 2NO_2 \quad (4.51)$$

$$O_3 + NO \longrightarrow O_2 + NO_2 \quad (4.52)$$

Besides, HO_2 radicals can be expected to be products of the interaction of NO_3 with formaldehyde, and HO_2 radicals generate OH radicals in reaction (**Equation 4.53**):

$$HO_2 + NO \longrightarrow HO + NO_2 \quad (4.53)$$

The reactive OH radicals arise also in this system via the reactions:

$$HO_2 + O_3 \longrightarrow OH + 2O_2 \quad (4.54)$$

$$OH + O_3 \longrightarrow HO_2 + O_2 \quad (4.55)$$

HO_2 radicals attack formaldehyde and form minor observed products, HCO_2H and HO_2CH_2OH:

$$HO_2 + CH_2O \rightleftharpoons HO_2CH_2O^{\bullet} \rightleftharpoons {}^{\bullet}O_2CH_2OH \quad (4.56)$$

$$2\ {}^{\bullet}O_2CH_2OH \longrightarrow 2\ {}^{\bullet}OCH_2OH + O_2 \quad (4.57)$$

$${}^{\bullet}O_2CH_2OH + NO \longrightarrow {}^{\bullet}OCH_2OH + NO_2 \quad (4.58)$$

$${}^{\bullet}O_2CH_2OH + HO_2 \longrightarrow HO_2CH_2OH + O_2 \quad (4.59)$$

$$^{\bullet}OCH_2OH + O_2 \longrightarrow HCO_2H + HO_2 \quad (4.60)$$

Another potential way for the consumption of the NO_3 radical in this system is the reaction with HO_2:

$$NO_3 + HO_2 \longrightarrow HONO_2 + O_2 \quad (4.61)$$

The OH radicals formed in reactions (**Equation 4.53**) and (**Equation 4.54**) react with several of the molecules present in this system:

$$OH + CH_2O \longrightarrow H_2O + HC^{\bullet}O \quad (4.62)$$

$$HC^{\bullet}O + O_2 \longrightarrow CO + HO_2 \quad (4.63)$$

$$OH + NO_2 \longrightarrow HNO_3 \quad (4.64)$$

$$OH + NO \longrightarrow HNO_2 \quad (4.65)$$

$$OH + CO + O_2 \longrightarrow HO_2 + CO_2 \quad (4.66)$$

$$OH + HO_2 \longrightarrow H_2O + O_2 \quad (4.67)$$

$$OH + O_3 \longrightarrow HO_2 + O_2 \quad (4.68)$$

Thus, many elementary reactions are required to describe the chemistry of the NO_2 – O_3 – CH_2O system. Therefore, the very simple treatment based upon only the reactions (**Equation 4.28**), (**Equation 4.45**)–(**Equation 4.47**) does not give consistent estimation of the rate constant of reaction (**Equation 4.45**). A more rigorous treatment of the reaction system in terms of the more complete mechanism gives the H-abstraction rate constant at room temperature $k_{IV.45}$ (CH_2CO) of $(6.3 \pm 1.1) \times 10^{-16}$ cm^3/molecule/s [37]. This value is sufficiently close (about a factor of two lower) to that for acetaldehyde [21].

The significant fraction of the organics emitted into polluted atmosphere are aromatic hydrocarbons [39, 40]. Substituted phenols are among the products of their photooxidation [41, 42]. The complete disappearance of cresols was observed upon the addition of O_3 to the cresol – NO_2 mixture [41]. The fact that O_3 and NO_2 are required for complete cresol consumption indicates a rapid reaction with NO_3

radicals. The rate constants derived from the kinetic study of these processes are (2.0 ± 0.4) × 10^{-12} cm^3/molecule/s for phenol, (12 ± 2) × 10^{-12} cm^3/molecule/s for *o*-cresol, (7 ± 1) × 10^{-12} cm^3/molecule/s for *m*-cresol, and (13 ± 2) × 10^{-12} cm^3/molecule/s for *p*-cresol. NO_3 reacts with phenolic compounds at least 250-times more rapidly than it does with the other aromatics (toluene, benzaldehyde, methoxybenzene). Carter and co-workers [41] believe that this effect could be due to rapid H-atom abstraction by NO_3 from the weak phenolic O–H bond or due to reversible addition of NO_3 to the aromatic ring followed by a six-centre rearrangement to give the same products as H abstraction:

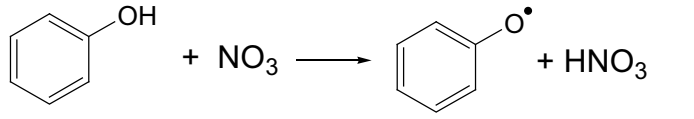

(4.69)

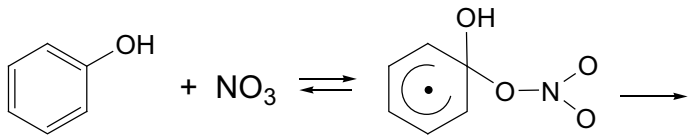

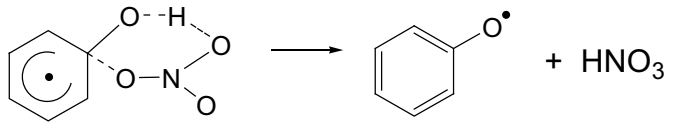

(4.70)

The mechanism of reactions of the nitrate radical with aromatic and substituted aromatic compounds has been studied in detail using the photolysis of CAN [43, 44]. The photochemical reaction of CAN (**Equation 4.4**) with toluene derivatives in acetonitrile was found to produce side-chain nitroxidation products in high yields:

$$ArCH_3 \xrightarrow{h\nu,CAN} ArCH_2ONO_2 \qquad (4.71)$$

NO_3 is a strong oxidising reagent [1] as well as a H-atom abstracting reagent, so the following reactions would be anticipated:

$$ArCH_3 + NO_3 \longrightarrow ArCH_2^{\bullet} + HNO_3 \qquad (4.72)$$

$$ArCH_3 + NO_3 \longrightarrow ArCH_3^{\bullet+} + NO_3^- \qquad (4.73)$$

$$ArCH_3^{\bullet+} \longrightarrow ArCH_2^{\bullet} + H^+ \quad (4.74)$$

The final product $ArCH_2ONO_2$ is formed in further oxidation of $ArCH_2^{\bullet}$ to $ArCH_2^+$ by CAN and the subsequent reaction with NO_3^-. For toluene derivatives with electron-donating substituents such as the methoxy group, the electron transfer reaction (**Equation 4.73**) was confirmed by the laser flash photolysis method [44]. For toluene, there is a probability for direct H-atom abstraction (**Equation 4.72**) with a highly polar transition state. Furthermore, for toluene derivatives with electron-withdrawing substituents, the addition ability of NO_3 to phenyl π-bonds can be considered on the basis of data for reactions with phenols [41] and furan [45]. To clarify the interchanges in the reaction paths by the substituent in toluene, reaction rate constants for various toluene derivatives were evaluated by flash photolysis [44]. The substituent effect of the rate constants for toluene derivatives was correlated with ionisation energies (IEs) of these substances. The reaction rate for anisole is too fast to obtain accurate rate constants, and only lower limits of the rate constants are obtained: k(anisole) $>3 \cdot 10^9$ $M^{-1} \cdot s^{-1}$. For *p*-nitrotoluene, the rate constant is $2.3 \cdot 10^5$ $M^{-1} \cdot s^{-1}$; IE = 9.5 eV. A deuterium kinetic isotope effect of 1.6 was observed for the reaction of NO_3 with toluene and toluene – d_8. This indicates that NO_3 predominantly abstracts the H atom from methyl groups. In the case of *p*-xylene, the deuterium isotope effect was not observed [43]. The rate constant for *p*-xylene ($> 2 \times 10^9$ M/s) is close to the diffusion-controlled limit in acetonitrile, and consequently selectivity becomes low.

Plots of rate constant against IE can be divided into three groups. One is anisole derivatives which have rate constants $>3 \times 10^9$ M/s. For *p*-methylanisole (IE = 8.25 eV), a transition absorption band (λ_{max} = 450 nm) attributed to cation radicals was observed [44]. Thereby, the electron transfer reaction (**Equation 4.73**) was confirmed, which is because of the high electron affinity of NO_3 (3.5 eV). The decay of the cation radical of *p*-methylanisole obeys first-order kinetics, from which the deprotonation process of the cation radical (**Equation 3.74**) forming benzyl radical follows. The first-order rate constant for the process:

$$CH_3OC_6H_4CH_3^{\bullet+} \longrightarrow CH_3OC_6H_4CH_2^{\bullet} + H^+ \quad (4.75)$$

was evaluated to be 2.1×10^4/s.

The second group contains xylene, toluene, and *p*-chlorotoluene, whose IEs are 8.45–8.80 eV. The rate constant of toluene is 1.3×10^8/M/s (IE = 8.76 eV). The deuterium isotope effect on the rate constants was observed for toluene and toluene – d_8, so direct H-atom abstraction is attributed to this group:

$$NO_3 + XC_6H_4CH_3 \longrightarrow HNO_3 + XC_6H_4CH_2^{\bullet}$$

$$(X = p - CH_3,\ m - CH_3,\ p - Cl) \tag{4.76}$$

A low activation energy was evaluated for the reaction with toluene, i.e., <1 kJ/mol.

Toluene derivatives with IEs >8.80 eV belong to the third group; the rate constants for *m*-chlorotoluene is 6.4×10^6/M/s (IE = 8.83 eV). The rate constants for toluene derivatives in this group also decrease linearly with an increase in IEs. The second-order rate constant for benzene is 10^6/M/s. The electron-withdrawing substituents on the benzene ring (F, CN) reduce the reaction rates. For these compounds, the transient absorption band due to the radical cation was not observed in the visible region. Thus, the addition of NO_3 to the double bonds of the benzene ring is responsible for the decay of NO_3:

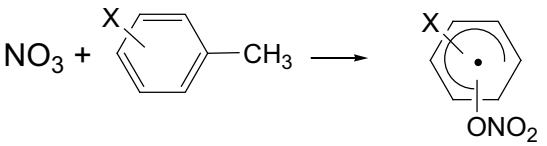

(4.77)

Absolute and relative rate constants have been reported for the addition of NO_3 to alkenes, dialkenes and terpenes [19, 21, 22, 24, 26, 46–48]. A kinetic technique using the equilibrium (**Equation 4.28**) was applied as the NO_3 radical source. The generalised reaction mechanism applicable to various alkenyl hydrocarbons involves the initial reactions [26]:

$$R{-}CH{=}CH{-}R + NO_3 \longrightarrow R{-}C^{\bullet}H{-}CH(ONO_2){-}R \tag{4.78}$$

$$R{-}C^{\bullet}H{-}CH(ONO_2){-}R + O_2 \longrightarrow R{-}CH(O_2^{\bullet}){-}CH(ONO_2){-}R \tag{4.79}$$

$$R{-}CH(O_2^{\bullet}){-}CH(ONO_2){-}R + NO_2 \leftrightarrow R{-}CH(O_2NO_2){-}CH(ONO_2){-}R \tag{4.80}$$

Further reactions of the peroxy radicals are:

$$2\ R{-}CH(O_2^{\bullet}){-}CH(ONO_2){-}R \longrightarrow 2\ R{-}CH(O^{\bullet}){-}CH(ONO_2){-}R + O_2 \tag{4.81}$$

$$2\ R{-}CH(O^{\bullet}){-}CH(ONO_2){-}R \longrightarrow R{-}CHOH{-}CH(ONO_2){-}R + R{-}CO{-}CH(ONO_2){-}R \tag{4.82}$$

$$R{-}CH(O_2^{\bullet}){-}CH(ONO_2){-}R + NO \longrightarrow$$

$$R{-}CH(O^{\bullet}){-}CH(ONO_2){-}R + NO_2 \longrightarrow R{-}CH(ONO_2){-}CH(ONO_2){-}R \quad (4.83)$$

The nitroxy-alkoxy radical reacts further:

$$R{-}CH(O^{\bullet}){-}CH(ONO_2){-}R + O_2 \longrightarrow R{-}CO{-}CH(ONO_2){-}R + HO_2 \quad (4.84)$$

$$R{-}CH(O^{\bullet}){-}CH(ONO_2){-}R \xrightarrow{kT} 2\ R{-}CHO + NO_2 \quad (4.85)$$

$$R{-}CH(O^{\bullet}){-}CH(ONO_2){-}R + NO_2 \longrightarrow R{-}CH(ONO_2){-}CH(ONO_2){-}R \quad (4.86)$$

If investigations are done with N_2O_5 as the NO_3 radical source, NO in the reaction system is suppressed due to reaction (**Equation 4.51**). However, the reaction involving NO can be taken into consideration for assessment of the chemistry in the 'real' atmosphere. For propene and 1-butene reactions with NO_3, aldehydes could be determined quantitatively: HCHO (8%), CH_3CHO (12%) (propene), and HCHO (11%) and CH_3CH_2CHO (12%) (1-butene). These aldehydes accounted in both cases for only minor quantities of the total products. Nitrates amount to ~60%. For the NO_3 reaction with *trans*-2-butene, the final products were 3-(nitrooxy)-2-butanone $CH_3C(=O)CH(ONO_2)CH_3$, 2,3-butandiol dinitrate $CH_3CH(ONO_2)CH(ONO_2)CH_3$, and acetaldehyde. For isobutene, the two main products are acetone and formaldehyde with yields of 85% and 80%, respectively.

For NO_3 + dialkenes (butadiene), the identified products were CO (4%), HCHO (12%) acrolein $CH_2{=}CH{-}CHO$ (12%), total nitrates (60%). For the NO_3 + isoprene reaction, yields of products were CO (4%), HCHO (11%), methacrolein $CH_2{=}CH(CH_3){-}CHO$ (uncertain yield), and total nitrates (80%). The aldehydes formed in the reactions of NO_3 with the dialkenes can be explained by the thermal decomposition of the related nitrooxy-alkoxy radicals as in reaction (**Equation 4.85**) for monoalkenes. The formation of small quantities of CO in both the NO_3 + dialkenes reaction systems is difficult to explain. It is unclear whether the CO is formed directly in the reaction of NO_3 with dialkenes or whether it is a product of secondary reactions of NO_3 with acrolein or methacrolein.

For reactions of NO_3 with monoterpenes (α- and β-pinenes), some spectral features in the FT-IR analyses indicate carbonyl- and nitrate-containing compounds [26].

The reactivity of NO_3 radicals toward furan, thiophene and pyrrole has been studied at 295 K as an important atmospheric process involving these constituents in aviation fuels [45]. The rate constants obtained for these reactions show that NO_3 radicals react rapidly with furan ($k = 1.4 \times 10^{-12}$ cm^3/molecule/s) and pyrrole ($k = 4.9 \times 10^{-11}$

cm^3/molecule/s), and substantially less rapidly with thiophene ($k = 3.2 \times 10^{-14}$ cm^3/molecule/s). This trend in reactivity of pyrrole > furan > thiophene corresponds to that for reactions of these compounds with OH radicals and O_3 [49]. The kinetics of the reactions of these heterocycles with NO_3 was determined, but the composition of products formed has not been ascertained. On the basis of the analogy with alkenes and dialkenes [22, 25, 46], it is expected that these NO_3 radical reactions with furan, thiophene and pyrrole proceed via initial addition of NO_3 to the olefin double bonds [45]:

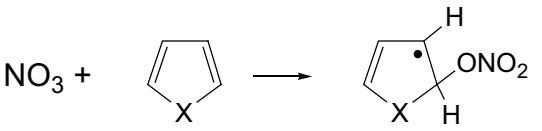

(4.87)

where X = O, S, or NH, followed by rapid addition O_2 to yield the peroxy radical

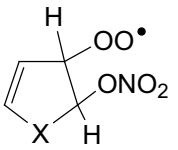

The reaction with NO_2 can then yield thermally unstable peroxynitrates:

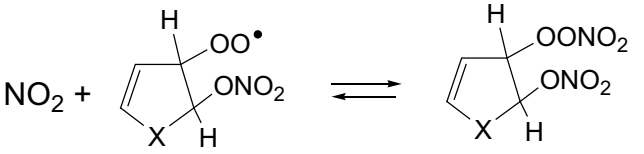

(4.88)

Peroxy radicals under nighttime conditions probably cause ring cleavage with the formation of species such as HC(=O)CH=CHXCHO.

4.4 Cross-linking of Macromolecules via the Photoreactions of NO_3

As mentioned above, in the course of CAN photolysis along with NO_3, other active radical species can be generated in reactions (**Equation 4.2**), (**Equation 4.4**), (**Equation 4.20**), and (**Equation 4.30**): NO, NO_2, and atomic oxygen. Use of light with different spectral distribution allows generation of the radicals in varying ratios. There is therefore an opportunity for research of the mechanism of radical reactions with participation of nitrogen oxides based on purposeful regulation of a yield of those or other products of these reactions. There is undoubted interest in the use of

CAN photolysis for generation of stable nitrogen-containing radicals, which find wide applications as spin labels [50]. NO readily reacts with free radicals (**Chapter 3**) to give nitroso compounds, which are effective spin traps. Therefore, photolysis and radiolysis of several polymers in an atmosphere of NO are accompanied by the appearance of stable nitrogen-containing radicals [51].

Stable radicals generated in this way occur in sufficiently drastic conditions of γ-radiolysis and direct action of UV light on macromolecules. This results in essential damage to the chemical structure and formation of various products owing to collateral thermal and photochemical reactions. From this viewpoint, CAN photolysis has certain advantages because light used for the generation of active radicals is not absorbed by macromolecules. In this case, primary macroradicals are formed in reactions of H-atom abstraction by atomic oxygen in the ground triplet state from the C–H bonds of monomer units [52]. Atomic oxygen should be active in reactions with C–H bonds, so generation of stable radicals during CAN photolysis does not require the availability of functional groups reactive to nitrogen oxides. By using the example of polyvinylpyrrolidone (PVP), which is widely used in pharmacology and medicine, the features of formation of stable aminoxyl radicals (ARs) during CAN photolysis have been considered [53–55].

PVP samples with additives of CAN (0.2–0.05 mol/kg) as coats of ~40-μm thickness on glass plates were irradiated in a vacuum by the filtered light of a mercury lamp. The formation of NO_2 by reactions (**Equation 4.1**) and (**Equation 4.4**) in the process of CAN photolysis is confirmed by the ESR spectrum recorded at 77 K. The spectrum at the initial stage of irradiation by light with $\lambda > 280$ nm is shown in **Figure 4.1a**. It represents a triplet signal with obviously expressed anisotropy of the *g*-factor and hyperfine structure belonging to NO_2 radicals stabilised at 77 K [56]. During further irradiation of samples, additional lines appeared on a background of the NO_2 signal, which corresponds to macroradicals of PVP (**Figure 4.1b**). NO_2 cannot abstract H atoms at 77 K, so macroradical formation is caused by the reaction of atomic oxygen with the weakest tertiary C–H bonds of macromolecules:

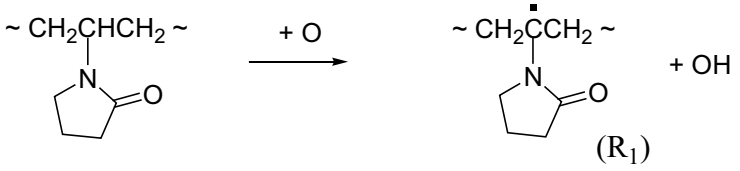

(4.89)

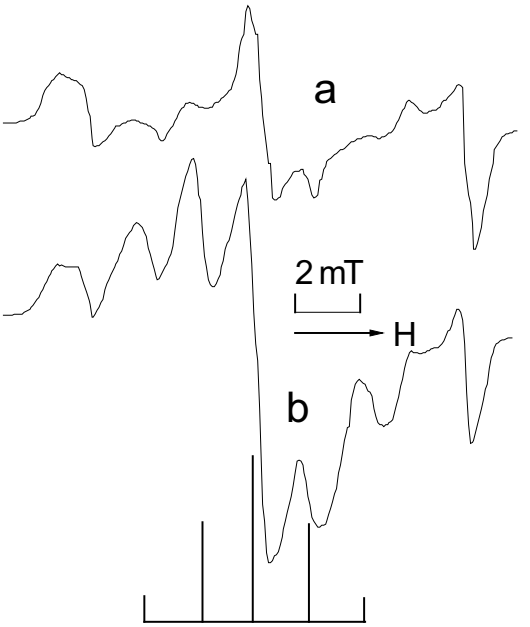

Figure 4.1 ESR spectra of PVP with CAN after irradiation by light with λ > 280 nm at 77 K during 2 min (a) and 69 min (b)

The spectrum of macroradicals R_1 in PVP represents a five-component signal with a distance between components of 1.8 mT [58], g = 2.0036. These macroradicals also arise from the subsequent reaction of sufficiently active hydroxyl radicals:

$$PVP + OH \longrightarrow R_1 + H_2O \tag{4.90}$$

In addition, formation of the radical R_1 takes place due to the reactions of NO_3 with tertiary C–H bonds [23]:

$$PVP + NO_3 \longrightarrow R_1 + HNO_3 \tag{4.91}$$

The radicals R_1 and NO_2 are stabilised only at low temperatures. Photolysis of the samples at room temperature results in formation of stable radicals, the ESR spectrum of which is shown in **Figure 4.2.** It represents a triplet with typical parameters for dialkylaminoxyl radicals with a hindered rotation: $A_{II}^{N} = 3.18\text{mT}$ and $g_{II} = 2.0024 \pm 0.0005$ (radical R_2). Spectra of this type are characteristic for ARs in

a polymeric matrix [51]. Their formation is explained by conversions of macroradicals R_1, which in reactions (**Equation 4.89**) and (**Equation 4.90**) are produced at very close distances in a polymeric matrix. This is because the intermediate radical pairs of macroradicals and OH radicals are formed in reaction (**Equation 4.89**). The species of this type detected by ESR in some glassy, crystal and polymeric media at low temperatures have characteristic distances between radicals of 0.5–0.6 nm [58]. If radicals are stabilised at a slightly longer distance, they appear in ESR spectra as isolated particles. This case is realised for radical R_1 at 77 K (**Figure 4.1b**).

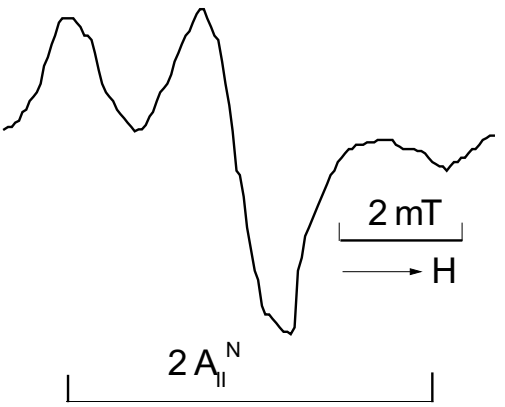

Figure 4.2 ESR spectrum of PVP with CAN after irradiation by light with λ > 280 nm at 295 K

The intermediate radical pairs of R_1 and OH radicals can efficiently recombine at room temperature, and this is the main process in PVP. Nevertheless, hydroxyl radicals are also capable of reacting with neighbouring macromolecules. Then, as a result of the following reaction (**Equation 4.90**), two closely located macroradicals R_1 are generated. The lifetime of the macroradicals until their contact in such arrangement is essentially more than that for previous radical pairs because of strong hindrance to molecular motions in solid polymers. Under conditions of photolysis by light with λ >280 nm, NO is formed in parallel with radicals R_1. The small-sized NO can diffuse relatively easily to radical R_1, giving nitroso compounds which, after accepting the close-spaced second radical, turns to radical R_2:

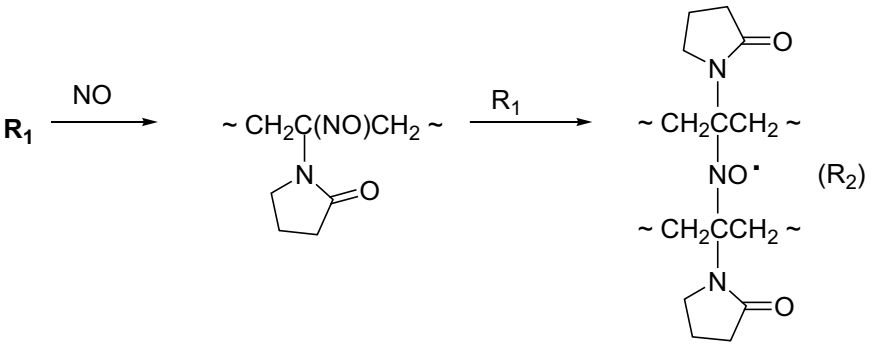

(4.92)

Similarly, stable ARs are formed in *N*-methyl-2-pyrrolidone (MP) chosen as a low-molecular analogue of PVP with additives of CAN under the same conditions [53]:

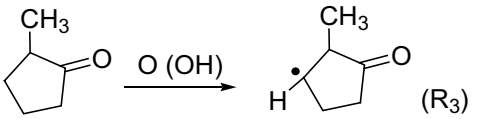

(4.93)

The radical R_3 is converted to aminoxyl R_4 by analogy with the scheme (**Equation 4.91**):

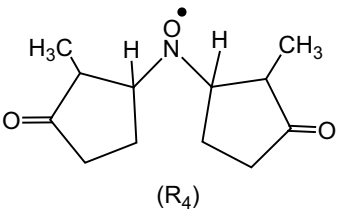

In principle, it is possible to assume H-atom abstraction by active atoms and radicals from the methyl groups of MP with the formation of radicals

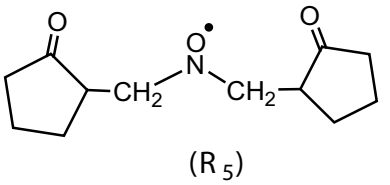

However, dialkylaminoxyl radicals containing methylene groups at the radical centre can disproportionate, giving a nitrone and hydroxylamine [59]:

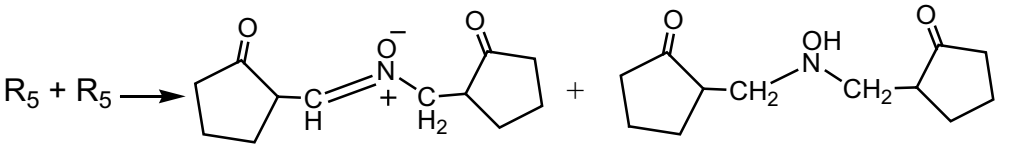

(4.94)

The disproportionation rate of the AR R_4 having α–alkyl – methine protons is strongly slowed down. The rate of this process for $(i\text{– Pr})_2NO^{\bullet}$ is approximately 340-times lower than for $Et_2NO^{\bullet}$ at 298 K [59]. These arguments lead us to believe that ARs in MP have the structure R_4.

From the ESR spectrum shown in **Figure 4.2**, it is clear that stable radicals of an aminoxyl type are formed during the initial generation of NO_3 in PVP. However, strong anisotropy of the hyperfine structure caused by hindered molecular mobility does not allow us to draw conclusions about the nature of the substituents at the radical centre. This spectrum gives only the prerequisites to represent the mechanism of the formation of stable radicals by the reactions (**Equation 4.89**)–(**Equation 4.92**). According to this mechanism, ARs are cross-links for macromolecules, and hence the radical concentration is connected with the yield of a gel-fraction (m_g / m_0) in the course of a sample photolysis.

Kinetic curves of gel accumulation under the action of light with $\lambda > 280$ nm and $280 < \lambda < 400$ nm are given in **Figure 4.3a** and **b**. As is evident from the figures, if light includes the UV and visible spectral region, the process is characterised from the outset by monotonous retardation with time. On the contrary, during photolysis only by UV light, some induction period is observed and it is especially noticeable at comparatively small initial concentrations of CAN. The availability of the induction period suggests that some intermediate product is formed and initiates cross-linking of macromolecules.

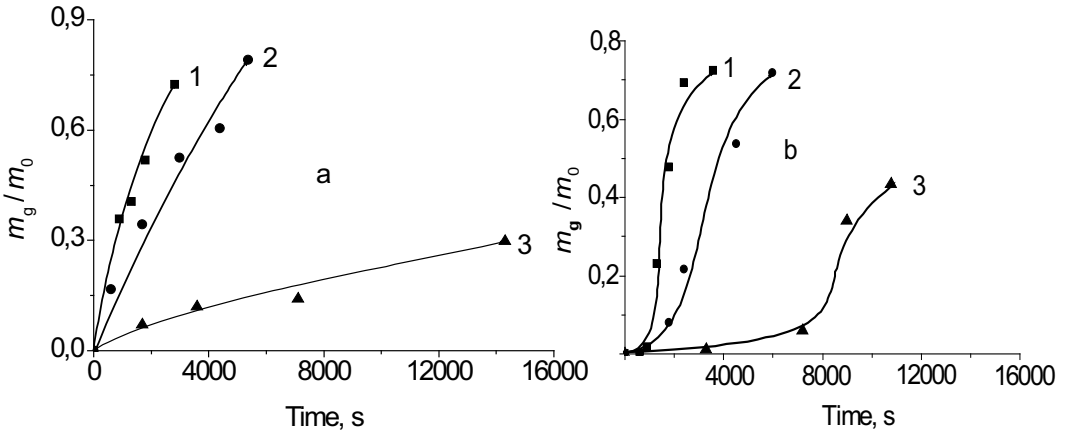

Figure 4.3 Kinetics of accumulation of gel fractions in PVP during photolysis by light with λ >280 nm (a) and 280 < λ < 400 nm (b) at $[CAN]_0$ = 0.19; 0.13 (2), 0.053 mol·kg^{-1} (3)

The kinetics of the accumulation of radical R_2 also demonstrates a qualitatively similar character. The process of gel formation and AR formation are in direct correlation during photolysis by light with λ > 280 nm. The linear dependencies shown in **Figure 4.4** indicate this feature.

The kinetics of formation of any product N with a monotonously decreasing rate can be represented by the equation:

$$N = at^n \tag{4.95}$$

where *a* and *n* are empirical parameters, and 0 < *n* < 1. As follows from **Figure 4.4**, kinetic curves are linearised in the co-ordinates of equation (**Equation 4.95**). The value of parameter $n = 0.8$ [53] is obtained from the analysis of kinetic dependencies by a least squares method. Such regularity confirms the mechanism (**Equation 4.92**), according to which the radical R_2 is formed with participation of NO and can be considered to be cross-links for macromolecules. The yield of cross-links is probably controlled by the effectiveness of the exit of the OH radical from intermediate radical pairs in reaction (**Equation 4.89**) and NO diffusion to radical R_1. If cross-linking were to mainly occur in another way, for example, by direct recombination of radical R_1, then the radical R_2 and gel accumulations would not be correlated as follows from **Figure 4.4**.

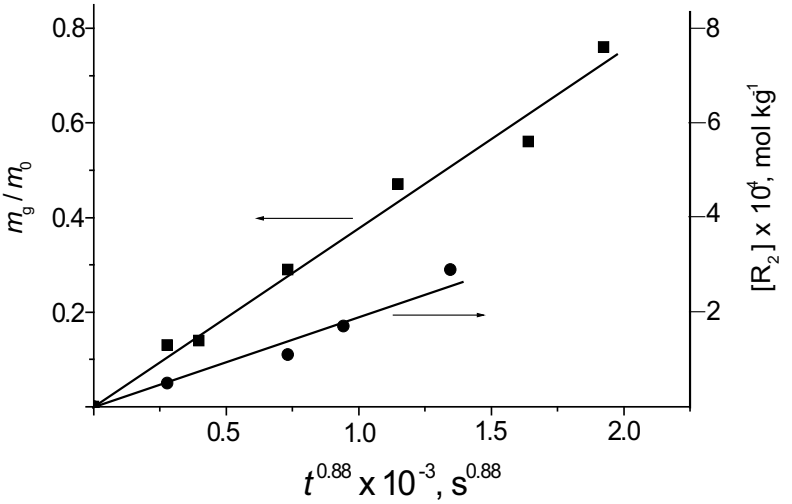

Figure 4.4 Linearisation of kinetics of the gel fraction and radical R_2 formation in PVP in the coordinates of **Equation 4.95**

The limiting concentration of ARs accumulated in samples does not exceed 10^{-3} mol/kg, which is much less than the initial concentrations of CAN in PVP. The reason is that the main part of macroradical R_1 is consumed in side processes without aminoxyl formation. That is why there are grounds to conclude that they recombine with OH radicals at the primary stage of radical generation.

Another situation is observed during UV photolysis of samples (**Figure 4.3b**). The induction period in the kinetics of gel formation assumes a peculiar mechanism of AR generation in these conditions. NO_3 dissociation via reaction (**Equation 4.30**) is strongly depressed, and the main path of photo-transformation of nitrate radicals is their decomposition into NO_2 and atomic oxygen. Thus, primary closely located macroradicals R_1 formed in reactions (**Equation 4.89**) and (**Equation 4.90**) can recombine with NO_2. Similarly to nitroso compounds, nitro compounds can add alkyl radicals with the formation of a stable spin adduct. Such an eventuality was shown by ESR in an example of aromatic nitro compounds [60]. For PVP, the mechanism resulting in radical R_2 is:

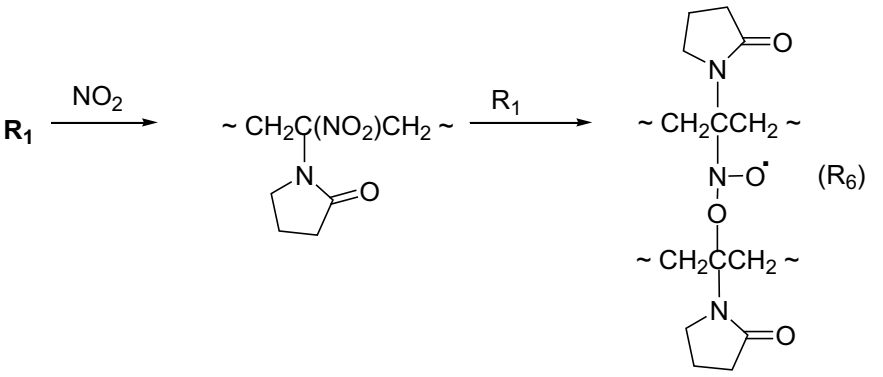

(4.96)

Alkoxyaminoxyl radicals R_6 are unstable at room temperature [61] and break down into alkoxy radicals and nitroso compounds:

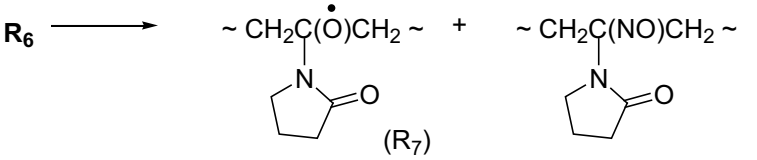

(4.97)

Alkoxy radicals R_7 are very active in reactions of H-atom abstraction [62] and are converted into radicals R_1 by interaction with tertiary C–H bonds of neighbouring macromolecules:

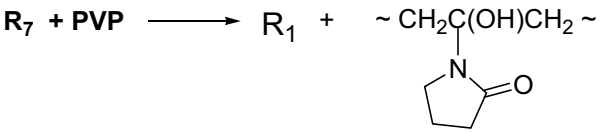

(4.98)

If radicals R_1 are allocated in the range of accepting with nitroso groups, they turn into radicals R_2 by reaction (**Equation 4.92**). However, additional intermediate reactions including decomposition of alkoxyaminoxyl radicals and changing of alkoxy to alkyl radicals make the spin trapping process in this case seemingly less preferable from a kinetic point of view. In the course of the reaction (**Equation 4.98**), a spatial separation implying an exit radical R_1 and nitroso groups from the reacting 'cage' occurs. As a consequence, a difficulty for their approach appears in conditions of hindered molecular mobility. This effect is especially appreciable at the beginning of photolysis when concentrations of nitroso groups in macromolecules are small, and the radical decay in recombination with NO_2 prevails over spin trapping. Owing

to this the induction period of a gel accumulation is observed in the absence of a competitive manner of aminosyl formation connected with the NO photo-generation (**Figure 4.3b**).

One can observe in **Figure 4.3a** and **b** that the gelation rate can be higher under the action of UV light after an induction period than during photolysis by light with $\lambda > 280$ nm. This effect is most pronounced at low concentrations of CAN. Such behaviour is explicable because light with $\lambda > 280$ nm generates oxygen in reaction (**Equation 4.2**). As oxygen is accumulated in samples, the oxidation of NO begins. Besides, the conversion of radicals R_1 to peroxy radicals takes place. Both processes decrease the yield of cross-links because peroxy radicals do not give stable adducts in reactions with nitroso compounds. In support of this interpretation, an induction period is apparent in gel formation during irradiation by light with $\lambda > 280$ nm in air. The presence of oxygen in samples inhibits the reactions of the formation of radical R_2 through NO and makes possible (to a certain extent) only the mechanism connected with reactions (**Equation 4.96**)–(**Equation 4.98**).

Measurements of the concentrations of radical R_2 separately in gel fractions [53] are represented in **Table 4.1**. The concentrations at late stages of photolysis become invariable, i.e., radicals R_2 are localised in the cross-links of macromolecules. The estimations on the basis of ESR spectra [53] show that one cross-link accounts for two original macromolecules of PVP.

Table 4.1 Concentrations of R_2 in gel fractions of PVP with $[CAN]_0 = 0.19$ mol/kg.

$[R_2]\cdot 10^4$, mol/kg		
$t\cdot 10^{-3}$, s	$\lambda > 280$ nm	$280 < \lambda < 400$
1.2	6.2	-
1.5	7.3	-
2.1	9.8	-
2.4	-	5.6
2.7	9.8	-
3.6	9.6	4.9
4.8	-	5.5

The considered method of obtaining the spin-labelled low-molecular compounds and solid polymers based on NO_3 photogeneration is comparatively simple, and can be used in systems in which CAN is sufficiently dissolved. Carrying out CAN photolysis in diluted solutions of polymers in specified solvents can prevent cross-

linking to a great extent, and give spin-labelled macromolecules as ARs containing low-molecular fragments of the solvent. CAN photolysis in solid polymers provides a way of preparing polymeric gels, in particular hydrogels which find use as specific sorbents [63]. In the considered procedure, estimation of the cross-link number does not require application of special techniques, and can be achieved by direct ESR measurements of concentrations of stable ARs.

References

1. P. Neta and R. Huie, *Journal of Physical Chemistry*, 1986, **90**, 19, 4644.

2. T.W. Martin and R.W. Glass, *Journal of the American Chemical Society*, 1970, **92**, 17, 5075.

3. R.W. Glass and T.W. Martin, *Journal of the American Chemical Society*, 1970, *92*, 17, 5084.

4. T.W. Martin, R.E. Rummel and R.C. Gross, *Journal of the American Chemical Society*, 1964, **86**, 13, 2595.

5. T.W. Martin, A. Henshell and R.C. Gross, *Journal of the American Chemical Society*, 1963, **85**, 1, 113.

6. L. Dogliotti and E. Hayon, *Journal of Physical Chemistry*, 1967, **71**, 12, 3802.

7. P.H. Wine, R.L. Mauldin and R.P. Thorn, *Journal of Physical Chemistry*, 1988, **92**, 5, 1156.

8. T.W. Martin, J.M. Burk and A. Henshell, *Journal of the American Chemical Society*, 1966, **88**, 6, 1097.

9. E. Hayon and E. Saito, *Journal of Chemical Physics*, 1965, **43**, 4314.

10. A.K. Pikaev, G.K. Sibirskaya, E.M. Shirshov, P.Ya. Glazunov and V.I. Spitsin, *Doklady Akademii Nauk SSSR*, 1974, **215**, 645.

11. M. Daniels, *Journal of Physical Chemistry*, 1969, **73**, 11, 3710.

12. R.K. Broszkiewicz, E. Kozlowska-Milner and A. Blum, *Journal of Physical Chemistry*, 1981, **85**, 15, 2258.

13. Y. Katsumura, P.Y. Jiang, R. Nagaishi, T. Oishi and K. Ishigure, *Journal of Physical Chemistry*, 1991, **95**, 11, 4435.

14. T.G. Hall and F.J. Blacet, *Journal of Chemical Physics*, 1952, **20**, 1745.

15. S. I. Bainov, V.K. Pack, V.A. Novostruev and B.A. Khisamov, *Khimiia Vysokikh Energii*, 1991, **25**, 92.

16. A. Mellouki, G. Le Brass and G. Poulet, *Journal of Physical Chemistry*, 1987, **91**, 22, 5760.

17. C.A. Smith, A.R. Ravishankara and P.H. Wine, *Journal of Physical Chemistry*, 1985, **89,** 8, 1423.

18. P.D. Hammer, E.J. Dlugokencky and C.J. Howard, *Journal of Physical Chemistry*, 1986, **90**, 11, 2491.

19. A.R. Ravishankara and R.L.Mauldin, *Journal of Physical Chemistry*, 1985, **89**, 14, 3144.

20. T.J. Wallington, R. Atkinson, A.M. Winer and J.N. Pitts, *Journal of Physical Chemistry*, 1986, **90**, 19, 4640.

21. E.D. Morris and H. Niki, *Journal of Physical Chemistry*, 1974, **78**, 1337.

22. S.M. Japar and H. Niki, *Journal of Physical Chemistry*, 1975, **79**, 1629.

23. R. Atkinson, C.N. Plum, W.P.L. Carter, A.M. Winer and J.N. Pitts, *Journal of Physical Chemistry*, 1984, **88**, 11, 2361.

24. R. Atkinson, C.N. Plum, W.P.L. Carter, A.M. Winer and J.N. Pitts, *Journal of Physical Chemistry*, 1984, **88**, 6, 1210.

25. R. Atkinson, S.M. Aschmann, A.M. Winer and N. Pitts, *Environmental Science and Technology*, 1984, **18**, 5, 370.

26. Barnes, V. Bastian, K.H. Becker and Z. Tong, *Journal of Physical Chemistry*, 1990, **94**, 6, 2413.

27. C.H. Wu, E.D. Morris and H. Niki, *Journal of Physical Chemistry*, 1973, **77**, 25, 2507.

28. H.S. Johnston and R. Graham, *Canadian Journal of Chemistry*, 1974, **52**, 8, 1415.

29. R. Graham and H.S. Johnston, *Journal of Physical Chemistry*, 1978, **82**, 3, 254.

30. C. Stroud, S. Madronich, E. Atlas, B. Ridley, F. Flocke, A.W. Talbot, A. Frid, B. Wert, R. Shetter, B. Lefer, M. Coffey and B. Heik, *Atmospheric Environment*, 2003, **37**, 24, 3351.

31. B. Venkatachalapathy and P. Ramamurthy, *Journal of Photochemistry and Photobiology A: Chemistry*, 1996, **93**, 1, 1.

32. A.D. Walsh, *Journal of the Chemical Society*, 1953, **88**, 2306.

33. J.F. Olsen and L. Burnell, *Journal of the American Chemical Society*, 1970, **92**, 12, 3659.

34. R.A. Rasmusen and M.A.K. Khalil, *Journal of Geophysical Research*, 1988, **93**, 1417.

35. P.R. Zimmerman, J.P. Greenberg and C.E. Westberg, *Journal of Geophysical Research*, 1988, **93**, 1407.

36. G. Schott and N. Davidson, *Journal of the American Chemical Society*, 1958, **80**, 8, 1841.

37. C.A. Cantrell, W.R. Stockwell, L.G. Anderson, K.L. Busarow, D. Perner, A. Schmeltekopf, J.G. Calvert and H.S. Johnston, *Journal of Physical Chemistry*, 1985, **89**, 1, 139.

38. R.A. Graham and H.S. Johnston, *Journal of Physical Chemistry*, 1978, **82**, 254.

39. W.A. Longeman, S.L. Kopczynski, P.E. Darley and F.E. Sutterfield, *Environmental Science and Technology*, 1974, **8**, 3, 229.

40. J.M. Heuss, G.J. Nebel and B.A. D'Alleva, *Environmental Science and Technology*, 1974, **8**, 7, 641.

41. W.P.L. Carter, A.M. Winer and J.N. Pitts, *Environmental Science and Technology*, 1981, **15**, 7, 829.

42. R.A. Kenley, J.E. Davenport and D.G. Hendry, *Journal of Physical Chemistry*, 1978, **82**, 9, 1095.

43. E. Baciochi, T. Del Giacco, S.M. Murgia and G.V. Sebastiani, *Journal of the Chemical Society Chemical Communications*, 1987, 16, 1246.

44. O. Ito, S. Akiho and M. Iino, *Journal of Organic Chemistry*, 1989, **54**, 10, 2436.

45. R. Atkinson, S.M. Aschmann, A.M. Winer and W.P.L. Carter, *Environmental Science and Technology*, 1985, **19**, 1, 87.

46. H. Bandow, M. Okuda and H. Akimoto, *Journal of Physical Chemistry*, 1980, **84**, 26, 3604.

47. P.B. Shepson, E.G. Edney, T.E. Kiendienst, J.H. Pittman, G.R. Namie and L.T. Cupitt, *Environmental Science and Technology*, 1985, **19**, 9, 849.

48. H. Akimoto, H. Bandow, F. Sakamaki, G. Inoue, M. Hoshino and M. Okuda, *Environmental Science and Technology*, 1980, **14**, 2, 172.

49. R. Atkinson, S.M. Aschmann, A.M. Winer and W.P.L. Carter, *Atmospheric Environment*, 1984, **18**, 2185.

50. A.M. Wasserman and A.L. Kovarsky, *Spin: Labels and Probes in Physical Chemistry of Polymers*, Nauka Publishers, Moscow, Russia, 1986.

51. G.B. Pariiskii, I.S. Gaponova and E.Ya. Davydov, *Russian Chemical Reviews*, 2000, **69**, 11, 985.

52. B. Ranby and J.F. Rabek, *Photodegradation, Photooxidation, and Photostabilisation of Polymers*, Wiley, London, UK, 1975.

53. E.Ya. Davydov, E.N. Afanas'eva, I.S. Gaponova and G.B. Pariiskii, *Organic and Biomolecular Chemistry*, 2004, **2**, 9, 1359.

54. E.Ya. Davydov, I.S. Gaponova and G.B. Pariiskii, *Polymer Science A*, 2003, **45**, 346.

55. E.Ya. Davydov, I.S. Gaponova, T.V. Pokholok, A.P. Vorotnikov, G.B. Pariiskii and G.E. Zaikov, *Polymers for Advanced Technologies*, 2008, **19**, 6, 475.

56. P.W. Atkins, N. Keen and M.C.R. Symons, *Journal of the Chemical Society*, 1962, 2873.

57. H. Monig and H. Ringsdorf, *Makromolekulare Chemie*, 1974, **B175**, 811.

58. E.Ya. Davydov, A.P. Vorotnikiv, G.B. Pariiskii and G.E. Zaikov, *Kinetic Peculiarities of Solid Phase Reactions*, Wiley, Chichester, UK, 1998.

59. D.F. Bowman, T. Gillan and K.U. Ingold, *Journal of the American Chemical Society*, 1971, **93**, 24, 6555.

60. W. Ahrens and A. Berndt, *Tetrahedron Letters*, 1973, **43**, 4281.

61. E.Ya. Davydov, I.S. Gaponova and G.B. Pariiskii, *Journal of the Chemical Society, Perkin Transactions 2*, 2002, **7**, 1359.

62. T. Bercés and A.E. Trotman-Dickenson, *Journal of the Chemical Society*, 1961, 348.

63. H.J. Naghash, A. Massah and A. Erfan, *European Polymer Journal*, 2002, **38**, 1, 147.

5 Reactions of Nitrogen Dioxide with Organic Compounds

Nitrogen dioxide (NO_2) is the air pollutant formed mainly by road traffic and energy production. It is one of the components of acid rain and may affect human health [1]. NO_2 represents a moderately reactive free radical in reactions of hydrogen-atom abstraction; the strength of the ONO–H bond is 327 kJ/mol [2]. It can initiate several types of reactions, e.g., hydrogen-atom abstraction from the weak C–H bonds of organic molecules at ambient temperatures and addition to carbon double bonds. Additionally, NO_2 and its dimers can enter into specific reactions with the functional groups of macromolecules.

5.1 Reactions of NO_2 with Alkanes

It is considered [3–6] that when NO_2 is used as a nitrating reagent, the following free-radical reaction occurs:

$$RH + NO_2 \rightarrow R^{\bullet} + HNO_2 \qquad (5.1)$$

The activation energy of the reaction for methane estimated experimentally is approximately 50 kcal/mol [4]. Calculations done on the basis of density functional molecular orbital theory give 35–40 kcal/mol for the reaction with methane, 32–35 kcal/mol for ethane, 28–32 kcal/mol for propane and 25–30 kcal/mol for isobutane [7]. For other cases, the activation energies decrease with the stabilisation energy of the radical $R^{\bullet}$ due to conjugation. For example, for the reaction of NO_2 with toluene, diphenylmethane and triphenylmethane, these values amount to 28–33 kcal/mol, 17–22 kcal/mol, and 5–10 kcal/mol, respectively. Therefore, *n*-alkanes almost fail to react with NO_2 under normal conditions even after several months, whereas the reaction with isoparaffins proceeds markedly, and the reaction (Equation **5.1**) with toluene goes to completion [4]. Nitration of diphenylmethane with NO_2 is complete in two days, and triphenylmethane reacts very quickly. The high reactivity of the paraffin chain of tetraline is probably due to the appearance of weak π-bonds between saturated carbon atoms, thus leading to the weakening of C – H bonds in the tetramethylene group – $(CH_2)_4$ – [4].

The vapour-phase nitration of alkanes with NO_2 is usually carried out in a reactor at 250–350 °C. In view of the partial dissociation of NO_2 which undoubtedly occurs under these conditions, the primary radical formation can be explained on the basis of the reaction of oxygen formed by the dissociation of NO_2 with the alkane by the chain mechanism [8]:

$$RH + O_2 \rightarrow RO_2H \quad (5.2)$$

$$RO_2H \rightarrow RO^{\bullet} + OH^{\bullet} \quad (5.3)$$

$$OH^{\bullet} + RH \rightarrow R^{\bullet} + H_2O \quad (5.4)$$

$$RO^{\bullet} + RH \rightarrow ROH + R^{\bullet} \quad (5.5)$$

$$R^{\bullet} + O_2 \rightarrow RO_2^{\bullet} \quad (5.6)$$

$$RO_2^{\bullet} + RH \rightarrow RO_2H + R^{\bullet} \quad (5.7)$$

It is also assumed that the oxidation of hydrocarbons is initiated by oxygen atoms formed by the thermal dissociation of a nitrogen oxide (NO) [3]. The use of gaseous initiation of liquid-phase oxidation of paraffins (127 °C), consisting of addition of NO_2 to air at the beginning of the reaction, allows considerable shortening of the induction period for the oxidation [9]. With a 30-minute initiation by air containing 0.35% NO_2, the induction period is 10 hours, as compared with 366 hours in the absence of the initiator.

Data obtained for the nitration of propane with NO_2 in the gas phase at ≤300 °C in the presence of oxygen shows [3] that a rise in oxygen concentration in the reaction zone by increasing the opportunities for radical formation appreciably increases the yield of nitroalkanes. If the same process is carried out at 350 °C, there is a sharp fall in the yield and extent of conversion, and there is an appreciable increase in the carbon monoxide (CO) content of the exit gases. It would appear that, in the high-temperature nitration of alkanes, conditions are created under which the rate of the reaction:

$$R^{\bullet} + NO_2 \rightarrow RNO_3 + RONO \quad (5.8)$$

is evidently less than that of the reaction:

$$R^{\bullet} + O_2 \rightarrow \text{oxidation products} \quad (5.9)$$

One of the possible causes of the development of an oxidative course in the nitration lies in the thermal decomposition of nitrocompounds and alkyl nitrites [4]. RONO decomposes between 300 °C and 500 °C. For instance, ethylnitrite produces a free

ethoxy and then a methyl radical to form, with NO_2, nitromethane and methyl nitrite:

$$CH_3CH_2ONO \xrightarrow{-NO} CH_3CH_2O^{\bullet} \xrightarrow{-CH_2O} CH_3^{\bullet} \xrightarrow{NO_2}$$

$$CH_3NO_2 + CH_3ONO \qquad (5.10)$$

The initiation of radical formation in the gas-phase nitration of alkanes with NO_2 is closely related to other phenomena connected with the catalysis of the reaction by chlorine [10], bromine [11], iodine [11], and mixtures of these halogens with oxygen. The observed accelerating effects of small additions of halogens with their initiation of radical formation can be represented by the scheme [10]:

$$X_2 \rightleftharpoons 2X \qquad (5.11)$$

$$RH + X \rightarrow R^{\bullet} + HX \qquad (5.12)$$

$$R^{\bullet} + NO_2 \rightarrow RNO_2 \qquad (5.13)$$

$$R^{\bullet} + X_2 \rightarrow RX + X \qquad (5.13)$$

$$HX \xrightarrow{O_2, NO_2} H_2O + X_2 + \text{lower nitrogen oxides} \qquad (5.14)$$

In the course of gas-phase nitration of alkanes with NO_2, increase in the yield of nitroalkane can be attained by increase in the rate of radical formation and retardation of oxidative reactions in which the free radicals take part. It is probable that the catalytic effect of molecular iodine on the nitration of propane with NO_2 is associated mainly with the tendency of inactive iodine atoms to retard the oxidation of hydrocarbons [11]. In the presence of 0.15% I_2, the CO content of the reaction products is reduced from 22.1% to 5.2%. Simultaneously, the yield of nitro compounds is increased by 10%.

The presence of free nitric oxide (NO) in the reaction zone has an unfavourable effect on the nitration reaction. NO may be formed by the dissociation of NO_2 and also by the reaction [3]:

$$2RH + 3NO_2 \rightarrow 2RNO_2 + NO + H_2O \qquad (5.15)$$

The effect of NO is particularly notable in the nitration of propane with nitric acid at 420 °C [10]. Being a powerful inhibitor of chain reactions (**Chapter 3**), NO reduces the rate of radical formation and the rate of recombination of radicals with NO_2. On the other hand, the increase observed in the content of CO and C_2H_4 of the exit gases indicates the development of processes of hydrocarbon breaking. The addition

of NO inhibits the oxidation of propane by nitrous oxide in the temperature range 505–605 °C [12]. Above 655 °C, the inhibiting effect of NO disappears. It was shown [8] that NO can simultaneously develop accelerating and retarding effects on chain reactions; the overall effect may be positive or negative.

The formation of trifluoronitroethane on nitration of 1,1,1–trifluoropropane at 395 °C [13] can be represented as follows:

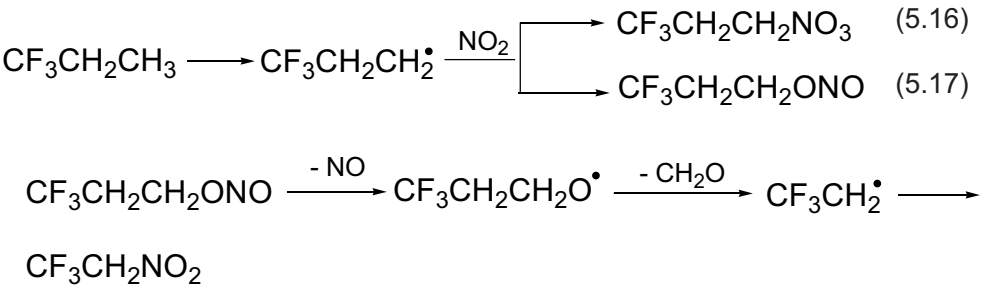

The study of gas-phase reactions between nitrogen dioxide and chlorinated derivatives of methane have been carried out over in the temperature range 290–335 °C [14]. The main feature of these reactions is their autocatalytic nature. The suggested mechanism of the reaction between methyl chloride and NO_2 initially involves hydrogen-atom abstraction:

$$CH_3Cl + NO_2 \rightarrow CH_2Cl + HNO_2 \quad (5.19)$$

Autocatalysis results from the production of chlorine atoms by the reaction of the products HCl and nitrosyl chloride (NOCl):

$$HCl + NO_2 \rightarrow Cl + HNO_2 \quad (5.20)$$

and

$$NOCl + M \rightarrow NO + Cl + M \quad (5.21)$$

The chlorine atoms then react with methyl chloride:

$$CH_3Cl + Cl \rightarrow CH_2Cl + HCl \quad (5.22)$$

Further evidence for the initial step (**Equation 5.19**) is that carbon tetrachloride (CCl_4) reacts with NO_2 at a temperature only 150 °C higher than that for the other chloromethanes. This confirms hydrogen (rather than chlorine) abstraction as the initial step.

The following mechanisms are postulated to account for the major products of NO_2 reactions with chloroform [14]:

$$CHCl_3 + NO_2 \rightarrow CCl_3 + HNO_2 \quad (5.23)$$

$$CCl_3 + NO_2 \rightarrow [CCl_3NO_2] + COCl_2 + NOCl \quad (5.24)$$

$$CCl_3 + COCl_2 \rightarrow COCl + CCl_4 \quad (5.25)$$

$$COCl \rightarrow CO + Cl \quad (5.26)$$

$$NO_2 + COCl \rightarrow CO_2 + NOCl \quad (5.27)$$

$$NOCl + M \rightleftharpoons NO + Cl + M \quad (5.28)$$

$$CHCl_3 + Cl \rightarrow CCl_3 + HCl \quad (5.29)$$

$$HCl + NO_2 \rightarrow Cl + HNO_2 \quad (5.30)$$

$$NO + Cl_2 \rightarrow NOCl + Cl \quad (5.31)$$

$$NOCl + Cl \rightarrow NO + Cl_2 \quad (5.32)$$

$$2HNO_2 \rightarrow H_2O + NO + NO_2 \quad (5.33)$$

$$2NO_2 \rightleftharpoons 2NO + O_2 \quad (5.34)$$

For methylene chloride, the similar scheme of reactions is suggested [14]:

$$CH_2Cl_2 + NO_2 \rightarrow CHCl_2 + HNO_2 \quad (5.35)$$

$$CHCl_2 + NO_2 \rightarrow [CHCl_2NO_2] + CHClO + NOCl \quad (5.36)$$

$$CHClO \rightarrow CO + HCl \quad (5.37)$$

$$CH_2Cl_2 + Cl \rightarrow CHCl + HCl \quad (5.38)$$

In addition, **Equations** (**5.28**), (**5.30**)–(**5.34**) as for chloroform take place.

The initial reaction is again hydrogen abstraction followed by addition of NO_2 to the $CHCl_2$ radical formed. Elimination of NOCl from this intermediate, in an analogous manner to that for the methyl chloride and chloroform reactions, would produce formyl chloride (**Equation 5.36**). At 290 °C this intermediate is unstable, [15] breaking to give CO and HCl and thus accounting for the relatively large amounts

of these products produced in this reaction. The mechanisms suggested account for the autocatalytic nature of these reactions and the products formed.

Alkyl nitrites in a liquid phase readily undergo hydrolysis, etherification, and other equilibrium reactions in terms of the following scheme yielding alcohols, alkyl nitrate, esters of organic acids, ethers and olefins [4]:

$$RONO \overset{H_2O}{\rightleftharpoons} ROH + HNO_2 \tag{5.39}$$

$$ROH \overset{HNO_3}{\rightleftharpoons} RONO_2 + H_2O \longrightarrow \text{olefins} + HNO_3 \tag{5.40}$$

$$ROH \overset{R'COOH}{\rightleftharpoons} R'COOR + H_2O \tag{5.41}$$

$$ROH \overset{ROH}{\rightleftharpoons} ROR + H_2O \tag{5.42}$$

Alcohols and alkyl nitrites are readily oxidised by NO_2 to aldehydes and ketones and then to acids R′COOH which react with alcohol according to (**Equation 5.41**).

The destructive nitration of alcohols, ethers, and ketones at 400 °C can be considered as a method of obtaining some nitro alkanes, for instance, $C_2H_5NO_2$ and CH_3NO_2 [16]:

$$(C_2H_5)_2O \xrightarrow{NO_2,400^o} CH_3CH_2^{\bullet} + CH_3CH_2ONO_2 \tag{5.43}$$

$$CH_3CH_2^{\bullet} + NO_2 \rightarrow CH_3CH_2NO_2 + CH_3CH_2ONO \tag{5.44}$$

$$CH_3CH_2ONO \xrightarrow{-NO} CH_3CH_2O^{\bullet} \xrightarrow{-CH_2O} CH_3^{\bullet} \xrightarrow{NO_2}$$

$$CH_3NO_2 + CH_3ONO \tag{5.45}$$

$$CH_3CH_2ONO_2 \xrightarrow{-NO_2} CH_3CH_2O^{\bullet} \xrightarrow{-CH_2O} CH_3^{\bullet} \xrightarrow{NO_2}$$

$$CH_3NO_2 + CH_3ONO \tag{5.46}$$

The paraffin chain shows high reactivity toward nitric anhydride [4]. The reaction of nitrogen pentoxide (N_2O_5) with paraffins and cyclohexane occurs quickly even at 0 °C in a solution of CCl_4 with the formation mainly of secondary alkyl nitrates and nitro compounds. This reaction is intensified by a very active NO_3 radicals resulting from the homolytic dissociation:

$$N_2O_5 \rightleftharpoons NO_2 + NO_3 \tag{5.47}$$

The mechanism of the N_2O_5 reaction with paraffins is represented as [4]:

$$RH + NO_3 \rightarrow R^{\bullet} + HNO_2 \tag{5.48}$$

$$R^{\bullet} + NO_2 \rightarrow RNO_2 + RONO \tag{5.49}$$

$$RONO \xrightarrow{N_2O_5} RONO_2 + N_2O_4 \tag{5.50}$$

$$R^{\bullet} + N_2O_5 \rightarrow RONO_2 + NO_2 \tag{5.51}$$

This scheme was confirmed by kinetic data for the nitration of cyclohexane by N_2O_5 in CCl_4 [17].

Aliphatic hydrocarbons are inert toward NO_2 under ambient conditions. However, this nitrating agent is activated in the presence of ozone at sufficiently low temperatures ('Kyodai nitration') [17]. This reaction has been used widely and is now the subject of industrial research. NO_2 and ozone form dinitrogen pentoxide through intermediate nitrogen trioxide and the formation of nitrogen trioxide (NO_3) has been established to be rate-determining [18]:

$$NO_2 + O_3 \rightarrow [NO_2 \cdot O_3] \rightarrow NO_3 + O_2 \tag{5.52}$$

$$2\ NO_2 \rightleftharpoons O_2N\text{-}NO_2 + O_3 \longrightarrow \left[\ \begin{array}{c} O \\ O \quad O \\ O_2N\text{-}NO_2 \end{array}\ \right] \longrightarrow NO_3 + O_2NOO^{\bullet} \tag{5.53}$$

$$O_2NOO^{\bullet} \rightarrow NO_2 + O_2 \tag{5.54}$$

$$NO_3 + NO_2 \rightleftharpoons N_2O_5 \rightleftharpoons NO_2^{+} + NO_3^{-} \tag{5.55}$$

The highly selective *N*- and *O*-functionalisation of adamantane based on the nitration procedure at –78 °C has been found [17]. Because of the symmetrical nature and high stability of the carbon framework, adamantane is a good model compound for examining the behaviour of alkanes toward the Kyodai nitration.

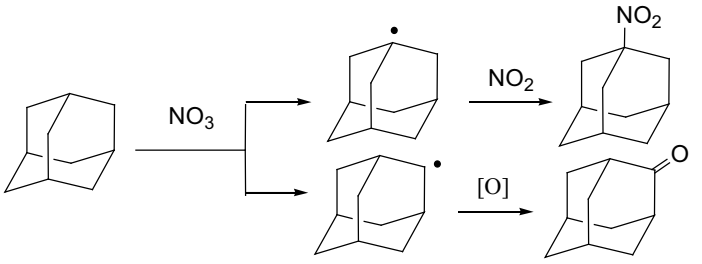

(5.56)

(5.57)

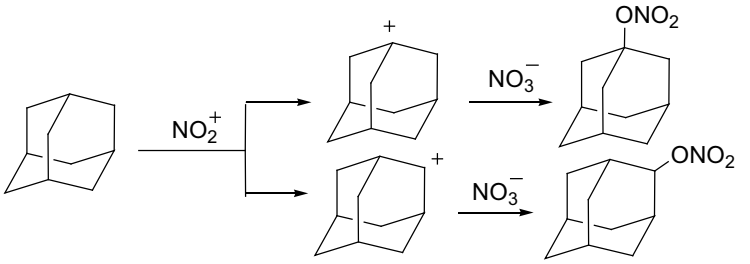

(5.58)

(5.59)

The nitration occurred with ease and high positional selectivity at the bridgehead to give 1-nitroadamantane as the major product (**Equation 5.56**). The best result was obtained at –78 °C in the presence of a large excess of NO_2, when tertiary/secondary positional selectivity was as high as 100. Skeletal rearrangement was not observed. Formation of nitrates (4–5%) in **Equations** (**5.58**) and (**5.59**) may be attributed to the oxidation of the initially formed adamantyl radicals to carbocations, followed by coupling with the nitrate ion.

Thus, the rate-determining step of alkane nitration is the formation of free alkyl radicals in (**Equation 5.1**), as well as in reaction of alkanes with O_2, NO_3, OH, Cl and other active radicals. The reactions of $R^{\bullet}$ with NO_2, NO, O_2, N_2O_5 [19], Br_2 [20] and other components of the reaction system (including solvents) results in a mixture of nitro compounds, nitrites, nitroso compounds, and nitrates. All these compounds with the exception of RNO_2 depending on the conditions undergo further conversions, resulting in the different composition of the end products of nitration.

5.2 Reactions of NO_2 with Aromatic Compounds

The attachment of NO_2 to organic molecules is successfully applied to the industrial production of nitroalkanes, but in the case of nitroarenes this method is frequently unsuitable because of the low affinity of NO_2 radicals toward aromatic nuclei. Under the same conditions, NO_2 reacts to produce a complicated mixture of products arising

from addition, substitution and oxidative degradation [4]. The radical mechanism is characterised by a greater diversity of reaction pathways and products which is an advantage and disadvantage from the synthetic point of view. Therefore, the electrophilic substitution (ionic mechanism) using nitric acid alone or in mixture with sulphuric acid is commonly used for aromatic nitration [21].

In accordance with the radical mechanism, the reaction in benzene yields trinitrobenzene, *p*- and *m*-dinitrobenzenes, 2,4-di- and 2,4,6-trinitrophenol and oxalic acid. The formation of *m*-dinitrobenzenes, and trinitrobenzene is accounted for by the addition of three and five NO_2 radicals to the primary nitrocyclohexadienyl radical followed by an abstraction of two or three nitrous acid (HNO_2) molecules from the adducts. For the trinitrobenzene formation, this process can be represented as follows [4]:

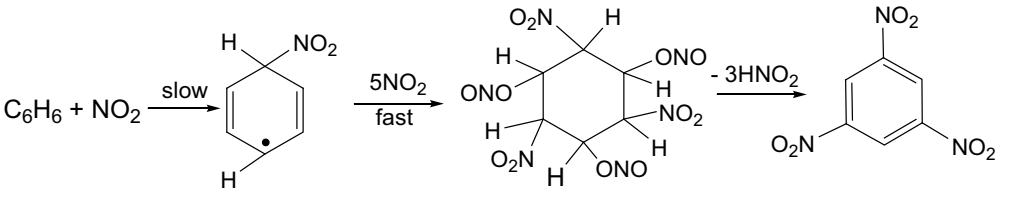

(5.52)

Study of the interaction of toluene, nitrobenzene, dimethylaniline, phenol, anisole, and chlorobenzene with pernitrous acid (HOONO) at 8–98 °C enabled formulation of the reaction mechanism [22]. HOONO is an important intermediate in the interconversion of nitrogen-containing species [23]. It forms upon reaction between hydrogen peroxide and nitrous acid. HOONO undergoes homolytic detachment:

$$HOONO \rightarrow OH + NO_2 \qquad (5.53)$$

The hydroxyl radical enters the aromatic nucleus almost exclusively in the *o*- and the *p*-position:

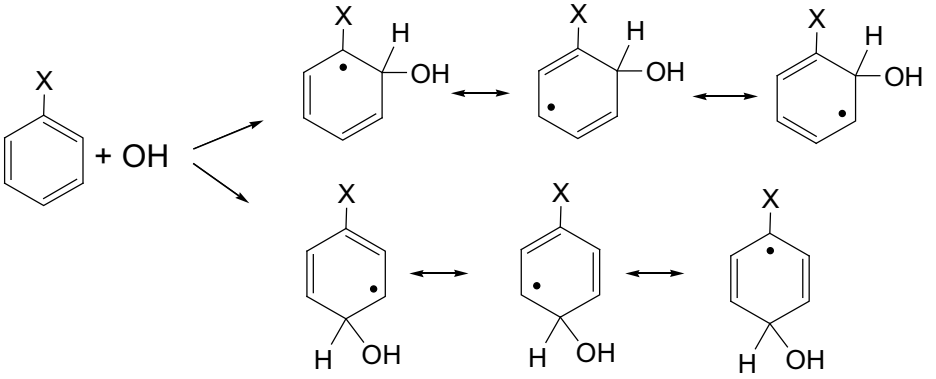

(5.54)

By reaction between the cyclohexadienyl radicals and NO_2, for which the activation energy will be practically zero, the nitro group is attached with the formation, for example, of the following nitro compounds:

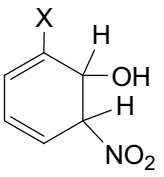

I

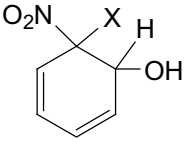

II

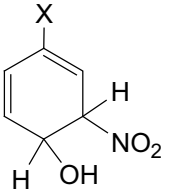

III

These compounds are unstable and liable to break down by the elimination of water, of nitrous acid, or of hydrogen:

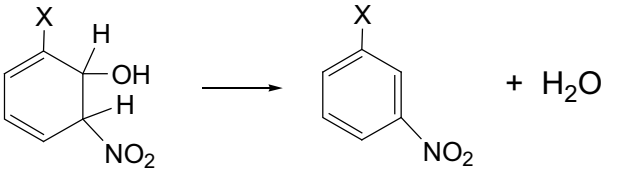

(5.55)

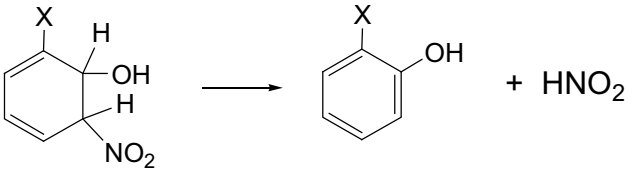

(5.56)

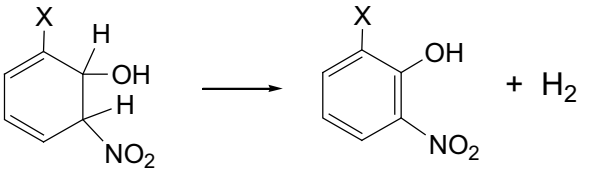

(5.57)

Similarly from **III** one can obtain

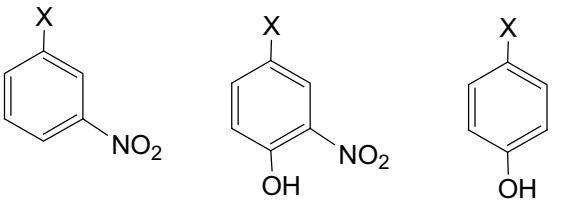

But in the case of **II**, the elimination of the original substituent X is possible:

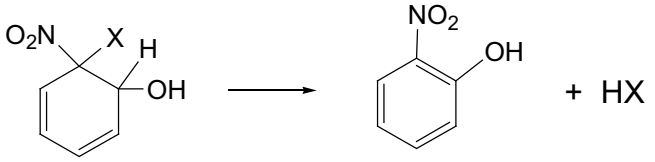

(5.58)

By such means hydroxyl and nitro groups may be introduced, individually or together, into the aromatic molecule. The hydroxyl group will always enter in *o*- or *p*-position, and the nitro group in the *m*-position relative to the original substituent. The course of the decomposition of the intermediate addition compound depends upon the nature of the original substituent which thus determines the product.

Analogous reactions in benzene give *o*-nitrophenol, and also two minor products, phenol and *p*-nitrophenol [22]. The diphenyl may result from the following sequences:

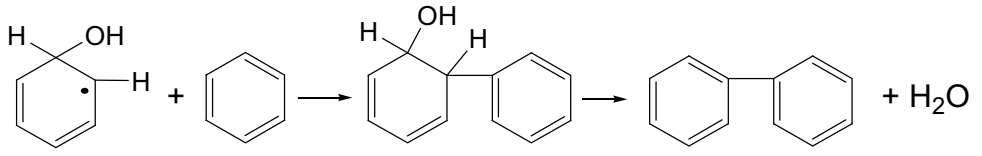

(5.59)

or

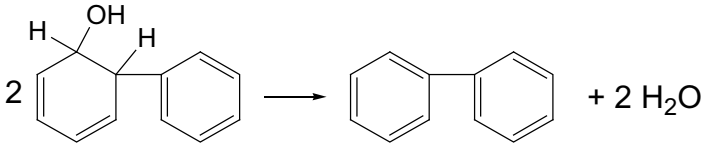

(5.60)

Benzaldehyde can be obtained from the direct oxidation of toluene by HOONO [22].

Anisole provides an example in which the original substituent is eliminated. The reactions involved are represented as:

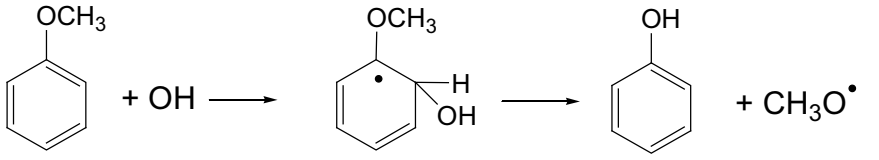

(5.61)

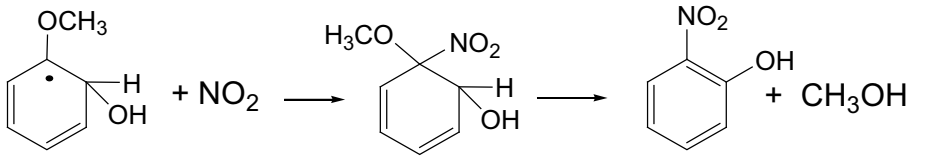

(5.62)

The reaction with participation of nitrous acid provides a method for nitration and hydroxylation of aromatic compounds, and for the preparation of *m*-nitro compounds and derivatives of *o*-nitrophenol. Unfortunately, the yields are very small and the products difficult to separate in many cases. Of the aromatic compounds used, nitrobenzene and anisole give the best yields of products in reactions with HOONO, correspondingly 8% and 30%. The corresponding yield for benzene, toluene, and chlorobenzene is <6% [22].

HOONO was applied in the nitration of polycyclic aromatic hydrocarbons, namely naphthalene [24]. The position 1 of naphthalene is more electron-rich. The interaction between HOONO and position 1 can induce a homolytic cleavage of HOONO, analogous to the following reaction:

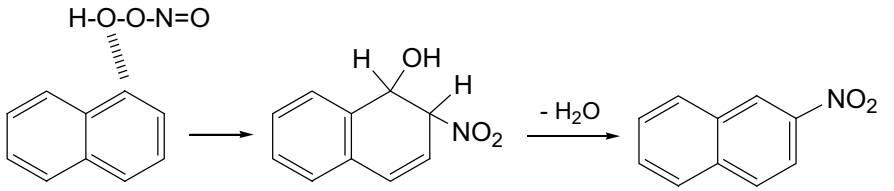

(5.63)

The hydroxyl group would then remain on position 1, and the nitro group might add to the adjacent position 2, yielding 1-hydroxy-2-nitro-1,2-dihydronaphthalene. This unstable intermediate might then evolve into 2-nitronaphthalene upon water elimination. It is possible that the nitration of naphthalene in the presence of HOONO occurs by the electrophilic pathway initiated by species originating from HOONO protonation; this pathway prevalently yields 1-nitronapthalene, but also affects the formation rate of 2-nitronaphthalene at pH < 2.

Ozone-mediated nitration by the Kyodai nitration is successfully applied for various aromatic compounds [18, 25–33]. The reaction proceeds by a double mode depending on the oxidation potential of the substrate. Deactivated aromatic compounds are likely to react with N_2O_5 in most cases via the nitronium ion forming in (**Equation 5.55**), but substrates of lower oxidation potential are easily oxidised by NO_3 to form the corresponding radical cations:

$$ArH + NO_3 \rightarrow [ArH^{\bullet+}, NO_3^-] \rightarrow ArH^{\bullet+} + NO_3^- \quad (5.64)$$

$$ArH^{\bullet+} + NO_2 \rightarrow Ar(H)NO_2^+ \xrightarrow{-H^+} ArNO_2 \quad (5.65)$$

$$ArH + NO_2^+ \rightarrow Ar(H)NO_2^+ \xrightarrow{-H^+} ArNO_2 \quad (5.65)$$

Bicumenes are readily oxidised to form radical cations and can be used as probes for electron transfer processes. These compounds have been chosen to confirm involvement of the electron transfer process in the Kyodai nitration [18]. Bicumene was stable toward NO_2 in a dilute dichloromethane solution at –20 °C. However, when ozone was introduced into this solution at the same temperature, the hydrocarbon was rapidly cleaved at the central position to produce 2-phenylpropene, 2-phenylpropan-2-ol and acetophenone:

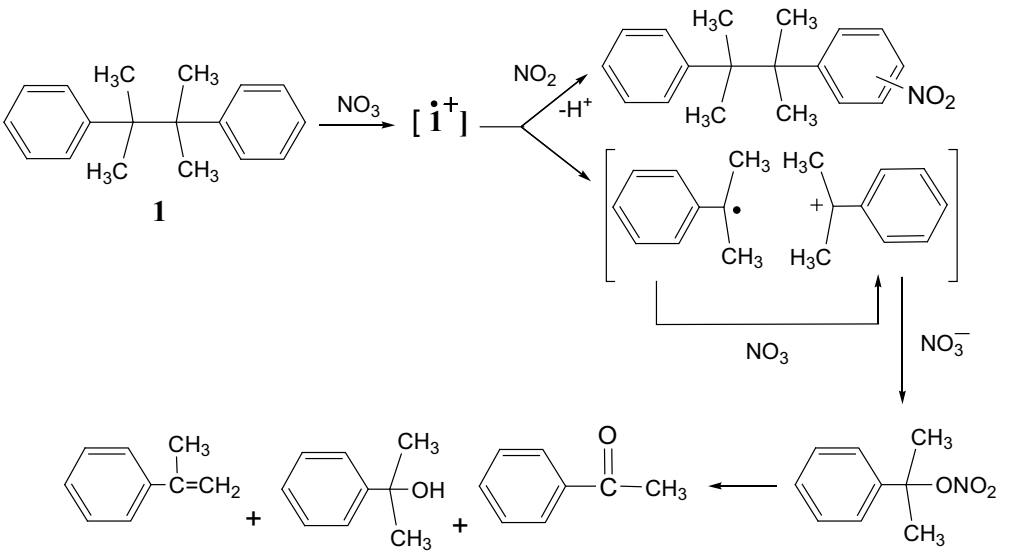

(5.66)

A few products of phenyl ring nitration are detected at –20 °C (9%). At 0 °C or in a more concentrated solution, the formation of nitro derivatives became extensive (40%), but even under these conditions the proportion of the fragmentation products was predominant in the product distribution. The formation of the fragmentation products apparently proves the occurrence of intermediate radical cations of bicumene.

The first importance of (**Equations 5.65** and **5.66**) has been pointed out for the ozone-mediated nitration of alkylbenzenes [25]. When a stream of ozonised air is introduced into a solution of an alkylbenzene C_6H_5X (X = H, Me, Et, Pr^i, Bu^t) in dry dichloromethane in the presence of an excess of NO_2 at <0 °C, the substrate is rapidly nitrated on the ring to afford an isomeric mixture of mononitro derivatives in good-to-moderate yield. The reaction of toluene occurred exclusively on the ring, giving a mixture of *o*-, *m*- and *p*-nitrotoluene in the proportions 57:2:41. Other alkylbenzenes also react actively to afford the corresponding mononitro compounds, mainly *o*- and *p*-nitroisomers in accord with the ion-radical nature of the reaction. Di- and tri-alkylated benzenes similarly undergo nitration, with the formation of mono- and polynitro derivatives. To see which one of two primary electrophiles, dinitrogen pentoxide and NO_3, has the more important role in nitration, the behaviours of benzyltrimethylsilane were compared toward N_2O_5 and nitrogen dioxide – ozone [25]. The silane is known to be easily oxidised to generate a radical cation [26], which then releases the trimethylsilylcation to give the benzyl radical. The reaction of the silane with N_2O_5 in dichloromethane at 0 °C gave a 5:2 mixture of 2- and 4- nitrobenzyltrimethylsilanes in 87% yield. In contrast, the ozone-mediated reaction of the silane with NO_2 under similar conditions led to extensive C–Si bond cleavage, giving a mixture of benzyl nitrates and nitro(phenyl)methanes. With NO_2 or ozone alone, the silane remains almost intact under the conditions used. The scheme of possible conversions of the silane is represented by:

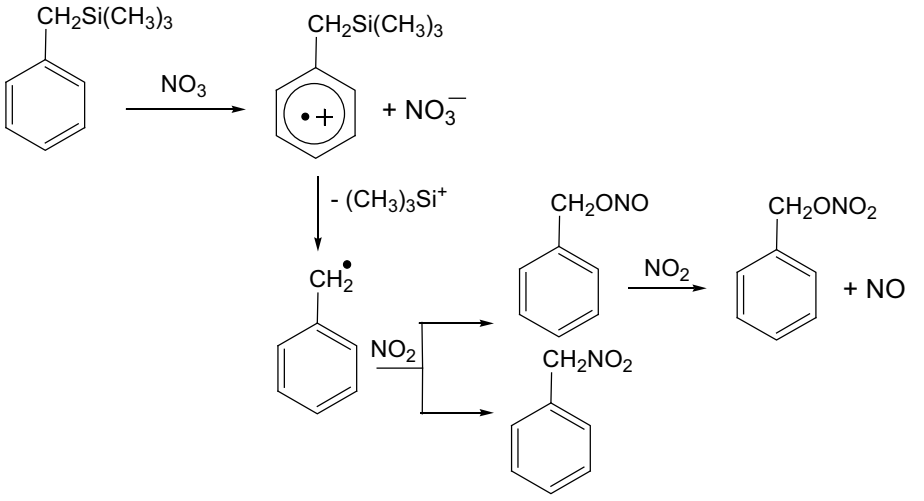

(5.67)

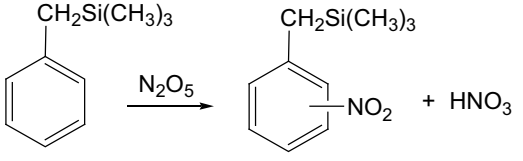

(5.68)

The ozone-mediated nitration of phenylalkyl ethers, phenylacetic esters, and some related compounds with NO_2 also demonstrates the mechanism based on radical cation intermediates [27]. Methyl phenylalkyl ethers are smoothly nitrated by the Kyodai method to give an isomeric mixture of nitro compounds in high yields (80–99%). The examination of methoxyalkyl groups of different chain length has revealed that the relative distance between the aromatic nucleus and the oxygen atom has a profound influence over the isomer composition of the products. NO_2 combines with the oxygen atom of the radical cation to form the intermediate ion, which then rearranges through an energetically favoured six-membered cyclic transition state to yield the *o*-nitro isomer:

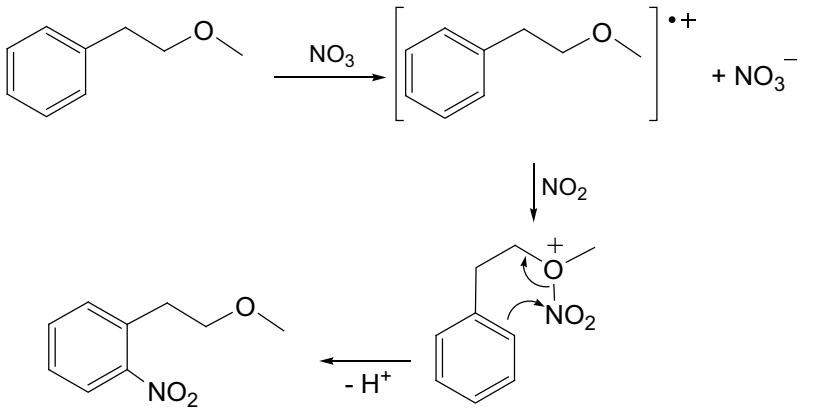

(5.69)

Under similar conditions, alkyl esters of phenylacetic acid were also easily nitrated to give a high proportion of the ortho isomers in good yields [27]:

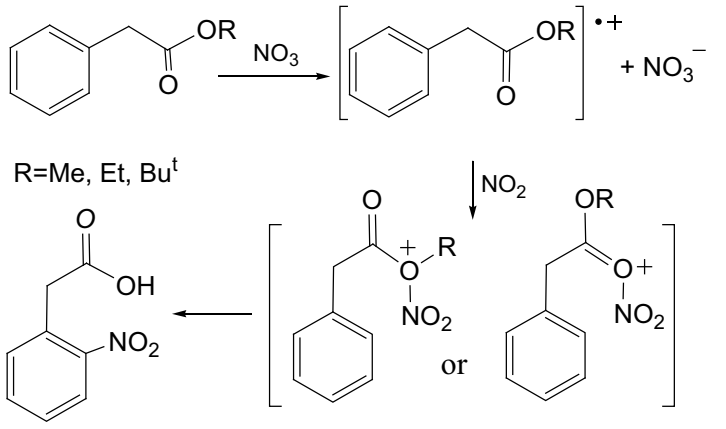

(5.70)

Thus, high *ortho* selectivity may be realised by the initial attachment of NO_2 to the oxygen atom of the substrate radical cation, followed by a rearrangement of the resulting oxonium ion intermediate.

Aromatic cyclic acetals can be successfully nitrated on the aromatic ring with NO_2 in ice-cooled dichloromethane in the presence of ozone to give mainly *o*- and *p*-nitro derivatives in good combined yields (90–95%) [28]:

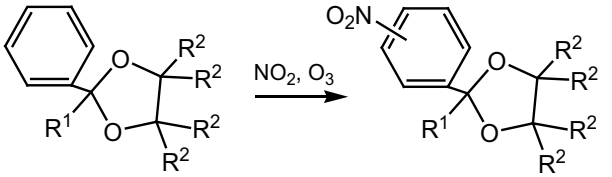

R^1=H, Me, Et, Pr^i, Bu^t
R^2=H, Me

(5.71)

If acetals contain protonated cycles (R^2 = H), the cleavage of the acetal ring occurs under similar conditions in preference to nuclear nitration to give a mixture of the original aldehyde, its nitration product, and small amounts of a nitrate ester:

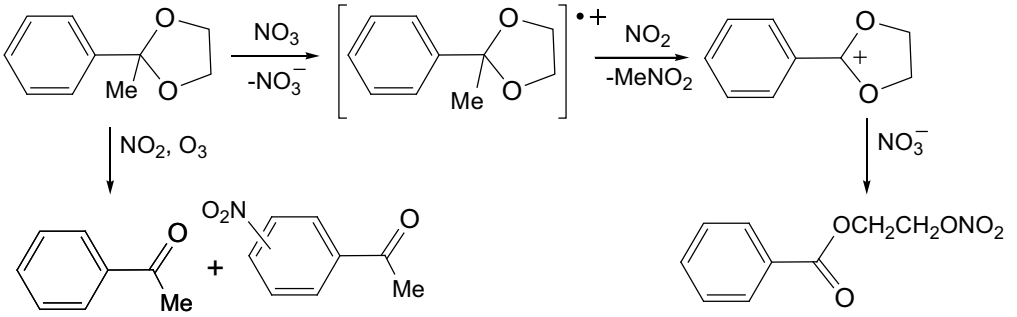

(5.72)

Of the wide variety of nitrobenzene derivatives which find uses in industry, 2- and 4-chloronitrobenzenes are the most important as precursors for chemical products used for the manufacture of dyes, medicines, agrochemicals, synthetic fibres, and other commodities. Commercial production of chloronitrobenzenes involves direct treatment of chlorobenzene with concentrated nitric acid or mixed acid [29]. The *ortho:para* isomer ratios can be varied to some extent according to the nitrating agent and solvent system employed, but modification of other factors such as temperature, concentration, reaction time, reagent/substrate ratio does not usually exert a significant influence on the isomer composition of the products. Along with this method, chloro and bromobenzenes can be efficiently nitrated with NO_2 in the presence of ozone to produce the products of nitration rich in the *ortho* isomer, and the *ortho/para* isomer ratio of the nitration products can be reversed from *ortho*-rich (*o*/*p* = 1.1 and 1.09) to *para*-predominant (*o*/*p* = 0.45 and 0.68) by altering the initial concentration of the substrate [30]. In contrast with chloro and bromobenzenes, the dependence of the isomer ratio on the initial concentration was not so marked with fluorobenzene. The *o*/*p* ratios varied in a narrow range from 0.16 to 0.11. It is assumed that halogen compounds are oxidised by NO_3 to generate radical cations, which subsequently undergo a coupling with NO_2 to yield ion intermediates:

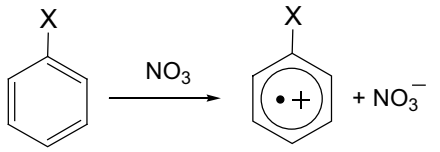

X = Cl, Br, F (5.73)

The reversal of the *ortho/para* isomer ratios depending on the initial concentration of a substrate may be interpreted in terms of equilibrium between the radical cation and its dimeric form, and the difference in their relative reactivity toward NO_2:

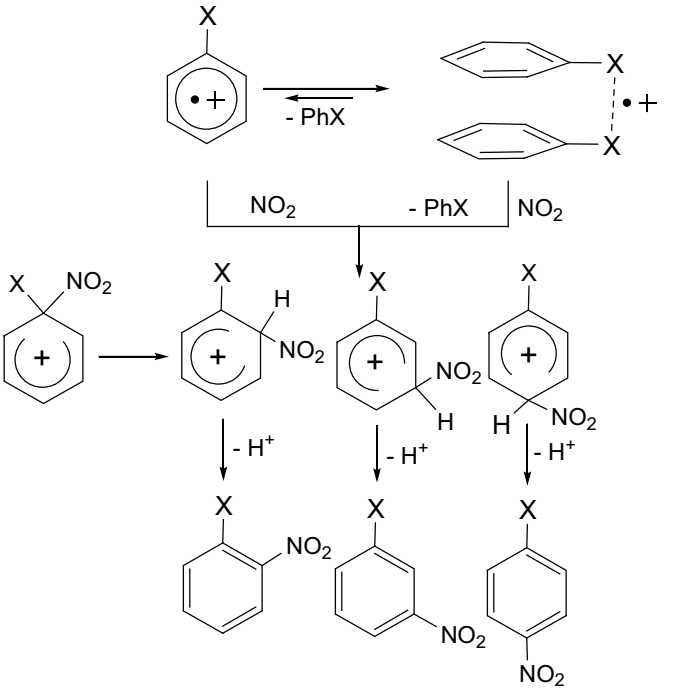

(5.74)

Semi-empirical calculations carried out for the radical cation and its dimer revealed that frontier electron density involved in a radical substitution reaction is highest on the chlorine atom in the monomer form, whereas it is most important at the *para*-carbon atom in the dimer form [30]. In dilute solution, the *hot* radical cation would be rapidly trapped by NO_2 present in large excess via the electronic interaction with the chlorine substituent, leading to the arenium ion intermediates. Such process would work favourably for *o*-substitution. In concentrated solution, the radical cation can be partially stabilised through coordination toward the chlorine atom of another chlorobenzene molecule to give a dimeric form, in which the frontier electron would

be extensively spread over the whole dimeric molecule. Under these conditions, NO_2 could react in a more regioselective manner, resulting in predominant substitution at the *para*-position.

The important role of NO_3 as the effective electrophile appears in the Kyodai nitration of electron-rich substrates such as alkylbenzenes. With electron-deficient substrates, however, the oxidative electron transfer would become a less favourable process for arenes, and NO_3 would react preferentially with NO_2 to form N_2O_5. Under these conditions, nitration is expected to follow the ionic mechanism. The strong deactivating effect of a carbonyl group on an aromatic ring as a result of inductive and mesomeric electron withdrawal directs an electrophile predominantly to the *meta* position. The aromatic ketones treated with NO_2 in dichloromethane in the presence of ozone at –10 °C readily undergo nitration on the ring to give *o*- and *m*-nitro derivatives in good yields (99–100%) [31]. For the reaction, attack on the alkyl groups of ketones was not observed, and in the absence of ozone, the nitration did not proceed.

The reaction of acetophenone with NO_2 gives a mixture of *o*- and *m*-nitroacetophenones in a ratio of 1.08, whereas the nitration of the acetophenone with nitric acid leads to the *ortho/meta* ratio of 0.37 [21]. The most remarkable feature of the nitration of aromatic ketones with $NO_2 + O_3$ is enhancement of the *ortho*-substitution as compared with classical nitration. The proportion of the *ortho*-isomer relative to two others increases with the increasing steric bulkiness of the alkyl moiety in ketones, from 1.08 for Ph–$COCH_3$ up to 3.8 for Ph–$COBu^t$. The increase of the *ortho/meta* ratio is accompanied by an increase in *para*-substitution, suggesting the decrease of the electron withdrawal by the bulky Bu^t substituent. In the reaction of aromatic carbonyl compounds, it is unlikely for ketones to be oxidised by NO_3 to form a radical cation, so N_2O_5 is the likely reactant for the nitration. There is good reason to believe [31] that nitrogen pentoxide forms a Lewis acid–base complex, which itself may act as the nitrating agent for ketones. As the reaction proceeds, the nitric acid formed would facilitate the heterolytic collapse of the complex, leading to the usual intermediates in *ortho*- and *meta*-nitration:

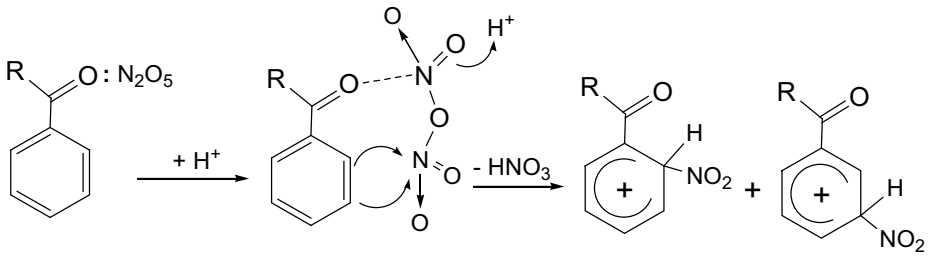

(5.75)

In view of the versatility of *o*-nitro ketones as the precursor for a variety of heterocyclic compounds, the present finding is of considerable synthetic importance.

Benzimidazole derivatives having electron-withdrawing or -donating substituents at the benzene ring were used as models of the imidazole moiety of bases and their nitration with NO_2 and O_3 [32]:

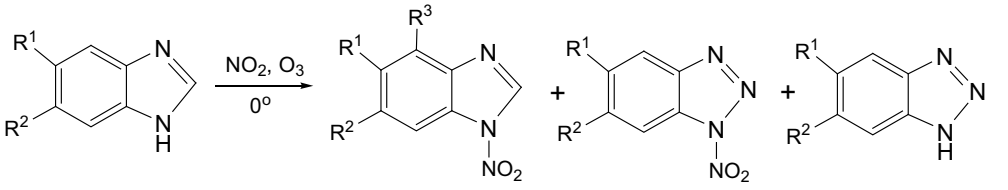

R^1 = H, CH_3, NO_2

R^2 = H, CH_3, CH_2NO_2, NO_2

R^3 = H, NO_2 (5.76)

The yields of (**Equation 5.76**) products are quite low (0.2–18%), except when R^1, R^2 = NO_2, R^3 = H (33% for 1,5,6-trinitro-benzimidazole). Benzimidazoles with electron-withdrawing substituents tend to give a higher yield of products. Pathways for the formation of products from benzimidazole by the Kyodai nitration are shown below:

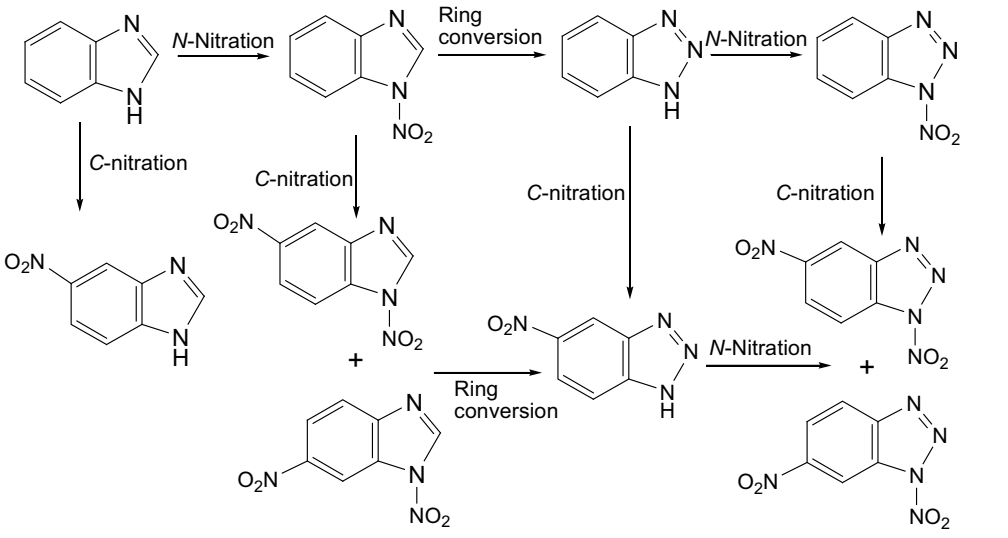

(5.77)

The yield of 1-nitrobenzotriazoles was increased by using a large amount of NO_2/O_3. Although 1-nitrobenzotriazoles were formed by nitration of benzotriazoles in the NO_2/O_3 system, it is not clear whether this system participates in ring conversion from 1-nitrobenzimidazoles to benzotriazoles. When imidazole itself was used as a substrate and examined by the Kyodai nitration, no triazole derivatives were found. For ring conversion from imidazoles to triazoles, imidazole ring opening is the initial step, and subsequent ring closure completes the conversion. In benzimidazoles, ring closure seems to proceed more easily than in imidazoles. It has been proposed that this kind of conversion from imidazole to triazole may occur in purine bases in deoxyribonucleic acid (DNA) as secondary DNA damage after DNA has been nitrated or aminated by certain mutagens [32].

On the assumption of NO_3 being the initial electrophile for the Kyodai nitration, the reaction of aromatic compounds with the ternary mixture of $NO–NO_2–O_2$ is of special interest because the gas-phase oxidation of NO to NO_2 is known to involve two isomeric unstable intermediates: the asymmetric (O–N–O–O) and the symmetric [O–N(O)–O] NO_3 [33]:

$$NO + O_2 \rightarrow O–N–O–O\ (\textit{asym}\text{-}NO_3) \tag{5.78}$$

$$(\textit{asym}\text{-}NO_3) + NO_2 \rightarrow ONO–O–NO_2 \tag{5.79}$$

$$ONO–O–NO_2 \rightarrow NO_2 + O–N(O)–O\ (\textit{sym}\text{-}NO_3) \tag{5.80}$$

The observation that the ternary mixture $NO–NO_2–O_2$ is more effective for nitrating aromatic substrate than a binary mixture of $NO_2–O_2$ may reveal a possible role of NO_3 as the initial electrophile in the Kyodai nitration. Toluene is inert towards NO alone, but in the presence of NO_2 it slowly undergoes ring nitration and side-chain oxidation, giving a mixture of nitrotoluenes, benzyl nitrate, phenylnitromethane and benzaldehyde:

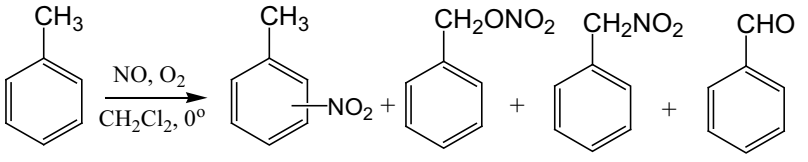

(5.81)

Upon admixture of oxygen, NO is rapidly converted into an equilibrium mixture of the NO, NO_2, NO_3 and N_2O_4, when this gaseous mixture is passed into a solution of toluene in dichloromethane containing an excess of NO_2 at 0 °C. The reaction is appreciably enhanced and the relative yield of the nitrotoluenes increased remarkably

at the expense of side-chain oxidation products. The reaction of toluene with NO_2 in the presence of O_2 is slow, and the relative proportion of ring substitution products was much less as compared with that obtained from the reaction carried out in the presence of NO. As expected, the addition of ozone makes the side-chain oxidation negligible. The side-chain oxidation products are derived from the capture of the benzyl radical by oxygen and NO_2 [33]:

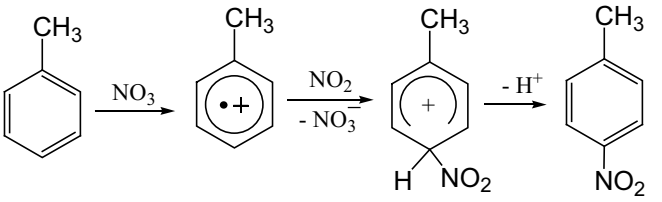

(5.82)

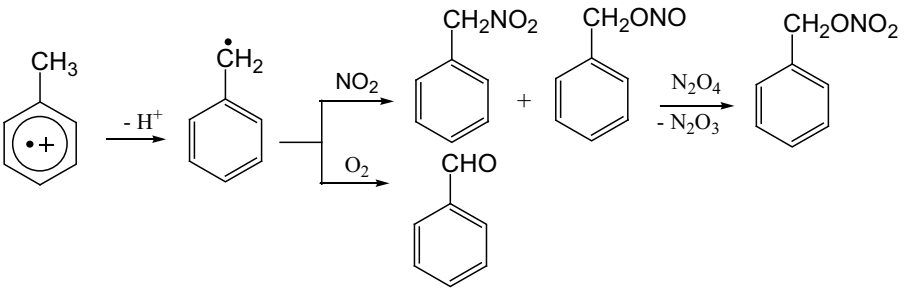

(5.83)

Under the same conditions, the nitration of chlorobenzene with the ternary system was quite slow. However, the chloronitrobenzenes obtained in low yield (6%) show high content of the *m*-isomer (*o*:*m*:*p* = 22:67:11).

The application of the standard Kyodai nitration procedure for pyridine gives a mixture of 5- and 3, 5-nitropyridine in only 2–5% yield [34]. However, pyridine can be efficiently nitrated by N_2O_5 in liquid sulphur dioxide to give 3-nitropyridine in 68% yield [35]. The role of sulphur dioxide in the process is evident from the following scheme [34]:

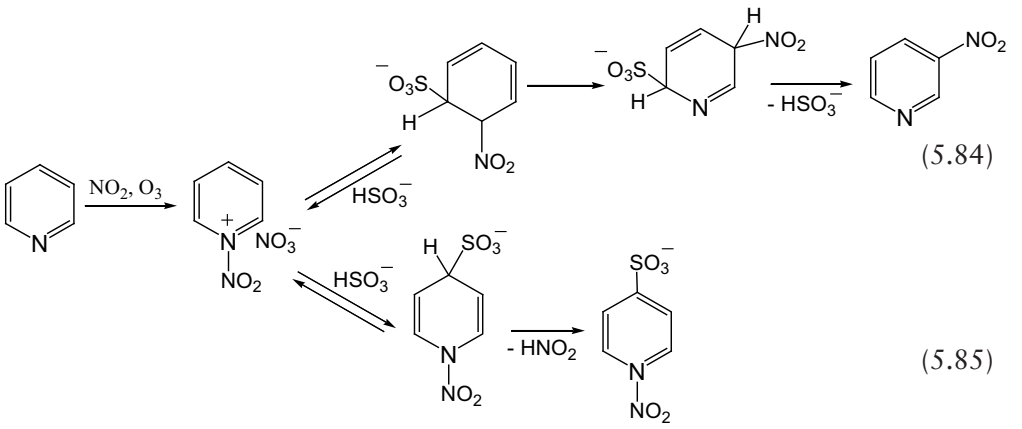

Upon aqueous workup of the reaction mixture, sulphur dioxide should form sulphurous acid (H_2SO_3) and sulphurous acid anion $(HSO_3\text{-})^-$ which make a nucleophilic attack on *N*-nitropyridinium salt to form adducts, eventually leading to the final products of (**Equations 5.84** and **5.85**). The 3-nitropyridine is most likely to be derived from the unstable adduct via the allylic rearrangement of the nitro group.

The methods of nitration of aromatic compounds based on using mixtures of nitric acid and sulphuric acid or NO_2 and ozone are generally unselective. Selectivity of the nitration process can be enhanced by solid catalysts such as clays, primarily zeolites [36]. Zeolites are crystalline aluminosilicates with uniform pore dimension. For instance, zeolite HZSM-5 represents a medium-pore material with elliptical pore size of 0.51–0.55 nm. It has been reported that certain zeolites can catalyze the process of nitration of halogenobenzenes by a nitrogen dioxide-oxygen system, simultaneously providing enhanced *para*-selectivity [37]. Zeolite β and zeolite Y with large pore sizes, mordenite with linear large pores, and ZSM-5 with a medium pore sizes were chosen for comparison. Additionally, variation of the cation type was studied with H^+, Na^+, K^+ and NH_4^+ in the case of zeolite β, and H^+ and Na^+ in the case of zeolite Y. Zeolite-5 was tested with two specific Si/Al ratios. The chlorobenzene nitration occurred in the presence of all zeolites, and all reactions gave higher yields (40–100%) than in the absence of any catalyst (6%). All of the zeolites demonstrated higher *para*-selectivity (*o*:*m*:*p* =39:0:61 without zeolite; *o*:*m*:*p* = 14:1:85 for zeolite Hβ). Mordenite and ZSM-5 gave lower *para*-selectivity as well as lower yields, which probably reflects more restricted diffusion through, and competition from, the reaction at the external surface of the solid. The ZSM-5 sample with the higher Si/Al ratio gave higher *para*-selectivity than that with the lower ratio. However, the yield with the higher Si/Al ratio was less, possibly because of the lower density of effective catalytic sites. The nature of cations shows a negligible effect on the reaction. Evidently, the process does not depend on strong acid catalysis and cation size. Perhaps the role of the

active site is merely to bring together the reagents and substrates within the confines of the pores by simple co-adsorption. Zeolites Hβ and Naβ produced the greatest selectivity for *para*-chloronitrobenzene (85%) and the highest yields (90% and 96%, respectively). Therefore, zeolite Hβ was tested with a range of other substrates [37]. After 24 hours, toluene had been completely consumed and produced a reasonable yield of mononitrotoluenes (85%). The *para*-selectivity was fairly low (45%), though greater than for mixed acid nitrations. The reaction with benzene was only 50% complete after 48 hours. However, all the halogenobenzenes gave good yields and reasonable *para*-selectivity. Thus, zeolites β and Y, with H^+, Na^+ or K^+ cations, can be efficient inorganic catalysts for the nitration of halogenobenzenes with NO_2 and oxygen (0 °C) and produce high *para*-selectivity and yields compared with classical nitration methods.

Toluene is moderately activated, so the Kyodai nitration of this hydrocarbon is always accompanied by more or less dinitration product. On inspecting the isomer composition of this byproduct in the course of the Kyodai nitration in the presence of montmorillonite K10 and zeolites HZSM-5 or HBEA-25, a considerable preponderance of 2,4-dinitrotoluene over the 2,6-dinitro isomer (2,4-/2,6- = 5.1–9.3) has been discovered [38]. In the classical nitration based on mixed acids, the 2,4-dinitro and 2,6-dinitro isomers were obtained in about a 4:1 ratio. The nature of organic solvent was found to exert considerable influence on the regioselectivity of dinitration. Of the four solvents of varied polarity (*n*-C_6H_{14}, CCl_4 CH_2Cl_2, MeCN), acetonitrile with a high dielectric constant exhibited the best result. The 2,4-/2,6-isomer ratio is enhanced up to 12 in acetonitrile, whereas these values are 5 in *n*-C_6H_{14}, 4.1 in CCl_4 and 9.3 in CH_2Cl_2.

At the dinitration of chlorobenzene, the regioselection in the presence of zeolites was again improved in favour of the 2,4-dinitro isomer (2,4-/2,6- = 48) [38]. In the presence of Faujasite-712, the nitration of *o*-chlorobenzene with N_2O_5 gives a mixture of 1-chloro-2,4-dinitro- and 1-chloro-2,6-dinitrobenzenes in about 30:1 ratio [39]. Thus, the procedure for the regioselective dinitration of toluene and chlorobenzene described above, which involves the Kyodai nitration in polar organic solvent in the presence of zeolites, provides a new efficient route to 2,4-dinitro derivatives under nonacid conditions. The method is easy to carry out, environmentally benign, and economical.

Highly activated aromatics such as polycyclic aromatic hydrocarbons can be easily nitrated with NO_2 alone. The investigation of the relative reactivity of the series of polycyclic aromatic hydrocarbons (naphthalene, triphenylene, phenantrene, chrysene, pyrene, anthracene, perylene) with NO_2 – N_2O_4 in solutions of dichloromethane at room temperature has been reported [40]. The nitration of naphthalene by NO_2 led to 1-nitro- and 2-nitronaphthalene in a ratio l-nitro:2-nitro = 11. The

nitration of pyrene under the same conditions gives a single product, 1-nitropyrene. Similar results are observed for the nitration of perylene with the formation of 3-nitroperylene. The nitration of phenanthrene led to a mixture of four nitrated products. The exclusive mononitrated product was 9-nitroanthracene. In addition to this compound, an appreciable amount of 9,10-anthraquinone is formed. The ratio of 9-nitroanthracene to 9,10-anthraquinone was 1.64 when approximately one-third of the initial anthracene present had reacted. In the course of further conversions, this value decreased to 1.42. This change is due to the accumulation of water as the reaction progresses. Water is inevitably present in these reaction mixtures because it is produced from nitrous acid:

$$2NO_2 + ArH \rightarrow HONO + ArNO_2 \tag{5.86}$$

$$2HNO_2 \rightarrow NO + NO_2 + H_2O \tag{5.87}$$

The nitration of polycyclic aromatic compounds by NO_2 is analogous to aromatic substitution by other electrophilic radicals. The mechanism involves a rate-determining σ-complex formation. This is illustrated in the following scheme using anthracene as the representative compound [40]:

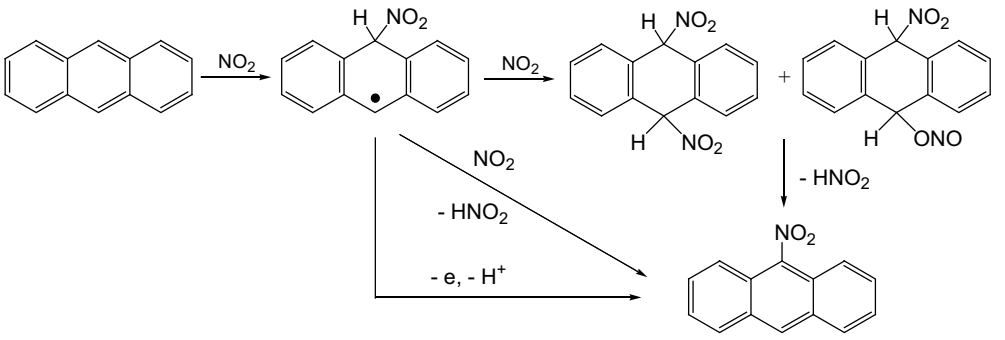

(5.88)

An entirely different mechanism for nitration by NO_2 is based on the initial electron transfer reaction:

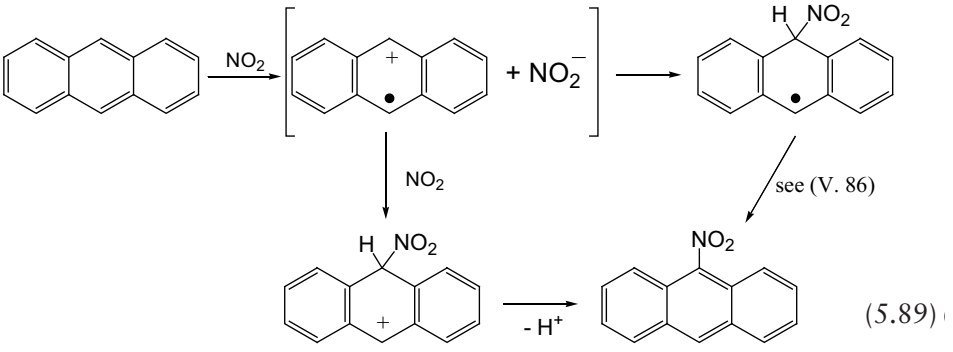

(5.89)

Electron transfer is the rate-determined step, and collapse of the intermediate species gives a σ-complex. Radical cations of polycyclic aromatic hydrocarbons react with nucleophiles and radicals to yield substituted compounds. The oxidation of anthracene to 9,10-anthraquinone involves the reaction of radical cations with water followed by one-electron transfer and deprotonation:

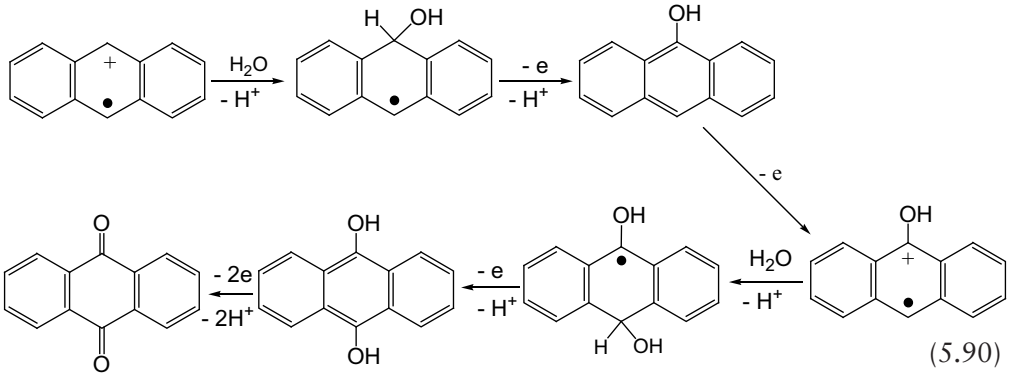

(5.90)

Relative rate constants of the nitration were obtained by direct competition between two aromatic hydrocarbons. The rate constants depend markedly on substrate structure, with $>10^4$ difference in values between the least reactive (benzene) and most reactive (perylene) compounds studied. The more reactive (and more easily ionised) polycyclic aromatic hydrocarbons interact with NO_2 in solution by an electron transfer mechanism.

5. 3 Reactions of NO_2 with Phenols

Nitration of substituted phenols by NO_2 proceeds quite easily. The commonly written description of the reaction of the phenols with NO_2 is given as follows [41, 42]:

$$ArOH + NO_2 \rightleftharpoons ArO^{\bullet} + HNO_2 \quad (5.91)$$

$$ArO^{\bullet} + NO_2 \longrightarrow \text{products} \quad (5.92)$$

In this reaction scheme, the first step is hydrogen-atom abstraction by NO_2 to give a corresponding phenoxy radical and nitrous acid. Subsequent radical coupling of a second NO_2 radical yields the immediate reaction products. For 2,4,6-tri-*t*-butyl phenol, these reactions give 2,4,6-tri-*t*-butyl-4-nitrocyclohexa-2,5-dienone and 2,4,6-tri-*t*-butyl-2-nitrocyclohexa-3,5-dienone:

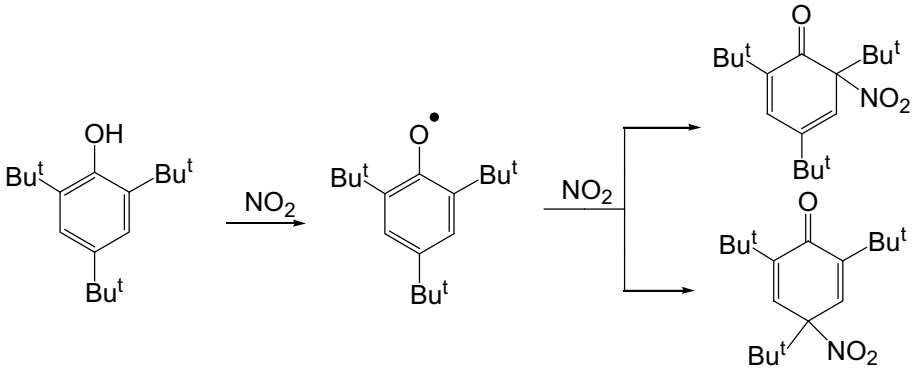

(5.93)

The study of the products of radical coupling of phenoxy radicals with NO_2 is complicated by the marked lability of some of those products. For instance, 2,4-dimethylphenol with NO_2 in chloroform at –60 °C gives three compounds:

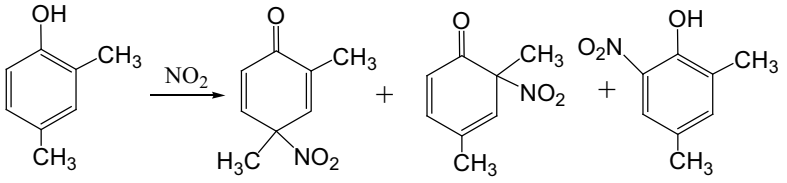

(5.94)

At ambient temperatures, the following consecutive rearrangements via a homolytic dissociation–recombination mechanism take place [43]:

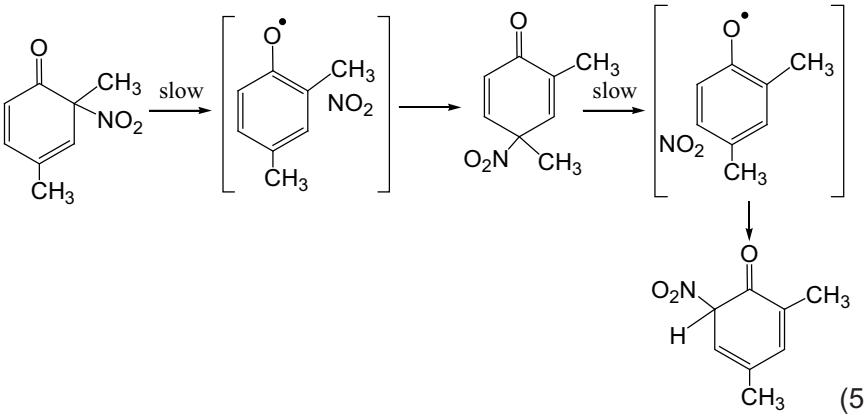

(5.95)

The initial dissociation to give the NO_2/phenoxy radical pair within the solvent cage is rate-limiting, and the rate of recombination of this radical pair to form the isomeric 6-nitrocyclohexa-2,4-dienone is comparable with the rate of diffusion of the radical pair from the solvent cage. The enolisation of this 6-nitrocyclohexa-2,4-dienone gives the 2,4-dimethyl-6-nitrophenol:

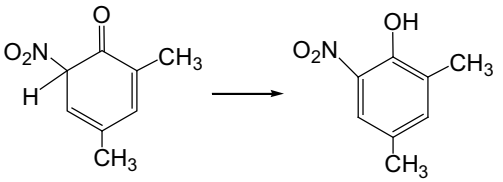

(5.96)

Although it is established that nitrous acid and a phenoxy radical are formed in reaction sequence (**Equation 5.91** and **5.92**), it is unlikely that this process involves direct phenolic hydrogen-atom abstraction by NO_2. The alternative mechanism, which includes electron transfer from the phenoxide ion to NO_2, is quite probable [41, 44]:

$$ArOH \rightleftharpoons ArO^- + H^+ \quad (5.97)$$

$$ArO^- + NO_2 \longrightarrow ArO^{\bullet} + NO_2^- \quad (5.98)$$

$$ArO^{\bullet} + NO_2 \longrightarrow \text{products} \quad (5.99)$$

NO_2 is a potent one-electron oxidant [44] and electron transfer is a common pathway in NO_2 reactivity. Factors such as the redox potentials of the species involved in the reactions, together with the specificity of solvents in which the reaction is carried out, have significant effect on the nitration mechanism. The influence of solvents on NO_2

reactivity in the reaction with alkylsubstituted phenols has been studied [44]. The reactions between phenols and gaseous NO_2 were carried out at room temperature by dissolving the phenol in the chosen solvent (benzene, methanol or dimethyl sulphoxide). Phenols were almost instantaneously converted into the corresponding products when the reaction was carried out in benzene, but the reactions were slower in methanol and in dimethyl sulphoxide. In particular, reactions of 2,4-di-*t*-butylphenol and 4-*t*-butylphenol were quite slow in methanol and dimethyl sulphoxide. The phenol with R = Bu^t, R^1 = Bu^t, R^2 = Bu^t was partially recovered after many hours in methanol. The presence of Bu^t groups in the *o*-positions of phenols enhances their reactivity in methanol and dimethyl sulphoxide with respect to phenols containing the H-atom in *o*-positions. This effect is conditional on steric hindrance, which reduces the solvation effect. H-bond formation between phenols and the solvent has an important role in every H-transfer process. The polarity of solvents may also determine the particular pathway followed. The possible mechanism of the formation of detected products in the reaction of 2,6-di-*t*-butylphenol is shown in the following scheme [44]:

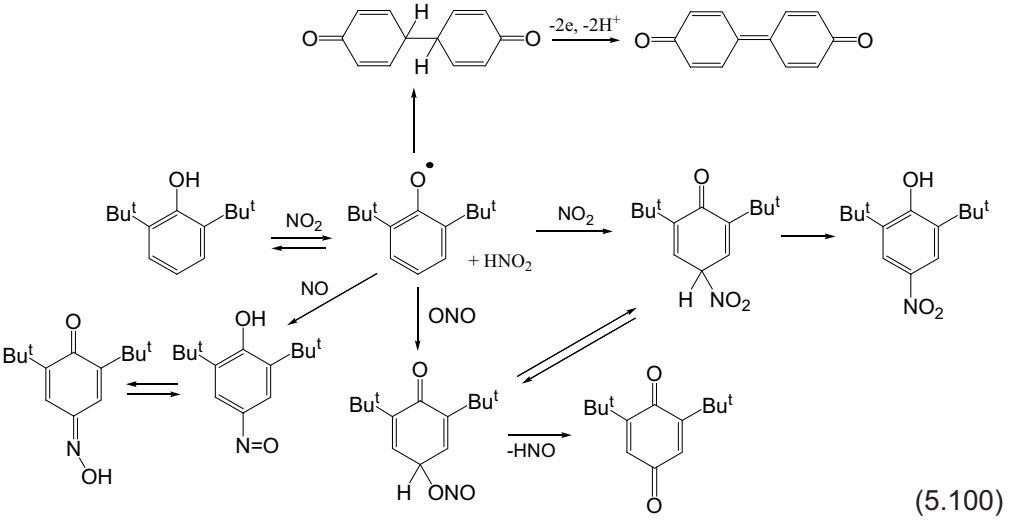

(5.100)

The phenoxy radical, derived from an H-abstraction reaction by $\cdot NO_2$, couples with another $\cdot NO_2$ molecule to give 4-nitrocyclohexa-2,5-dienone, which readily rearranges, after a keto-enol tautomerism to 2,6-di-*t*-butyl-4-nitrophenol. 2,4-di-*t*-butylphenol and 4-*t*-butylphenol react in the same way, whereas the presence of three substituents on the aromatic ring of 2,4,6-tri-*t*-butylphenol and 2,6-di-*t*-butyl-4-methylphenol does not allow keto-enol tautomerism; in these cases 2,4,6-tri-*t*-butyl-4-nitrocyclohexa-2,5-dienone and 2,6-di-*t*-butyl-4-methylnitrocyclohexa-2,5-dienone were the sole nitro compounds obtained. The reaction between NO_2 and 2,6-di-*t*-butylphenol or 2,4-di-*t*-butylphenol in methanol resulted in phenoxyl radical dimerisation together with nitration. As shown in (**Scheme 5.100**), phenoxyl radical dimerises to give an

unstable intermediate, which is easily oxidised to diphenoquinone. The phenoxyl radical is also involved in the formation of benzoquinone monooxime (the tautomeric form of the corresponding nitroso phenol), which is obtained, as the main product, in the reaction between 2,6-di-*t*-butylphenol and NO_2 in dimethyl sulphoxide.

NO_2 is a good one-electron oxidant and it could oxidise phenols, but the oxidation potentials of phenols are very high in organic solvents. For example, 2,6-di-*t*-butylphenol and 4-*t*-butylphenol have oxidation potentials measured in acetonitrile against an Ag/AgI electrode referenced to ferrocenium couple of 2.12 and 2.00 V, respectively; for 2,4,6-tri-*t*-butylphenol under the same conditions, *energy of oxidation (Eox)* = 1.85 V [45]. However, these phenols in polar solvents such as methanol or dimethyl sulphoxide may be dissociated and may exist in equilibrium with the corresponding phenoxide anions, which have much smaller oxidation potentials (*E*ox = 0.256, 0.44, and 0.23 V) measured in dimethyl sulphoxide relative to Ag/AgI taken with the ferrocenium couple as an internal standard [45]. NO_2 may easily oxidise the phenoxide anion to the corresponding radical, which can then react with other NO_2 (**Equations 5.97–5.99**). Thus, in polar solvents, phenoxyl radicals are formed by the oxidation of phenoxide anions, whereas in a solvent which does not support ionisation, such as benzene, they are formed by direct hydrogen abstraction by NO_2.

One of the main products obtained in the reaction between 2,6-di-*t*-butylphenol and NO_2 in dimethyl sulphoxide is the nitroso derivative [44]. Nitrosation, as well as nitration, is a common reaction for NO_2 [46, 47]. However, this process is due not to NO_2 but to its dimeric form $NO^+NO_3^-$ or $ONONO_2$. The possible mechanism for nitrosation of 2,6-di-*t*-butylphenol can be represented as:

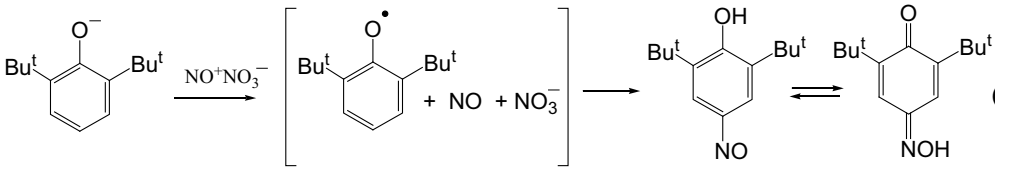

(5.101)

Thus, different pathways leading to the products of nitration and nitrosation are possible depending on the experimental conditions and, in particular, on the solvent used: Hydrogen-atom abstraction in solvents such as benzene, which have a low hydrogen-bond-accepting ability and electron transfer in hydrogen-bond-accepting and polar solvents such as methanol and dimethyl sulphoxide.

NO_2 and hindered phenols present the important constituents of different free radical processes, and knowledge of the kinetic peculiarities of reactions of NO_2 with phenols in the liquid phase is required to find out the mechanism in conditions modeling the environmental exposure. From this viewpoint it is appropriate to conduct reactions at reasonably low concentrations of NO_2 in mixture with nitrogen or air using a batch reactor [48]. The application of this technique enables the reaction mechanism to be investigated under change over a wide range of phenol concentrations and flow rates of the gas mixtures [49, 50]. The liquid-phase nitration of 2,4,6-tri-*t*-butylphenol in a batch reactor by gas mixture containing NO_2 (750 ppm) and air produces a variety of products of nitration and oxidation. The phenol solution (2×10^{-1} mol/l) in hexadecane was bubbled at various flow rates of gas mixture. Besides nitrocyclohexadienone, the formation of other products was revealed at room temperature from ultraviolet (UV) spectra (**Figure 5.1**).

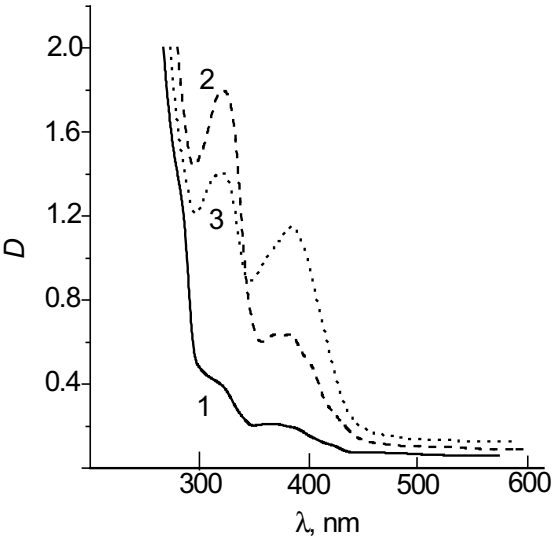

Figure 5.1 UV spectra 2,4,6-tri-*t*-butylphenol solution in the course of NO_2 bubbling (1), after completion of 15 hours of bubbling (2), after 10 minutes of heating at 333 K (3)

Two absorbance bands at 320 nm and 380 nm are observed in the course of NO_2 bubbling (1). The 320 nm band is substantially increased if to keep the solution after complete decay of the phenol in reactions (**5.93**) for 15-20 hours keep outside of the reactor (2). In these conditions, a decrease of the original phenol band intensity is also exhibited. It is obvious that the 320 nm band corresponds to *o*-quinolide peroxy groups (QHP) (lgε ≈ 3) [51]. The formation of these compounds is attributed to reactions of the intermediate phenoxy radical oxidation:

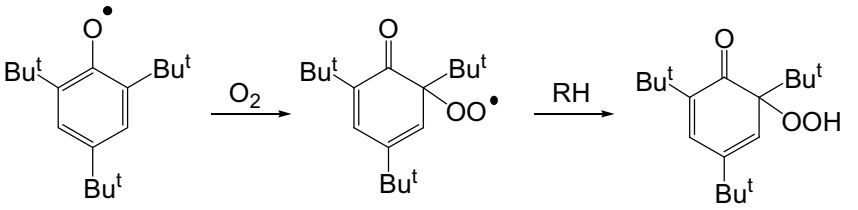

(5.102)

It is known that the thermal decay of these compounds at not very high concentrations (<10^{-2} mol/l) is a unimolecular reaction with activation energy of ~120 kJ/mol and pre-exponential factor of 10^{14}–10^{15} s^{-1} [52]. The kinetics of the 320 nm band decrease in the temperature range of 323 K to 346 K are also described by a first-order equation with the rate constant $k_d = 10^{15} \cdot \exp(-114 \pm 4/RT)s^{-1}$ [50].

The mechanism of the thermal *o*-QHP decay involves two consecutive reactions. The primary step is the breaking of the O – O bond, and the resulting cyclohexadienone alkoxy radical is capable of dissociating with *o*-quinone formation:

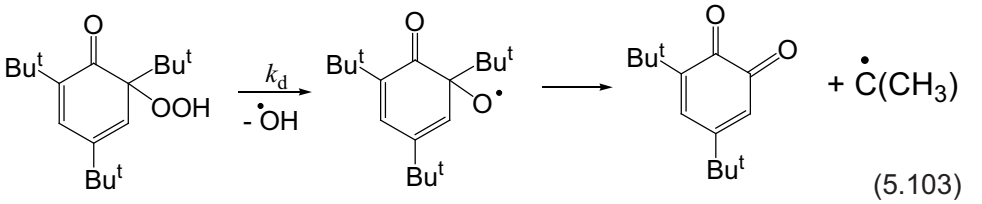

(5.103)

The UV spectrum of *o*-quinone has an intense absorbance band in the region 380–390 nm [53]. An increase in absorbance at 380 nm is observed in the course of QHP thermal decomposition (**Figure 5.1, curve 3**). The kinetics of QHP decay in hexadecane solutions during NO_2 bubbling at 295 K is described by a second-order equation [50]. The following scheme has been proposed for explanation of the kinetics:

$$QHP + NO_2 \underset{k_{-1}}{\overset{k_1}{\rightleftharpoons}} QHP \cdot NO_2 \tag{5.104}$$

$$QHP \cdot NO_2 + QHP \xrightarrow[RH]{k_2} \text{products} \tag{5.105}$$

In a primary reversible step, QHP forms the intermediate with NO_2, which is subsequently transformed into products in a reaction with the other QHP molecule. Assuming that QHP·NO_2 and soluble NO_2 concentrations are steady state, one can obtain the following equation of the QHP decay rate:

$$\frac{d[QHP]}{dt} = -\frac{k_1 k_2 [QHP]^2 k_s [NO_2]_{lim}}{k_1 k_2 [QHP]^2 + k_1 k_2 [QHP] + k_s k_{-1}} \tag{5.106}$$

where $[NO_2]_{lim}$ is the limiting concentration of soluble NO_2 in hexadecane determined by UV spectroscopy, k_s is a constant depending on the flow rate of the gas mixture in solutions [50]. If $k_1[QHP]^2 < k_2[QHP] < k_{-1}$, then (**Equation 5.106**) is transformed to the equation which is in agreement with the experimental kinetic dependence:

$$\frac{d[QHP]}{dt} = -\frac{k_1 k_2}{k_{-1}} [NO_2]_{lim} [QHP]^2 \tag{5.107}$$

The specific mechanism of reaction (**Equation 5.105**) includes formation and decomposition of the highly ordered cyclic hydrogen-bonded transition state:

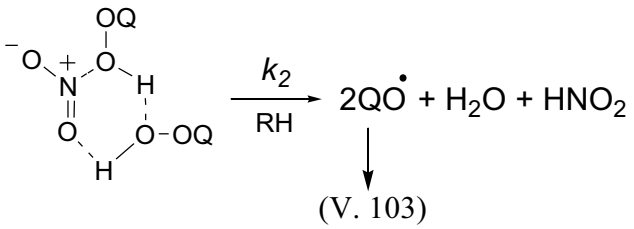

(5.108)

The formation and conversion reactions of QHP are initiated by decomposition of nitrohexadienones:

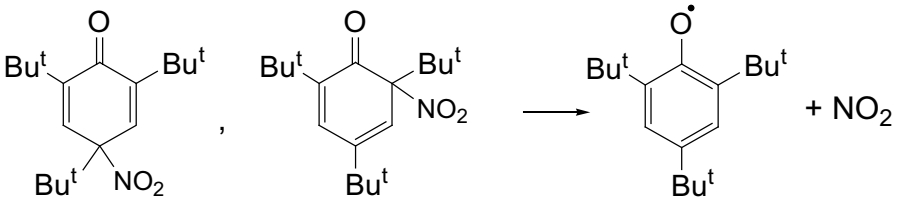

(5.109)

For determining the kinetic parameters of (**Equation 5.109**), the phenol solution was bubbled at room temperature until complete transformation of the phenol into nitrocyclohexadienones. Thereafter, their thermal decay was measured at 323–343 K. This reaction is described by a first-order equation. The effective values of activation energy and pre-exponent are 60 kJ/mol and 3.5×10^6 s^{-1}, respectively [50]. An approximate estimation taking into consideration these values shows that the nitrocyclohexadienone half conversion time is about 7 hours at room temperature. This fact correlates with the noted instability of these compounds [41, 42].

The effect of NO_2 on discoloration of some commercial phenolic stabilisers has been studied [54]. The antioxidants, all of which are initially white powder, were exposed to an atmosphere of 3% NO_2 gas for 30 minutes at ambient temperature. Fully hindered phenols (2,6-di-*t*-butylphenol derivatives) were changed to yellow. A bisphenol, which is known to be discoloured under oxidative conditions, was also discoloured to yellow. A thiobisphenol was discoloured to a greater extent to brick red. GA-80 remained almost undiscoloured. Hindered phenol not only gave extensive coloured products. but also reacted to give many products. In contrast, although GA-80 gave a small quantity of coloured products, it was found to react with NO_2.

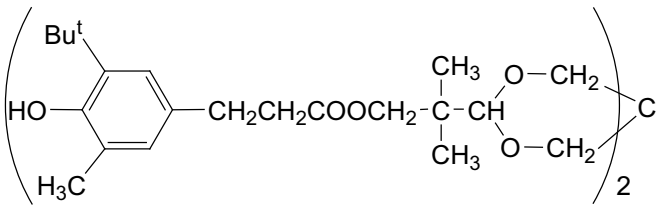

To clarify why GA-80, which is not inert to NO_2, was not discoloured, product analyses were done by chromatography. The chemical structures of products formed were determined spectroscopically, and were found to be a *meta*-nitrated spiro compound (C), a *meta*-nitrated compound (A) and a *meta*-nitrated hydroxyl compound (B), all of which were almost colourless. Product analyses suggest the reaction pathway shown in the following scheme:

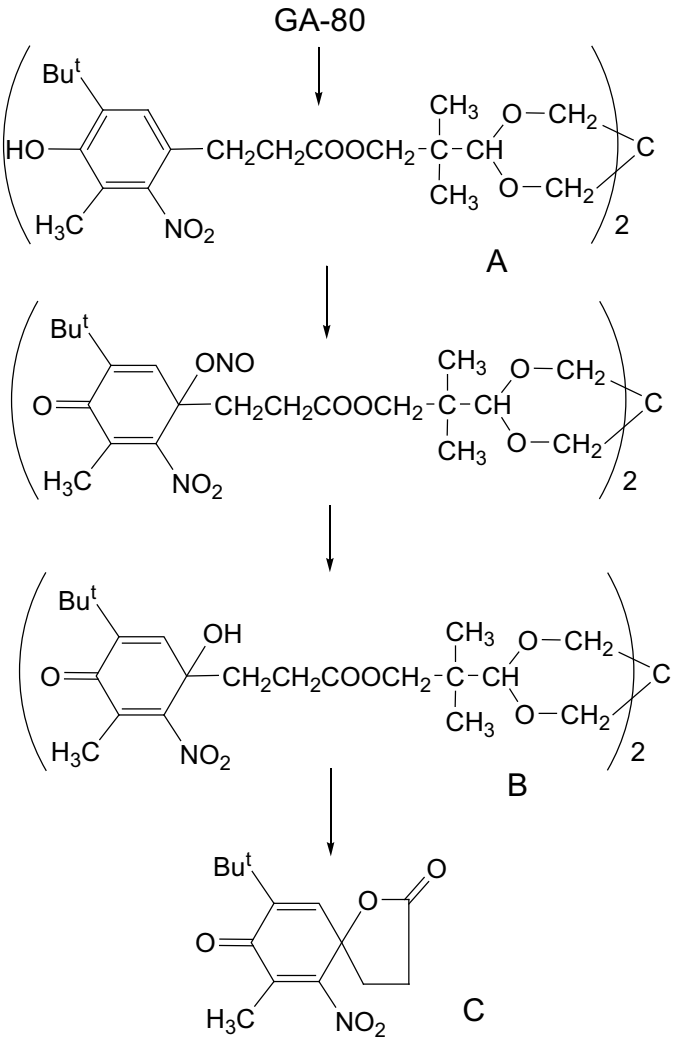

(5.110)

In *meta*-nitrated compound (A), the *para*-position is attacked with subsequent hydrolysis to give a *meta*-nitrated hydroxy compound (B) and cyclisation to give a stable colourless *meta*-nitrated spiro compound (C). Nitration of fully hindered phenols at the *para*-position gives coloured materials with quinine-like structures:

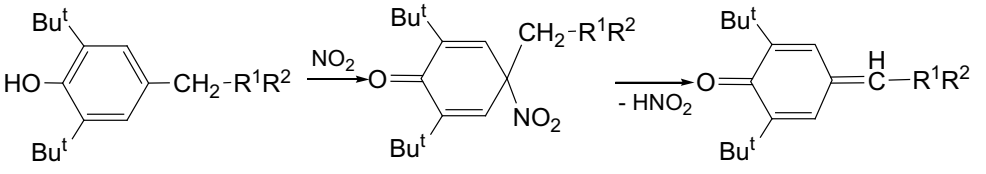

(5.111)

Thiophenols in organic solvents (ethanol, benzene, hexane) are rapidly oxidised by NO_2 [55]. The reaction is exothermic and becomes quite hot if the rate of addition of NO_2 is appreciable. A strong green colour develops immediately when the NO_2 comes into contact with the thiophenol solution, and then fades to pale-yellow at the end of the reaction. This colour is due to the S-nitroso thiol. The following scheme of reaction has been proposed:

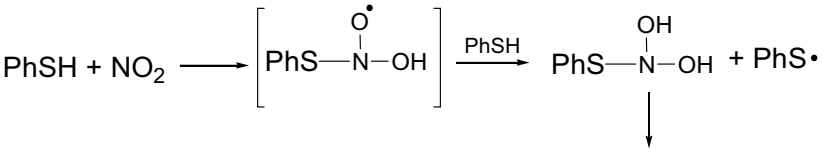

(5.112)

$$PhSN{=}O \rightarrow PhS^{\bullet} + NO \qquad (5.113)$$

$$2PhS^{\bullet} \rightarrow PhSSPh \qquad (5.114)$$

The S-nitroso thiol is an intermediate, and NO is the immediate gaseous product that is formed. The feature of conversions of thiophenols in the presence of NO_2 lies in the recombination of phenylthyil radicals with the formation of disulphide.

p-Nitrocalixarenes are a class of useful intermediates for the introduction of other functional groups to obtain N-containing substituted calixarenes [56]. The synthesis of *p*-nitrocalix[6]arene *via p*-sulfonatocalix[6]arene by nitric acid has been carried out, but the overall yield was low [57]. A facile synthetic method of obtaining *p*-nitrocalix[4]arenes by blowing gaseous NO_2 into the chloroform solution of calix[4]arene containing phenolic groups has been proposed [58]. The synthesis was accomplished at ambient temperature. Soon the solution turned to yellow, and the precipitate appeared rapidly within a few minutes. It was found that this reaction proceeded almost quantitatively (yield >90%):

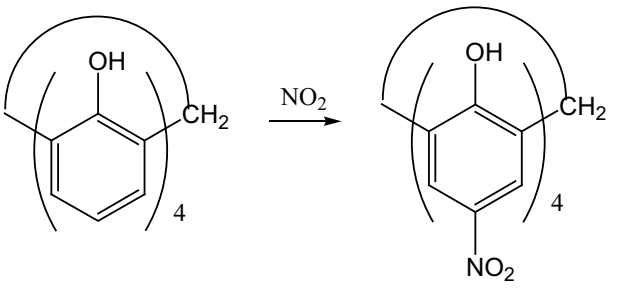

(5.115)

Other conventional solvents such as toluene give the same results. The ^{1}H-NMR spectrum of the nitro compound obtained shows that nitro groups were introduced in the *para* positions. The same nitration method was also used for calix[n]arene (n = 6, 8). Although the reactions occurred, the products were much more complicated than that for calix[4]arene.

Tetramethoxycalix[4]arene cannot be nitrated by means of the present method [58]. This shows that the hydroxyl groups have an important role in the nitration. The mechanism of nitration by NO_2 apparently includes (**Equations 5.97–5.99**). Calix[4] arenes carrying phenolic OH groups usually have acidic properties because the first dissociation of phenolic hydrogens easily occurs due to the stabilisation of the calix[4] arene anion by resonance structures of strong intramolecular hydrogen bonds. When the abstraction of one phenolic hydrogen of calix[4]arene takes place, the negative electrical charge can be freely moved among the OH groups. As a result, the nitration of the calix[4]arene occurs most effectively over the whole molecule. Furthermore, the yield obtained is much higher than those for general phenols and other aromatic compounds because of the peculiar acidity of the calix[4]arene.

5.4. Interaction of NO_2 with Alkenes, Dienes and Polyenes

NO_2 reacts with alkenes at room temperature by a free-radical mechanism [4, 59–62]. Gas-phase and liquid-phase studies revealed the formation of two types of products: addition products and allylic substitution products [62]. The change in concentrations of NO_2 leads to variation of the addition/substitution ratio. As the NO_2 concentration is decreased, the relative amounts of substitution products increase. These observations were made with cyclohexene as substrate [61]. In principle, NO_2 or its dimer N_2O_4 may be involved in these reactions. One pathway is represented by the following scheme [4, 63-65]:

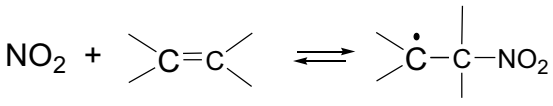

(5.116)

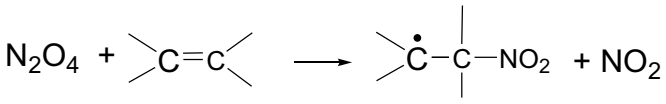

(5.117)

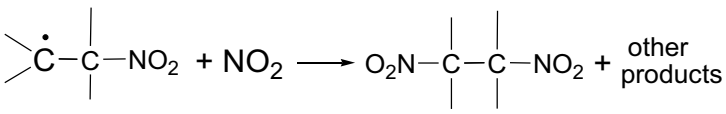

(5.118)

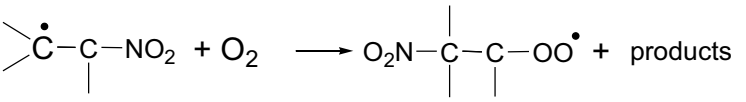

(5.119)

The NO_2 addition to double bonds results in geometrical olefin isomerisation by bond rotation in nitroalkyl radicals [59, 60]. For the reaction:

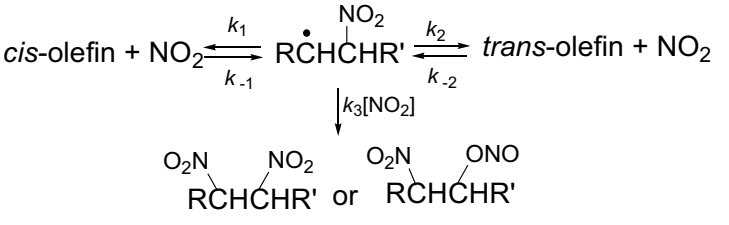

(5.120)

the equilibrium constant for the isomerisation may be calculated as $K = ([trans]/[cis])_{eq}$ considering that the rate of product formation is negligible compared with the rates of the steps involved in maintaining the isomerisation equilibrium. The values of K at several temperatures for the NO_2-catalysed geometric isomerisation of 2-butene (298–370 K) and 2-pentene (298–400 K) in the gas phase have been determined [59]. For 2-butene, the K values change from 2.977 at 298 K to 2.203 at 370 K. For 2-pentene, corresponding values are 4.648 at 298 K and 2.978 at 400 K. For the NO_2-catalysed geometric isomerisation of *cis*-2-butene, it has been shown that $k_2 \approx k_1$ and $k_{-2} \approx k_{-1}$. Kinetic analysis indicates that the deviation of the measured equilibrium ratio $([trans]/[cis])_{eq}$ from the true value K, which would be obtained when $k_3 = 0$, must be no greater than 3%. Thus, the effect of the product formation on the position of the geometric equilibrium is wholly negligible.

If NO_2 can abstract the allylic hydrogen of alkyl-substituted alkenes, the following scheme has been proposed [59, 61, 62]:

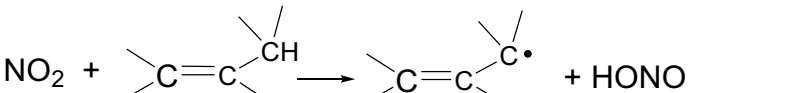

(5.121)

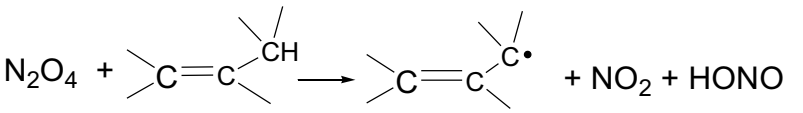

(5.122)

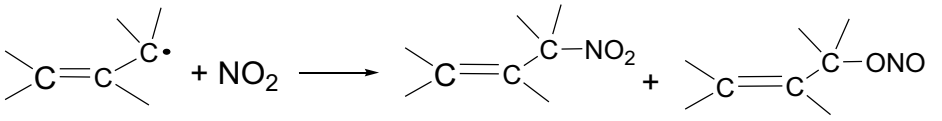

(5.123)

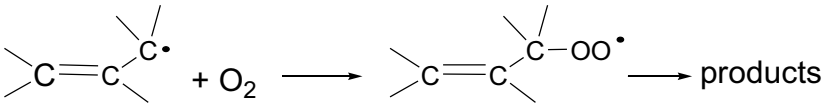

(5.124)

The isomerisation of *cis*- or *trans*-2-olefin to 1-olefin in reactions with NO_2 has not been detected by the chromatographic analysis [59].

The kinetics of the formation of nitration products in reactions of various alkenes with NO_2 + N_2O_4 in CCl_4, CH_2Cl_2 and hexane were investigated by stopped-flow spectroscopy [62]. The rates of reactions of 2,3-dimethyl-2-butene, cyclohexene, and 1-hexene were measured over a wide range of NO_2 concentrations, from <0.1 mM to 760 mM. For all of these substrates, the order in NO_2 is ~2 at high NO_2 and decreases to ~1 as the concentration of NO_2 decreases. These data indicate the presence of at least two reaction pathways. One involves the diamagnetic dimer N_2O_4 in an addition mechanism (**Equation 5.117**), and the other involves monomer NO_2 (**Equation 5.116**). The reaction of the monomer NO_2 proceeds also through abstraction of allylic hydrogen atoms.

The nitration of hexafluoropropene, CF_3–CF=CF_2 and octafluoroisobutene $(CF_3)_2$C=CF_2 has been described, and it was found that the reactivity of perfluoro olefins toward NO_2 falls from tetrafluoroethylene to hexafluoropropene, and further to octafluoroisobutene [66]. Whereas tetrafluoroethylene reacts explosively with NO_2 and nitration must be conducted in a solvent, hexafluoropropene reacts gently in the absence of solvents over 7 days at room temperature or 4–6 hours at 100 °C, and octafluoroisobutene reacts only at 170–180 °C. The nitration of hexafluoropropene is in accordance with the scheme:

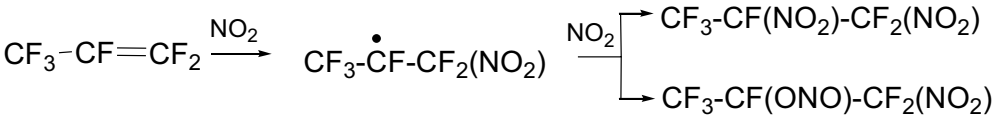

(5.125)

A small amount of a hexafluoronitrosopropane CF_3–CF(NO)–$CF_2(NO_2)$ also was detected.

The reaction of alkenes with NO_2 gives, as a rule, complex mixtures of products arising from competing addition, substitution, and oxidation. The cleavage of C–C bonds is also possible in intermediates radicals. As for styrene, the yields of nitroolefins are quite poor, and the nitro alcohols ($ArCH(OH)CH_2NO_2$) obtained are usually accompanied by a mixture of other products [67]. However, the synthesis of β-nitrostyrenes is the important problem because these compounds can be used for obtaining aryl-substituted nitroalkanes, hydroxylamines, aldoximes, ketoximes, amines, and ketones. In this connection, the reaction of styrene with NO_2 and ozone (Kyodai nitration) represents a convenient method for the direct side-chain nitration of styrene and its *p*-substituted derivatives [68]. The reaction has been investigated using mainly *p*-chlorostyrene as the substrate in dichloromethane from –20 °C to 0 °C. Under these conditions, *p*-chlorostyrene gave the best combined yield (88–98%) of nitro-nitrates.

The pathway from styrene to the side-chain nitration products in the Kyodai nitration is depicted by the following reactions:

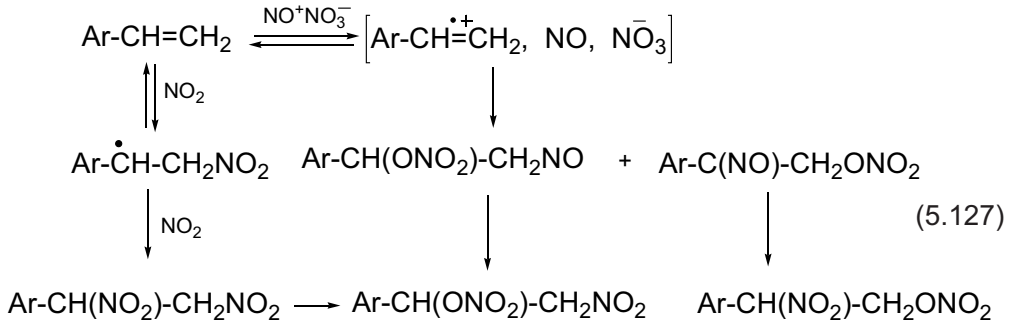

(5.127)

In dichloromethane, addition of NO_2 to the olefinic double bond may occur via heterolytic mode, where NO^+ and NO_3^- yield the corresponding nitroso-nitrate adducts. The reversible addition of nitrosonium nitrate to the styrene may be initiated via electron transfer between the olefin donor and nitrosonium cation. Therefore, the first intermediate is a styrene radical cation which subsequently couples with the nitrate anion or NO. The nitrosonitrates formed undergo rapid oxidation of the nitroso group to the nitro group in the presence of ozone to yield the nitro-nitrates as the final products. The β–nitro-α-nitrate adducts easily release the elements of nitric acid by the action of a weak base such as sodium hydrogen carbonate or alumina, giving the corresponding β–nitrostyrenes in good yield (50%):

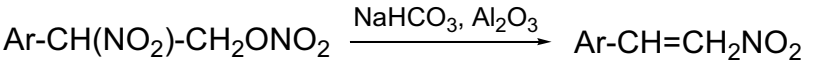

(5.127)

Using the reactions of NO_2 with several hexenes, the variation of product composition with substrate structure and reaction conditions has been studied [69]. The substrate used were the hexenes $C(CH_3)_2{=}C(CH_3)_2$ (I), $C(CH_3)(CH_3){=}CH(C_2H_5)$ (II), $CH(C_2H_5){=}CH(C_2H_5)$ (III), $CH_2{=}C(C_2H_5)_2$ (IV) and $CH_2{=}CH(C_4H_9)$ (IV). The hexene (I) reacts in $CHCl_3$ solution with NO_2 by the heterolytic route with participation of NO_2 dimers to give the nitrosonitrate as the only product. This reaction in hexane simultaneously gives a mixture of different nitration products:

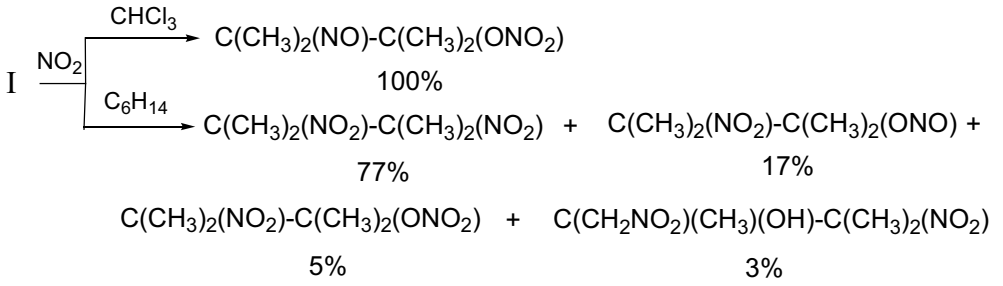

(5.128)

Thus, the heterolytic reaction path connected with nitrosyl nitrate $ONONO_2$ is apparently eliminated by the use of non-polar solvents.

Some investigations have been done on the reaction of several dienes with NO_2 [70, 71]. In these experiments, a solution of NO_2 in an organic solvent was added slowly to a stirred solution of the organic substrate in the same solvent at room temperature. The products obtained from conjugated 2,5-dimethylhexa-2,4-diene are shown in the scheme:

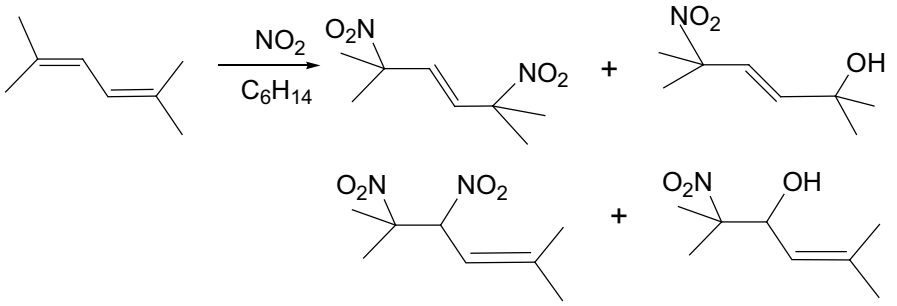

(5.129)

The four products obtained are those expected from the initial addition of NO_2 to give dinitro compounds or nitro nitrites at the 1:2 and 1:4 positions. The nitro nitrites

undergo rapid conversion to the corresponding nitro alcohols. The absolute and relative yields of these products depend very much on the conditions of reaction. In *n*-hexane as solvent, the 1,4-dinitro compound is formed in significant yields (70%) when relatively low concentrations of NO_2 (<1 mol/l) are used. The use of greater concentrations of NO_2 gives lower yields of the dinitro compound and significant yields of 1:2 adducts. In benzene and in diethyl ether, no initial precipitation of the 1,4-dinitro compound occurs. Evidence of a further reaction between this compound and NO_2 was not found.

The interaction of NO_2 with the *trans, trans* and *cis, trans* forms of hexa-2,4-diene is represented by the following reactions:

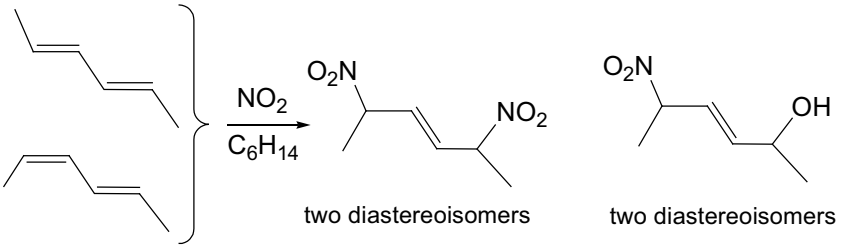

(5.130)

The yields varied with the conditions, but usually about 50% of the dinitro compound and 18% of the nitro alcohol. In diethyl ether, the yield of the dinitro alcohol increases up to 40%.

In reactions of 2,3-dimethylbuta-1,3-diene with NO_2, only two products were identified [71]:

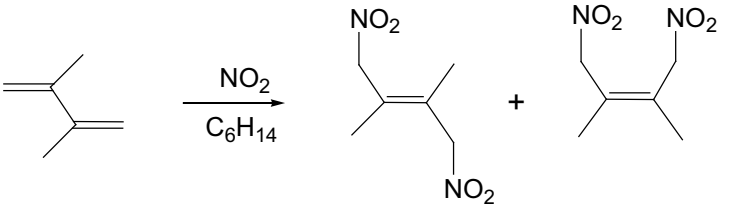

(5.130)

The absolute and relative yields of the two products are sensitive to the solvent used. In the more polar solvents, the ratio *trans*:*cis* is increased (5.8 in diethyl ether and 1 in CCl_4).

Dienes with non-conjugated double bonds, for example, hepta 1,6-diene, do not give products of 1,4-addition in reactions with NO_2:

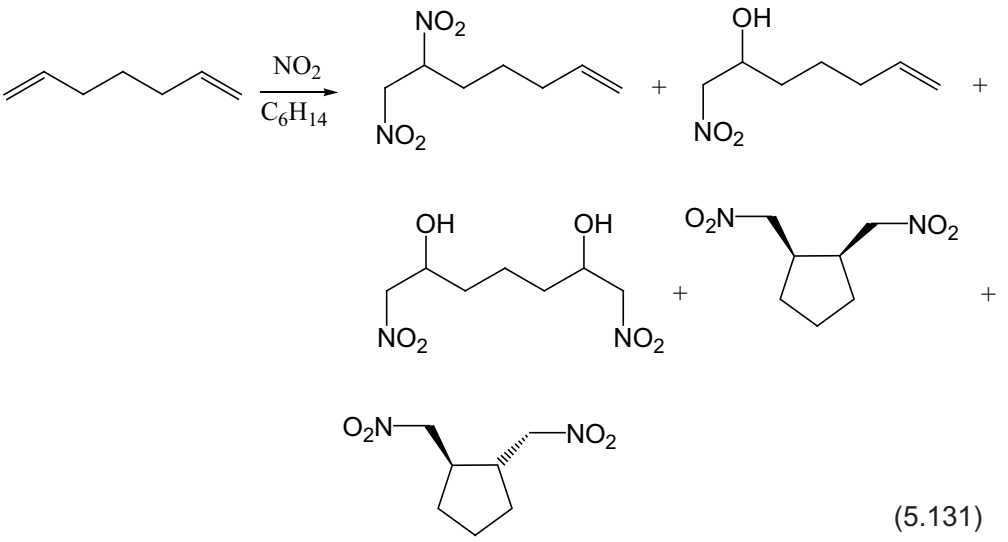

(5.131)

The formation of the two cyclic compounds shows that the reaction of the substrate with two separate NO_2 radicals takes place [65].

Fluorinated dienes react vigorously with NO_2 in the liquid and gas phase, and at ambient temperatures [72]. In its reactivity toward NO_2, hexafluoro-1,3-butadiene may be compared with tetrafluoroethylene. The addition of NO_2 to hexafluoro-l,3-butadiene goes at the two end carbon atoms of the system of conjugated bonds, as a result of which hexafluoro-l,4-dinitro-2-butene and the nitrous ester of hexafluoro-4-nitro-2-buten-l-ol are formed:

$$CF_2{=}CF\text{-}CF{=}CF_2 + N_2O_4 \longrightarrow \begin{cases} O_2N\text{-}CF_2\text{-}CF{=}CF\text{-}CF_2\text{-}\ NO_2 \\ O_2N\text{-}CF_2\text{-}CF{=}CF\text{-}CF_2\text{-}\ ONO \end{cases}$$

(5.132)

The formation of difluoronitroacetyl fluoride by the oxidation of the dinitro derivative with NO_2 occurs in the reaction:

$$O_2N\text{-}CF_2\text{-}CF{=}CF\text{-}CF_2\text{-}\ NO_2 \xrightarrow[\text{heat}]{N_2O_4} 2O_2N\text{-}CF_2\text{-}COF \qquad (5.133)$$

Alkenes and conjugated dienes can react with NO_2 under the action of visible light in low-temperature matrices [73–77]. The chemical reaction has been observed upon irradiation of ethylene – NO_2 pairs in solid Ar at 12 K with continuous-wave dye

laser light at wavelengths as long as 574 nm, well below the 398-nm dissociation limit of isolated NO_2 [74, 76]. The mechanism involves formation of a transient oxirane biradical:

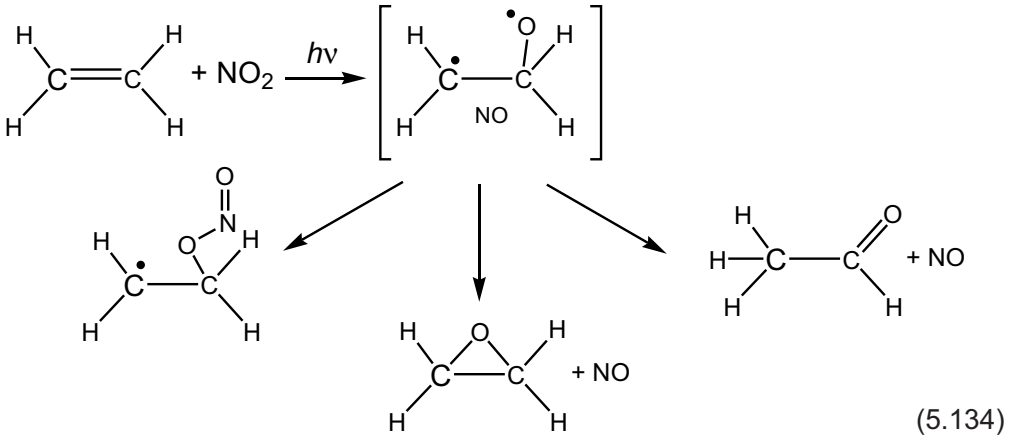

(5.134)

The nitrite radical and the epoxide have a common transient precursor: the oxirane biradical. This conclusion is confirmed by the observed photolysis wavelength-dependence of the branching between the two products and with the observed high degree stereochemical retention upon photolysis of alkene – NO_2 pairs [74]. The primary step of the visible-light-induced reaction is the atomic oxygen transfer from NO_2 to the C=C bond to generate an oxirane biradical. The stabilisation of the transient biradical so formed involves competition between three ultrafast (picosecond) processes, namely, ring closure to give epoxide, 1,2-H migration to yield acetaldehyde, and trapping by the NO cage neighbour to produce the ethyl nitrite radical.

The visible light excitation of diene – NO_2 reactant pairs has been also found to cause an oxygen-atom transfer from NO_2 to diene to form the oxirane biradical [77], which is similar to the photochemical reactions observed in the alkene – NO_2 – Ar systems. Two isomers are considered for the nitrite radical of butadiene:

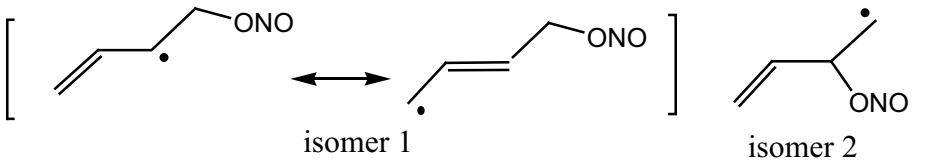

Isomer 2 has a C–O bond at the inner C atom of the butadiene skeleton and is unstable due to the non-resonance structure. Therefore, the nitrite radical is isomer 1, that is, the reaction sites are at the terminal C atoms of butadiene. The quantum yield for dissociation of nitrite radicals is much larger in alkene – NO_2 systems than in those for

dienes. The difference in the ΔH_r values might be a reason why the photodissociation yields of nitrite radical are much smaller in the diene – NO_2 systems than in the alkene – NO_2 systems:

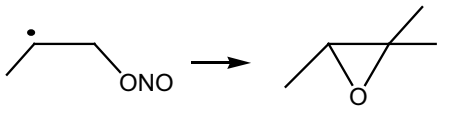

ΔH = - 14 kcal mol^{-1} (5.135)

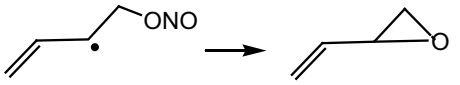

ΔH = + 13 kcal mol^{-1} (5.136)

In the case of allene + NO_2 reaction in solid Ar during the visible-light photolysis (585 nm), 2-allylnitrite radical was detected by Fourier transform infrared (FT-IR) spectroscopy, whereas excitation of dimethylacetylene – NO_2 systems (610 nm) gives the acetylmethyliminoxy radical and dimethylketene [75]. As a result of oxygen atom transfer from NO_2 to the central carbon atom, 2-allenylidoxy transient biradical is generated in allene:

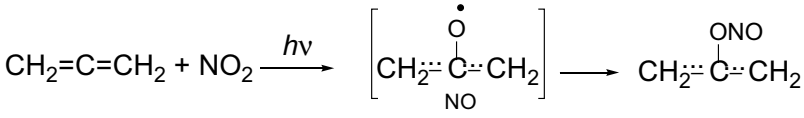

(5.137)

The biradical forms from large amplitude oxygen-atom transfer from highly vibrationally excited NO_2 in the unstable twisted conformation. The fact that no allene oxide is formed upon direct excitation of the NO_2 – allene system at any visible wavelength can readily be rationalised by fast conformational relaxation of initially formed twisted biradical to the stable planar conformer, followed by NO trapping.

In dimethylacetylene, the triplet ground state intermediate biradical has a ketocarbene structure with a C=O double bond, a central C–C single bond, and a carbene C atom:

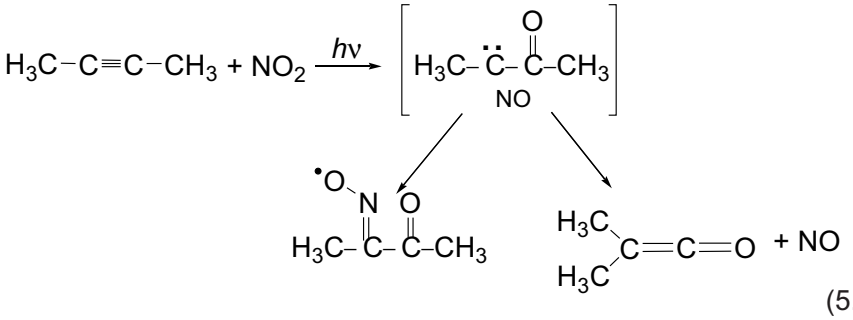

(5.138)

The iminoxyl radical observed by electron spin resonance (ESR) proves the formation of ketocarbene in the process of triple-bond oxidation by NO_2 under the action of visible light.

Carotenoids, in particular β-carotene, are well-known free-radical quenchers [78]. It has been shown that peroxy radicals can oxidise β-carotene to the corresponding radical cations [78]. Absorption spectra demonstrate the appearance of broad bands in the range 600–1000 nm with λ_{max} = 910 nm ($\varepsilon = 9.4 \times 10^4$/M/cm) during pulse radiolysis of solutions of β-carotene in tert-butyl alcohol – water mixtures containing nitrate [79]. These bands were attributed to β-carotene radical cations generated by electron abstraction from the substrate by NO_2 radicals:

$$NO_2 + \beta\text{-carotene} \rightarrow [\beta\text{-carotene}]^{+\bullet} + NO_2^- \qquad (5.139)$$

NO_2 is known to be a moderately strong one-electron oxidant with the redox potential E^0 (NO_2/NO_2^-) = + 1.04 V). The absolute rate constant k[NO_2 + β-carotene] is (1.1 ± 0.1) × 10^8 M/s. The antioxidant properties of β-carotene not only reflect rates of free-radical scavenging, but also the reactivity of the resultant carotenoid radicals. Radical cations formed are highly resonance-stabilised and therefore relatively unreactive.

Radical addition is the main chemical reaction of fullerene C_{60} due to its high electron affinity, allowing a direct chemical attack by the radicals [80, 81]. It has been suggested that C_{60} acts like a 'closed-cage' alkene rather than an aromatic molecule due to its poor electron delocalisation [82]. For example, C_{60} undergoes reactions associated with electron-deficient alkenes. Such reactions include various addition reactions such as cycloaddition, nucleophilic addition, and radical addition. Therefore, radical NO_2 was used for direct multiple addition to get polynitrofullerene [83, 84]. NO_2 was obtained in the reaction of concentrated NO and copper powder or sodium nitrite. Gaseous NO_2 in excess quantity was carried at 15–20 °C over into a solution of C_{60} in benzene or toluene by a stream of dried nitrogen. The progress of C_{60} was monitored by the disappearance of the purple colour of a solution of C_{60} and the formation of the red polynitrated fullerene product. At a reaction period of 2.5–5.5 hours, the quantity of the nitro products reaches a relatively steady ratio of di-, tetra-, and hexanitro[60]fullerenes. The fraction of tetraisomers is the major product of reaction. The yield of tetranitro[60]fullerenes is 2.7- and fourfold higher than that of di- and hexaisomers respectively:

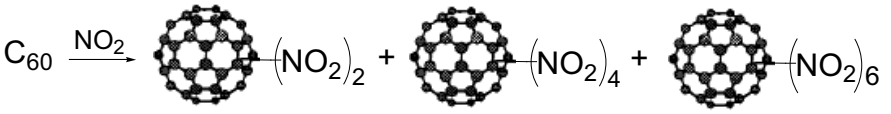

(5.140)

Further nitration of the C_{60} molecules for 5–6 days gives products consisting mainly of hexanitro[60]fullerenes. As the nitration temperature increases to 60 °C, the production rate of hexanitrated C_{60} isomers is raised sharply within a reaction period of 5 hours. However, the increase in rate is accompanied by products showing a more complicated composition owing to the formation of several polynitrated C_{60} isomers containing several nitro groups higher than 6. In addition, constant evaporation of NO_2 at >50 °C tended to result in additional product fractions with a low nitration level. This broadens the number distribution of nitro groups per C_{60} in the final products.

Fullerene nitro functional groups were found to be unstable thermally in solution or in SO_2, which prohibits the direct purification and separation of polynitrated isomers. The instability of these compounds arises from the facile occurrence of the intramolecular rearrangement into corresponding nitrites and further polyhydroxylated C_{60} by hydrolysis:

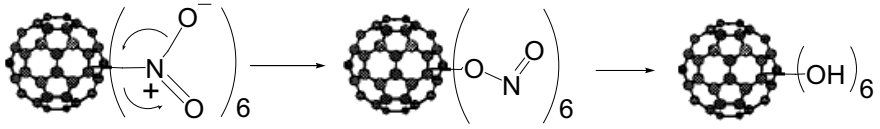

(5.141)

Hexanitro[60]fullerenes are highly electrophilic molecules toward reactions with various nucleophiles. Upon treatment of $C_{60}(NO_2)_6$ in tetrahydrofuran (THF) with aniline in the presence of triethylamine at 50 °C for 6 hours, hexanitroanilino[60] fullerenes $C_{60}(NHC_6H_5)_6$ were obtained in a yield of 94% [84].

5.5 Radical Conversions of p-benzoquinones in Reactions with NO_2

Quinones are found in the structures of several biologically active substances, such as ferments, vitamins and pigments [85]. Hence, kinetic studies of reactions of NO_2 with quinones are important for understanding the mechanism of conversions of such natural unsaturated substances in an aggressive atmosphere. Such investigations have been done for *p*-benzoquinone and 2,6-di-*tert*-butyl-*p*-benzoquinone (TBQ) [86]. Investigation into the reaction mechanism was mainly concentrated on the structures of nitrogen-containing radicals and the kinetic features of their accumulation. After exposure of TBQ to NO_2 at pressures of $2.5 \times 10^5 - 1.45 \times 10^4$ Pa, the slow growth of ESR spectra was observed over several days up to the maximum level dependent on the gas pressure. The electron paramagnetic resonance (EPR) spectrum recorded at room temperature is shown in **Figure 5.2**.

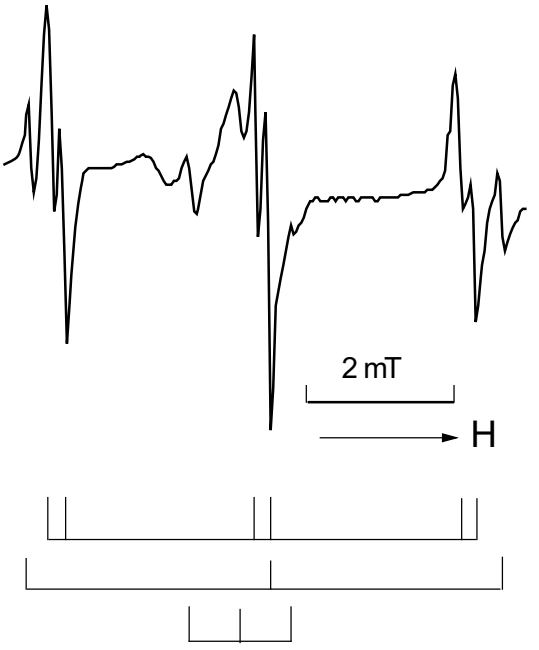

Figure 5.2 ESR spectrum of TBQ after exposure to NO_2 at 293 K

Essentially the same spectrum was observed for *p*-benzoquinone. In the spectrum shown in **Figure 5.2,** it is possible to distinguish the signals of three types of radicals. The triplet signal, characterised by the nitrogen coupling constant a_N =2.82 mT and g = 2.0053, corresponds to oxyaminoxyl radicals [70, 87] arising from the addition of NO_2 to the double bonds of the quinines:

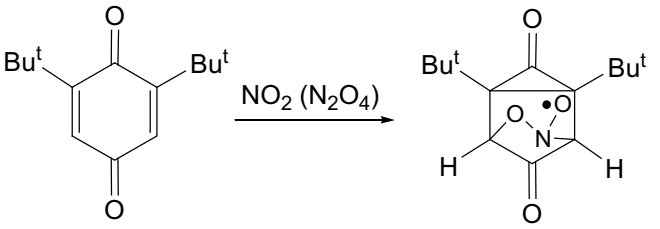

(5.142)

A doublet splitting of the triplet components with a_H =0.17 mT is also observed because of the hydrogen atom adjacent to the nitrogen [88].

Oxyaminoxyl radicals with similar ESR parameters have been detected in reactions of NO_2 with phorone [70] in which it is believed that these radicals are produced by NO_2 addition to the double bonds of the ketone:

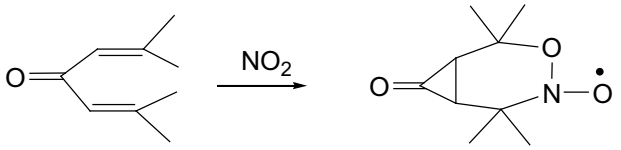

(5.143)

In this connection, the analogous structure of oxyaminoxyl radicals in TBQ seems the most preferable.

The absence of anisotropy of the ESR spectrum shown in **Figure 5.2**, which is characteristic of the ESR spectra of aminoxyl radicals (ARs) in the solid phase, is explained by the gradual 'melting' of quinines and their transformation into a viscous liquid on exposure to NO_2. In addition to oxyaminoxyl radicals, two other radicals are detected from the ESR spectrum (**Figure 5.2**). The triplet signal with parameters a_N =3.21 mT and g = 2.0045 belongs to the iminoxyl radicals with averaged anisotropy of interaction of unpaired electrons with nitrogen nuclei [89]. Another type of radical is characterised by a triplet signal with a_N =0.71 mT and g = 2.0072. Such ESR parameters are typical of g = 2.0045 [90]. The fraction of iminoxyl radicals and acyl(alkyl)aminoxyl radicals is fairly small; the estimation shows that their signals do not exceed 29% of the total ESR spectrum [86].

Obviously, iminoxyl and acyl(alkyl)aminoxyl radicals cannot be formed by the direct interaction of NO_2 with the double bonds of the quinines, but these radicals are produced as a result of thermal conversions of primary oxyaminoxyl radicals most likely because of the strong angular strain arising from their bicyclic structure. Oxyaminoxyl radicals can decompose, giving alkoxyl radicals, which subsequently break down, leading to the destruction of the quinine structure with the formation of acyl radicals containing nitroso groups:

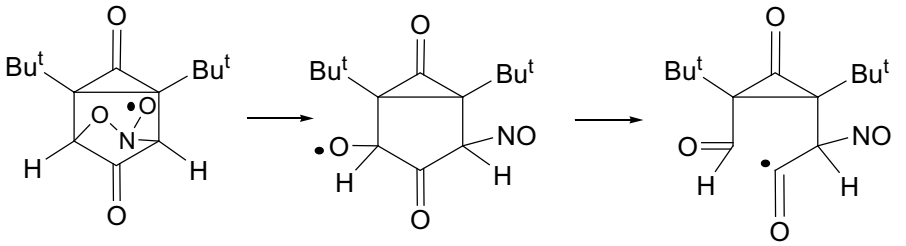

(5.144)

The cyclopropanone fragments of radicals appear to be unstable and [91], and elimination of CO leads to the following conversion:

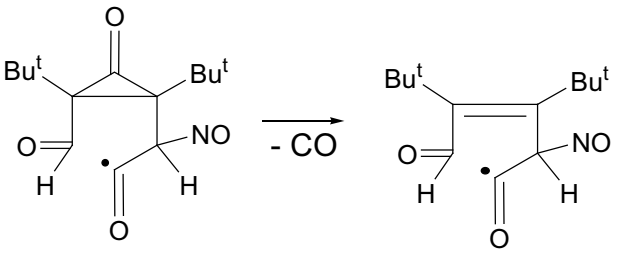

(5.145)

Further transformations produce molecular products (nitro compounds or nitrites) and ARs:

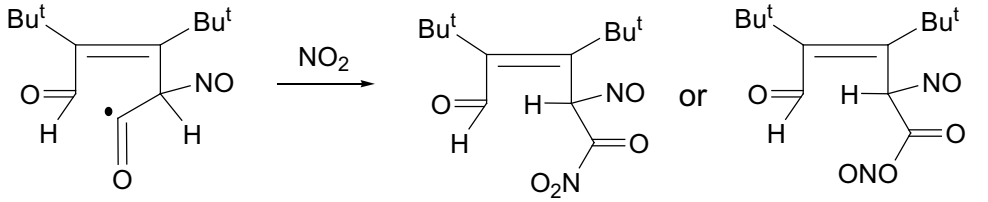

(5.146)

The nitroso groups of products having an α-hydrogen atom undergo isomerisation into oximes [85] which react with NO_2 to produce iminoxyl radicals:

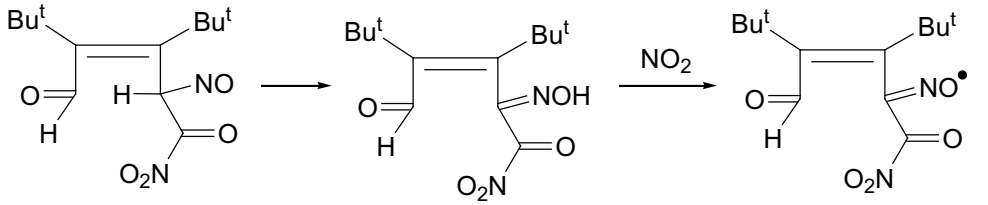

(5.147)

Simultaneously to (**Equation 5.147**), acyl radicals are transformed into acyl(alkyl) aminoxyl radicals, for instance, by attaching to the nitroso groups of (**Equation 5.146**) products with the formation of structures in which the substituents R^1 and R^2 are fragments of the quinine molecules:

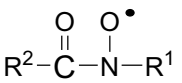

The detection of some molecular products using IR spectra confirms the free-radical processes taking place in *p*-benzoquinones under the action of NO_2 [86]. Two new bands at 1560 cm^{-1} and 1340 cm^{-1} are due to the asymmetric stretches of NO_2 groups in nitro compounds observed in the IR spectrum of TBQ exposed to NO_2. The formation of nitroso groups is also traced by the band at 1120 cm^{-1}, indicating the presence of the nitroso *trans*-dimers [92]. Evidence for the conversion of oxyaminoxyl radicals according to (**Equations 5.144–5.146**) is provided by the appearance of the absorption band at 1704 cm^{-1}, which can be assigned to the carbonyl stretch in α,β-unsaturated aldehydes.

Oxyaminoxyl radicals of *p*-benzoquinones are sensitive to temperature; a stationary concentration of the radicals varies reversibly with changes in temperature in an atmosphere of NO_2. The corresponding temperature dependence is given in **Figure 5.3**.

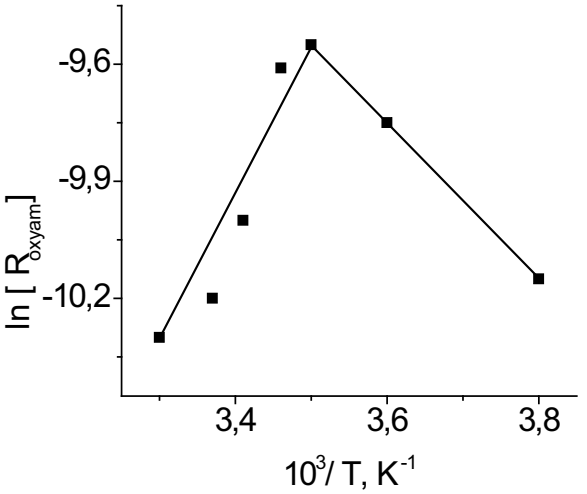

Figure 5.3 Temperature dependence of stationary concentrations of oxyaminoxyl radicals in *p*–benzoquinone

At first at T < 300, the radical concentration increases and attains a maximum at 12 °C, but then it decreases with further lowering of temperature. Oxyaminoxyl radicals quickly disappear at room temperature within several minutes after pumping out NO_2 from the samples. The mechanism of decay involves recombination of oxyaminoxyl radicals with the resulting formation of N_2O_4 and two molecules of TBQ. The increase

in the stationary concentration of the radicals with decreasing temperature in the range from 12 °C to 27 °C occurs due to the formation of the NO_2 dimer, as the equilibrium $2NO_2 \rightleftarrows N_2O_4$ is also shifted to the right with decreasing temperature [93]. The decisive role of N_2O_4 in the mechanism of the formation of oxyaminoxyl radicals is confirmed by the results of kinetic measurements at various pressures of NO_2. The relationships between the initial rates and partial pressures of NO_2 and N_2O_4 calculated from known equilibrium constants [93] are shown in **Figure 5.4**.

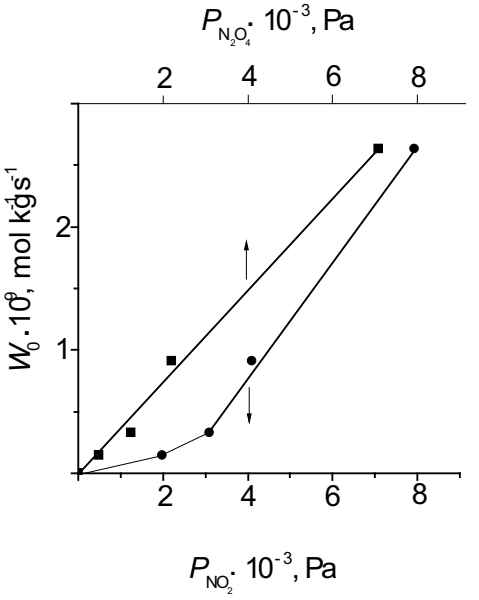

Figure 5.4 Dependencies of initial rates of accumulation of oxyaminoxyl radical at 20 °C on the partial pressures of NO_2 and N_2O_4

It is clear that the experimental values of the initial rates depend linearly on the partial pressures of N_2O_4 and not of NO_2.

Based on the kinetic data obtained, the formation and decay of oxyaminoxyl radicals can be presented by the following scheme:

$$2NO_2 \underset{k_{-1}}{\overset{k_1}{\rightleftarrows}} N_2O_4 + Q \quad \underset{k_{-2}}{\overset{k_2}{\rightleftarrows}} \quad \left[N_2O_4 \bullet Q \right] \xrightarrow{k_3} R_{oxy} + NO_2 \qquad (5.148)$$

$$R_{oxy} + R_{oxy} \xrightarrow{k_4} \text{products} \qquad (5.149)$$

where Q is quinine, and R_{oxy} is the oxyaminoxyl radical. If it is assumed that $k_{-2} >> k_3$ and $k_{-1} >> k_2$, then the equation for the concentration of radicals at the steady state takes the form:

$$[R_{oxy}]_{st} = \left(\frac{k_1 k_2 k_3}{k_{-1} k_{-2} k_4} \right)^{1/2} [NO_2] \tag{5.150}$$

Then the temperature dependence of the radical concentration in steady-state conditions is determined as follows:

$$\ln[R_{oxy}]_{st} = \frac{A + (E_4 - E_3 + \Delta H_1 + \Delta H_2)}{2RT} \tag{5.151}$$

where A is a parameter dependent on the NO_2 pressure, E_3 and E_4 are activation energies of the formation and decay of oxyaminoxyl radicals, ΔH_1 is the heat of equilibrium dissociation of N_2O_4 dissolved in the quinine samples, and ΔH_2 is the dissociation heat of an intermediate complex N_2O_4 with quinine molecules. The temperature coefficient E_4–E_3 + ΔH_1 + ΔH_2 in (**Equation 5.151**) at 12–27 °C (**Figure 5.3**) is 64 kJ/mol for TBQ. At –43 °C to 17 °C, the equilibrium is practically completely shifted towards N_2O_4·Q, and the temperature coefficient of the dependence takes the opposite sign. The change in the stationary concentrations of oxyaminoxyl radicals is determined in this temperature range from the $E_2 - E_1$ values which is –32 kJ/mol for TBQ, then $\Delta H_1 + \Delta H_2$ is 96 kJ/mol. As is known, the enthalpy of the N_2O_4 dissociation in the gas phase is 60 kJ/mol [93]. The complexes involving quinine molecules act as spin traps for NO_2 in the irreversible dissociation of N_2O_4. The appearance of such complexes is accompanied by an essential heat effect ΔH_2. If it is supposed that ΔH_1 in TBQ is in the range 60–70 kJ/mol, then values of 26–36 kJ/mol for ΔH_2 can be estimated [86].

As discussed previously [69], nitrogen tetroxide can react with unsaturated compounds in solution by different mechanisms depending on the polarity of the solvent. These two mechanisms are connected with existence of the dimer in the planar form and as nitrosyl nitrate, which dissociate by homolytic and heterolytic pathways, respectively. The heterolytic pathway leads to the formation of nitroso nitrates as the main products of alkene nitration, whereas homolytic dissociation of nitrogen tetroxide gives dinitro compounds and nitro nitrites. Generation of the quinine radicals is also dependent on the homolytic dissociation of nitrogen tetroxide. The features of this process appear to be the formation of an intermediate complex involving N_2O_4 coordination with two double bonds of *p*-benzoquinones. This conclusion follows from the analysis of temperature dependence of the stationary concentration of radicals. The free-radical considered may therefore be useful as specific test for similar quinine structures in various chemical and biological systems.

References

1. M.A. Arbex, L.C. Martins, A.A. Pereira, F. Negrini, A.A. Cardoso, W.R. Melchert, R.F. Arbex, P.H.N. Saldiva, A. Zanobetti and A.L.F. Brage, *Brazilian Journal of Medical and Biological Research*, 2007, **40**, 4, 527.

2. B. Ranby and J.F. Rabek, *Photodegradation, Photooxidation, Photostabilisation of Polymers*, Wiley, London, UK, 1975.

3. A.V. Topchiev and N.N. Kaptsov, *Russian Chemical Bulletin*, 1956, **5**, 883.

4. A.I. Titov, *Tetrahedron*, 1963, **19**, 557.

5. G.B. Bachman, L.M. Addison, J.V. Hewett, L. Kohn and A. Millikan, *Journal of Organic Chemistry*, 1952, **17**, 7, 906.

6. A.P. Ballod and V.Ya. Shtern, *Russian Chemical Reviews*, 1976, **45**, 721.

7. W.T. Chan, S.M. Heck and H.O. Pritchard, *Physical Chemistry Chemical Physics*, 2001, **3**, 1, 56.

8. N.N. Semenov, *Some Problems of Chemical Kinetics and Reactivity*, Academy of Sciences USSR Press, Moscow, Russia, 1954.

9. E.A. Blyumberg and N.M. Emanuel, *Russian Chemical Bulletin*, 1956, **6**, 289.

10. G.B. Bachman and L. Kohn, *Journal of Organic Chemistry*, 1952, **17**, 7, 942.

11. G.B. Bachman, J.V. Hewett, L. Kohn and A.G. Millikan, *Journal of Organic Chemistry*, 1952, **17**, 7, 935.

12. R. Smith, *Journal of the Chemical Society*, 1953, 1271.

13. E. McBee, H. Hass and J. Robinson, *Journal of the American Chemical Society*, 1950, **72**, 8, 3579.

14. D.V.E. George and J.H. Thomas, *Transactions of the Faraday Society*, 1962, **58**, 58, 262.

15. K.B. Krauskopf and G.K. Rollefson, *Journal of the American Chemical Society*, 1934, **56**, 12, 2542.

16. H.B. Hass and D.E. Hudgin, *Journal of the American Chemical Society*, 1954, **76**, 10, 2692.

17. H. Suzuki and N. Nonoyama, *Chemical Communications*, 1996, **15**, 1783.

18. H. Suzuki and T. Mori, *Journal of the Chemical Society, Perkin Transactions 2*, 1997, **7**, 1265.

19. J.C.D. Brand, *Journal of the American Chemical Society*, 1955, **77**, 10, 2703.

20. G.B. Bachman, M.T. Atwood and M. Pollack, *Journal of Organic Chemistry*, 1954, **19**, 3, 312.

21. L. Eberson and F. Radner, *Accounts of Chemical Research*, 1987, **20**, 2, 53.

22. E. Halfpenny and P.L. Robinson, *Journal of the Chemical Society*, 1952, 939.

23. T. Logoger and K. Sehested, *Journal of Physical Chemistry*, 1993, **97**, 25, 6664.

24. D. Vione, V. Maurino, C. Minero and E. Pelizzetti, *Environmental Science and Technology*, 2005, **39**, 4, 1101.

25. H. Suzuki, T. Murashima, I. Kozai and T. Mori, *Journal of the Chemical Society - Perkin Transactions 2*, 1993, **9**, 1591.

26. E. Bacciocchi, M. Crescenzi, E. Fasella and M. Mattioli, *Journal of Organic Chemistry*, 1992, **57**, 17, 4684.

27. H. Suzuki, T. Takeuchi and T. Mori, *Journal of Organic Chemistry*, 1996, **61**, 17, 5944.

28. H. Suzuki, S. Yonezawa, T. Mori and K. Maeda, *Journal of the Chemical Society - Perkin Transactions 2*, 1994, **6**, 1367.

29. G.A. Olah, R. Malhotra and S.C. Narang, *Nitration Methods and Mechanics*, VCH, New York, NY, USA, 1989.

30. H. Suzuki and T. Mori, *Journal of the Chemical Society, Perkin Transactions 2*, 1994, **3**, 479.

31. H. Suzuki and T. Murashima, *Journal of the Chemical Society, Perkin Transactions 1*, 1994, **7**, 903.

32. T. Kajya, K. Nakamura, M. Tanaka, N. Niyata and K. Kohda, *Chemical & Pharmaceutical Bulletin*, 2004, **52**, 5, 570.

33. H. Suzuki and T. Mori, *Journal of the Chemical Society, Perkin Transactions 1*, 1995, **3**, 291.

34. H. Suzuki, M. Iwaya and T. Mori, *Tetrahedron Letters*, 1997, **32**, 5647.

35. J.M. Bakke and I. Hegbom, *Journal of the Chemical Society - Perkin Transactions 2*, 1995, **6**, 1211.

36. O.V. Bakhvalov, *Chemistry for Sustainable Development*, 2003, **3**, 439.

37. K. Smith, S. Almeer and S.J. Black, *Chemical Commununications*, 2000, 17, 1571.

38. X. Peng and H. Suzuki, *Organic Letters*, 2001, **3**, 22, 3431.

39. R.P. Claridge, N.L. Lancaster, R.W. Millar, R.B. Moodie and J.P.B. Sandall, *Journal of the Chemical Society, Perkin Transactions 2*, 2001, **2**, 197.

40. W.A. Pryor, G.J. Gleicher, J.P. Cosgrove and D.F. Chuech, *Journal of Organic Chemistry*, 1984, **49**, 26, 5189.

41. M.P. Hartshorn, *Acta Chemica Scandinavica*, 1998, **52**, 2.

42. C.D. Cook and R.C. Woodworth, *Journal of the American Chemical Society*, 1953, **75**, 24, 6242.

43. C.E. Barnes and P.C. Myhre, *Journal of the American Chemical Society*, 1978, **100**, 3, 973.

44. P. Astolfi, M. Panagiotaki and L. Greci, *European Journal of Organic Chemistry*, 2005, 14, 3052.

45. F.G. Bordwell and J.P. Cheng, *Journal of the American Chemical Society*, 1991, **113**, 5, 1743.

46. L. Parts and J.T. Miller, *Journal of Chemical Physics*, 1965, **43,** 136.

47. S.V. Lindeman, E. Bosch and J.K. Kochi, *Journal of the Chemical Society*, *Perkin Transactions 2*, 2000, **9**, 1919.

48. R.K. Jensen, S. Korsek, L.R. Mahoney and M. Zinbo, *Journal of the American Chemical Society*, 1979, **101**, 25, 7574.

49. E.Ya. Davydov, S. Korsek, R.K. Jensen and G.E. Zaikov, *Oxidation Communications*, 1997, **20**, 214.

50. E.Ya. Davydov, S. Korsek, R.K. Jensen and G.E. Zaikov, *Oxidation Communications*, 1997, **20**, 225.

51. A.F. Bickel and E.C. Kooyman, *Journal of the Chemical Society*, 1953, 3211.

52. V.A. Roginskii, V.Z. Dubinskii, I.A. Shlyapnikova and V.B. Miller, *European Polymer Journal*, 1977, **13**, 11, 1043.

53. S. Nagakura and A. Kuboyama, *Journal of the American Chemical Society*, 1954, **76**, 4, 1003.

54. S. Yachigo, M. Sasaki, T. Ishii and S. Tanaka, *Polymer Degradation and Stability*, 1992, **37**, 2, 99.

55. W.A. Pryor, D.F. Church, C.K. Govindan and G. Crank, *Journal of Organic Chemistry*, 1988, **47**, 1, 156.

56. H.M. Chawla and K. Srinivas, *Journal of the Chemical Society - Chemical Commununications*, 1994, **22**, 2593.

57. S. Shinkai, K. Araki, T. Tsubaki, T. Arimura and O. Manaba, *Journal of the Chemical Society, Perkin Transactions 1*, 1987, 2297.

58. Y. Li, J.S. Wang and D.S. Li, *Chinese Chemical Letters*, 2004, **15**, 400.

59. H. Akimoto, J.L. Sprung and J.N. Pitts, *Journal of the American Chemical Society*, 1972, **94**, 14, 4850.

60. J.L. Sprung, H. Akimoto and J.N. Pitts, *Journal of the American Chemical Society*, 1974, **96**, 21, 6549.

61. W.A. Pryor, J.W. Lightsey and D.F. Church, *Journal of the American Chemical Society*, 1982, **104**, 24, 6685.

62. D.H. Giamalwa, G.B. Kenion, D.F. Church and W.A. Pryor, *Journal of the American Chemical Society*, 1987, **109**, 23, 7059.

63. H. Shechter, J.J. Gardikas, T.S. Cantrell and G.V.D. Tiers, *Journal of the American Chemical Society*, 1967, **89**, 12, 3005.

64. H. Baldock, N. Levy and C.W. Scaife, *Journal of the Chemical Society*, 1949, 2627.

65. J.C.D. Brand and I.D.R. Stevens, *Journal of the Chemical Society*, 1958, 629.

66. I.L. Knunyants, A.V. Fokin and V.A. Komarov, *Izvestiya Akademii Nauk SSSR Seriya Khimichestkaya*, 1966, 466.

67. D.K. Bryant, B.C. Challis and J. Iley, *Journal of the Chemical Society - Chemical Communications*, 1989, **15**, 1027.

68. H. Suzuki and T. Mori, *Journal of Organic Chemistry*, 1997, **62**, 19, 6498.

69. R. Golding, J.L. Powell and J.H. Ridd, *Journal of the Chemical Society, Perkin Transactions 2*, 1996, **5**, 813.

70. I. Gabr and M.C.R. Symons, *Journal of the Chemical Society - Faraday Transactions*, 1996, **92**, 10, 1767.

71. R.P. Claridge, J. Deeming, N. Paul, D.A. Tocher and J.H. Ridd, *Journal of the Chemical Society - Perkin Transactions 1*, 1998, **21**, 3523.

72. I.L. Knunyants, A.V. Fokin, Yu.M. Kosyrev, I.N. Sorochkin and K.V. Frosina, *Izvestiya Akademii Nauk SSSR Seriya Khimichestkaya*, 1963, 1772.

73. M. Nakata and H. Frei, *Journal of the American Chemical Society*, 1989, **111**, 14, 5340.

74. M. Nakata, M. Shibuya and H. Frei, *Journal of Physical Chemistry*, 1990, **94**, 21, 8168.

75. M. Nakata and H. Frei, *Journal of the American Chemistry Society*, 1992, **114**, 4, 1363.

76. D.J. Fitzmaurice and H. Frei, *Journal of Physical Chemistry*, 1992, **96**, 25, 10308.

77. N. Tanaka, Y. Kajii, K. Shibuya and M. Nakata, *Journal of Physical Chemistry*, 1993, **97**, 27, 7048.

78. T.J. Hill, E.J. Land, D.J. McGarvey, W. Schalch, J.H. Tinkler and T.G. Truscott, *Journal of the American Chemical Society*, 1995, **117**, 32, 8322.

79. S.A. Everett, M.F. Dennis and K.B. Patel, *Journal of Biological Chemistry*, 1996, **271**, 7, 3968.

80. C. Corvaja, M. Maggini, M. Prato, C. Scorranno and M. Venzin, *Journal of the American Chemical Society*, 1995, **117**, 34, 8857.

81. G-W. Wang, L-H. Shu, S-H. Wu, H-M. Wu and X-F. Lao, *Journal of the Chemical Society - Chemical Communications*, 1995, **10**, 1071.

82. M. Yan, S.X. Cai and J.F.W. Keana, *Journal of Organic Chemistry*, 1994, **59**, 20, 5951.

83. N.X. Wang, *Propellants, Explosives, Pyrotechnics*, 2001, **26**, 3, 109.

84. V. Anantharaj, J. Bhonsle, T. Canteenwala and L.Y. Chiang, *Journal of the Chemical Society, Perkin Transactions 1*, 1999, **1**, 31.

85. J.D. Roberts and M.C. Caserio, *Basic Principles of Organic Chemistry*, W. A. Benjamin, Inc., New York, NY, USA, 1964.

86. E.Ya. Davydov, I.S. Gaponova and G.B. Pariiskii, *Journal of the Chemical Society, Perkin Transactions 2*, 2002, **7**, 1359.

87. H.G. Korth, R. Sustmann, P. Lommes, T. Paul, A. Ernst, H. de Groot, L. Hughes and K.U. Ingold, *Journal of the American Chemical Society*, 1994, **116**, 7, 2767.

88. A. Rockenbauer, M. Gyor and F. Tudos, *Tetrahedron Letters*, 1986, 4325.

89. P.S. Lakkaraju, J. Zhang and H.D. Roth, *Journal of the Chemical Society, Perkin Transactions 2*, 1993, **12**, 2319.

90. J.S.B. Park and J.C. Walton, *Journal of the Chemical Society, Perkin Transactions 2*, 1997, **12**, 2579.

91. E.F. Rothgery, R.J. Holt and H.A. McGee, *Journal of the American Chemical Society*, 1975, **97**, 17, 4971.

92. *The Chemistry of the Nitro and Nitroso Groups*, Ed., H. Feuer, Wiley, New York, NY, USA, 1969.

93. F.H. Verhoeck and F. Daniels, *Journal of the American Chemical Society*, 1931, **53**, 4, 1250.

6 Nitrogen Dioxide Monoradicals in Reactions of Modification and Degradation of Macromolecules

As discussed in **Chapters 1 and 5**, nitrogen dioxide (NO_2) is a relatively low-active free radical. Therefore, it virtually does not react at ambient temperatures with polymers that do not contain specific functional groups. However, NO_2 interacts very actively with the double C–C bonds of macromolecules as well as with macroradicals. These reactions result in the formation of various products of nitration and nitrosation. Subsequent processes can involve the degradation of macromolecules, and the formation of stable nitrogen-containing radicals.

6.1 Formation of Spin-Labelled Polymers in Reactions of NO_2 with the Double Bonds of Macromolecules

Some polymers that do not react directly with NO_2 demonstrate high reactivity after the action of, for instance, light irradiation. For example, polymethylmethacrylate (PMMA) has been considered [1, 2]. The irradiation of this polymer by ultraviolet (UV) causes elimination of the ester groups as methyl formate and macromolecular structures containing double bonds in the main chain [3]. The formation of paramagnetic species under the action of NO_2 in PMMA containing 0.3–0.4 mol/kg of monomer units with double C–C bonds and produced upon photolysis has been studied by electron spin resonance (ESR) spectroscopy. The experimental ESR spectrum of PMMA is a superposition of two triplet anisotropic signals of dialkykaminoxyl radicals $R_1R_2N(O^{\bullet})$ ($A_{II}^{N} = 3.2 \pm 0.1$ mT, $g_{II} = 2.0026 \pm 0.0005$) and acylalkylaminoxyl radicals $R_1C(=O)N(O^{\bullet})R_2$ ($A_{II}^{N} = 2.1 \pm 0.1$ mT, $g_{II} = 2.0027 \pm 0.0005$). In samples of PMMA exposed to NO_2 and soluted in benzene, these radicals exhibit triplet ESR spectra with the parameters $a^{N} = 1.5 \pm 0.1$ mT, $g = 2.0064 \pm 0.0005$ and $a^{N} = 0.8 \pm 0.1$, $g = 2.0065 \pm 0.0005$. The absence of additional hyperfine splitting in spectra obtained in the benzene solution indicates that the carbon atoms neighbouring the $NO^{\bullet}$ group are tertiary. The initial rate of accumulation of these macroradicals is proportional to the concentration of NO_2 in the gas phase. The reaction scheme proposed [1] explains features of the nitrogen-containing radical formation:

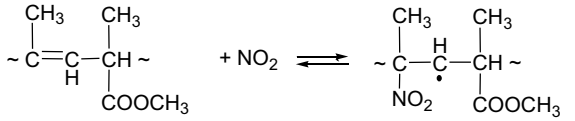

(6.1)

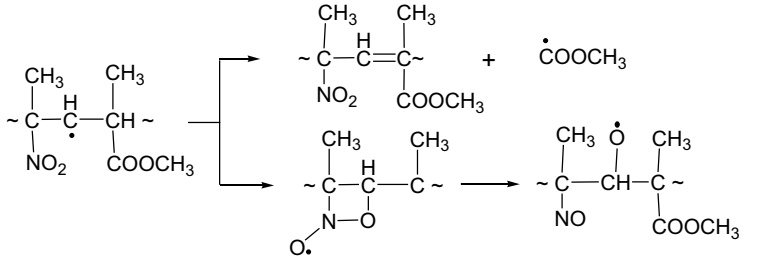

(6.2)

(6.3)

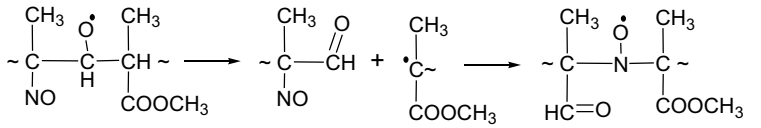

(6.4)

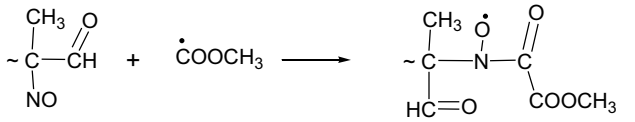

(6.5)

According to the scheme, the primary nitroalkyl radical is converted into unstable four-membered alkoxyalkylaminoxyl radicals which decompose to give the alkoxyl radical and nitroso group at the adjacent carbon atom. Subsequent decomposition of alkoxyl macroradicals results in an alkyl radical and nitroso compound located in the immediate vicinity of each other. The reaction between them, resulting in the formation of dialkylaminoxyl macroradicals, can be initiated by small-amplitude translational and rotational motions. Acylalkylaminoxyl radicals appear in the reactions of the low-molecular methoxycarbonyl radicals with tertiary nitroso compounds. This reaction scheme ignores concurrent transformations of reactive free radicals, which proceed without formation of aminoxyl radicals (ARs). These processes seem to be responsible for the low yield (~1%) of ARs relative to consumed NO_2 molecules. The similar reduction of nitro compounds to nitroso compounds through the stage of formation and decomposition of alkoxyalkylaminoxyl radicals (**Equation 6.3**) has been pointed out in the liquid-phase reactions [4–6]. As the reaction scheme suggests, the interaction between the double bonds of PMMA and NO_2 is accompanied by chain scissions in the macromolecules and elimination of the ester side groups.

Spin labels produced in the reactions of NO_2 with the double bonds of polymers give information on macromolecular dynamics. This approach was used for polyisoprene

(PI) [2, 7]. Samples having a cylindrical shape (diameter of 4 mm, height of 1.5 cm) were placed into tubes for ESR measurements. The tubes were connected with a glass flask. After evacuation, samples were exposed to NO_2 ($[NO_2] = 10^{-5}$ mol/l to $2 \times 3 \cdot 10^{-3}$ mol/l) or an $NO_2 + O_2$ mixture ($[NO_2] = 10^{-4}$ mol/l to 2×10^{-3} mol/l and $[O_2] = 2 \times 10^{-3}$ mol/l to 1.4×10^{-2} mol/l), and ESR measurements were started immediately after gas entry into the tubes. Interaction of NO_2 with the PI sample gives rise to the ESR spectrum shown in **Figure 6.1a**.

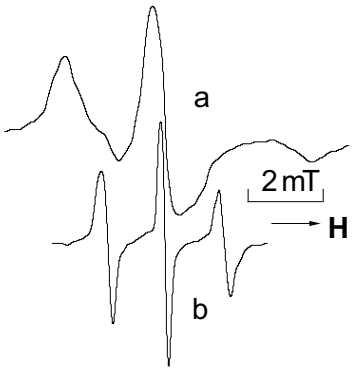

Figure 6.1 ESR spectra of aminoxyl radicals obtained in the reaction of a block PI sample with NO_2 at 20 °C (a) and 100 °C (b)

The spectrum represents a characteristic anisotropic triplet signal of ARs in the region of their slow motions (10^{-9} s < τ_c < 10^{-7} s) with $A_{II}^{N} = 3.1$ mT and $g_{II} = 2.0028 \pm 0.0005$. On dissolving the polymer in benzene or toluene, the spectrum exhibits a triplet signal with $a^{N} = 1.53 \pm 0.03$, $g = 2.0057 \pm 0.0005$ and a component intensity ratio of 1:1:1. This spectrum is characteristic of radicals having fast motions (10^{-9} s > τ_c > 10^{-11} s). These parameters coincide with those of ARs obtained by interaction of NO + O_2 with PI in solution [8]. The same a^{N} and g values were observed for block PI samples at 373 K (**Figure 6.1b**). The initial rates of the accumulation of ARs are proportional to NO_2 concentrations in the gas phase. Kinetic curves have the maximum dependence on NO_2 concentrations. As the concentration increases, the maximum amount of the aminoxyl macroradicals initially grows, reaches a maximum of $(4–5) \times 10^{16}$ spin/sample at $[NO_2] = (7–8) \times 10^{-4}$ mol/l, and then gradually decreases. The time required for accumulating the maximum amount of the radicals increases from 10 minutes to >400 minutes when the $[NO_2]$ decreases from $2.3 \cdot 10^{-3}$ mol/l to 10^{-5} mol/l.

The accumulation of ARs during the interaction of PI with a mixture of NO_2 and oxygen obeys other kinetic regularities. The presence of O_2 leads to the appearance of a certain induction period in the process. The ESR signal of PI exposed to the NO_2 + O_2 mixture is similar to that shown in **Figure 6.1a**. In the absence of NO_2, the iminoxyl macroradicals formed in both cases are stable for many months in an inert atmosphere and in air. The proposed scheme of possible reactions of the radical formation in PI involves four main stages [7]: (i) generation of alkyl macroradicals by the reaction of NO_2 with elastomers; (ii) synthesis of tertiary macromolecular nitroso compounds; (iii) acceptance of tertiary alkyl or allyl macroradicals; and (iv) decay of ARs.

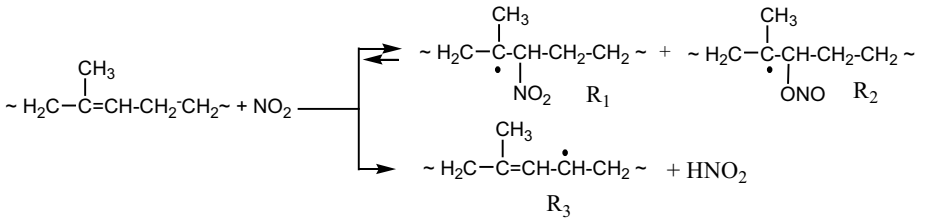
(6.2)

(6.3)

$$R_1(R_2, R_3) + NO_2 \rightarrow \text{products } (RNO_2) \quad (6.8)$$

$$2HNO_2 \rightleftharpoons NO + NO_2 + H_2O \quad (6.9)$$

$$R_1 (R_2, R_3) + NO \rightarrow R_1NO\ (R_2NO, R_3NO) \quad (6.10)$$

$$RNO_2 + R \rightarrow [R\text{-}N(O^{\bullet})\text{-}OR] \rightarrow R\text{-}NO + RO^{\bullet} \quad (6.11)$$

$$RO^{\bullet} \xrightarrow{RH} R\text{-}OH \quad (6.12)$$

$$R\text{-}NO + R_1(R_2, R_3) \rightarrow (R)_2N\text{-}O^{\bullet} \quad (6.13)$$

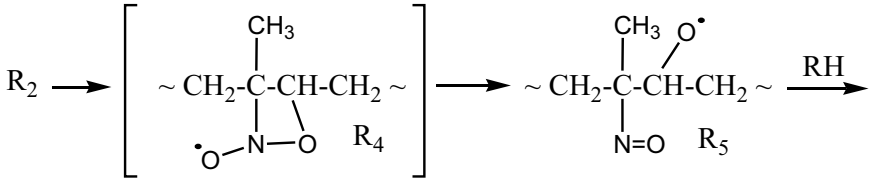

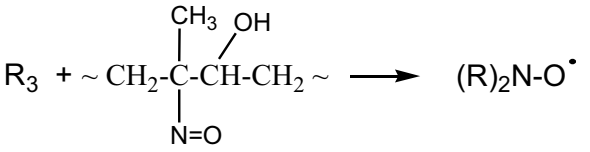
(6.14)

$$(R)_2NO^{\bullet} + N_2O_4 \rightarrow [(R)_2N^{+}{=}O\ NO_3^{-}] + NO \quad (6.15)$$

The synthesis of macromolecular nitroso compounds may take place in at least two ways: as a result of attachment of nitric oxide (NO), rapidly formed by reaction (**Equation 6.9**), to R_1, R_2 or R_3 radicals; and the nitro compounds, according to [5], can be reduced by radicals to nitroso compounds via the stage involving the formation of alkoxyalkylaminoxyl radicals by reaction (**Equation 6.11**). As in the case of PMMA with double C–C bonds, the nitrate group of radical R_2 may convert into a tertiary nitroso compound and alkoxy radical via an intermediate stage involving formation of a four-membered alkoxyalkylaminoxyl radical R_4. Reaction of the resulting radical R_5 with an adjacent macromolecule leads eventually to the formation of a tertiary nitroso compound and a tertiary allyl radical R_3. Interaction of the latter two compounds leads to the formation of ARs by reaction (**Equation 6.14**). The mixture of NO_2 + O_2 with a large excess of O_2 produces intense oxidation of the primary alkyl and allyl macroradicals to peroxide, whereas the NO formed also oxidised to higher nitrogen oxides. Under these conditions, reaction (**Equation 6.14**) is strongly inhibited, and the considerable induction period corresponding to attaining the stationary concentrations of the nitroso compounds is observed.

The study of ESR spectra of dilute PI solutions, nitrated for various times, shows that the spectrum represents a superposition of the spectra of ARs corresponding to their fast and slow rotation [7]. This is related to a significant cross-linking of the elastomer at large exposure durations ($t >> t_{max}$). For $t < t_{max}$, the ESR spectrum exhibits only the signal of ARs corresponding to fast rotations. For this reason, the molecular dynamics has been studied using only the samples exposed to NO_2 during a time period lower than or equal to the time of the maximum amount of aminoxyl macroradicals. According to the above scheme, the formation of macromolecular nitroso compounds may lead to cyclisation or to the cross-linking of macromolecules, depending on whether the nitroso compounds and the accepted radical occur at the same or at different macromolecules. Thus, the question arises whether the macromolecules, spin-labelled by the considered method, can be used for investigation of the rotational dynamics in solution and in the block at various temperatures. The correlation times τ_c for the rotational diffusion of macromolecules, estimated for nitrated PI at NO_2 are $7 \cdot 10^{-4}$ mol/l, with the other published data obtained for PI by the spin label and spin probe techniques. The correlation times for a 1% toluene solution of PI were calculated using the simplest model of isotropic rotation [9]:

$$\tau_c = 6.5 \cdot 10^{-10} \Delta H_0 [(I_0 / I_{-1})^{1/2} - (I_0 / I_{+1})^{-1/2}] \qquad (6.16)$$

where ΔH_0 is the distance between the extreme points for the central component of the spectrum, and $I(0,\pm)$ are the intensities of components in the weak (+), medium (0), and strong (–) magnetic field. The calculated correlation time τ_c = $1.3 \cdot 10^{-10}$ s approximately coincides with that obtained for a 0.5% toluene solution of PI with the spin label attached to the macromolecule as a side group.

For the analysis of the correlation time temperature dependence, the equation (**Equation 6.16**) was used in the region of fast rotation of ARs. In the region of slow rotations, τ_c values were estimated using the *S* parameter [10]:

$$\tau_c = a(1-S)^b(32/A_{zz}) \tag{6.17}$$

where $S = 2A'_{zz}/2A_{zz}$; $2A_{zz}$ and $2A'_{zz}$ are the distances between the outer extreme of the ESR spectrum for the maximum ($\tau_c >> 10^{-7}$ s at –196 °C) and experimental ($T = T_{exp}$) correlation times. The parameters *a* and *b* depend on the mobility model selected and the contribution of non-resolved hyperfine coupling to the line width. Estimation of the τ_c at 20 °C obtained within the framework of the models of Brownian diffusion, free diffusion, and free diffusion by large angles gives $\tau_c = 1.38 \times 10^{-4}$, 1.2×10^{-8} and 1.07×10^{-8} s, respectively. The temperature dependence of the rotational correlation time is described by the equation [10]: $\tau_c = \tau_0 \exp(E/RT)$. **Figure 6.2** shows the plot of $\log\tau_c$ *versus* 1/*T*.

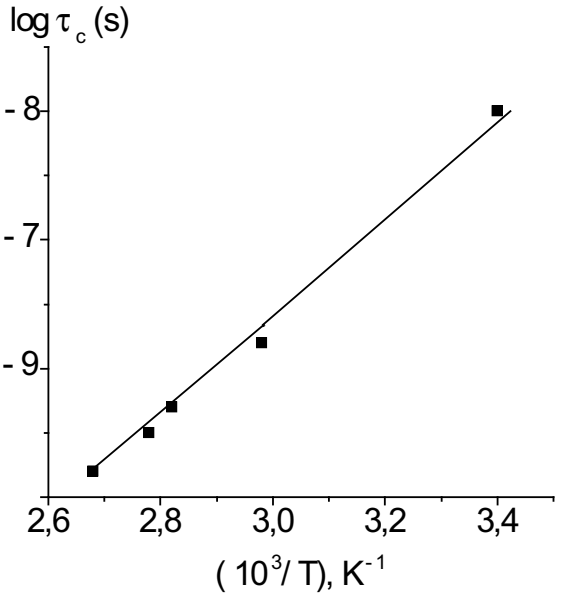

Figure 6.2 Temperature dependence of the correlation time of rotational diffusion of PI macromolecules measured with the aid of aminoxyl radicals synthesised by the reaction with NO_2

As is seen, the τ_c values are well described by the above function with the parameters E = 34.7 kJ·mol^{-1} and log τ_c = –14.2. It was assumed that the aminoxyl fragment participates in a sufficiently rapid cooperative motion involving the aminoxyl group and several carbon atoms of the main chain linked to this group. This additional mobility produces additional averaging of A and g-tensors to virtually an isotropic level. For this reason, the correlation times estimated in the considered system are close to the τ_c values for the rotation of spin probes determined by the motion of molecular segments.

6.2 ESR Imaging in Studies of the Spatial Distribution of the Reaction Front of NO_2 in Polymers

The interaction of NO_2 with solid polymers involves the diffusion of molecules from the gas phase and their reactions in the bulk of the polymer. These reactions are, and are accompanied by, structural changes of a matrix, so their quantitative kinetic analysis is complicated. For this reason, the method based on the determination of one (but informative) characteristic of the process is of interest. The structure of the reaction front may serve as such a characteristic. The method of ESR imaging has been developed for determining the spatial distribution of paramagnetic species [11–13]. In this method, tomograms representing ESR spectra in non-uniform magnetic fields are recorded at the field constant gradient. The spatial distribution of aminoxyl macroradicals has been exhibited in the reaction of NO_2 with the double bonds of PI [14]. It characterises the structure of the reaction front during nitration of cylinder samples (d = 0.4 cm) of the polymer in the initial and deep stages of the process.

The absorption of NO_2 proceeds at least during 50 hours according to the equation:

$$\frac{\Delta[NO_2]_t}{[NO_2]_t} = k_{ef} t \qquad (6.18)$$

The spatial distribution of ARs of the type $(R)_2NO^{\bullet}$ in the form of lines is shown in **Figure 6.3**. The level values are given in arbitrary units with interval ΔI = 0.018 relative to the maximum intensity I_{max} = 0.1145.

As seen from **Figure 6.3**, the spatial distribution of radicals with the maximum local concentration is attained in a superficial layer. The width of the distribution varies from 20% to 30% for 740 hours. The concentration of radicals decreases towards a centre of the sample. The size of layers containing ARs is about 1 mm, and radicals are absent in the centre of samples. The width of the reaction front does not depend on the diameter of samples (d = 2–4 mm) The focal character of the level distribution at

the fixed distance from the sample surface is due to the presence of pores, microcracks as well as an non-homogeneity of the sample density. The very slow subsequent change of the reaction front width is explained by essential structural transformations and decreasing the coefficient of diffusion of NO_2 in the course of nitration. In this process, the protective layer consisting of the less penetrable polymer is formed during a short initial time. The synthesis of aminoxyl macroradicals leads to cross-linking of polymer chains with the formation of a spatial lattice, making molecular mobility difficult. This effect is confirmed by the comparative estimation of rates of the spin probe diffusion from a gas phase to exposed samples of PI. PI samples were exposed to NO_2 during 0 minutes, 40 minutes and 315 hours. The detection time for spin probes was correspondingly 2, 60 and 3000 minutes. Thus, the ESR imaging method allows appreciation of the structural changes in solid polymers under the action of aggressive gases via regularities of diffusion of low-molecular ARs.

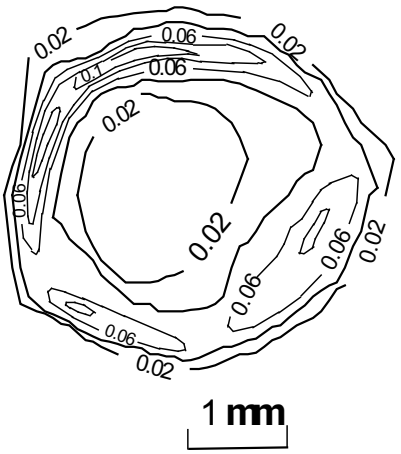

Figure 6.3 The pseudo-three-dimensional spatial distribution of aminoxyl radicals generated by NO_2 (p_{NO_2} = 935 Pa) in PI for 2.5 h

In the presence of O_2, the form of radical distribution and the character of its alteration are, on the whole, similar to those in pure NO_2, but the distribution width is smaller [14]. It is evident that oxygen decreases rates of formation of ARs due to competition between alkyl macroradicals in reactions with O_2 and RNO, and the ratio $W_R(NO_2)/W_R(NO_2+O_2)$ in these conditions amounts to 10^2. The width of the reaction front is determined by a probability of NO_2 addition to C=C double bonds.

The probability is greater, the reaction front is narrower. The consumption of double bonds in the course of the reaction is negligible, and therefore the reaction front does not practically migrate after its formation. Thus, the ESR imaging method allows appreciation of the structural changes in solid polymers under the action of NO_2 via regularities of the spatial distribution of ARs.

6.3 Polymer Degradation in Reactions of Peroxide Macroradicals with NO_2

In air, alkyl or allyl macroradicals produced in reactions with NO_2 can oxidise to give peroxide radicals. The reactions of the latter with NO_2 result in relatively unstable peroxy nitrates similar to low-molecular peroxide radicals [15, 16]:

$$rO_2^{\bullet} + NO_2 \rightarrow rOONO_2 \tag{6.19}$$

Two mechanisms were proposed for the decomposition of peroxyacetyl nitrate [17]:

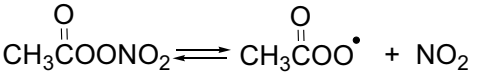

(6.20)

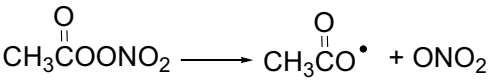

(6.21)

The reaction of perfluoroperoxide macroradicals also yields peroxy nitrate. In this case, the decomposition similar to (**Equation 6.21**) results in destruction of the macromolecule because the resultant alkoxyl radicals in fluorinated polymers cannot enter into the substitution reaction [18]:

$$\sim CF_2–CF(O^{\bullet})–CF_2 \sim \rightarrow \sim CF_2–CFO + {}^{\bullet}CF_2–CF_2 \sim \tag{6.22}$$

To predict the stability of fluorinated polymers in the atmosphere polluted with nitrogen oxides, the ratio of rates of peroxynitrates in polytetrafluoroethylene (PTFE) by two mechanisms has been determined [19]. Chain peroxide radicals $R_cO_2^{\bullet}$ were obtained by photolysis of PTFE powder in a vacuum with the subsequent oxidation of fluoroalkyl macroradicals. The end peroxide radicals $R_eO_2^{\bullet}$ were generated by photolysis of the $R_cO_2^{\bullet}$ containing PTFE in the air. The exposure of PTFE samples containing chain or end peroxide macroradicals to NO_2 results in decay of these radicals. The kinetics of the decay of peroxide radicals of both types is practically identical, and is likely to be determined by the rate of diffusion of NO_2 into the

polymer. After evacuation of the samples, the accumulation of radicals resulting from the decomposition of the products of the reaction between peroxide radicals and NO_2 was observed by ESR at room temperature. The ability of these products to decompose depends on the type of the initial peroxide radicals.

The samples initially containing chain peroxide radicals partially regenerate $R_cO_2^{\bullet}$. The kinetics of this process are shown in **Figure 6.4**.

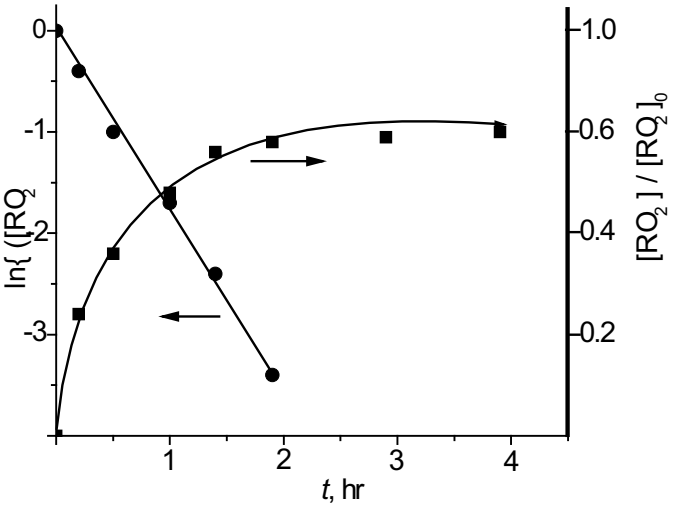

Figure 6.4 The kinetics of $R_cO_2^{\bullet}$ regeneration in PTFE at 40 °C and its semi-logarithmic anamorphosis

However, in PTFE containing end peroxide radicals, no regeneration of these radicals after the removal of NO_2 was observed, though the decomposition temperature was raised to 140 °C. Nevertheless, the reappearance of peroxide radicals in PTFE upon evacuating shows that the product of the $R_cO_2^{\bullet}$ reaction with NO_2 is peroxy nitrate, and fluorinated compounds also exhibit the reversible reaction:

$$R_cO_2NO_2 \underset{k_{-1}}{\overset{k_1}{\rightleftharpoons}} R_cO_2^{\bullet} + NO_2 \qquad (6.23)$$

If the reversible decay is the only process occurring in the polymer, the regeneration of $R_cO_2^{\bullet}$ would be complete and satisfy the relationship $[R_cO_2^{\bullet}]_{lim} = [R_cO_2^{\bullet}]_0$. The

degree of regeneration never reaches 100%. This difference is not due to the decay of peroxide radicals during evacuation at 40 °C, but indicates additional processes other than reversible reactions (**Equation 6.23**) leading to a decreasing content of $[R_cO_2^{\bullet}]_{lim}$. One pathway is the decomposition of peroxy nitrate into alkoxyl radicals and nitrogen trioxide [17]:

$$R_cO_2NO_2 \xrightarrow{k_2} R_2O^{\bullet} + NO_3 \rightarrow \text{products} \tag{6.24}$$

Hydrolysis of peroxy nitrate due to the possible presence of water vapour can also take place:

$$R_cO_2NO_2 + H_2O \rightarrow R_cO_2H + HNO_3 \tag{6.25}$$

Peroxide radicals can react with nitric oxide present in the initial gas mixture or formed in the given system [17]:

$$R_cO_2NO_2 + NO \xrightarrow{k_3} R_cO^{\bullet} + NO_2 \rightarrow \text{products} \tag{6.26}$$

The conversion of peroxy nitrate can also occur upon storage of the sample in an atmosphere containing nitrogen oxides by the formal scheme:

$$R_cO_2NO_2 + X_i \xrightarrow{k_i} \text{products} \tag{6.27}$$

where X_i is the component of this gas mixture. The kinetic analysis gives the following equation for the decay of peroxy nitrate in equilibrium conditions [19]:

$$-\frac{d[R_cO_2NO_2]}{dt} = K^*[R_cO_2NO_2] \tag{6.28}$$

where the parameter $K^* = k_2 + \sum_i k_i X_i + \frac{k_1}{1 + \frac{k_{-1}[NO_2]}{k_3[NO]}}$. If the concentrations of X_i and NO do not change much during the PTFE exposure to NO_2, then the K^* value is constant and the decay of peroxy nitrate is described by the first-order equation. After the gas-phase removal the concentration of the remaining peroxy nitrate is equal to:

$$[R_cO_2NO_2]_t = [R_cO_2NO_2]_0 \exp(-K^* t) \tag{6.29}$$

When NO_2 enters the reacting system, the initial peroxide radicals quantitatively convert into peroxy nitrate and $[R_cO_2NO_2]_0 = [R_cO_2^{\bullet}]_0$. The regeneration process of peroxide radicals in vacuum should follow the equation:

$$\frac{d[R_cO_2]}{dt} = k_1[R_cO_2NO_2]_t \cdot e^{-(k_1+k_2)t} \tag{6.30}$$

$$[R_cO_2^{\bullet}] = \frac{k_1}{k_1+k_2}[R_cO_2^{\bullet}]_0 \cdot e^{-K^*t} \cdot [1-e^{-(k_1+k_2)t}] \tag{6.31}$$

The upper limit of k_2 value reflecting the probability of possible degradation of macromolecules at 40 °C was found to be $\leq 7.6 \cdot 10^{-5}$ s^{-1} and $4.0 \cdot 10^{-4} \leq k_1 \leq 4.8 \cdot 10^{-4}$ s^{-1}, i.e., $k_2 \leq 0.2k_1$.

The difference in thermal behaviour of the products of the interaction of chain and end peroxide radicals with NO_2 is conditional upon conversions of $R_eO_2^{\bullet}$ R into end stable products, for example, via a six-membered transition state:

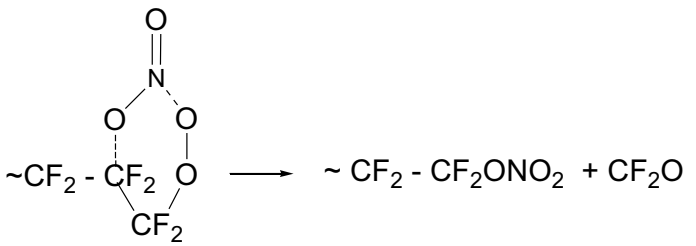

(6.32)

An identical process is proposed for conversion of peroxyacetyl nitrate [20]. This reaction requires high mobility of the molecular fragments to build up six-membered complexes. In contrast to $R_eO_2^{\bullet}$, the chain peroxide radicals in a rigid matrix of PTFE form such transition states with difficulty [21].

Thus, if a polymer containing stable peroxide radicals is exposed to NO_2 for a long time, the second decomposition pathway of peroxynitrate can lead to a high degree of degradation of the polymer due to reaction (**Equation 6.22**) even though the corresponding rate constant is five or more times smaller than that for the decomposition reaction (**Equation 6.23**).

References

1. T.V. Pokholok, G.B. Pariiskii and G. Bragina, *Vysokomolekulyarnye Soedineniya Seria A*, 1989, **31**, 2048.

2. G.B. Pariiskii, I.S. Gaponova and E.Ya. Davydov, *Russian Chemical Reviews*, 2000, **69**, 985.

3. T.S. Popravko, Yu.A. Mikheev and D.Ya. Toptygin, *Doklady Akademii Nauk SSSR*, 1977, **232**, 856.

4. E.Ya. Davydov, I.S. Gaponova and G.B. Pariiskii, *Journal of the Chemical Society - Perkin Transactions 2*, 2002, **7**, 1359.

5. R.A. Jackson and W.A. Waters, *Journal of the Chemical Society*, 1960, 1653.

6. G.R. Chalfont, D.H. Hey, K.S.Y. Liang and M.J. Perkins, *Journal of the Chemical Society B*: *Physical Organic Articles*, 1971, 233.

7. T.V. Pokholok and G.B. Pariiskii, Polymer Science A, 1997, **39**, 765.

8. M. Gyór, A. Rockenbauer and F. Tüdos, *Tetrahedron Letters*, 1986, **27**, 4795.

9. A.L. Buchachenko and A.M. Vasserman, *Stable Radicals*, Khimiya Publishers, Moscow, Russia, 1973.

10. A.M. Vasserman and A.L. Kovarskii, *Spin Labels and Probes in Physical Chemistry of Polymers*, Nauka Publishers, Moscow, Russia, 1986.

11. O.E. Yakimchenko, A.I. Smirnov and Ya.S. Lebedev, *Applied Magnetic Resonance*, 1990, **1**, 1.

12. A.I. Smirnov, O.E. Yakimchenko, H.A. Golovina, Sh.Kh. Bekova and Ya.S. Lebedev, *Journal of Magnetic Resonance*, 1991, **91**, 386.

13. A.I. Smirnov, O.G. Poluektov and Ya.S. Lebedev, *Journal of Magnetic Resonance*, 1992, **97**, 1.

14. E.N. Degtyarev, T.V. Pokholok, G.B. Pariiskii and O.E. Yakimchenko, *Zhurnal Fizicheskoi Khimii*, 1994, **68**, 461.

15. C.W. Spicer, A. Villa, H.A. Wiebe and J. Heicklen, *Journal of the American Chemical Society*, 1973, **95**, 1, 13.

16. F. Zabel, A. Reimer, K.H. Becker and E.H. Fink, *Journal of Physical Chemistry*, 1989, **93**, 14, 5500.

17. D.G. Hendry and R.A. Kenley, *Journal of the American Chemical Society*, 1977, **99**, 9, 3198.

18. V.P. Mel'nikov, L.S. Gulyaeva and A.M. Markevich, *Zhurnal Fizicheskoi Khimii*, 1983, **2,** 637.

19. I.S. Gaponova and G.B. Pariiskii, *Journal of Chemical and Biochemical Kinetics*, 1991, **1**, 349.

20. G.I. Senum, R. Fajer and J.S. Gaffney, *Journal of Physical Chemistry*, 1986, **90**, 1, 152.

21. D. Suryanarayana, L. Kevan and S. Schlick, *Journal of the American Chemical Society*, 1982, **104,** 3, 668.

7 Role of Nitrogen Dioxide Dimers in Reactions with Polymers

Because nitrogen dioxide (NO_2) is a free radical of moderate reactivity, it can initiate free-radical reactions by abstracting hydrogen atoms only from the least strong C–H bonds or by attaching to double C–C bonds [1–4]. Nevertheless, effective formation of stable radicals is observed also in polymers not containing labile hydrogen atoms or double bonds. Aromatic polyamidoimides [5], Nylon, polyvinylpyrrolidone [6], aromatic polyamides [7] and polyimides [8] therefore exhibit high activity in respect to NO_2. These facts allow consideration of other probable mechanisms of radical initiation. The major stable radical products of the interaction of NO_2 with aromatic polyamides and polyvinilpyrrolidone are iminoxyl and acylalkylaminoxyl radicals that are produced from oximes and acylnitroso compounds [6, 7]. The occurrence of these precursors of stable radicals in turn is associated with the presence of nitric oxide. In this connection, it is necessary to suppose a participation of NO_2 dimeric forms in radical initiation.

7.1 Formation of Nitrosonium Complexes from Organic Compounds and NO_2

Transitory formation of nitrosonium nitrate, $NO^+NO_3^-$, occurs in reactions involving dinitrogen tetroxide [9]. There is the evidence for the isomerisation of the planar dimer and its subsequent ionisation

$$O_2NNO_2 \rightleftharpoons ONONO_2 \rightleftharpoons NO^+ + NO_3^- \tag{7.1}$$

from the observation that the Raman spectrum of a solution of nitrogen tetroxide (N_2O_4) in nitric acid exhibits no lines at the known frequencies of planar dimers [10]. A strong Raman line at 2240 cm^{-1}, which is within the range of nitrosonium-ion stretching frequencies, suggests heterolytic dissociation of N_2O_4 in a solvent of high dielectric constant. Infrared (IR) spectra of compounds containing nitrosonium ion have absorption bands between 2150 cm^{-1} and 2400 cm^{-1} [11].

The reactions of NO_2 dimers in the form of nitrosonium nitrate with amides provide a general method for the preparation of nitroso amides [12]. The reaction is carried

out rapidly for 10 minutes at 0 °C with yields of 77–95%:

$$RNH{-}COR' + ONONO_2 \rightarrow RN(NO){-}COR' + HNO_3 \tag{7.2}$$

Aromatic hydrocarbons form with NO_2 red-coloured metastable complexes in dichloromethane at room temperature [13]. The distinctive colouration observed immediately upon the mixing of NO_2 (dinitrogen tetroxide) with methylsubsituted benzenes was strongly dependent on the number of methyl groups. Thus, intense red-brown colours could be produced from 0.1 M hexamethylbenzene, whereas comparable colourations were obtained with the slower reacting mesitylene only at significantly higher (1 M) concentrations. Spectral ultraviolet–visible (UV–Vis) examination of the coloured solutions showed new absorption bands assigned to the charge-transfer intermolecular electron donor–acceptor complexes of the nitrosinium nitrate with corresponding aromatic donors. The batochromic shifts, together with the strongly varying intensities of the charge-transfer bands, relate to the strong dependence for the complexation constant on the aromatic donor strength, as evaluated by the ionisation potential. For example, for hexaethylbenzene with IP = 7.71 eV and hexamethylbenzene with IP = 7.85 eV, charge-transfer bands are correspondingly observed at 495 nm and 516 nm. The charge-transfer colouration is readily assigned to ArH/NO^+ interactions in the donor–acceptor complexes resulting from the disproportionation of NO_2 [14]:

$$2\,NO_2 + ArH \rightleftharpoons [ArH, NO^+]\,NO_3^- \tag{7.3}$$

Ionic disproportionation of NO_2 can be promoted in non-polar media by the addition of Bronsted acids and Lewis acids [10]. The photochemical activation of the nitrosonium donor–acceptor complex via irradiation of the charge-transfer absorption band produces the aromatic radical cation. The most direct pathway to aromatic nitration proceeds via homolytic coupling of the aromatic radical cation with NO_2 [16] because the intermediate subsequently undergoes very rapid deprotonation:

$$[ArH, NO^+]\,NO_3^- \rightleftharpoons [\overset{\bullet+}{A}rH, NO]\,NO_3^- \tag{7.4}$$

$$\overset{\bullet+}{A}rH + NO_2 \longrightarrow Ar\overset{+}{\underset{NO_2}{\overset{H}{<}}} \longrightarrow ArNO_2 + H^+ \tag{7.5}$$

The photochemical and thermal nitrations of aromatic hydrocarbons with NO_2 dimers are carried out under essentially the same experimental conditions. The charge-transfer activation by light is merely effected at lower temperatures, where competition from the thermal process is unimportant.

Treatment of the hydroquinone ethers with NO_2 in dichloromethane at room temperature readily leads to the corresponding 1,4-quinones and alkylnitrite [17]. The trivial work-up procedure for the ready isolation of pure quinones in essentially quantitative yields, establish this to be the method of choice for the oxidative dealkylation of fully substituted hydroquinone ethers. The formation of radical cations of hydroquinone ethers ($R_2Q^{\bullet+}$) as intermediates provides the key to understand how the alkoxy bonds are cleaved in these compounds. The activation for this oxidative process depends on the ability of the aromatic ether to undergo one-electron transfer to the nitrosonium ion [15]:

$$R_2Q + NO^+NO_3^- \rightarrow R_2Q^{\bullet+}\ NO_3^- + NO \qquad (7.6)$$

The electron-donating properties of the hydroquinone ethers decrease from (E_{ox} = 1.12 V) to (E_{ox} = 1.57 V).

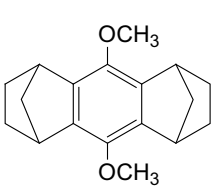

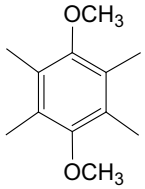

Based on the reduction potential for nitrosonium of E_{ox} = 1.50 V, the free energy changes for electron transfer by (**Equation 7.6**) are sufficient to promote oxidative dealkylation with

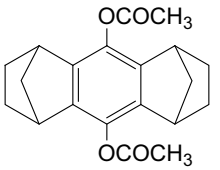

NO_2. It is noteworthy that the acetate analogue with the more positive oxidation potential of E_{ox} = 1.86 V is not oxidised. Likewise, four chlorine substituents reduce the donor

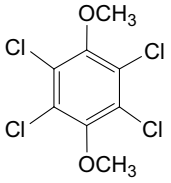

strength of the hydrochloranil ether (E_{ox} > 2 V) sufficiently to inhibit its oxidative

dealkylation with NO_2. The series of one-electron transformations are represented in scheme (**Equation 7.7**) [17]:

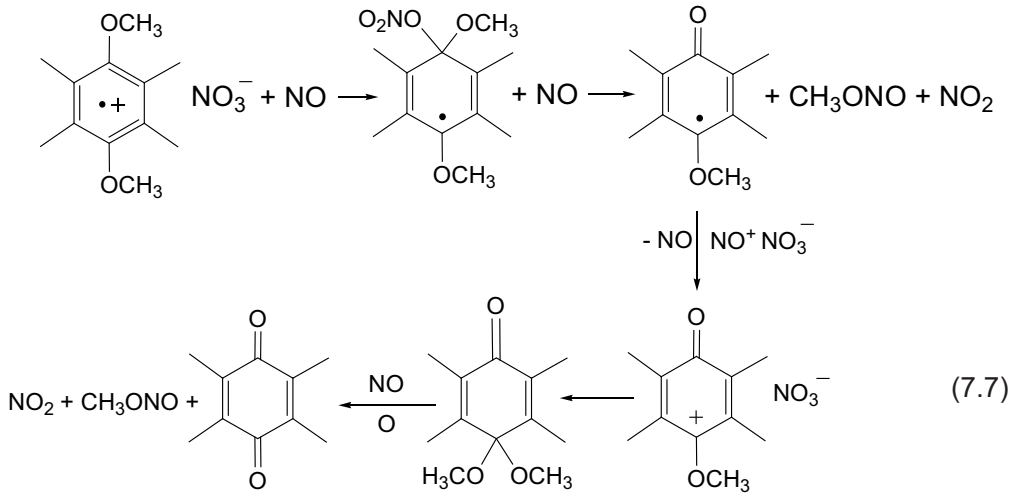

(7.7)

The oxidative conversions of quinone dioximes into dinitroso benzenes can be carried out by interaction with nitrosonium nitrate [18]:

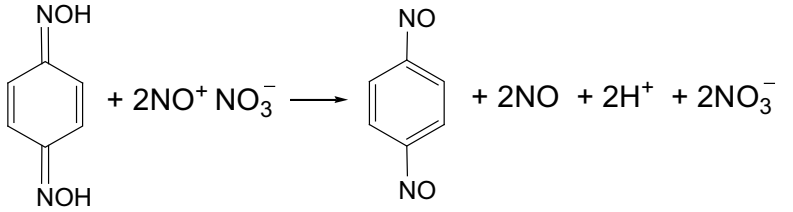

(7.8)

A mixture of nitric acid and nitric oxide (NO) is metastable, undergoing rapid transformation to dinitrogen trioxide and dinitrogen tetroxide with the liberation of water:

$$HNO_3 + 2NO \xrightarrow[-H_2O]{} N_2O_3 + N_2O_4 \qquad (7.9)$$

Because dinitrogen trioxide is in reversible equilibrium with NO and NO_2, it is readily converted into N_2O_4 (NO_2) in the presence of oxygen. Reactions (**Equation 7.8**) and (**Equation 7.9**) therefore represent a complete catalytic cycle of the dioxime autoxidation by NO_2 to dinitroso benzenes. This catalytic cycle is reminiscent of the mechanism presented for the autoxidation of hydroquinones to quinones [19]. Formally, the oxidation of hydroquinones (H_2Q) to quinones (Q) involves the removal of two electrons and two protons:

$$H_2Q + 2NO^+ \rightarrow Q + 2NO + 2H^+ \qquad (7.10)$$

The reaction (**Equation 7.10**), together with subsequent reoxidation of nitric oxide with oxygen, constitutes the reduction–oxidation cycle for the catalytic autoxidation with NO_2. On the basis of the understanding of the interaction of nitrosonium with aromatic donors [15], hydroquinones are expected to strongly shift the equilibrium (**Equation 7.3**) to favour the nitrosonium complex in conformity with enhanced donor properties of the aromatic substrates. Accordingly, the oxidation of hydroquinone with NO_2 proceeds via the nitrosonium nitrate ion pair. The overall two-electron oxidation of hydroquinone to quinone by 2 equivalent NO^+ probably proceeds via successive one-electron steps. The ^{18}O labelling studies in the process

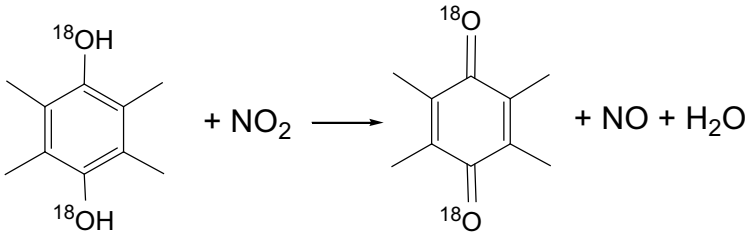

(7.11)

show that it occurs by scission of both oxygen-hydrogen bonds [20]. In the one-electron mechanism, the hydroquinone radical cation ($H_2Q^{\bullet+}$) is the obligatory intermediate:

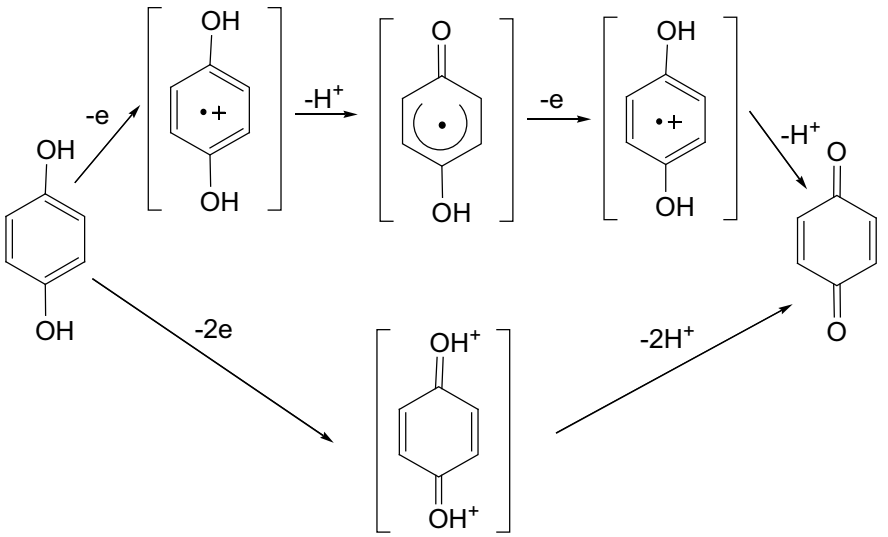

(7.12)

However, the hydroquinone radical cation undergoes rapid deprotonation, and attempts to detect independently radical cations were unsuccessful in these works.

In such processes, the catalytic efficiency depends on effective electron transfer from the hydroquinone to NO^+, and the step of the hydroquinone radical cation rapid proton loss. The driving force for the electron transfer

$$H_2Q + NO^+ \rightarrow H_2Q^{\bullet+} + NO \tag{7.13}$$

was estimated to be $\Delta G \approx -5$ kcal·mol^{-1}, based on $E^0_{ox} = 1.3V$ for hydroquinone and $E^0_{red} = 1.5V$ for nitrosonium in dichloromethane [19]. Such a moderate driving force for electron transfer, coupled with the short lifetime of the $H_2Q^{\bullet+}$ ($\tau < 10^{-10}$ s), is sufficient to promote hydroquinone oxidations with NO^+.

The molecular association of various aromatic hydrocarbons, including sterically hindered donors, with diverse acceptors (in particular nitrosonium ions) is visually apparent in solution by the spontaneous appearance of distinctive colours. Spectral measurements (UV–Vis) represent a sensitive analytical tool for evaluating the steric hindrance of donor–acceptor association [21]. Exposure of nitrosonium tetrafluoroborate $NO^+BF_4^-$ to hexamethylbenzene (HMB) in acetonitrile immediately resulted in an intense red colouration and appearance of a well-resolved charge-transfer absorption band (λ_{CT} = 337 nm) with a characteristic low-energy band extending beyond 600 nm. Although the extinction coefficient of ε_{CT} =3100 M^{-1} cm^{-1} is similar to that evaluated for HMB complexes with π-acceptors, for example, chloranil, the association constant in (**Equation 7.3**) K_{DA} is 31000 M^{-1} is more than four orders of magnitude larger. This is indicative of an exceptionally strong donor–acceptor association of NO^+ with the substrate. More surprising is that the highly hindered tris-annulated donors (cyclooctatriene derivatives) show a high association, with $K_{DA} > 3 \cdot 10^4$ M^{-1}.

The critical role of the nitrosonium complex in thioether oxidations with NO_2 was probed by its selective activation at –78 °C in dichloromethane solution [22]:

$$2NO_2 \rightleftharpoons NO^+NO_3^- \overset{R_2S}{\rightleftharpoons} [R_2S, NO^+] + NO_3^- \tag{7.14}$$

Experimentally, the brightly coloured solutions of thioanisole were held at this low temperature and continuously exposed to light with λ > 410 nm. Under these conditions, the monotonic bleaching of the charge-transfer band and the formation of methyl phenyl sulphoxide were observed (quantum yield φ: = 0.5 ± 0.3):

$$[PhSMe, NO^+]NO_3^- \xrightarrow{h\nu} PhS(O)Me \tag{7.15}$$

Charge-transfer oxidations of a series of dialkyl and mixed alkylaryl sulphides leads to high yields of sulphoxides by the same photochemical procedure. Intermediates formed in the charge-transfer activation of the thioether complexes were probed by time-resolved spectroscopy. The spectra transient with λ_{max} =500 nm in tetrahydrothiophene were attributed to the corresponding radical cations:

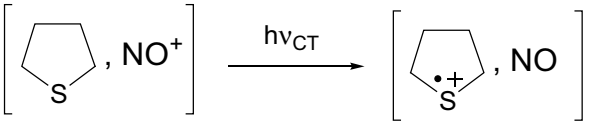

(7.16)

Intermediates in the thermal oxidations of thioethers with NO_2 are generally difficult to detect owing to the limiting reaction rates. The exceptions are oxidations of strong sulphur-containing donors derived from thianthrene. The stoichiometric oxidation of thianthrene in dichloromethane at −78 °C produces a pink-coloured solution (λ_{max} =544 nm) that finally leads to a pale-yellow solution from which thianthrene 5-oxide was isolated in 94% yield. This process involves the intermediate stage of the thianthrene radical cation formation [23]:

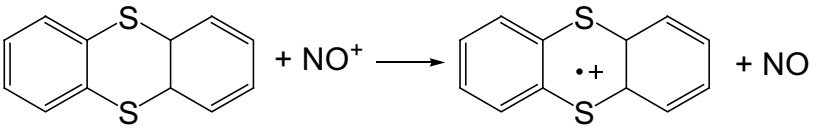

(7.17)

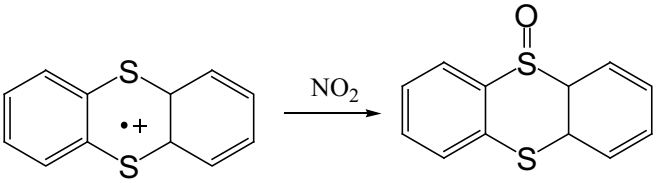

(7.18)

Even in the presence of excess NO_2, there is no evidence for the further oxidation or nitration of thianthrene sulphoxide.

NO_2 used for thioether oxidation to sulphoxides is unique in that it can be employed as a reagent in stoichiometric amounts or as a catalyst for O_2 autoxidation. Oxygen alone cannot oxidise thioethers at ambient temperatures and atmospheric pressures, so NO_2 must be the active agent in the catalytic oxidation. There is strong correlation between the oxidative conversion of thioethers to sulphoxides and the concentration of [R_2S, NO^+] complexes. The enhanced reactivity of an alkyl thioether such as dibutyl sulphide relative to diphenyl sulphide directly parallels the difference in the steady-state concentrations of the corresponding nitrosonium donor–acceptor complexes [22]: [Bu_2S, NO^+], [Ph_2S, NO^+]. The same trend in the structure/reactivity relationship is more clearly shown in the oxidative conversion of the homologous thioethers in

the order *p*-$MeOC_6H_4SMe$ > *p*-MeC_6H_4SMe > PhSEt that parallels the batochromic shifts of the charge-transfer bands of the corresponding nitrosonium complexes. Moreover, additives such as antimony pentachloride (Lewis acid) that effectively enhance the ionic disproportionation of NO_2 into $NO^+NO_3^-$ also greatly promote the oxidative conversion of a given thioether. From these facts one can conclude that the nitrosonium donor–acceptor complexes are the critical intermediates in the oxidative conversion of thioethers with NO_2. Nitrosonium complexes are directly activated by light irradiation of the charge-transfer absorption band to afford high sulphoxide yields at temperatures too low (–78 °C) to effect the thermal oxidation of thioethers. Under these conditions, the radical cation generation of thioethers takes place. Further conversions of the radical cations proceed via ion-pair collapse.

$$R_2S + 2NO_2 \rightleftharpoons [R_2S, NO^+]\, NO_3^- \tag{7.19}$$

$$[R_2S, NO^+]\, NO_3 \overset{h\nu_{CT}}{\rightleftharpoons} [R_2S^{\bullet+}, NO]\, NO_3^- \tag{7.20}$$

$$[R_2S^{\bullet+}, NO_3^-] \longrightarrow R_3SO + NO_2 \tag{7.21}$$

The thermal oxidation of thioethers with NO_2 proceeds via similar intermediates:

$$[R_2S, NO^+]\, NO_3 \rightleftharpoons [R_2S^{\bullet+}, NO] + NO_3^- \tag{7.22}$$

$$R_2S^{\bullet+} + NO_3^- \xrightarrow{\text{fast}} R_2SO + NO_2 \tag{7.23}$$

In a biological context, the high formation constant ($K > 10^4\ M^{-1}$) for the nitrosonium donor–acceptor complex with dialkylsulfides provides a ready mechanism for the biochemical formation of the powerful one-electron oxidant, NO^+, from NO in oxygenated media.

7.2 Direct Experimental Detection of Primary Radical Cations and Products of Their Decomposition in the Reactions of Nitrosyl Nitrate

The ion-radical mechanism postulated for interaction of aromatic compounds with nitrosyl nitrate [13–19, 21, 22] is mainly based on an analysis of indirect

spectrophotometric data and final products. The radical cation revealed by electron spin resonance (ESR) could provide direct experimental evidence that initiation in these processes proceeds through the primary reaction:

$$[RH, NO^+ NO_3^-] \rightleftharpoons [\overset{\bullet +}{R}H, NO, NO_3^-] \tag{7.24}$$

where R can be low- and high-molecular radicals. However, because of high reactivity [24], the primary radical cations cannot be always registered by this direct method.

The examination of the occurrence of radical cations via their decomposition accompanied by proton detachment has been undertaken with the use of interactions of NO_2 with poly-(2-vinylpyridine) (PVPR) [25]. Pyridine can accept protons to yield pyridinium cations. Hence, if protons are formed in PVPR during decomposition of radical cations, they can be detected easily from IR spectra typical of pyridiniun cations. Pyridine itself can be nitrated only under quite severe conditions using a NO_2 – ozone mixture (**Chapter 5**). However, NO_2 efficiently interacts with PVPR films, as seen from **Figure 7.1**.

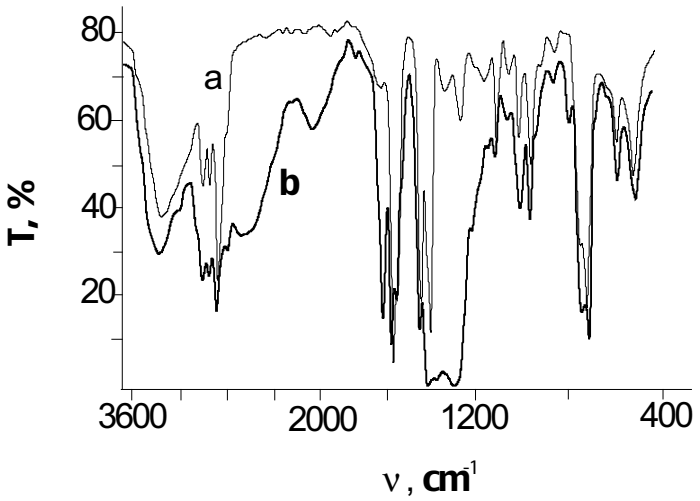

Figure 7.1 IR spectra of the original PVPR film (a) and (b) the same film after exposure for 90 minutes to NO_2; $[NO_2] = 5 \times 10^{-4}$ mol/l

After exposure at 25 °C, two intense bands were observed at 2400–2600 cm^{-1} and 2200 cm^{-1} corresponding to the stretching vibrations of NH^+ pyridinium cations [26]. The bands at 1600–1430 cm^{-1}, attributed to the stretching vibrations of C=C and C=N bonds of pyridine rings, are present in the initial spectrum of PVPR [27]. During exposure to NO_2, a band at 1650 cm^{-1} corresponding to the stretching vibrations of $C=N^+$ bonds arises in the spectrum simultaneously with the bands at 2400-2600 and 2200 cm^{-1}. Moreover, an intense absorption typical of nitrate ions NO_3^- is observed at 1300–1400 cm^{-1} [26]. Hence, alkyl substitutients that build up the backbone of the macromolecules provide a higher reactivity of PVPR as compared with pyridine. The presence of these substituents substantially decreases the ionisation potential of pyridine rings and thus enhances the formation of intermediate radical cations through reaction (**Equation 7.24**). These radical cations are precursors of the molecular and radical products of PVPR conversions:

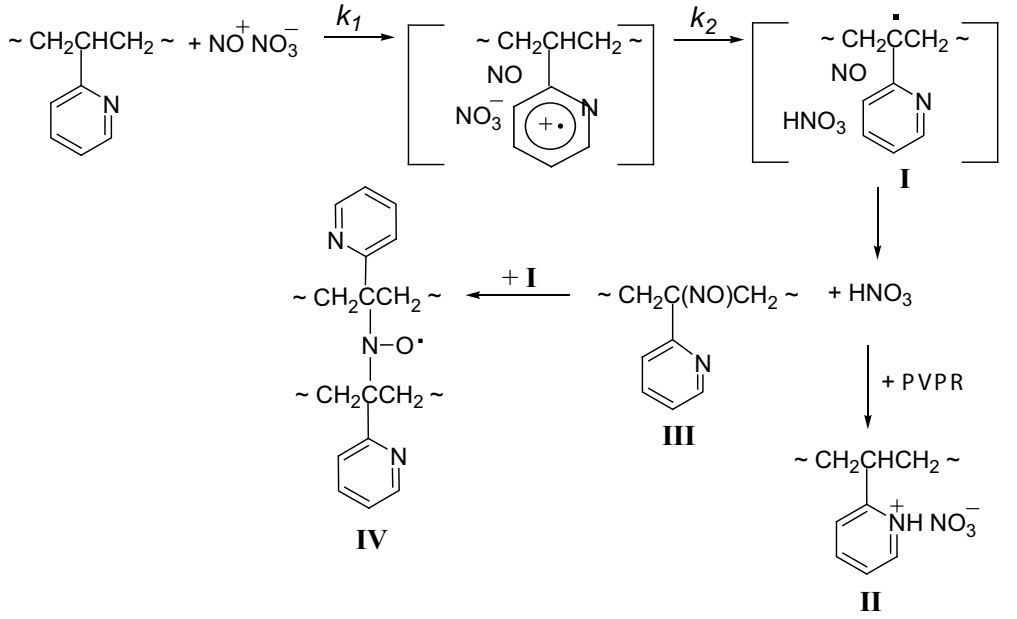

(7.25)

The formation of nitroso compounds **III** is confirmed by the ESR spectrum obtained during exposure of PVPR to NO_2 (**Figure 7.2**).

The spectrum is an anisotropic triplet with parameters typical of aminoxyl radicals (ARs) with hindered rotations in a solid polymer matrix: $A_{\mathbf{I}}^{\mathrm{N}} = 3.1$ mT and $g_{\mathbf{I}} = 2.0028$ [2]. The formation of radicals **IV** directly results from the

acceptance of one part of alkyl macroradicals **I,** leaving the reaction cage by nitroso compounds **III.** ARs generated in reactions (**Equation 7.25**) lead to the cross-linking of macromolecules, and PVPR films partially lose their solubility in chloroform after treatment with NO_2 [25].

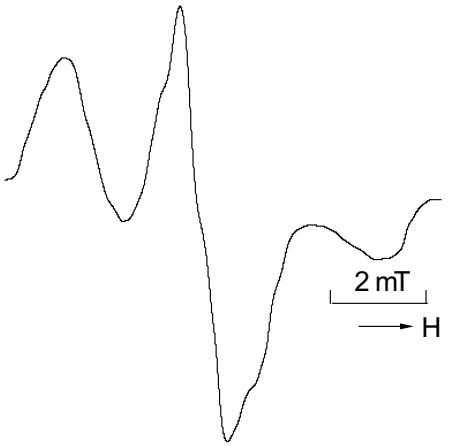

Figure 7.2 ESR spectrum of PVPR after exposure to NO_2

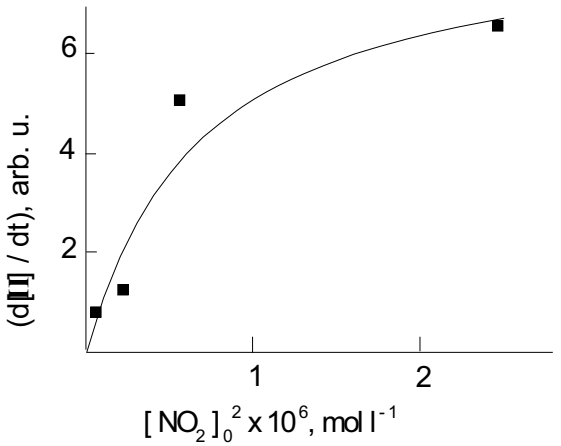

Figure 7.3 Dependence of the initial rates of the accumulation of compound **II** on NO_2 concentrations

The key role of nitrosyl nitrate in the formation of **II** via the ion-radical mechanism is confirmed by kinetic measurements done at different NO_2 concentrations in the gas phase. The initial rates of accumulation of this compound plotted against the square of the initial concentrations of NO_2 are shown in **Figure 7.3**.

As follows from **Figure 7.3**, the experimental rates (dots) are proportional to $[NO_2]_0^2$ at relatively low concentrations of NO_2 (< 7 x 10^{-4} mol/l). As the concentration of NO_2 is increased, the plot drastically deviates from linearity because of an increase in the probability of intermediate radical cation decay in side reactions of oxidation with nitrosonium cations through the following reaction:

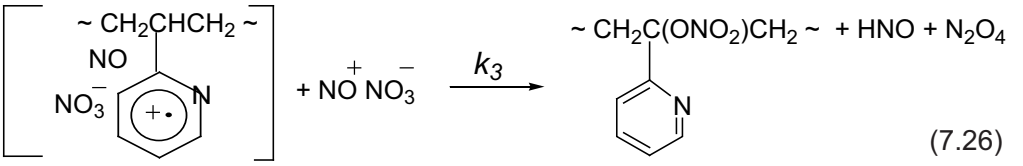

(7.26)

The solid line in **Figure 7.3** represents the calculated function for the initial rates of compound **II** accumulation according to scheme 7.25 taking into account reaction 7.26 and stationary concentrations of HNO_3 and radical cations:

$$\left(\frac{d[\mathrm{II}]}{\mathrm{dt}}\right)_0 = \frac{k_1 k_2 [\mathrm{NO_2}]_0^2}{k_2 + k_3 [\mathrm{NO_2}]_0^2} \qquad (7.27)$$

where k_1, k_2, and k_3 are empirical constants. The optimal values of these constants are selected using the least-squares method for the most adequate description of the experimental data. At low concentrations of NO_2, ($[NO_2] << \sqrt{k_3 / k_2}$), (**Equation 7.27**) is approximated by a linear function, as follows from the initial part of the curve in **Figure 7.3**. Hence, the kinetics demonstrate that the radical conversions of PVPR are initiated by NO_2 dimers.

Pyridine, which does not react with NO_2, has the role of a trap for protons resulting from ion-radical reactions induced by $NO^+NO_3^-$ ion pairs. The reaction products of NO_2 and 1:1 pyridine –*N*-methylpyrrolidone liquid mixture contain pyridinium cations (the same IR bands as in **Figure 7.1**) [25]. The scheme of reactions proceeding in this system includes the following consecutive stages:

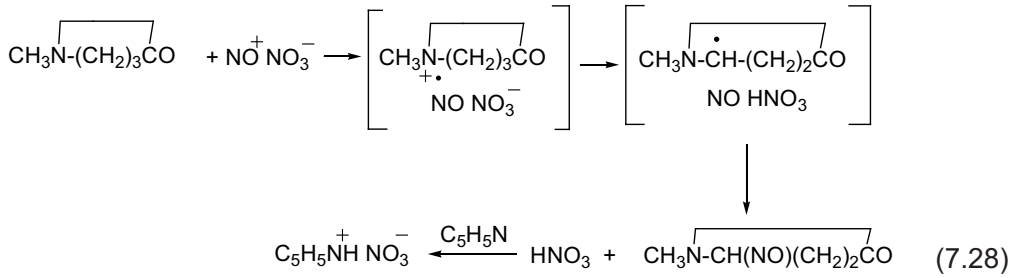

(7.28)

Thus, in liquid and solid phases, electron transfer to nitrosonium cations gives rise to the formation of cation-radicals.

The planar dimers of NO_2, $O_2N–NO_2$, are therefore also capable of initiating free-radical reactions. This form is active in compounds containing conjugated double bonds, for example, in *p*-benzoquinone (**Chapter 5**). However, protons are not generated in this system via the ion-radical mechanism; pyridinium cations are not observed in the IR spectra after pyridine is added to benzoquinone preliminarily treated with NO_2. Therefore, $NO^+NO_3^-$ ion pairs exhibit a noticeable reactivity in compounds whose ionising potential assumes electron transfer from donor groups of molecules to NO^+ [13]. Seemingly, this is the reason why NO_2 efficiently interacts with PVPR, whereas pyridine is inert with respect to this compound. From this point of view, initiation involving $NO^+NO_3^-$ ion pairs in benzoquinone is probably less energetically advantageous than dissociation of $O_2N–NO_2$ affording NO_2 radicals. The reasons underlying the ion-radical mechanism for conversions of polymers under the action of NO_2 were revealed from comparative *ab-initio* calculations for energies of model reactions representing separate stages in Scheme (**Equation 7.25**). 2-Isopropylpyridine and pyridine were selected as models [25]. The calculations were done using the GAMESS software package (Gordon Research Group of Iowa State University) under the spin-restricted Hartree–Fock approximation for closed and open shells with 6-31G* basis set [28]. By analogy with Scheme (**Equation 7.25**), model processes are presented as follows:

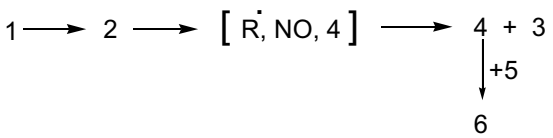

(7.29)

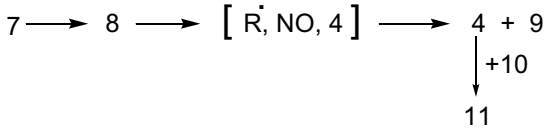

(7.30)

In reactions (**Equation 7.29**) and (**Equation 7.30**), R• refers to radicals resulting from the deprotonation of corresponding radical cations of 2-isopropylpyridine and pyridine. As follows from the energy values listed in **Table 7.1**, the nitrosation of pyridines must be, on the whole, an exothermic process (1 → 4 + 3 and 7 → 4 +9). However, this consecutive process comprises two endothermic stages related to electron transfer and formation of radical cations (1 → 2 and 7 → 8), which represent activated states of reaction systems characterised by maximum energies. The calculations suggest that the energy required to reach this stage for pyridine is ~1.7-times higher than that for 2-isopropylpyridine. At the following stage of

deprotonation and the formation of nitroso compounds, a large amount of energy is released. However, a large difference between energy consumptions at the initial stage of the electron transfer makes the nitrosation of pyridine a low-efficiency process as compared with that of 2-isopropylpyridine.

Hence, reactions considered for PVPR illustrate the mechanism connected with the conversions of primary radical cations generated by nitrosyl nitrate. Nevertheless, the direct detection of radical cations by ESR fails in this system apparently because of fast detachment of protons. For confirmation of the ion-radical initiation concept under the action of NO_2, triphenylamine (TPA) is a suitable model compound. TPA does not contain chemical bonds capable of reacting with monoradicals of NO_2. The formation of radical cations in TPA has been revealed in reactions with some Lewis acids as salts $(Ph)_3\overset{+\bullet}{N}$ A where A = $SbCl_6^-$, ClO_4^-, FB_4^- [29-32]. On exposure of TPA crystals at room temperature during 1 minute, the very narrow single line of $\Delta H_{1/2}$ = 0.25 mT and g = 2.0024±0.0005 is observed in the ESR spectrum (**Figure 7.4a**).

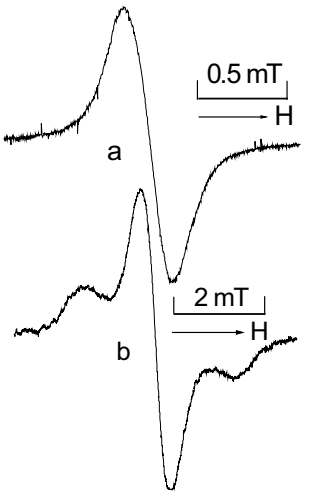

Figure 7.4 ESR spectra of TPA exposed to NO_2 during 1 minute (a) and 3 days (b) at 22 °C

Taking into consideration that radical cations of TPA formed by the reaction:

$$(Ph)_3N + NO\ {}^+ONO_2^- \rightarrow (Ph)_3\overset{+\bullet}{\underset{V}{N}} + NO + ONO_2^- \qquad (7.31)$$

should have, in the isolated state, a triplet ESR spectrum due to hyperfine interaction (HFI) of unpaired electrons with nitrogen nuclei, the narrow line observed can be caused by an electron exchange between radical cations **V** and neutral molecules of TPA owing to the overlap of molecular orbitals [33]. In this case, electron spins are exchanged so rapidly that the time-averaged value of a magnetic field caused by HFI is close to zero. At room temperature in an atmosphere of NO_2, this single line quickly disappears (for 6-7 minutes it decreases twice). On further exposure during 3 days, the ESR spectrum is transformed to an anisotropic triplet signal (**Figure 7.4b**) with the distance between components of 1.86 mT and the same *g*-factor as for the singlet line. After exposure to NO_2 during 1 minute to pump out NO_2, the disappearance of the signal also takes place. However, in contrast with the process in an NO_2 atmosphere, the spectrum shown in **Figure 1b** in this case does not occur. The kinetics of the decay of paramagnetic species in vacuum obeys the second-order equation. It means that the main path of decay of radical cations **V** is their recombination [34]:

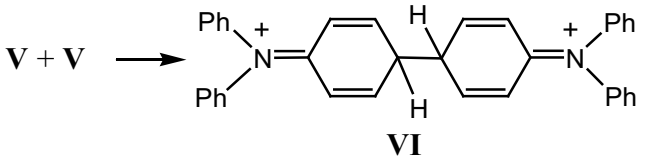

VI (7.32)

As a result of reaction (**Equation 7.32**), the formation of tetraphenylbenzidine [32] along with nitric acid occurs through the deprotonation of the dications **VI**:

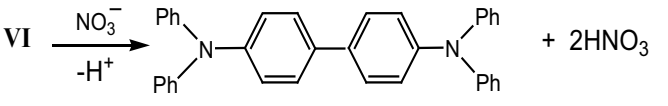

VII (7.33)

Radical species with the spectrum shown in **Figure 7.4b** are a product of conversions of primary radical cations **V** under the action of NO_2, as a result of which, *p*-nitroderivatives of radical cations are sequentially formed:

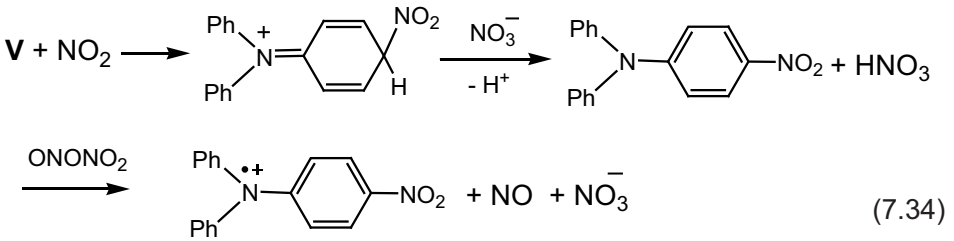

(7.34)

The derivatives nitrated into all *p* – positions of phenyl rings are similarly obtained:

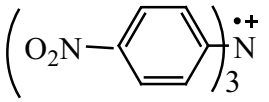

V'

It is obvious that radical cations **V′** are not capable of recombining by reaction (**Equation 7.32**) and are stabilised in the given conditions. At the same time, these nitrosubstituted radical cations cannot rapidly exchange electrons with TPA molecules because of structural distinctions. Therefore, the triplet ESR spectrum recorded instead of a narrow line on later stages of TPA exposure (**Figure 7.4b**) belongs to radical cations **V′**. The scheme of reactions (**Equation 7.34**) is confirmed by IR measurements. Under the action of NO_2, the absorption band corresponding to asymmetric stretch vibrations of $N \cdots O$ groups in aromatic nitro compounds appears at 1360 cm^{-1}. Two intense bands are also observed at 1320 cm^{-1} and 840 cm^{-1} owing to nitrate anions formed by oxidative reactions (**Equation 7.31**) and (**Equation 7.34**).

Though the chemical structure of radical cations **V** cannot be derived from a singlet ESR spectrum (**Figure 7.4a**), this information follows from products obtained by dissolving TPA in dichloromethane preliminarily exposed to NO_2. The ESR spectrum recorded at once after TPA dissolution is given in **Figure 7.5a**.

In this case instead of a narrow single line (**Figure 7a**), a wide line with $\Delta H_{1/2}$ = 1.7 mT is observed. The concentration of paramagnetic species is lowered by a factor of 30. The effect observed shows that as a result of TPA dissolving, the rate of electron exchange between radical cations **V** and neutral molecules sharply decreases due to dilution, and the singlet spectrum is broadened. An overwhelming fraction of radical cations **V** recombines, yielding dications **VI**. Such a conclusion is substantiated by the fact that the ESR spectrum of the solution gradually varies, and after 70 minutes it turns into a quintet with a distance between components of 0.57 mT and g = 2.0033 (**Figure 7.5b**). The amount of paramagnetic species for this time becomes fourfold as much. The quintet spectrum specifies the presence of two equivalent nitrogen atoms in the given particles, which can be attributed to radical cations of tetraphenylbenzidine:

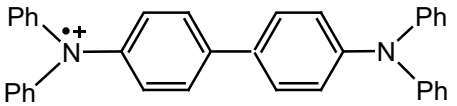

VIII

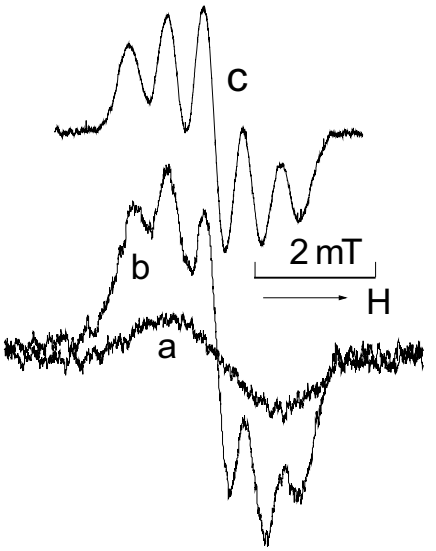

Figure 7.5 ESR spectra of TPA exposed to NO_2 (1 minute): immediately after dissolving in CH_2Cl_2 (a), after 70 minutes (b), after dissolving in CH_2Cl_2 without oxygen (c)

The formation of radical cations **VIII** in a solution of TPA is conditioned by the oxidative action of dications **VI:**

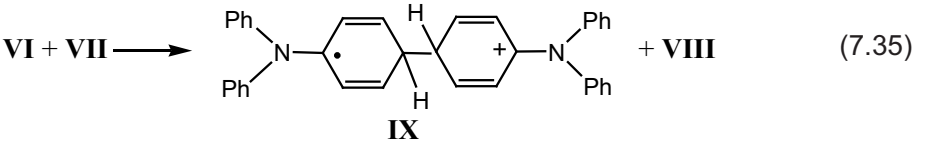

(7.35)

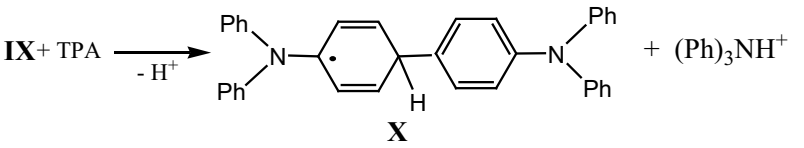

(7.36)

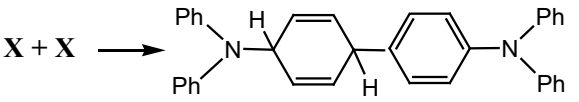

(7.37)

or

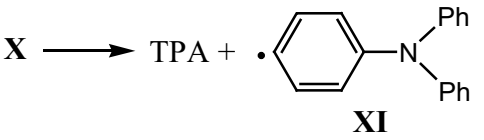

(7.38)

$$\mathbf{XI} + \mathbf{XI} \longrightarrow \mathbf{VII} \qquad (7.39)$$

On evidence derived from the literature, organic cations and dications are capable of oxidising bases, resulting in the formation of radical cations [35]. In the given system, tetraphenylbenzidine **VII** reacts as the organic base. In the absence of oxygen in similar systems, the oxidation results quickly and with a high yield. The presence of oxygen influences the mechanism of further transformations of radical cations. The pyridinium ion gives rise to stable radicals, but these radicals react rapidly with oxygen, producing hydrogen peroxides [36]. The TPA sample exposed to NO_2 during one minute was freezed at - 196 ^oC immediately after addition of methylene chloride. Then the solution was degassed by consecutive ,freezing - pumping out - thawing™ procedure. The concentration of radical cations **VIII** in these conditions was approximately 8 times greater than that in the presence of oxygen (Figure 7.5b) (2.8 x 10^{-2} mol/l and 3.6 x 10^{-3} mol/l respectively). As this takes place, radical cations **VIII** appear instantly at room temperature, and they have a more resolved ESR spectrum (**Figure 7.5c**). The increase of the spectrum resolution is obviously connected with the absence of the broadening effect of paramagnetic oxygen molecules. These facts show that oxygen effects strongly on the conversions of radical cations in stages (**Equation 7.36-7.39**), since free radicals formed in these reactions can be oxidised. Because of the high reactivity of the primary radical cations **V,** their ESR spectrum was not observed in solutions. Nevertheless, occurrence of the five-component spectrum unequivocally points to the formation of radical cations **V** in the primary reaction of NO_2 with TPA.

7.3 Oxidative Generation of Stable Nitrogen-Containing Radicals in Aliphatic Polyamides and Polyvinylpyrrolidone

The oxidative ion-radical mechanism of conversions induced by nitrosyl nitrate explains the high reactivity of aliphatic polyamides and polyvinylpyrrolidone (PVP) to NO_2 as well as the nature of stable radicals and the molecular products of nitration. Amide groups can appear as electron donors, and regularities of the conversions for aliphatic polyamides, in particular polycaproamide (PCA), [6, 37] is described by the following scheme:

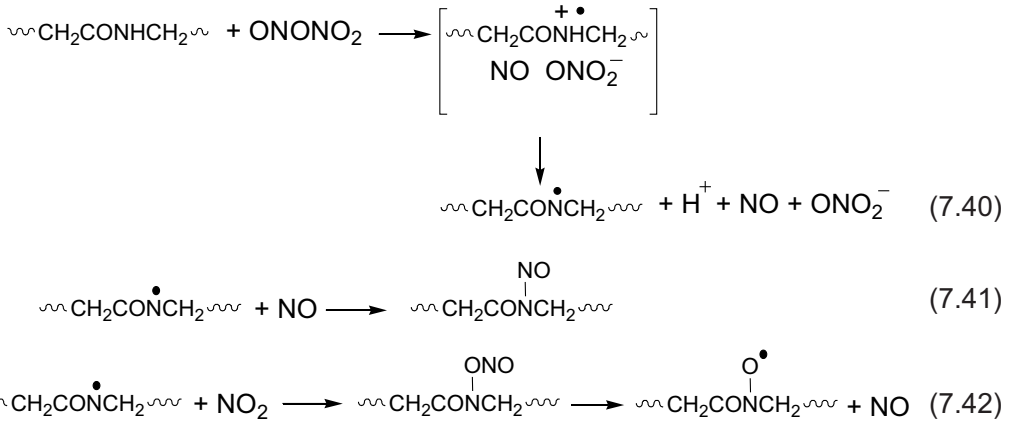

The conversion of N–H groups of PCA into nitrosoamides in reactions (**Equation 7.40**) and (**Equation 7.41**) follows from IR spectra (**Figure 7.6**) which show a decreasing band at 3293 cm^{-1} (stretching vibrations of H-bonded N–H groups). The intensity of amide I (ν = 1642 cm^{-1}) and amide II (ν = 1563 cm^{-1}) also drops markedly. Instead of these bands, the band at 1730 cm^{-1}, which corresponds to the C=O group of nitrosoamides, and the bands 1504 cm^{-1} and 1387 cm^{-1}, corresponding to the asymmetric and symmetric stretching vibrations of N=O groups of nitrosoamides [12], appear in the spectrum of PCA exposed to NO_2.

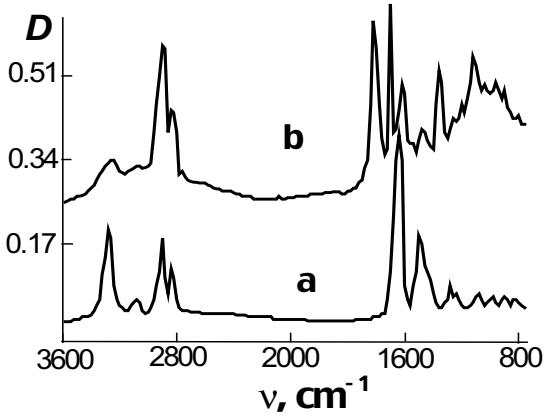

Figure 7.6 IR spectra of the original PCA films (a) and those after exposure to NO_2 (b).

The initial rate for the accumulation of C=O groups of nitrosoamides in the NO_2 concentration range of 4×10^{-5} to 4×10^{-4} mol/l is proportional to $[NO_2]^n$, where $n \approx 2$. This fact confirms the participation of nitrosyl nitrate in PCA conversions. In reaction (**Equation 7.42**), an unstable intermediate nitrite is initially generated. The latter gives the detectable acylalkylaminoxyl radicals with an anisotropic triplet spectrum ($A_{II}^{N} = 1.94$ mT, $g_{II} = 2.003$) (**Figure 7.7**).

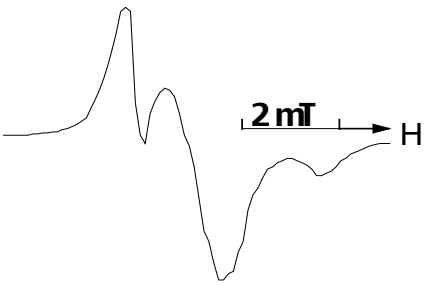

Figure 7.7 ESR spectrum of PCA radicals generated by NO_2 at 22 °C

The ESR study of the PVP exposed to NO_2 at concentration $[NO_2]_{gas.} = 4 \times 10^{-4}$ mol/l [6, 37] shows that two types of stable nitrogen-containing macroradicals are formed: iminoxyl radical $R_1(R_2)C{=}N\text{-}O^{\bullet}$ with parameters A_{II}^{N} = 4,33 mT, $A_{\perp}^{N}$ =2,44 mT, g_{II} = 2,0029, $g_{\perp}$ =2,0053, and acylalkylaminoxyl macroradicals $R_1C(=O)\text{-}N(O^{\bullet})\text{-}R_2$ with practically the same parameters as in PVP (**Figure 7.8**).

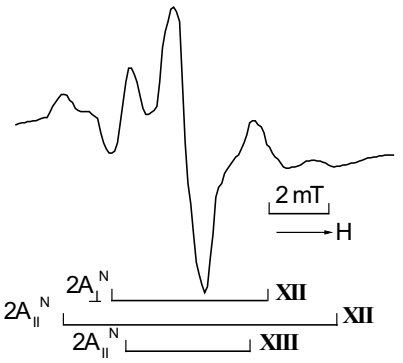

Figure 7.8 ESR spectrum of PVP exposed to NO_2

The scheme of processes of the PVP conversion in reactions with nitrogen dioxide is shown below.

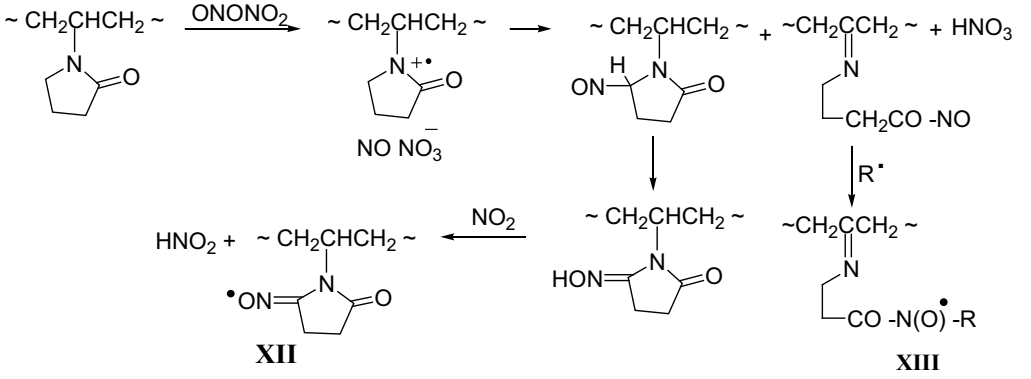

(7.42)

As in the case of PCA, a radical-generating reagent is nitrosyl nitrate, which reacts with the tertiary amide group, forming the amide radical cations and nitric oxide. The possible conversions of this cation-radical presented in scheme (**Equation 7.42**) are similar to those in low-molecular *N*,*N*-dialkylamides [38]. The first direction is a decomposition of the radical cations with the detachment of proton from CH_2-group of the side-cyclic fragment. Produced in this reaction, the secondary alkyl radical combining 'in cage' with NO yields the secondary nitroso compound. Such nitroso compounds undergo isomerisation into oximes to produce iminoxyl macroradicals **XII** in the reaction with NO_2. The second pathway includes the decomposition of the radical cations with the rupture of –N–C(=O)– bond. Acyl radicals produced react 'in cage' with NO to give an acylnitroso compound. The latter interact with alkyl radical, forming acylalkylaminoxyl radical **XIII**.

Thus, the structure of stable nitrogen-containing radicals and the mechanism of their formation provide evidence for the selectivity of primary oxidative reaction resulting in hydrogen abstraction from macromolecules. N–H bonds (PCA) or C–H bonds at the α-position with respect to the amide group (PVP) are involved in this reaction.

7.4 Ion-Radical Conversions of Aromatic Polyamides in the Presence of NO_2

The feature of **Equation 7.24** in aromatic polyamides lies in the fact that the formation of radical cations can be caused by the electron transfer from amide groups and phenyl rings. The mechanism of generation of stable radicals in aromatic polyamides

on exposure to NO_2 has been considered by the example of poly-*m*-phenylene isophthalamide (PPIA) [7]. At the initial stage of PPIA exposure to NO_2 at 22 °C, the ESR spectrum shown in **Figure 7.9a** is obtained. It represents an anisotropic triplet with A_{II}^{N} = 4.8 mT, g_{II} = 2.0021 and $A_{\perp}^{N}$ =3.2 mT, $g_{\perp}$ =2,0047. This signal corresponds to a spectrum of iminoxyl radicals **XIV** in a solid phase with a hindered rotational mobility [39, 40]. At later stages (**Figure 7.9b**), a signal of the second iminoxyl radical **XV** appears. The spectrum of radical **XV** is also an anisotropic triplet but with other parameters: A_{II}^{N} = 4.1 mT, g_{II} = 2,0024 and $A_{\perp}^{N}$ =2.6 mT, $g_{\perp}$ =2.0050. On long exposure of PPIA, the ESR with the prevailing signal of radicals **XV** was recorded (**Figure 7.9c**). As a result of subsequent pumping out of the sample at 295 K, the components of radicals **XIV** appeared again (**Figure 7.9d**). The total concentration of iminoxyl radicals is increased fourfold. This effect is explained by the ability of radicals **XIV** to form nonparamagnetic complexes with NO_2, which are easily decomposed by pumping.

Based on formal mechanism (**Equation 7.24**), one can conclude that the primary act is the oxidising interaction of amide groups with aminoxyl nitrate:

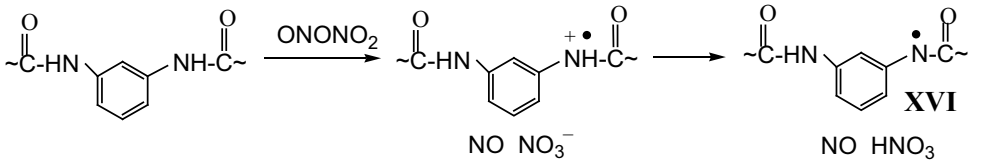

(7.43)

As a result of a primary stage, a radical pair involving NO and radical **XVI** is formed. The recombination of radical **XVI** with NO gives the *N*-nitroso compound **XVII**:

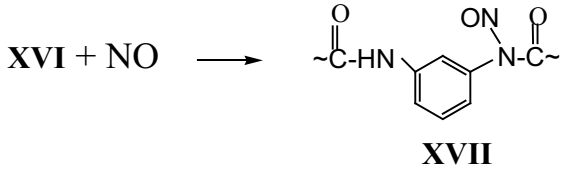

(7.44)

Isomeric forms of radical **XVI** are radicals of the cyclohexadienyl type:

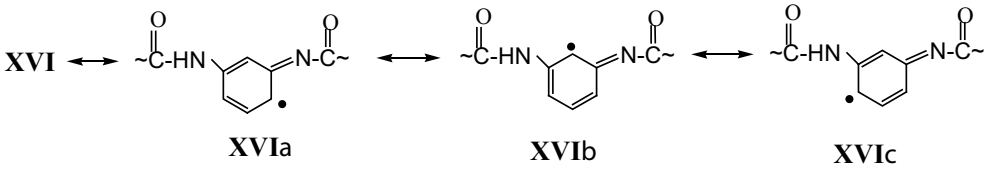

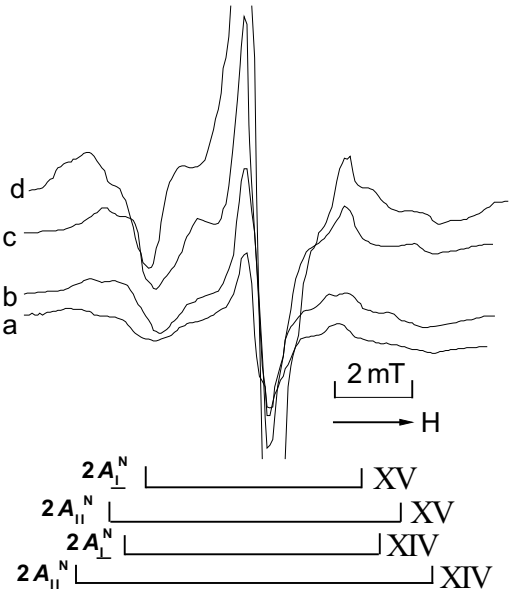

Figure 7.9 ESR spectra of PPIA after exposure to NO_2 at 295 K: (a) 0.5 h, (b) 4.5 h, (c) 95 h, and (d) is (c) after pumping-out

Therefore, along with the formation of compounds **XVII** in the recombination reaction (**Equation 7.44**), other nitroso compounds should be expected:

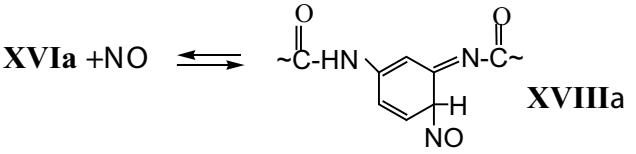

(7.45)

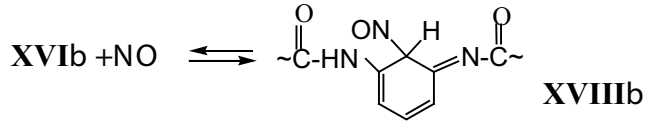

(7.46)

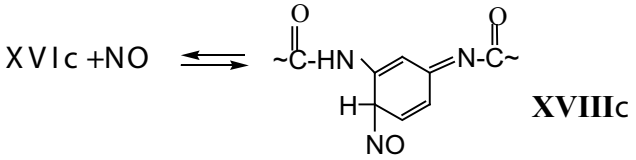

(7.47)

Nitroso compounds **XVIIIa**, **XVIIIb** and **XVIIIc** containing α-hydrogen are easily isomerised [41] into the respective oximes:

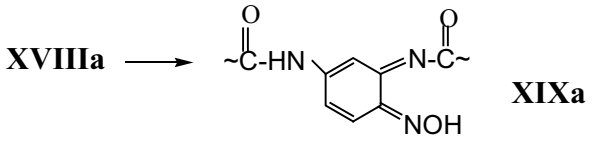

(7.48)

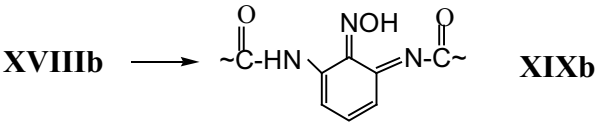

(7.49)

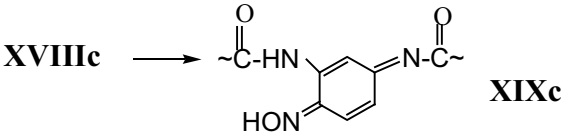

(7.50)

In the following stage, hydrogen-atom abstraction from oximes leads to formation of stable iminoxyl radicals:

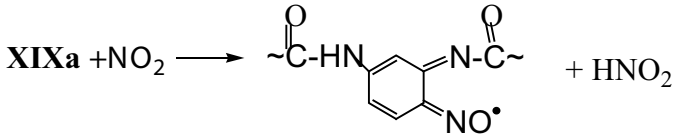

(7.51)

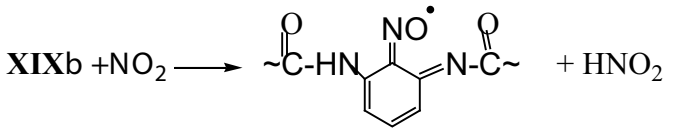

(7.52)

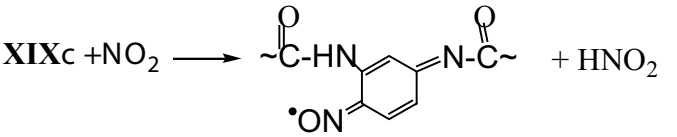

(7.53)

Thus, the interaction of PPIA with NO_2 by the ion-radical mechanism is capable of initiating conversions of chemically inert phenyl rings into much more reactive cyclohexadiene groups.

The formal scheme of reactions explains the appearance of stable radicals **XIV** and **XV** (**Figure 7.9a** and **b**) in the given system. However, to attribute concrete structures to these radicals, *ab-initio* calculations of isotropic hyperfine coupling constants were done for the following iminoxyl radicals [7]:

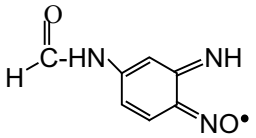

XXa

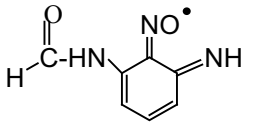

XXb

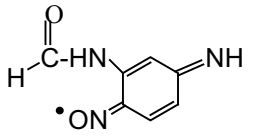

XXc

Calculations were accomplished by the Gaussian 98W program [42] using density functional theory in B3LYP approximation. The basis set 3-21G has been applied for the geometry optimisation of model structures. Hyperfine coupling constants were calculated using EPR-II and 6-31 (d, p) basis sets [43]. The results obtained are given in **Table 7.2**. For comparison, the average values of constants determined from experimental ESR spectra (**Figure 7.9 a** and **b**) are also given : $A^{N}_{av} = \frac{1}{3}\left(A^{N}_{\parallel} + 2A^{N}_{\perp} \right)$.

Table 7.2 Calculated isotropic and averaged experimental hyperfine coupling constants for iminoxyl radicals

Radical	A^{N}_{i}, mT		A^{N}_{av}, mT
	Basis set		
	EPR-II	6-31G(d, p)	
XIV	-	-	3.7 ± 0.1
XV	-	-	3.1 ± 0.1
XXa	3.29	3.27	-
XXb	4.01	3.84	-
XXc	3.93	3.77	-

As is obvious from results of the calculation, model structures **XXb** and **XXc** are in general agreement with radicals **XIV**, while structure **XXa** most likely belongs to radicals **XV**.

An application of the B3LYP method also allows explanation of the peculiarities of accumulations of radicals **XIV** and **XV** at 295 K, namely, later appearance of the radical **XV** signal in the ESR spectrum as compared with radicals **XIV**. For that the energy variations in a model reacting system in the course of consecutive conversions to iminoxyl radicals **XXa**, **XXb** and **XXc** (structural analogues of radicals **XIV** and **XV**) by reactions similar to (**Equation 7.43**)–(**Equation 7.53**) were calculated. As a primitive model compound, *N*–(3–aminophenyl)formamide **XXI** has been chosen. The results obtained are represented in **Figure 7.10**.

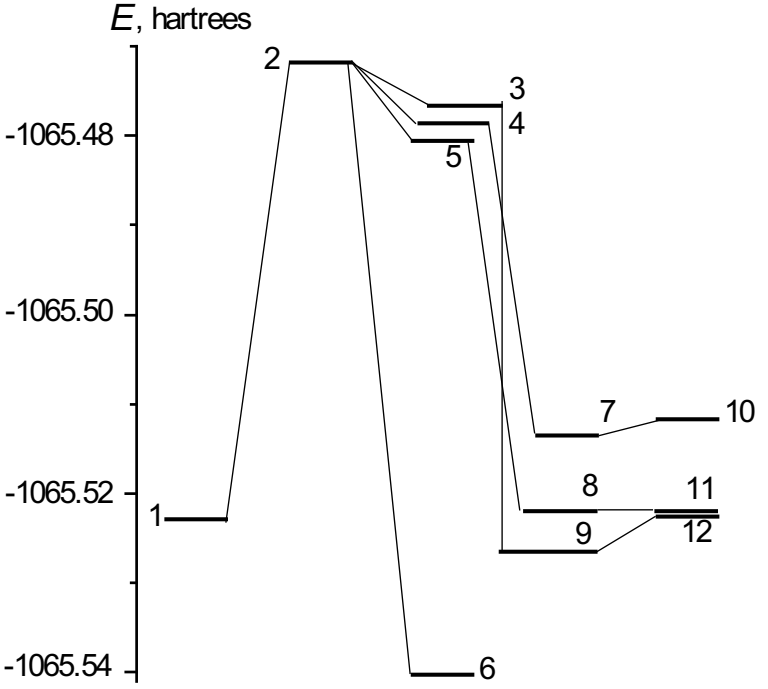

Figure 7.10 Variations of calculated energies in the generation of iminoxyl radicals:

XXI+ONONO$_2$ + NO$_2$ (1); XVI (XVIa, XVIb, XVIc) + NO + HNO$_3$ + NO$_2$ (2); XVIIIa

+ HNO$_3$ + NO$_2$ (3); XVIIIc + HNO$_3$ + NO$_2$ (4); XVIIIb + HNO$_3$ + NO$_2$ (5); XVII +

HNO$_3$ + NO$_2$ (6); XIXc + HNO$_3$ + NO$_2$ (7); XIXb + HNO$_3$ + NO$_2$ (8); XIXa + HNO$_3$ +

NO$_2$ (9); XXc + HNO$_3$ + HNO$_2$ (10); XXb + HNO$_3$ + HNO$_2$ (11); XXa + HNO$_3$ + HNO$_2$ (12)

All designations in **Figure 7.10** for intermediate products of conversions **XXI** are the same as for PPIA. As evident from the figure, the first stage similar to reaction (**Equation 7.43**) requires significant energy consumption. In the subsequent reaction

(**Equation 7.44**), a large amount of energy is released (level 6), and in whole this transformation is an exothermic process. However, the recombination of NO and cyclohexadienyl radicals (**Equations 7.45–7.47**) decreases insignificantly the energy (levels 3–5) of the system ($-\Delta E$ = 0.0047–0.0092 hartrees). Because of this, the reverse reaction from levels 3-5 to radicals **XVIa**, **XVIb** and **XVIc** is possible until nitroso compounds **XVIIIa, XVIIIb** and **XVIIIc** are isomerised to corresponding oximes (levels 7-9) with the large energy release (- = 0.05 hartrees). The greatest probability of back transition to the cyclohexadienyl radical with an exit of NO from the reacting 'cage' would be expected for compounds **XVIIIa** (level 3), which according to the scheme of process are the precursors of stable radicals **XV** recorded at later stages of PPIA exposure to NO_2 (**Figure 7.10 b** and **c**). For compounds **XVIIIb** and **XVIIIc** (levels 4 and 5), which transform into radicals **XIV**, the back transition is least probable, and consequently these radicals are effectively formed at the beginning of exposure (**Figure 7.9a**). As a whole, the stable radical generation in PPIA in the presence of NO_2 by reactions (**Equations 7.43–7.53**) is a thermo-neutral or poorly endothermic process (ΔE = 0.011 hartrees ≈ 28 kJ mol^{-1}).

The observed ability of iminoxyl radicals **XIV** to form unstable compounds with NO_2 allows choosing between the structures **XXb** and **XXc** having approximately identical ESR spectra (**Table 7.1**). As shown previously (**Section 5.5**), interaction of the conjugated double bonds of *p*-benzoquinone with NO_2 results in the formation of appropriate oxyaminoxyl radicals. Based on this fact, one can believe that the radicals **XIV** of structure **XXc**, having a system of conjugated double bonds similar to those in *p*-benzoquinone, are capable of recombining with NO_2:

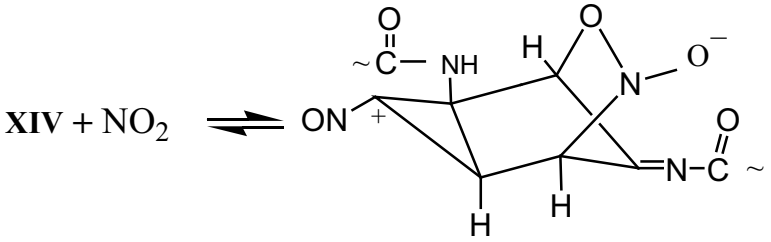

(7.54)

The strong structural tensions cause instability of the compound formed in reaction (**Equation 7.54**); it quickly turns into initial iminoxyl radicals during the pumping-out of NO_2. For structure **XXa** with conjugated double bonds similar to those of *o*-benzoquinone, the reaction (**Equation 7.54**) is less probable, and radicals **XV** are substantially accumulated on long-term exposure of samples. On this basis one can conclude that the mechanism of generation of iminoxyl radicals with structure **XXc** is realised in practice. Significant steric hindrances created by substituents of a phenylene ring make the mechanism including reactions (**Equation 7.46**, **7.49** and **7.52**) energetically less preferable in PPIA.

Iminoxyl radicals are also formed in PPIA after exposure to NO_2 if samples are further warmed in a vacuum at 100 °C (**Figure 7.11**). Parameters of the ESR spectrum of iminoxyls recorded in these conditions are the same as for radicals **XV**. The concentration of these radicals during heating for a long time is found to be a lot more than those initially obtained in PPIA in an atmosphere of NO_2 at 22 °C. This is evident from **Figure 7.12**, where kinetic plots of the accumulation of iminoxyls are shown for two samples preliminarily exposed to NO_2 within one and four days. As indicated in the figure, the initial rates of the accumulation roughly correlate with duration of the sample exposure at 22 °C. Along with iminoxyls, acylarylaminoxyl radicals **XXII** are formed during heating of exposed PPIA at 100 °C (**Figure 7.11**). These radicals are identified by an anisotropic triplet signal with $A_{\|}^{N}$ = 1.94 mT and $g_{\|}$ = 2.003 [44].

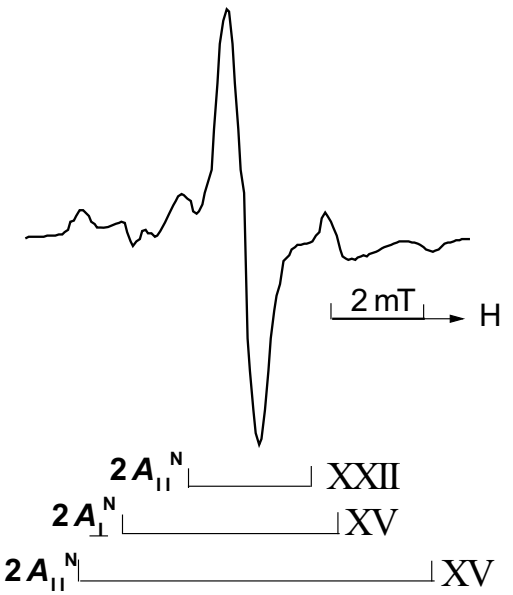

Figure 7.11 ESR spectrum of PPIA preliminarily exposed to NO_2 after subsequent heating in A vacuum at 100 °C

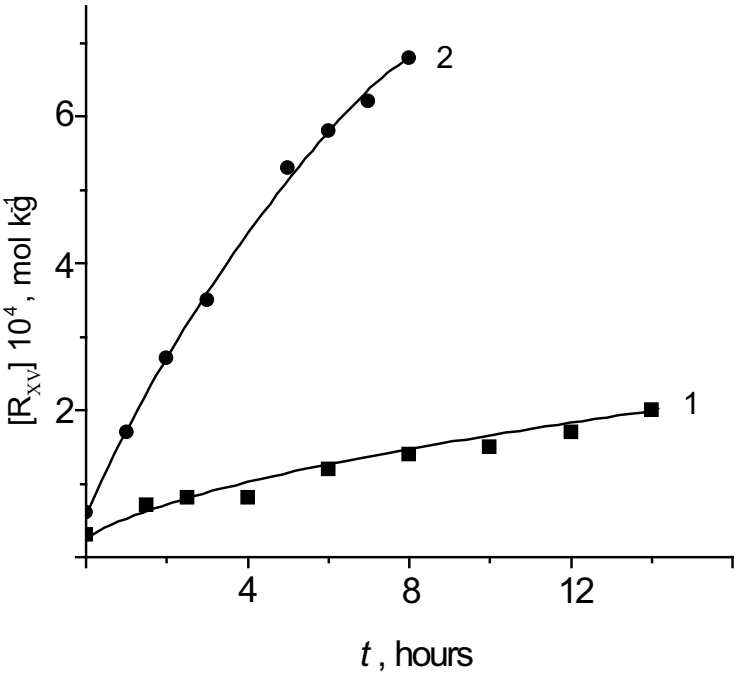

Figure 7.12 Kinetics of the accumulation of radical XV in the course of heating (100 °C) of PPIA preliminarily exposed to NO_2 for (1) one day and (2) four days

The effects observed are seemingly conditioned by the formation of some molecular products on exposure of PPIA to NO_2, which are further converted to stable radicals **XV** and **XXII** at elevated temperatures. Such products are compounds **XVII**, whose formation in the presence of NO_2 is energetically favourable (**Figure 7.10**). It should be remembered that primary radical cations can be generated in aromatic polyamide (PA) by reaction (**Equation 7.4**) owing to an electron transfer from phenyl rings to nitrosyl nitrate [13]. As a result of oxidising reactions, aryl radical cations are formed in monomer units containing *N*-nitroso groups. These radical cations by subsequent recombination with NO give intermediate nitroso aryl cations and then aryl nitroso compounds after detachment of a proton. Because the characteristics of the ESR spectrum (**Figure 7.11**) correspond to a spectrum of radicals **XVII**, these consecutive reactions can be presented as follows:

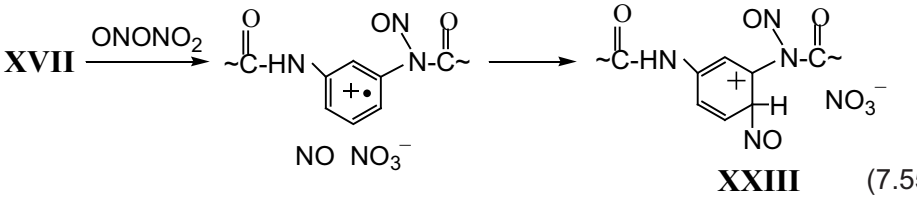

(7.55)

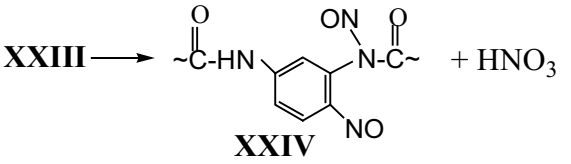

(7.56)

Due to thermal decomposition of compounds XXIV during heating, iminoxyl radicals (XV) are formed:

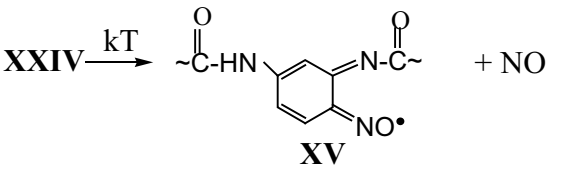

(7.57)

The precursors of other stable radicals **XXII** are formed by recombination of radicals **XVI** and NO_2:

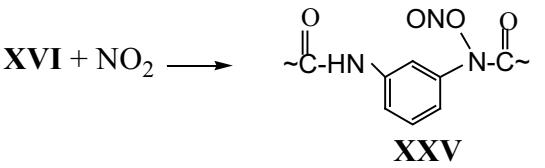

(7.58)

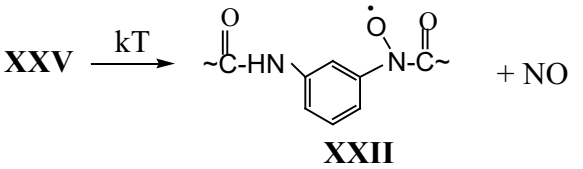

(7.59)

The IR spectra of nitrated PPIA confirm the considered mechanism (**Figure 7.13**). From **Figure 7.13**, the appreciable decrease of intensity of the stretch band at 3340 cm^{-1} of N-H bonds by reaction (**Equation 7.43**) is observed. The appearance of new intensive bands at 1370 cm^{-1} and 810 cm^{-1} belonging to nitrate-anions indicates ion-radical conversions of the polymer. The reaction (**Equation 7.58**) proves to be true

by two stretch bands at 1680 cm^{-1} and 1610 cm^{-1} of nitrite groups, respectively, in *trans*- and *cis*-forms [26].

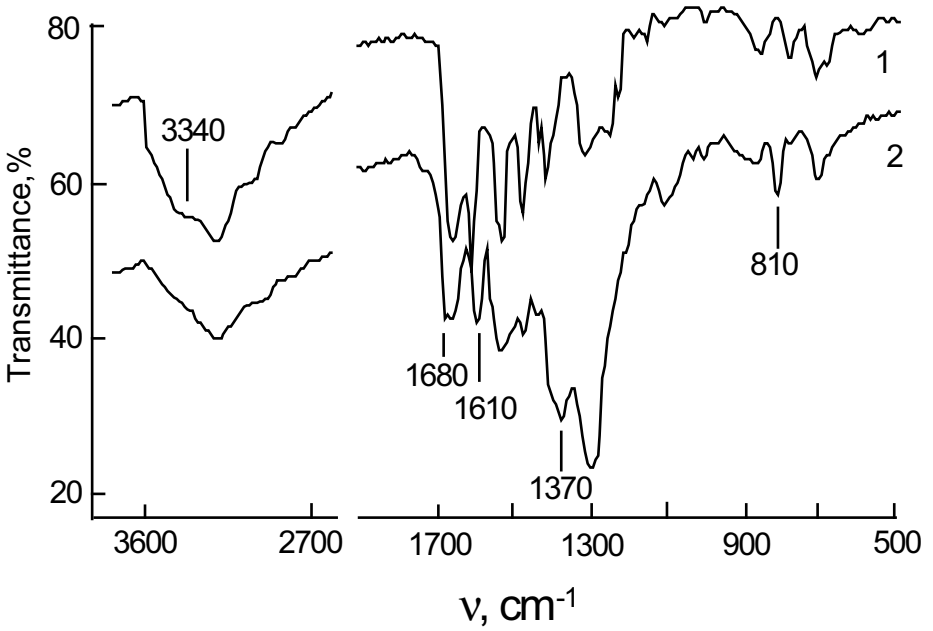

Figure 7.13 IR spectra of (1) original PPIA and (2) after exposure to NO_2 at 22 °C

Thus, widely used aromatic polyamides with high mechanical characteristics and thermal stability [45] are rather reactive relative to NO_2. This is because of the specific ion-radical initiation. In this process, chemically inert aromatic rings are transformed into active cyclohexadiene structures, and in this way simple synthesis of spin-labeled macromolecules can be carried out.

7.5 Oxidative Radical Generation via NO_2 Dimer Conversions Induced by the Amide Groups of Macromolecules

The equilibrium (**Equation 7.1**) involving planar dimer (PD) and nitrosyl nitrate (NN) could explain an appearance of stable radicals in the polymers not containing specific chemical bonds reacting with NO_2 mono radicals. However, there are certain obstacles connected with the energetic properties of NO_2 dimers for realising the

mechanism connected with reactions of NN; the energy of syn- and anti- forms of NN exceeds that of PD, respectively, 29.8 and 18.4 kJ/mol [10]; that is the equilibrium (**Equation 7.1**) should be shifted to PD in the gas phase. Nevertheless, nitroso nitrate formation was observed during the interaction of olefins with NO_2 in the liquid phase [10, 46]. This fact is indicative of the participation of NN in these reactions. The shift of equilibrium (**Equation 7.1**)) to NN can occur in liquid-phase reactions, for instance, because of increasing the polarity of medium. In solid polymers with small macroscopic dielectric permeability (ε = 2–3), the formation of NN could be promoted by coordination of NO_2 with polar functional groups. However, stable nitrogen-containing radicals were not registered in such polymers with polar ester groups as poly(methylmethacrylate), polycarbonate, acetyl cellulose on exposure to NO_2. On the basis of this fact, one can assume that the effective formation of NN and consequently realisation of the ion-radical process (**Equation 7.24**) are conditioned by specific donor–acceptor interactions of NO_2 dimers with certain functional groups facilitating the isomerisation of PD into NN. The possibility of PD conversion into NN under the influence of amide groups of PPIA and PVP with further generation of stable radicals has been considered [47]. As the indicator of dimer conversion, the dependence of yield of typical radicals in the reaction of PD with *p*-benzoquinone (BQ) [48] on the contents of PPIA and PVP in the reacting system was used.

As noted in **Chapter 5**, the formation of oxyaminoxyl radicals

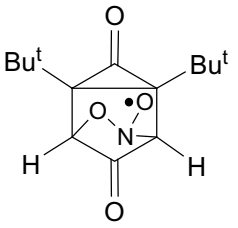

(**XXVI**) takes place with participation of PD by the reaction (5-142) [48]. In addition to **XXVI**, iminoxyl radicals **XV** occur in composites of BQ with PPIA on exposure to NO_2. Under the same conditions, the sum of iminoxyl radicals **XII** and acylalkylaminoxyl radicals **XIII,** along with **XXVI,** was revealed in composites of BQ with PVP. The maximum concentrations of radicals **XXVI**, **XV**, **XII** and **XIII** were separately determined in composites with the various contents of BQ, poly-*m*-phenylene isophthalamide (PPIA) and PVP after exposure to NO_2 within 24 hours.

As seen from **Figure 7.14a** and **b**, the maximum concentration of radicals **XXVI** monotonously falls as the relative contents of PPIA and PVP is increased, whereas concentrations of radicals **XV** and **XII** + **XIII** vary from 10% to 20% of the average value that is within the accuracy of integration of ESR spectra. This fact is indicative of obvious dependence of the radical **XXVI** yield on the contents of polymers with

amide groups in composites, suggesting that PD is converted under the influence of amide groups into NN that generates stable radicals **XV**, **XII** and **XIII** in the polymeric phases. It is significant that an appreciable decrease of the yield of radicals **XXVI** was not observed in control experiments when polymers of other chemical structure, for example, acetyl cellulose, were used in composites [47]. Therefore, one can conclude that amide groups have a special role in the process PD → NN.

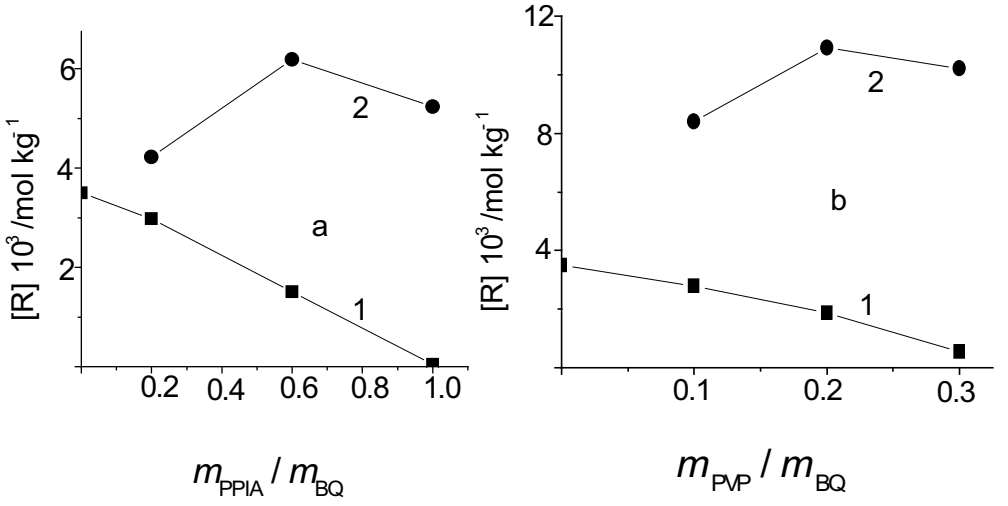

Figure 7.14 Dependencies of concentrations of radicals **XXVI** (1), **XV** (2) in BQ + PPIA (a) and **XXVI** (1), **XII** + **XIII** (2) in BQ + PVP (b) after exposure to NO_2 on a weight ratio of BQ, PPIA, and PVP

The decrease of the relative yield of radicals I on addition of polymers with amide groups to composites is apparent from the formal kinetic scheme:

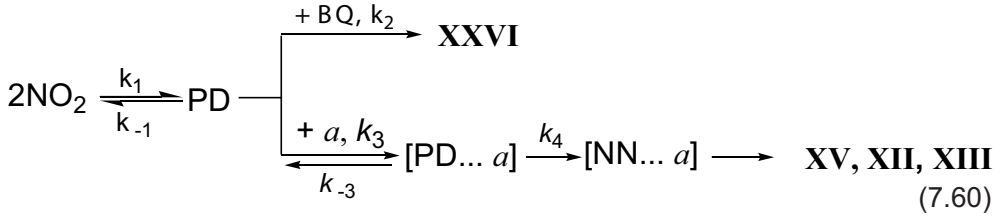

(7.60)

where *a* is an amide group. Taking into consideration the stationary state for concentrations of PD, NN, [PD···*a*], [NN···*a*], the following equations for rates of accumulation of radicals **XXVI, XV XII,** and **XIII** are obtained:

$$\frac{d[\mathrm{XXVI}]}{dt} = \frac{k_1 k_2 [\mathrm{BQ}](k_{-3} + k_4)[\mathrm{NO_2}]^2}{(k_{-3} + k_4)(k_{-1} + k_2[\mathrm{BQ}] + k_3[a]) - k_{-3}k_3[a]} \tag{7.61}$$

$$\frac{d[\mathrm{XV, XII, XIII}]}{dt} = \frac{k_1 k_3 k_4 [a][\mathrm{NO_2}]^2}{(k_{-3} + k_4)(k_{-1} + k_2[\mathrm{BQ}] + k_3[a]) - k_{-3}k_3[a]} \tag{7.62}$$

where $[\mathrm{NO_2}]$ is the concentration of NO_2 in the gas phase, and [*a*] is the concentration of amide groups. These equations are simplified if the conversion of amide groups in composites is comparatively large, and the conversion of PD into NN occurs sufficiently effectively, that is, $k_3[a] > k_{-1} + k_2$ [BQ]. Then

$$\frac{d[\mathrm{XVI}]}{dt} = \frac{k_1 k_2 [\mathrm{BQ}](k_{-3} + k_4)[\mathrm{NO_2}]^2}{k_3 k_4 [a]} \tag{7.63}$$

$$\frac{d[\mathrm{XV, XII, XIII}]}{dt} = k_1[\mathrm{NO_2}]^2 \tag{7.64}$$

Thus the rate of accumulation of radicals **XVI, XII** and **XIII** is determined by $[\mathrm{NO_2}]^2$, and maximum concentrations of these radicals not depend appreciably on AP and PVP contents (**Figure 7.14a** and **b** (curve 2)). In contrast, the yield of radicals **XVI** decreases as polyamides are added to composites and [*a*] is increased. These plots are representative of competitive pathways for PD interactions with BQ and amide groups. Moreover, the yield of radicals XVI is not changed in the NO_2 atmosphere in composites of BQ with other polymers, for instance, acetyl cellulose at any ratio of the components.

For validating the mechanism proposed for the conversion of PD into NN, the calculations of energy changes in process of NO_2 interaction with the simplest amide (formamide) have been carried out [47] within the framework of density functional theory by the Gaussian 98 program [42]. The B3LYP/6-31G(d, p) restricted method for closed and open shells was used. The intention of the calculations is to correlate energy consumptions for PD → NN with those for other stages of the radical generation process. Energies of the following states according to scheme (**Equation 7.60**) were calculated:

$$2NO_2 + NH_2COH \quad (7.65)$$

$$O_2N\text{-}NO_2 + NH_2COH \quad (7.66)$$

$$ONONO_2 + NH_2COH \quad (7.67)$$

$$[O_2N\text{-}NO_2 \cdots NH_2COH] \quad (7.68)$$

$$[ONONO_2 \cdots NH_2COH] \quad (7.69)$$

$$N^{\cdot}HCOH + NO + HNO_3 \quad (7.70)$$

$$NH_2C^{\cdot}O + NO + HNO_3 \quad (7.71)$$

The given process includes intermediate molecular complexes of PD and NN with formamide (**Equation 7.68**, **Equation 7.69**). The changes of minimum energies are shown in **Figure 7.15a**. One can see that the formation of PD from NO_2 is an energetically advantageous process [4], whereas NN is generated from NO_2 in an endothermic reaction. The complexation of PD with formamide is accompanied by a release of energy: Δ = 28 kJ/mol. However, PD in complex (**Equation 7.68**) cannot react with formamide, and can only leave the reacting cage. At the same time, PD in the complex can be converted approximately with the same energy consumption into NN (**Equation 7.69**), which further reacts by the electron transfer reactions (**Equation 7.70**, **Equation 7.71**) giving radicals, NO, nitric acid and a significant release of energy (44–57 kJ/mol). Such a sequence of transformations seems to be more efficient in comparison with a direct interaction of NN and formamide in state (**Equation 7.67**) because the energy of dimers in complexes (**Equation 7.68**) and (**Equation 7.69**) is lower than that of the initial state (**Equation 7.65**). Thus, the results of calculations are not contrary to the mechanism proposed on the basis of the experimental plots of **Figure 7.14**.

The specific role of the amide groups of macromolecules in the process of PD into NN conversion is also apparent from similar calculations carried out for the interaction of the dimers with different functional groups, for instance, carbonyls [47]. The results of calculations for the following reaction stages of the NO_2 interaction with acetaldehyde:

$$2NO_2 + CH_3COH \quad (7.72)$$

$$O_2N\text{-}NO_2 + CH_3COH \quad (7.73)$$

$$ONONO_2 + CH_3COH \quad (7.74)$$

$$[O_2N\text{-}NO_2 \cdots CH_3COH] \quad (7.75)$$

$$[ONONO_2 \cdots CH_3COH] \quad (7.76)$$

$$C^{\cdot}H_2COH + NO + HNO_3 \quad (7.77)$$

$$CH_3C^{\cdot}O + NO + HNO_3 \quad (7.78)$$

are represented in **Figure 7.15b**. There are principal distinctions associated with the capability for isomerisation of PD into NN in complexes (**Equation 7.68**) and (**Equation 7.75**). As indicated by **Figure 7.15b,** this process for complex (**Equation 7.75**) necessitates additional expenditure of ~24 kJ/mol as compared with an energy for transforming (**Equation 7.75**) into (**Equation 7.73**) with an exit of PD from reacting cage. Thus the coordination of PD with polar carbonyl groups can make difficulties for conversion of PD into NN.

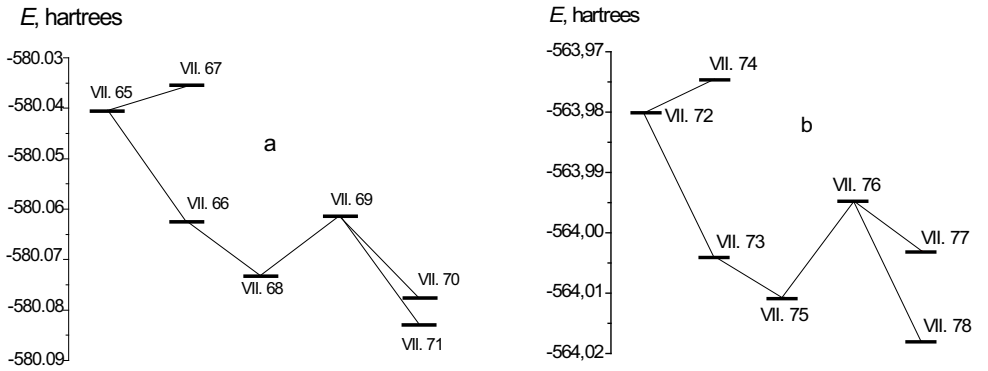

Figure 7.15 Changes in minimum energies calculated for the reactions of NO_2 with formamide (a) and acetaldehyde (b)

7.6 Interaction of Aromatic Polyimides with NO_2

The materials based on polyimides have valuable mechanical and chemical properties [45]. Currently, these thermostable polymers are used extensively in aerospace engineering. Investigations of the thermal and thermo-oxidative stability of polyimides have been carried out in detail [49]. However, the mechanism of action of such aggressive gases as nitrogen oxides on these materials remains practically unexplored. The efficiency of initiation by the ion-radical mechanism (**Equation**

7.24) is caused by donor properties of functional groups of macromolecules as well as by possible conversions of intermediate radical cations into free radicals. Apparently, these conditions are realised in aliphatic and aromatic polyamides and polyamidoimides [5–7]. However, the chemical structure of some polyimides, for example, polypyromellitimide (PPI), does not involve disintegration of radical cations with detachment of protons through the mechanism similar to that shown by reaction (**Equation 7.40**). Thus, the study of interaction of PPI with NO_2 enables other probable ways of ion-radical transformations of macromolecules to be established. The mechanism of stable radical generation in PPI under the action of NO_2 has been considered using ESR measurements [8].

The exposure of PPI to NO_2 at room temperature for up to 7 days does not give significant ESR signals. After the-pumping out of NO_2 from exposed samples, the anisotropic ESR spectrum, shown in **Figure 7.16a**, was observed. The parameters of this spectrum ($A_{II}^{N} = (2.0 \pm 0.1)$ mT; $g_{II} = 2.0018 \pm 0.0005$) entirely correspond to acylarylaminoxyl radicals 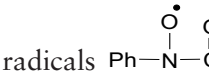 (**XXVII**) detected in solid polymers [6]. If the same samples are heated at 100 °C in a vacuum, additional signals appear in the spectrum (**Figure 7.16b** and **c**). In this case, the total concentration of radicals considerably increases. The new signals can be divided into two types: four anisotropic side components and a central singlet line. The content of these novel components increases if the exposure of PPI to NO_2 is longer. Such a conclusion is reached by comparing ESR spectra obtained after the same time of warming PPI in vacuum (8 hours), but durations of exposure of the samples to NO_2 are 5 hours and 7 days, correspondingly (**Figure 7.16c** and **d**). On the basis of spectral splitting and *g*-factor values, the side components can be unequivocally attributed to a signal of iminoxyl radicals 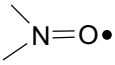 (**XXVIII**) with the parameters: A_{II}^{N} = (4.4 ± 0.1) mT; g_{II} = 2.0022 ± 0.0003; $A_{\perp}^{N}$ = (2.4 ± 0.1) mT; $g_{\perp}$ = 2.0056 ± 0.0003.

The kinetic dependencies of the radical **XXVIII** accumulation in vacuum at 100 °C for PPI samples exposed to NO_2 during 7 days in conditions of various NO_2 concentrations are shown in **Figure 7.17a**. As indicated in the figure, radicals **XXVIII** are formed within 14 hours at a constant rate. The linear dependence of these rates on concentrations of NO_2 is given in **Figure 7.17b**.

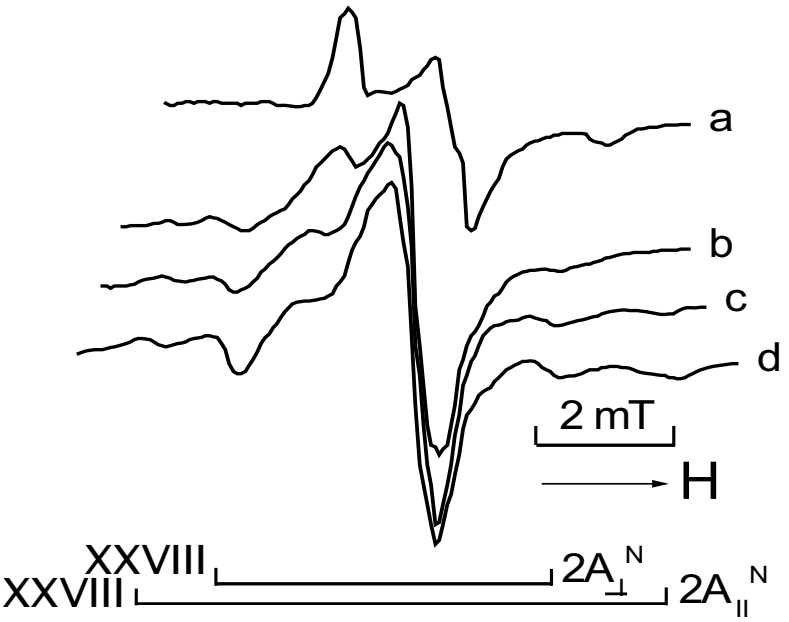

Figure 7.16 ESR spectra of PPI exposed to NO_2 at 22 °C during 5 h (a–c) and 7 days (d) after Pumping-out at 22 °C (a) and subsequent heating at 100 °C in a vacuum for 1 h (b) and 8 h (c, d)

In contrast with the exposure at room temperature, practically only iminoxyl radicals **XXVIII** are accumulated in an NO_2 atmosphere at 100 °C (**Figure 7.18a**). However, the concentration of radicals **XXVIII** in these conditions becomes steady in 2–3 hours (**Figure 7.19a**). A significant increase of radical **XXVIII** concentrations is observed at subsequent heating these samples at 100 °C in a vacuum as shown by **Figure 7.19b**. Their signal in the ESR spectrum remains prevailing (**Figure 7.19b**).

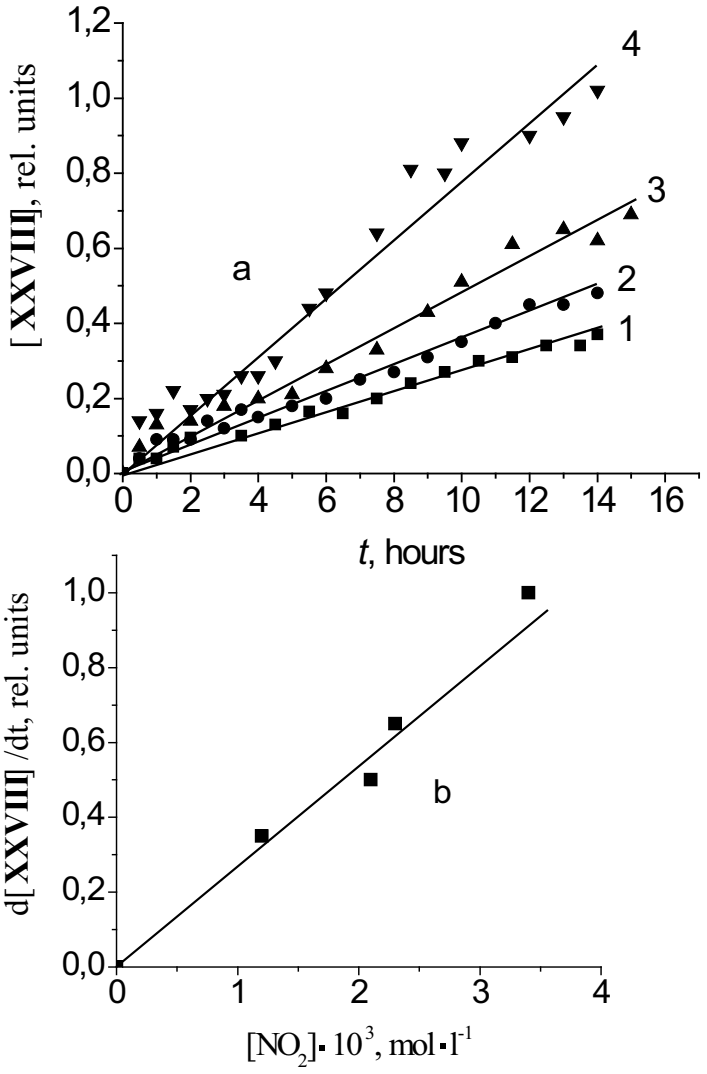

Figure 7.17 Kinetics of radical **XXVIII** accumulation during heating (100 °C) PPI pre-exposed to NO_2 at 22 °C for 7 days. (a) $[NO_2] = 1.2 \times 10^{-3}$(1); 2.1×10^{-3}(2); 2.3×10^{-3}(3); 3.4×10^{-3} mol/l (4), and the dependence of rates of the radical **XXVIII** accumulation on NO_2 concentrations (b)

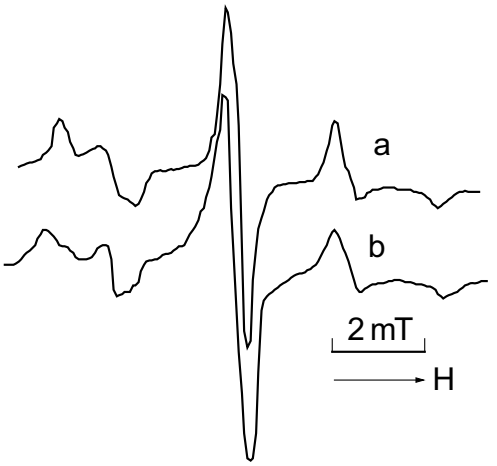

Figure 7.18 ESR spectra of PPI exposed to NO_2 for 5 h at 100 °C (a) and after subsequent heating at 100 °C in a vacuum (b)

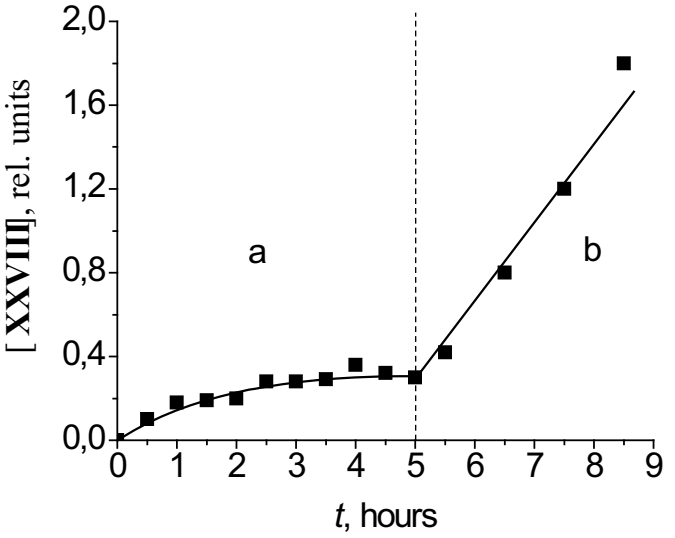

Figure 7.19 Kinetics of radical **XXVIII** accumulation on exposure of PPI to NO_2 at 100 °C (a) and after subsequent heating at 100 °C in a vacuum (b)

It is expected that the primary act is the oxidative interaction of imide groups with NO_2 dimers (nitrosyl nitrate):

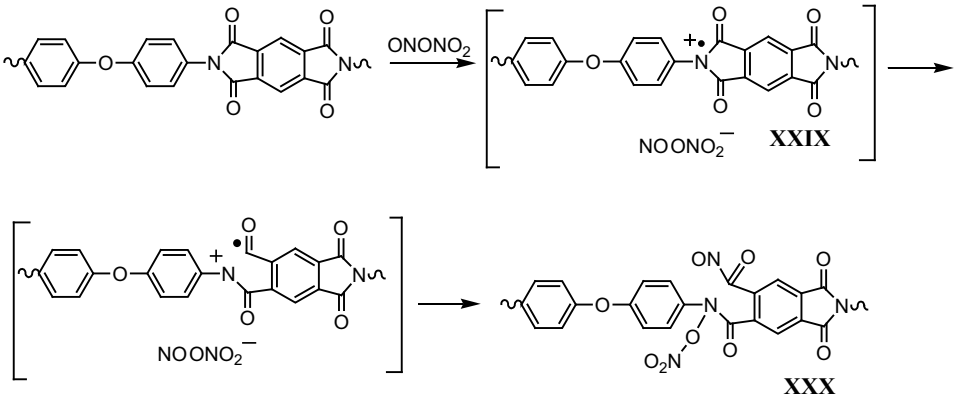

(7.79)

As a result of this primary stage, radical cations **XXIX**, NO and nitrate-anion are formed. The dissociating decomposition of radical cations and subsequent cage recombination of the primary stage products give compounds **XXX**. These compounds, being apparently intermediates, are converted into stable acylarylaminoxyl radicals **XXVII** due to reversible dissociation with detachment of NO_2:

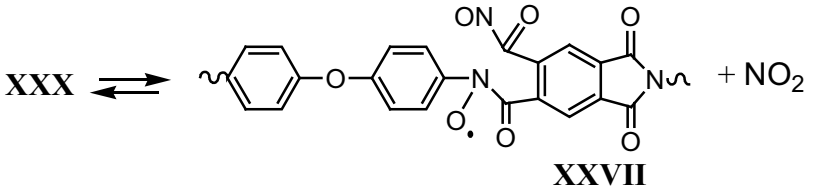

(7.80)

In an NO_2 atmosphere at room temperature, the equilibrium (**Equation 7.80**) is shifted to the left, and paramagnetic products are not detected in PPI in these conditions. However, this equilibrium is shifted to radicals **XXXVII** by pumping out NO_2 from samples (**Figure 7.16a**).

The disintegration of radical cations **XXIX** arises probably as a result of dissociation of other bonds of imide cycles:

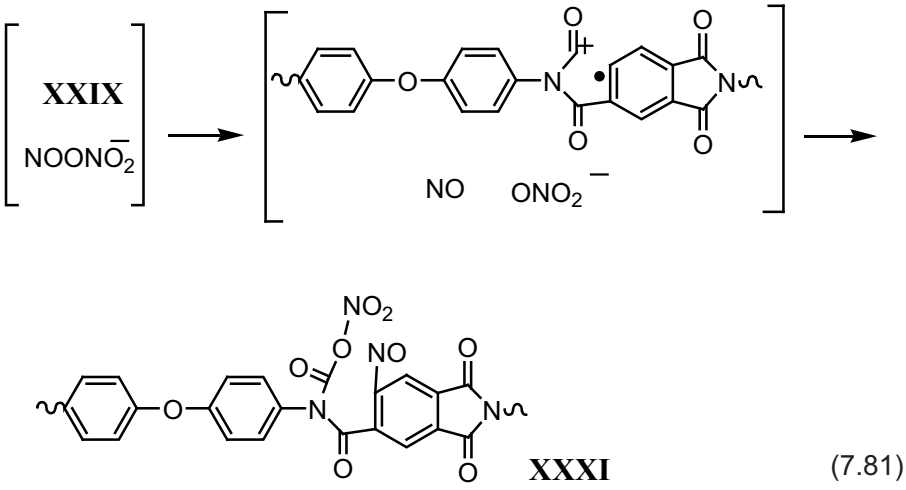

(7.81)

The compounds **XXXI** formed as a result of consecutive cage reactions (**Equation 7.81**) can be considered as precursors of iminoxyl radicals **XXVIII** and radicals **XXXII** characterised by a singlet EPR spectrum (**Figure 7.16c** and **d**). The amidyl radicals XXXIII are formed by thermal decomposition of XXXI while heating in vacuum of PPI previously exposed to NO_2:

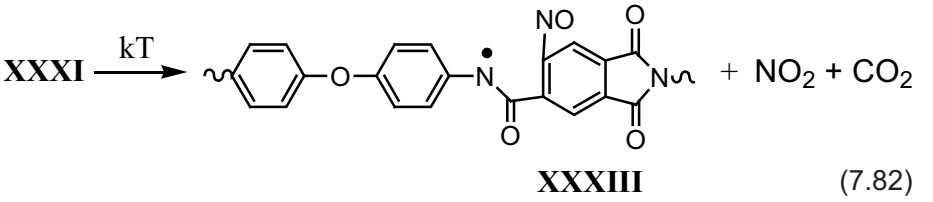

(7.82)

The isomerisation of radicals **XXXIII** gives phenoxyl radicals **XXXII** which have sufficient high thermal stability [50]:

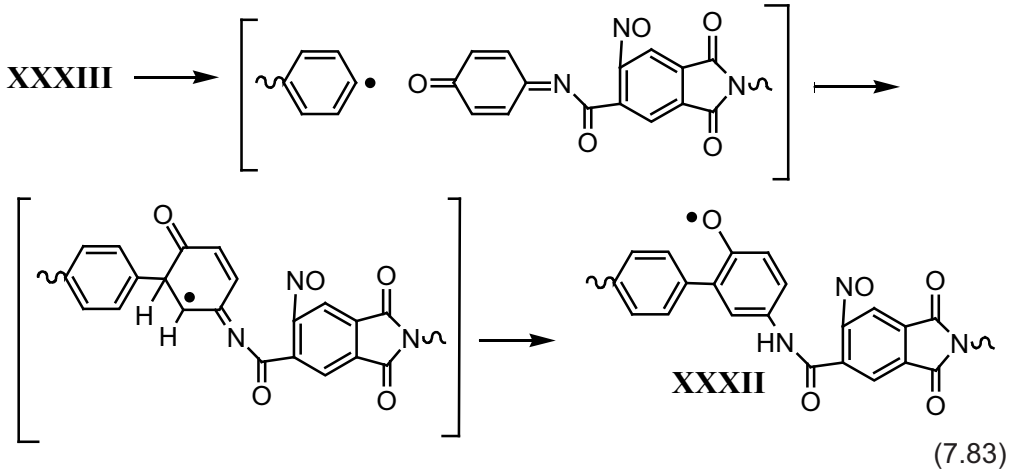

(7.83)

Similarly, isomeric phenoxyl radicals **XXXIIa** or **XXXIIb** can be formed:

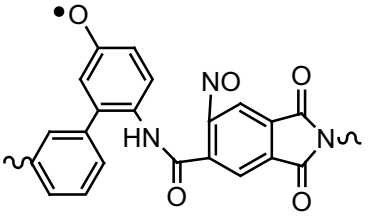

XXXIIa

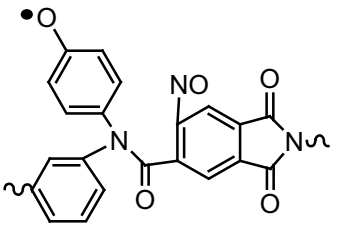

XXXIIb

Ab-initio calculations [8] show that the thermal conversions of **XXXIII** into phenoxyl radicals are energetically efficient; the energy of model amidyl radicals far exceeds that of model phenoxyl radicals (ΔE = 58–85 kJ/mol/1). In addition, among probable structures of phenoxyl radicals formed by the exothermic reaction (**Equation 7.83**) the structures **XXXII** and **XXXIIa** are energetically more preferable in comparison with **XXXIIb**.

The generation of iminoxyl radicals **XXVIII** after exposure of PPI to NO_2 at room temperature followed by warming samples in vacuum at 100 °C (**Figure 7.16b, c** and **d**) or in the course of exposure to NO_2 at the same temperature (**Figure 7.18a**) is seemingly conditioned by specific products. In the primary oxidative reaction, the formation of radical cations of PPI can take place also owing to an electron transfer from phenyl rings to nitrosyl nitrate. Such possibility follows from the available data of UV spectroscopy according to which nitrosyl nitrate is capable of forming charge transfer complexes with aromatic compounds [13]. As a result of the oxidative reaction, aryl radical cations appear. These species give intermediate aryl nitroso compounds after detachment of protons. If the nitrosation process takes place in monomer units modified by nitrogen-containing groups as in **XXXI**, these consecutive reactions can be represented as follows:

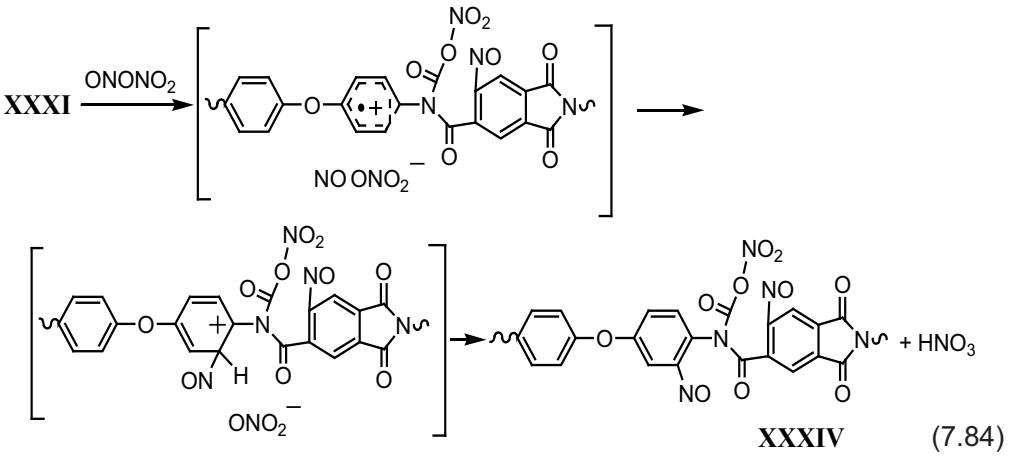

XXXIV (7.84)

Due to the thermal decomposition of compounds **XXXIV** during heating, amidyl radicals **XXXV** are formed:

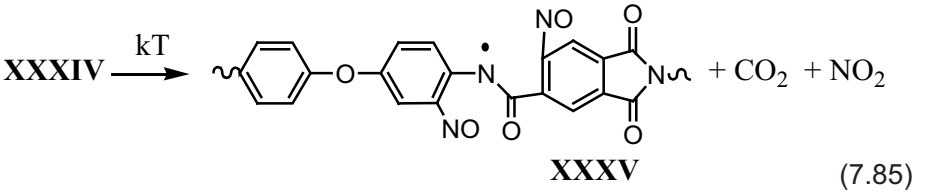

XXXV (7.85)

The radicals **XXXV** may also present in other isomeric forms, for instance, as nitrosoalkyl radicals which in turn isomerised into iminoxyl radicals **XXVIII** [51, 52]:

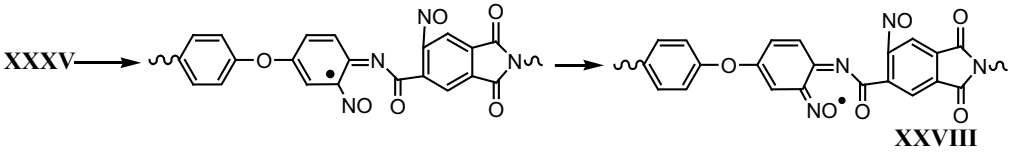

XXVIII (7.86)

The steady-state level of radical **XXVIII** concentration on exposure of PPI to NO_2 at 100 °C (**Figure 7.19a**) is caused by the recombination of formed iminoxyl radicals with NO_2:

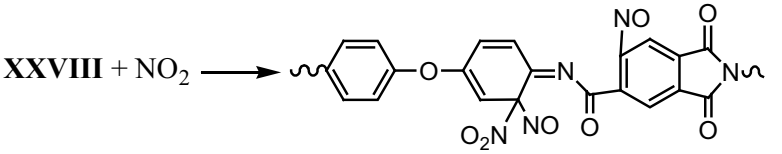

XXXVI (7.87)

The products **XXXVI** are thermally less stable compared with **XXXIV,** and decompose into the initial components. In this case, the replacement of **XXXIV** by **XXXVI** takes place during exposure of PPI to NO_2 at 100 °C. Therefore, the rate of accumulation of **XXVIII** at subsequent heating of PPI in a vacuum (**Figure 7.19b**) is four-times higher than that for samples exposed at room temperature (**Figure 7.17a** (4)) when products **XXXVI** are not generated and **XXXIV** is the sole precursor of iminoxyl radicals.

Figure 7.17b demonstrates that the rate of accumulation of radicals **XXVIII** during thermolysis of PPI pre-exposed to NO_2 linearly depends on concentrations of NO_2 in the gas phase. At first glance, this result contradicts the mechanism with participation of nitrosyl nitrate as an initiator, according to which the square-low dependence should be observed for the rate. However, if we take into account that aromatic nitroso

compounds are oxidised by monoradicals of NO_2 to nitro compounds [53], one can explain the experimentally observed linear dependence. Indeed, if nitroso compounds **XXXIV** are formed by consecutive reactions (**Equation 7.81**), (**Equation 7.84**), and concentrations of **XXXI** and **XXXIV** become stationary during long exposure of PPI to NO_2 at room temperature, then k_1 $[NO_2]^2 = k_2$ [**XXXIV**] $[NO_2]$ and d[**XXVIII**]/$dt = k_1 k_3 k_2^{-1}[NO_2]$ where k_1 and k_2 are effective rate constant of formation and decay of **XXXIV** in NO_2 atmosphere, k_3 is the rate constant of thermal conversion of **XXXIV** into **XXVIII**.

One can assume other parallel process when aromatic nitroso compounds are initially formed and transformed later into **XXXIV** in the reaction with nitrosyl nitrate:

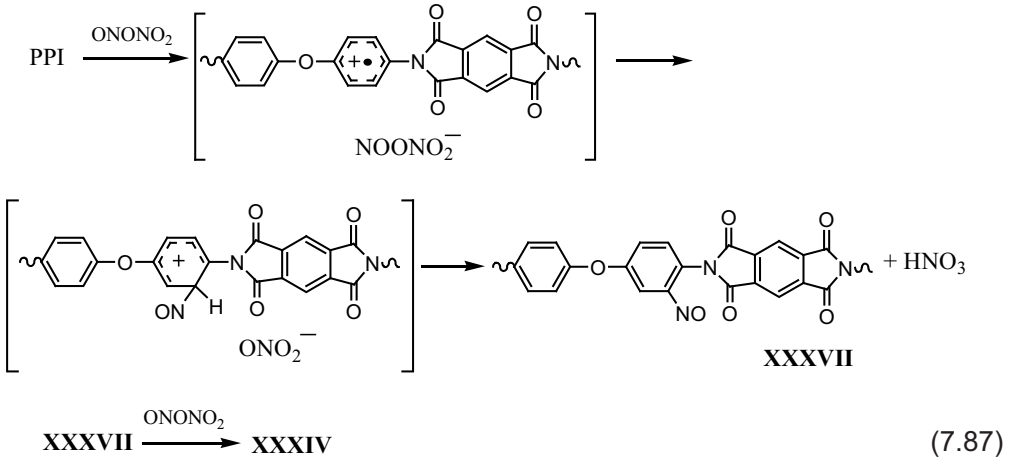

(7.87)

The formal kinetic scheme for the sequence of reactions (**Equation 7.87**) taking into account NO_2 reactions can be represented as follows:

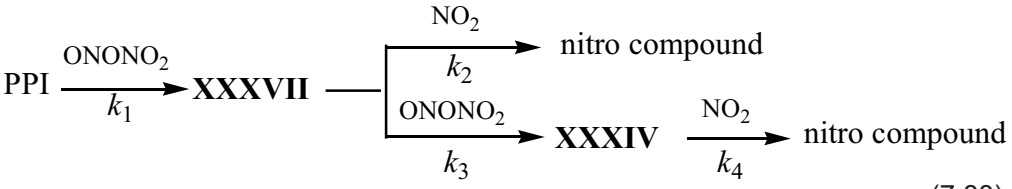

(7.88)

Then the equation for stationary concentrations of **XXXIV** is

$$[\mathrm{XXXIV}] = \frac{k_1 k_3 [\mathrm{NO_2}]^3}{k_4 (k_2 [\mathrm{NO_2}] + k_3 [\mathrm{NO_2}]^2)} \tag{7.89}$$

If the conversion of nitroso compound **XXXVII** takes place sufficiently efficiently,

that is, $k_3[NO_2]^2 > k_2[NO_2]$, then $[XXXIV] = \frac{k_1[NO_2]}{k_4}$. In this case, too, the linear dependence on NO_2 concentrations should be observed for the kinetics of the iminoxyl radical **XXVIII** formation by reaction (**Equation 7.85**).

Thus, thermally and chemically stable, PPI is reactive with respect to NO_2. The significant reactivity of polyimides can be explained by the concept of intermediate radical cations formed as a result of the primary oxidising reaction with participation of nitrosyl nitrate.

References

1. D.H. Giamalva, G.B. Kenion, D.F. Church and W.A. Pryor, *Journal of the American Chemical Society*, 1987, **109**, 23, 7059.

2. T.V. Pokholok and G.B. Pariiskii, *Journal of Polymer Science Part A: Polymer Chemistry Edition*, 1997, **39**, 765.

3. J.S.B. Park and J.C. Walton, *Journal of the Chemical Society*, *Perkin Transactions 2*, 1997, **12**, 2579.

4. P. Golding, J.L. Powell and J.H. Ridd, *Journal of the Chemical Society*, *Perkin Transactions 2*, 1996, **5**, 813.

5. I.S. Gaponova, E.Ya. Davydov, G.B. Pariiskii and V.P. Pustoshnyi, *Vysokomolekulyarnye Soedineniya Seria A*, 2001, **43**, 98.

6. I.S. Gaponova, E.Ya. Davydov, G.G. Makarov, G.B. Pariiskii and V.P. Pustoshnyi, *Journal of Polymer Science: Polymer Chemistry Edition*, 1998, **40**, 309.

7. T.V. Pokholok, I.S. Gaponova, E.Ya. Davydov and G.B. Pariiskii, *Polymer Degradation and Stability*, 2006, **91**, 40, 2423.

8. I.S. Gaponova, G.B. Pariiskii, T.V. Pkholok and E.Ya. Davydov, *Polymer Degradation and Stability*, 2008, **93**, 6, 1164.

9. L. Parts and J.T. Miller, *Journal of Physical Chemistry,* 1965, **43**, 136.

10. D.S. Goulden and D.J. Millen, *Journal of the Chemical Society*, 1950, 2620.

11. W.A. Sharp and J. Thorley, *Journal of the Chemical Society*, 1963, 3557.

12. E.H. White, *Journal of the American Chemical Society*, 1955, **77**, 22, 6008.

13. E. Bosch and J.K. Kochi, *Journal of Organic Chemistry*, 1994, **59**, 12, 3314.

14. E. Bosch and J.K. Kochi, *Journal of Organic Chemistry*, 1994, **59**, 19, 5573.

15. E. Kim and J.K. Kochi, *Journal of the American Chemical Society*, 1991, **113**, 13, 4962.

16. E.K. Kim, T.M. Bockman and J.K. Kochi, *Journal of the American Chemical Society*, 1993, **115**, 8, 3091.

17. R. Rathore, E. Bosch and J.K. Kochi, *Journal of the Chemical Society, Perkin Transactions 2*, 1994, **6**, 1157.

18. R. Rathore, J.S. Kim and J.K. Kochi, *Journal of the Chemical Society*, *Perkin Transactions 1*, 1994, **19**, 2675.

19. E. Bosch, R. Rathore and J.K. Kochi, *Journal of Organic Chemistry*, 1994, **59**, 9, 2529.

20. C.D. Snyder and H. Rapoport, *Journal of the American Chemical Society*, 1972, **94**, 1, 227.

21. R. Rathore, S.V. Lindeman and J.K. Kochi, *Journal of the American Chemical Society*, 1997, **119**, 40, 9393.

22. E. Bosch and J.K. Kochi, *Journal of Organic Chemistry*, 1995, **60**, 10, 3172.

23. Y. Mao and J.K. Thomas, *Journal of Organic Chemistry*, 1993, **58**, 24, 6641.

24. D. Greatorex and T.J. Kemp, *Journal of the Chemical Society - Faraday Transactions 1*, 1979, **68**, 121.

25. E.Ya. Davydov, I.S. Gaponova, G.B. Pariiskii and T.V. Pokholok, *Journal of Polymer Science: Polymer Chemistry Edition*, 2006, **48**, 375.

26. K. Nakanishi, *Infrared Absorption Spectroscopy*, Holden Day, San Francisco, CA, USA, 1962.

27. R. Silverstein, G. Bassler and T. Morril, *Spectroscopic Identification of Organic Compounds*, Wiley, New York, NY, USA, 1974.

28. T. Clark, *Handbook of Computational Chemistry*, Wiley, New York, NY, USA, 1985.

29. H.J. Tricker, T.B. Tennakoon, J.M. Thomas and J. Heald, *Clays and Clay Minerals*, 1975, **23**, 1, 77.

30. V.G. Koshechko, V.E. Titov and V.D. Pohodenko, *Theoretical and Experimental Chemistry*, 1983, **19**, 2, 143.

31. V.G. Koshechko, V.Yu. Atamanyuk and V.D. Pohodenko, *Theoretical and Experimental Chemistry*, 1977, **13**, 6, 570.

32. K. Sreenath, C.V. Suneesh, K.R. Kumar and K.R. Gopidas, *Journal of Organic Chemistry*, 2008, **73**, 8, 3245.

33. J.E. Wertz and J.R. Bolton, *Electron Spin Resonance*, McGraw-Hill, New York, NY, USA, 1972.

34. F.A. Bell, P. Beresford, L.J. Kricka and A. Ledwith, *Journal of the Chemical Society*, *Perkin Transactions 1*, 1974, 1788.

35. A. Ledwith, *Accounts of Chemical Research*, 1972, **5**, 4, 133.

36. E.M. Kosower and E.J. Poziomek, *Journal of the American Chemical Society*, 1964, **86**, 24, 5515.

37. G.B. Pariiskii, I.S. Gaponova, E.Ya. Davydov and T.V. Pokholok in *Aging of Polymers, Polymer Blends and Polymer Composites*, Volume 1, Eds., G.E. Zaikov, A.L. Buchachenko and V.B. Ivanov, Nova Science Publishers, New York, NY, USA, 2002, p.31.

38. V.N. Belevskii, D.A. Tyurin and N.D. Chuvylkin, *Khimiia Vysokikh Energii*, 1998, **32**, 342.

39. P.S. Lakkaraju, J. Zhang and H.D. Roth, *Journal of Physical Chemistry*, 1994, **98**, 11, 2722.

40. W.M. Fox and N.C.R. Symons, *Journal of the Chemical Society A: Inorganic, Physical, Theoretical,* 1966, 1503.

41. H. Feuer, *The Chemistry of the Nitro and Nitroso Groups*, Wiley, New York, NY, USA, 1969.

42. M.J. Frisch, G.W. Trucks, H.B. Schlegel, G.E. Scuseria, M.A. Robb, J.R. Cheeseman, and co-workers, *Gaussian 98*, Gaussian Inc., Pittsburgh, PA, USA, 1998.

43. A.R. Jaszewski, J. Jeziewska and A. Jezierski, *Chemical Physical Letters*, 2000, **319**, 5-6, 611.

44. G.B. Pariiskii, I.S. Gaponova and E.Ya. Davydov, *Russian Chemical Reviews*, 2000, **69**, 985.

45. K.U. Bühler, *Spezialplaste*, Academic Verlag, Berlin, Germany, 1978.

46. E.F. Shoenbrunn and J.H. Gardner, *Journal of the American Chemical Society*, 1960, **82**, 18, 4905.

47. E.Ya. Davydov, I.S. Gaponova, T.V. Pokholok, G.B. Pariiskii and G.E. Zaikov, *Journal of Applied Polymer Science*, 2008, **108**, 1, 128.

48. E.Ya. Davydov, I.S. Gaponova and G.B. Pariiskii, *Journal of the Chemical Society, Perkin Transactions 2*, 2002, **7**, 1359.

49. W. Xie, R. Heitsley, X. Cai, F. Deng, J. Lieu and C. Lee, *Journal of Applied Polymer Science*, 2002, **83**, 7, 1219.

50. D.C. Nonhebel, J.M. Tedder and J.C. Walton, *Radicals*, Cambridge University Press, Cambridge, UK, 1979.

51. F.G. Bordwell and S. Zhang, *Journal of the American Chemical Society*, 1995, **117**, 17, 4858.

52. H.J. Peter de Lijser, J.S. Kim, S.M. McGrorty and E.M. Ulloa, *Canadian Journal of Chemistry*, 2003, **81**, 575.

53. B.G. Gowenlock, J. Pfab and V.M. Young, *Journal of the Chemical Society, Perkin Transactions 2*, 1997, **9**, 1793.

Abbreviations

AC	Acetyl Cellulose
AIBN	2,2'-azobisisobutyronitrile
AR	Aminoxyl radical(s)
BNB	2,4,6-tri-*t*-butylnitroso benzene
BQ	Benzoquinone
BR	Butyl rubber
BTNO	Benzotriazole-*N*-oxyl
CAN	Ceric ammonium nitrate
CCl_4	Carbon tetrachloride
CH_2Cl	$^{\bullet}CH_2Cl$ radical
$CHCl_2$	$^{\bullet}CHCl_2$ radical
CO	Carbon monoxide
CO_2	Carbon dioxide
DMAA	Dimethylacetamide
DME	dimethylether
DMF	dimethylformamide
DNA	Deoxyribonucleic acid
DNIC	Dinitrosyl iron complexes
DPN	Diphenylnitron
*E*ox	Energy of oxidation
EPR	Electron Paramagnetic resonance
ESR	Electron spin resonance
EtOEt	Ethoxy ethane
FT-IR	Fourier transform infrared technology
FT-IR	Fourier transform infrared technology
GPC	Gel permeation chromatography
H_2Q	Hydroquinones

H_2SO_3	Sulphurous acid
HBEA-25	Trademark of zeolite
HBT	1-hydroxybenzotriazole
HCl	Hydrogen chloride
HFC	Hyperfine coupling
HFI	Hyperfine interaction
HFP	Hexafluoropropylene
HFS	Hyperfine splitting
HMB	Hexamethylbenzene
HNO_2	Nitrous acid
HNO_3	Nitric acid
HOONO	Pernitrous acid
HSO_3^-	Sulphurous acid anion
HZSM-5	Trademark of zeolite
IE	Ionisation energie(s)
INDO	Intermediate Neglect of Differential Overlap
IP	Ionisation potential
IR	Infrared
LMW	Low molecular weight
MN	Methylene-*t*-butylnitron
MP	*N*-methyl-2-pyrrolidone
N_2O_4	Nitrogen tetroxide
N_2O_5	Nitrogen pentoxide
NB	Nitroso benzene
ND	Nitroso durene
NMR	Nuclear magnetic resonance
NN	Nitrosyl nitrate
NO	Nitric oxide
NO_2	Nitrogen dioxide
NO_3	Nitrogen trioxide
NOCl	Nitrosyl chloride
O_2	Oxygen
O_3	Ozone
PA	Polyamide

PBN	-Phenyl-*N*-*t*-butylnitron
PCA	Polycaproamide
PD	Planar dimer
PE	Polyethylene
PI	1,4-cis-polyisoprene
PMMA	Polymethylmethacrylate
PP	Polypropylene
PPI	Polypyromellitimide
PPIA	Poly-m-phenylene isophthalamide
PPM	Parts per million
PS	Polystyrene
PTBMA	Poly-t-butylmethacrylate
PTFE	Polytetrafluoroethylene
PVP	Polyvinylpyrrolidone
PVPR	poly-(2-vinylpyridine)
QHP	o-quinolide peroxy groups
SO_2	Sulfur dioxide
TBQ	2,6-di-tert-butyl-p-benzoquinone
TFE-HFP	Tetrafluoroethylene with Hexafluoropropylene
THF	Tetrahydrofuran
TNB	t-nitroso butane
TPA	Triphenylamine
UV	Ultarviolet
UV-VIS	Ultraviolet-visible
ZSM-5	Trademark of zeolite

Index

A

B

C

D

H

I

O

P

Q

R

S

T

U

V

Z

Published by Smithers Rapra, 2009

Nitrogen oxides are common by-products of fossil fuel combustion and are one of the most important types of air pollution. The nitric oxides react with UV radiation to form oxides of nitrogen, ozones and acids. The nitrogen oxides can have considerable impact of the life of polymers in the environment and can be responsible for failure of polymer products, so it is important to know how these effects will be manifest.

In this book, novel results obtained by physicochemical methods especially electron spin resonance spectroscopy are considered for various polymers. The influence of different functional groups on the mechanism of interaction of nitrogen oxides with polymers are discussed. The features of ion-radical initiation of conversions of polymers by dimers of nitrogen dioxide are also considered. Various other techniques for studying these interactions are also discussed.

This book will be of interest to all those who produce polymer products that are likely to spend their life in an outdoors environment. It will also be useful to the manufacturers of raw materials used in these products. Technicians who are involved in material testing will also find a wealth of information about testing for the effects of ozone on polymers.

Shawbury, Shrewsbury, Shropshire, SY4 4NR, UK
Telephone: +44 (0)1939 250383
Fax: +44 (0)1939 251118
Web: www.rapra.net